

Injectable drug delivery systems for steroids

Dissertation

zur Erlangung des akademischen Grades des
Doktors der Naturwissenschaften (Dr. rer. nat.)

eingereicht im Fachbereich Biologie, Chemie, Pharmazie
der Freien Universität Berlin

vorgelegt von

Stefanie Nippe

aus Lübben

März 2014

1. Gutachter: Professor Dr. R. Bodmeier
2. Gutachter: Privatdozent Dr. H. Kranz

Disputation am 16.10.2014

To my family

Danksagung

Die vorliegende Arbeit wurde unter der Leitung von Herrn Professor Dr. Roland Bodmeier vom Institut für Pharmazie der Freien Universität Berlin sowie in der Abteilung Early Development der Bayer HealthCare AG angefertigt und vor Ort von Herrn Dr. Sascha General betreut.

Mein besonderer Dank gilt meinem Doktorvater Herrn **Prof. Dr. Roland Bodmeier** für seine fachliche Betreuung und sein entgegengebrachtes Vertrauen, während der Zeit meiner wissenschaftlichen Arbeit.

Herrn **Priv.-doz. Dr. Heiko Kranz** danke ich ganz herzlich für die Bereitschaft die vorliegende Arbeit zu begutachten.

Meinem Mentor Herrn **Dr. Sascha General** danke ich für die Bereitstellung meines Promotionsthemas, die Initiierung interdisziplinärer Zusammenarbeiten sowie die überlassene Freiheit zur Gestaltung der Arbeit.

Bei Herrn **Dr. Stefan Bracht** möchte ich mich für die Möglichkeit zur Anfertigung dieser Dissertation sowie die finanzielle Unterstützung bedanken.

Der Abteilung Analytical Development Physical Chemistry danke ich für die Möglichkeit zur Durchführung der umfangreichen Partikelgrößenuntersuchungen. Mein besonderer Dank gilt Herrn **Sven Wegner** für die hervorragende Einführung in die Messmethoden und seine Hilfsbereitschaft.

Dr. Oliver-Martin Fischer und **Dr. Andrea Rotgeri** sowie der früheren Abteilung Nonclinical Pharmacokinetics, insbesondere **Dr. Cornelia Preuße**, danke ich herzlich für die Durchführung der *in vivo* Studien. Besonders bedanken möchte ich mich bei **Andreas Eckermann** für die gute Zusammenarbeit und Unterstützung.

Ein herzlicher Dank geht auch an die Abteilung Pharmaceutical Technology Packaging für die Unterstützung bei den Versuchen zur Applizierbarkeit. Insbesondere bedanken möchte ich mich bei **Torsten Wollenberg** für die Hilfe bei der Interpretation der Ergebnisse.

Meinen Kollegen der ehemaligen Abteilungen Early Development and Drug Delivery Systems sowie Early Development danke ich für die stetige Unterstützung bei allen technische Fragestellungen. Besonders danken möchte ich **Markus Hafke**, **Thomas Trill** und **Stephan Elze** für die Einführung in zahlreiche Analytikmethoden sowie in die Polymerpartikelherstellung.

Ganz herzlich danken möchte ich der Firma Intendis für die Möglichkeit zur Durchführung der Rheologiestudien sowie die Einführung in die komplexe Messmethodik.

Der Abteilung Analytical Development Project Laboratory II danke ich für die Möglichkeit der Durchführung der HPLC/FD Untersuchungen.

Meinen Kollegen der IVIVC Gruppe der Hexal AG danke ich für ihr Verständnis sowie für die Möglichkeit flexibel Zeit für die Fertigstellung der Arbeit zu bekommen. Besonders bedanken möchte ich mich bei **Jörg Nink** und **Dr. Markus Wiedmann** für die intensive und konstruktive Durchsicht der Arbeit.

Den Mitdoktoranden der Bayer HealthCare AG danke für die schöne Zeit in Labor, den Mittagspausen und nach Feierabend. Ganz herzlich danke ich **Dr. Annett Richter** für das kritische Korrekturlesen der Arbeit sowie die vielen hilfreichen und aufmunternden Anmerkungen.

Ein großes Dankeschön geht auch an **Julia, Jens, Nicole, Martin, Lisa** und **Christine** für die schönen, ablenkenden Feierabende, die vielen aufbauenden Worte und ihr Verständnis.

Mein größter Dank gilt meinen **Eltern** und meiner **Schwester** für ihre unermüdliche Unterstützung in allen Lebenslagen.

Table of Contents

Abbreviations.....	VIII
--------------------	------

CHAPTER 1 Introduction..... 1

1.1 Injectable drug delivery systems	2
1.1.1 General aspects	2
1.1.2 Conventional versus controlled-release injectable drug delivery systems	4
1.2 S.c. and i.m. injectable drug delivery systems for lipophilic APIs	5
1.2.1 Oil-based solutions as well as aqueous and oil-based microcrystal suspensions (MCSs).....	5
1.2.2 Organogels	10
1.2.3 Biodegradable polymeric particulate systems – Poly(n-butyl-2-cyanoacrylate) (PBCA) and poly(D,L-lactid-co-glycolide) (PLGA) particle	15
1.3 Combined drug delivery	24
1.4 S.c. and i.m. injectable drug delivery systems for steroids	24
1.4.1 General aspects	24
1.4.2 Parenteral s.c. and i.m. injectable contraceptives	24
1.4.3 The steroidal model APIs DRSP, EE, and ZK28.....	29
1.4.4 Summary	30
1.5 Objectives.....	31
References	32

CHAPTER 2 Parenteral oil-based drosiprenone microcrystal suspensions - Evaluation of physicochemical stability and influence of stabilising agents..... 43

Abstract	44
Graphical Abstract.....	45
1. Introduction	46
2. Materials and methods	47
3. Results and discussion	51
4. Conclusion	58
References	60

CHAPTER 3 Investigation of injectable drospirenone organogels with regard to their rheology and comparison to non-stabilized oil-based drospirenone suspensions.....	62
Abstract	63
1. Introduction	64
2. Materials and methods	64
3. Results and discussion	69
4. Conclusion	80
5. Supplement.....	81
References	82
CHAPTER 4 Evaluation of the <i>in vitro</i> release and pharmacokinetics of parenteral injectable formulations for steroids.....	84
Abstract	85
Graphical Abstract.....	86
1. Introduction	87
2. Materials and methods	88
3. Results	94
4. Discussion	104
5. Conclusion	110
6. Supplement.....	111
References	112
CHAPTER 5 Combination of injectable ethinyl estradiol and drospirenone drug-delivery systems and characterization of their <i>in vitro</i> release	115
Abstract	116
Graphical Abstract.....	117
1. Introduction	118
2. Materials and methods	119
3. Results and discussion	126
4. Conclusion	136
5. Supplement.....	138
References	139
CHAPTER 6 Summary - Zusammenfassung	142
CHAPTER 7 Appendices.....	152
List of Publications.....	153
Curriculum Vitae.....	154

Abbreviations

English

τ	Shear stress
η^*	Complex viscosity
17HSD	17 β -hydroxysteroid dehydrogenase
ACN	Acetonitrile
API	Active pharmaceutical ingredient
Approx.	Approximately
AS	Aluminum stearate
AUC	Area under the curve
Bb	Benzyl benzoate
BCA	n-Butyl cyanoacrylate
C_{\max}	Maximum plasma concentration
CMC	Critical micelle concentration
C_{\min}	Minimum plasma concentration
Co	Castor oil
COC	Combined oral contraceptives
CS	Cholesteryl stearate
DRSP	Drospirenone
E2	Estradiol
EE	17 α -ethinyl estradiol
F	Sedimentation volume
f_1	Difference factor
f_2	Similarity factor
FDA	US Food and Drug Administration agency
Fig.	Figure
G	Gauge
G'	Elastic modulus
G''	Viscous modulus
GLP	Good laboratory practice
HCl	Hydrochloric acid
HPLC	High performance liquid chromatography
HPLC/FD	High performance liquid chromatography with fluorescence detection
HPLC/UV	High performance liquid chromatography with UV detection
HP- β -CD	Hydroxypropyl- β -cyclodextrin

HP- β -cyclodextrin	Hydroxypropyl- β -cyclodextrin
I.m.	Intramuscular(ly)
I.v.	Intravenous
IsoDRSP	Isodrospirenone
LC-MS/MS	Liquid-liquid extraction, separation by high-pressure liquid chromatography and tandem mass spectrometric detection
LLOQ	Lower limit of quantification
LNG	Levonorgestrel
LOQ	Limit of quantification
LVR	Linear viscoelastic region
MC	Methyl cholate
MCS	Microcrystal suspension
MCT	Medium chain triglycerides
MeOH	Methanol
MPA	Medroxyprogesterone acetate
MRM	Multiple reaction monitoring
n.c.	not considered
NET	Norethisterone
NET-EN	Norethisterone enanthate
Nw-mp	Median of number-weighted particle size distribution
PACA	Poly(alkylcyanoacrylate)
PBCA	Poly(n-butyl-2-cyanoacrylate)
PBCAEEC	PBCA microcapsules incorporating ethinyl estradiol in the core
PBCAEES	PBCA microcapsules incorporating ethinyl estradiol in the shell
PCS	Photon correlation spectroscopy
pK_a	logarithmic acid dissociation constant
PLGA	Poly(D,L-lactid-co-glycolide)
Po	Peanut oil
PSD	Particle size distribution
PVA	Poly(vinyl alcohol)
QC	Quality control
r^2	Square root of correlation coefficient
RKL2	Rheopearl® KL2
RT	Room temperature
RTL2	Rheopearl® TL2
RTT2	Rheopearl® TT2
S.c.	Subcutaneous(ly)

SEM	Scanning electron microscopy
SHBG	Sex hormone-binding globulin
Tab.	Table
$\tan\delta$	quotient of elastic and viscous modulus
TIS	Turbo ion spray ion source
T_{\max}	Time to maximum plasma concentration
ULOQ	Upper limit of quantification
USP	United States Pharmacopeia
VTE	Venous thromboembolism
Vw-mp	Median of volume-weighted particle size distribution

German

DRSP	Drospirenon
EE	Ethinylestradiol
IsoDRSP	Isodrospirenon
MKS	Mikrokristallsuspension
MKT	Mittelkettige Triglyceride
PBCA	Poly(n-butyl-2-cyanoacrylat)
PBCAEEC	PBCA Mikrokapseln, die EE im Kern enthalten
PBCAEES	PBCA Mikrokapseln, die EE in der Hülle enthalten
PLGA	Poly(D,L-laktid-co-glykolid)

CHAPTER 1

Introduction

1.1 Injectable drug delivery systems

1.1.1 General aspects

The first official parenteral injected drug was a morphine injection mentioned in the British Pharmacopeia in 1867 [1]. Since that time their number has been increased dramatically. Injectable drug delivery systems are formulations or carrier systems for active pharmaceutical ingredients (APIs) which are administered by subcutaneous (s.c.), intramuscular (i.m.), and intravenous (i.v.) routes as well as at other specific sites such as intra-articulate [1,2]. The following work is focused on injectable s.c. and i.m. drug delivery systems. In comparison to conventional oral dosage forms, these systems provide numerous advantages summarized in **Fig. 1**. However, the application of oral dosage forms is often preferred, due to disadvantages which are associated with the injectable administration route and the high requirements for the manufacturing of injectable drug delivery systems [1-3]. These issues must be considered during the development of injectable drugs in order to use their advantages in an optimal way.

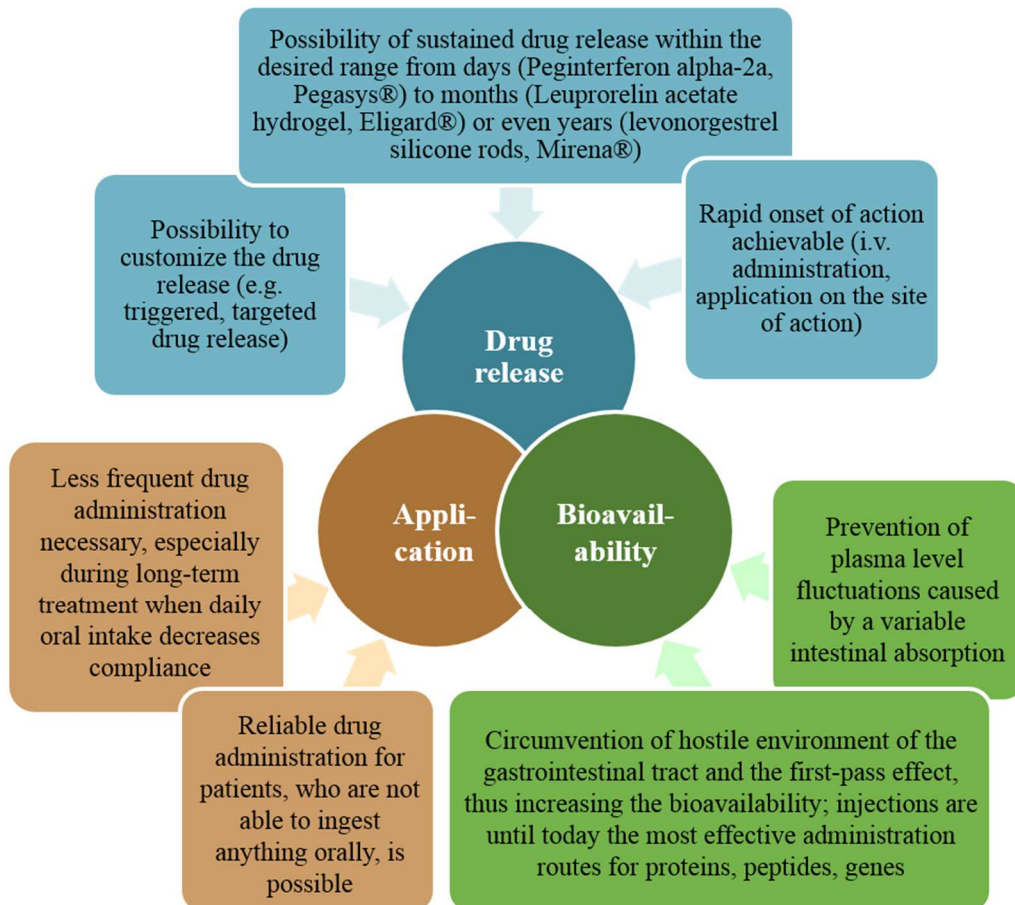


Fig. 1 Advantages of injectable drug delivery systems [1,2,4-7].

Issues during application of injectable drug delivery systems

Major problems during the application are pain and tissue damage at the injection site decreasing the patients' compliance.

Different methods are used to reduce these issues including [3,8]:

- Co-administration of anesthetics (e.g. lidocaine) to reduce pain
- Reduction of injection speed as well as use of the optimal injection needles (size, shape), site, depth, technique and temperature of dosage form to minimize pain and tissue damage
- Optimization of the formulations with respect to injection volume, viscosity, particle size, pH, tonicity, osmolarity, drug concentration, dosage form (e.g. diazepam formulated as an emulsion reduces the injection pain), excipients (e.g. co-solvents, microbial preservatives, chelating agents) to decrease pain and tissue damage

There is a general consensus that a maximum injection volume should not be exceeded in order to reduce injection pain and tissue damage, but the specification of the optimum and maximum volume varies in dependence on the drug formulation and the literature source. It is frequently recommended that the volume injected i.m. should be less than 5 ml into large muscle groups [8,9]. The overall liquid amount administered s.c. should be less than 2 ml with the optimum at 0.5 ml [1]. The limits of injection speed are difficult to define. Empirically determined, injections should be administered within 10 s. Too long duration of application decreases the patients' compliance, but a rapid injection is restricted by high viscosity of drug formulations or large suspended particles. A wide-broad opinion is that large needle diameters generally increase the injection pain. Interestingly, clinical trials show that a certain increase in the needle size does not or only slightly intensify the injection pain [10,11]. However, the application of voluminous dosage forms, i.e. implants, require the use of large needles and, thus, a minor surgical procedure is necessary which can cause hematoma, bleedings, and pain [12]. Therefore, in dependence on injection pain and tissue damage, the application frequency should be in a tolerable mode to increase the compliance of injectable drug delivery systems. Implants typically provide long dose intervals of year(s) (Vantas® is injected every year, Implanon® every 3 years) [12,13]. Oil-based formulations and polymeric microparticles are injected non-surgically but may cause higher injection resistance than most aqueous solutions. They are commonly administered with 20-23 gauge (G) injection needles every 2-12 weeks [14-16].

Another challenge for the application of injectable drug delivery systems is related to the long-term efficacy. Although the sustained drug delivery is frequently appreciated, this characteristic is unintended in case of hypersensitivity because the systems are often difficult to remove [17]. Consequently, complete baseline assessment should be performed on each patient before administration to reduce the incidence of hypersensitive reactions to a minimum. Furthermore, the application of a lower non-sustained dose is recommended, prior to the first injection of the reservoir system [18]. A further disadvantage, compared to oral application forms, is that injectable dosage forms can usually not be administered by the patients themselves and require therefore a visit to a physician. Moreover, the individual application procedure has to be trained because a

wrong application can cause injection pain, burst of the depot system, or insufficient efficacy [12,18]. S.c. and i.m. injections should be placed away from big nerve fibers and blood vessels to avoid embolism and/ or gangrenes. As a consequence, new and better injection devices are developed which are easier to apply or even allow a home treatment by the patients themselves [1]. Such systems include autoinjectors or portable syringe pumps.

Manufacturing issues of injectable drug delivery systems

Since injectable drug delivery systems bypass natural barriers of the body (gut, skin, mucosa), highest quality and purity standards must be ensured to protect the patients from physical, chemical, and microbial contamination [2]. Consequently, injectable dosage forms as well as the included API and excipients have to be fulfill special requirements which are not prerequisite for oral dosage forms (**Fig. 2**).

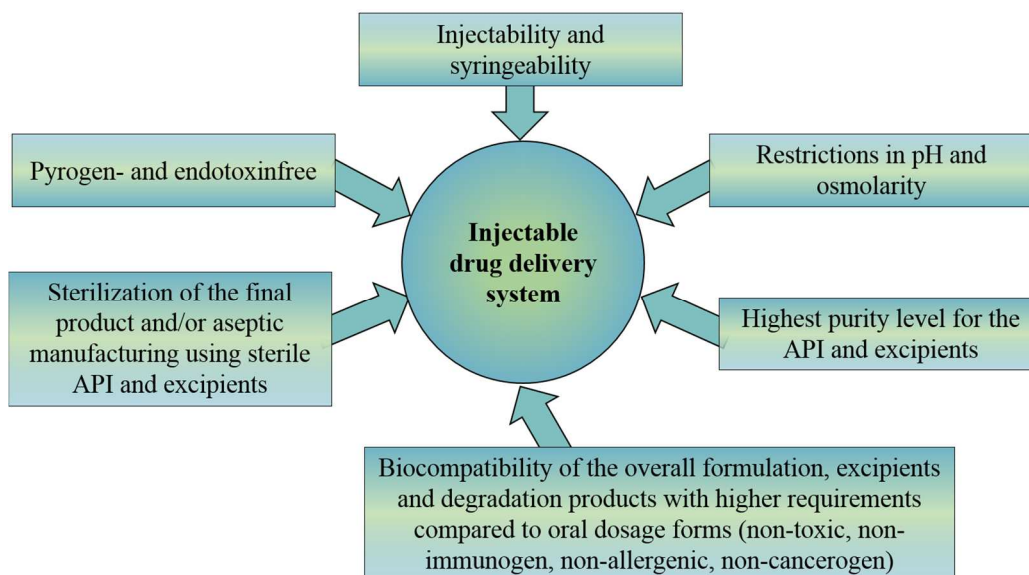


Fig. 2 Special manufacturing challenges of injectable drug delivery systems (additional requirements compared to oral dosage forms) [2,4,19].

1.1.2 Conventional versus controlled-release injectable drug delivery systems

The difference between conventional and controlled drug delivery systems is difficult to define. *A.T. Florence* [20] gives a broad definition of the term controlled drug delivery systems, as he suggested that the systems provide a “true control of drug release rates”. The history of controlled drug delivery systems includes earlier “uncontrolled” or “conventional” systems which ensure stability, activity, and bioavailability of the API but do not reach sufficient drug release control [20,21]. Unwanted pharmacokinetic drug behavior of conventional systems is then most often the driving force for the development of controlled-release systems [20]. Therapeutic advantages of controlled-release systems include prolonged dosing frequency, improved efficacy-dose relationship, reduced drug plasma level fluctuations and adverse effects, as well as higher patients’ compliance [17]. In order to realize the desired therapeutic outcome, the delivery system should

achieve the optimal effective drug concentration at a pre-determined rate and/ or at the preferred location [22]. There are various terms to describe drug release from drug delivery systems which overlap with the term “controlled drug release” [20]:

- Sustained or prolonged drug release: continuous long-term release from the formulation
- Modified drug release: release rates which are different from immediate release
- Pulsatile drug release: release of more than one drug dose from a given system
- Timed drug release: release after a specified period of time
- Triggered drug release: release that is stimulated by an external or endogenous signal
- Targeted drug release: release at a specific location (e.g. in tumor or brain)

Three elements are critical for the controlled release: the API, the formulation and the administration route [20]. Accordingly, drug modification i.e. PEGylation (Interferon alpha 2-a), synthesis of drug esters (estradiol esters) or salts (benzathine benzylpenicillin), or complexation (insulin-zinc-complexes) are used to prolong the drug release. In addition, the drug release can be regulated by suitable carrier systems. *A.S. Hoffmann* [5] suggested a categorization of controlled-release carrier systems into “macro-“, “micro-“ and “nanocarriers”. “Nanocarriers” have a size between 10-1000 nm and include i.e. nanoparticles, liposomes, and polymeric micelles. Injectable “microcarriers” are i.e. biodegradable polymeric or lipid-based microparticles. Their size ranges in a 1-1000 μm scale. Injectable “macrocarriers” are not limited to gels or implants [7]. Sometimes, controlled drug delivery systems are directly applied to the site of action to increase the local efficacy and reduce systemic drug circulation (Gliadel®) [17].

1.2 S.c. and i.m. injectable drug delivery systems for lipophilic APIs

Next, selected examples of s.c. and i.m. injectable drug delivery systems are introduced. Since the work is focused on steroids, drug delivery systems, which are suitable carrier systems for lipophilic APIs, are discussed.

1.2.1 Oil-based solutions as well as aqueous and oil-based microcrystal suspensions (MCSs)

General aspects and considerations for preparation

Oil-based solutions as well as oil-based and aqueous MCSs are the most commonly used injectable formulation options for the large number of lipophilic APIs [23]. Some APIs are not only poorly soluble in aqueous but also in oil-based vehicles and/or are unstable in aqueous fluids. For these molecules, oil-based MCSs might be suitable dosage forms. Vegetable or semi-synthetic oils, i.e. medium chain triglycerides, sesame, castor and peanut oil, are typical vehicles for the preparation of oil-based formulations. Most of these oils are regarded as essentially nontoxic and nonirritant materials [24]. Peanut and sesame oil are sometimes reported to cause hypersensitivity but allergens are inactivated by heating or removed in highly refined qualities [24].

Advantageously, no further addition of any excipients to the vehicles is frequently required to prepare oil-based solutions (**Tab. 1**). However, antioxidants and antimicrobial preservatives may be necessary because oils can tend to oxidation and hydrolytic or microbial rancidity upon contact with moisture [24]. Moreover, co-solvents are added to achieve API solubility in the desired concentration. For i.m. and s.c. injections, the organic solvent concentration can be increased up to 100%; however, the injection volume is then constrained to prevent pain, inflammation, and hemolysis caused by solvents [3,9]. The limits for injection volume and solvent concentration are tighter for s.c. injections due to the slow *in vivo* dilution [9]. The organic solvent benzyl benzoate is not only added to castor oil to increase drug solubility but also to reduce viscosity and to ensure consequently syringeability and injectability.

Tab. 1 Excipients used in injectable oil-based solutions and aqueous and oil-based MCSs [1,25-27].

Excipients	Oil-based solutions	Aqueous MCSs	Oil-based MCSs
Buffer, pH-adjusting agents		X	
Solvents, co-solvents, solubilizing agents	X		
Surfactants as suspending agents, wetting agents		X	X
Viscosity-imparting agents		X	X
Antimicrobial preservatives	(X)	X	(X)
Antioxidants, reducing agents	(X)	X	(X)
Tonicity adjustors		X	
Flocculating and deflocculating agents		X	

In advantage to solutions, chemical API instabilities such as hydrolysis or oxidation are typically reduced in MCSs [25]. However, MCSs are thermodynamically unfavorable systems which show numerous physical instabilities, i.e. aggregation or crystal growth. Crystal growth is caused by temperature fluctuations, polymorphic transformation, or Ostwald ripening [25]. The latter is more an issue for small particles of less than 1 μm [28]. Aggregation and crystal growth affect the particle size distribution and shape. These particle characteristics influence the sedimentation rate and resuspendability, the API dissolution, the viscosity and, consequently, the product appearance, product stability, and the drug release [25]. Moreover, needle-shaped and other particles with sharp edges could lead to irritations. Sedimentation is another physical instability that leads, in the worst case, to irreversible sediment compaction (caking). With respect to the Stoke's law (**Equation 1**), sedimentation is reduced by viscosity increase and reduction of particle sizes and the density difference between particle and vehicle. However, too small particles increase the risk of caking and Ostwald ripening. Sedimentation during the manufacturing can cause deviations in the content uniformity. For injectable MCSs prefilled in syringes, sedimentation could cause clogging of the injection needle during administration. Thus, reconstitution is often a prior step to injection.

$$v = \frac{g \cdot d^2(\rho_1 - \rho_2)}{18 \cdot \eta}$$

Equation 1 Stoke's law; v = sedimentation velocity, g =gravity of earth; d = diameter of suspended particles, ρ_1 = particle density, ρ_2 = density of continuous phase, η = viscosity of continuous phase.

To prevent physical instabilities of suspensions, different techniques can be employed such as selection of a narrow particle size distribution and more stable drug crystal forms, the avoidance of high-energy milling during micronization and temperature extremes during storage as well as the incorporation of stabilizing agents, i.e. surfactants, viscosity-increasing or (de)floculating agents [25] (**Tab. 1**). Steric or electrostatic repulsion of suspended particles play an important role for the prevention of aggregation [25]. It is generally assumed that oil-based MCSs provide higher physical stability than aqueous MCSs, i.e. due to the high viscosity of the continuous phase. Thus, stabilization approaches for oil-based MCSs are much less investigated than for aqueous MCSs. However, during long-term storage, physical instability can also be an issue for oil-based MCSs.

***In vivo* release and absorption processes**

Injectable oil-based solutions and aqueous or oil-based MCSs deliver APIs mostly, more or less constant, over weeks to months. They are often referred to as conventional parenteral drug delivery systems [29,30]. Nevertheless, there are possibilities to manipulate the drug release kinetics. The understanding of the complex interaction of many different mechanisms that affect the pharmacokinetics (LADME) is the basis for influencing the drug release. In the literature, various parameters are described which influence the drug release and uptake into the systemic circulation after s.c. and i.m. injection [29,31,32]:

- **API:** molecular weight, pK_a , solubility in the vehicle and the surrounding fluid, crystalline structure, lipophilicity (oil-water partition coefficient), irritating properties
- **Formulation:** vehicle characteristics (irritating properties, viscosity, interfacial tension, chemical/enzymatical degradability), excipient properties (e.g. co-solvents and surfactants), vehicle volume (drug concentration), dissolved or dispersed API, surface area of drug microcrystals, shape of the depot (needle/spherical)
- **Application:** injection technique and depth, injection trauma which can cause a change in the physiology of the injection site
- **Injection site:** body movement, muscle activity, drainage and blood flow, osmolarity, pH, tissue structure, distribution of enzymes and proteins, inflammation

In vivo release and absorption of aqueous MCSs

Low API amounts are dissolved in the aqueous vehicle and dissolved drug molecules are assumed to be transported through the tissue together with the flow of the aqueous vehicle from the injection site [29]. After complete drainage of the aqueous vehicle, API remaining at the injection site is

dissolved in the tissue fluid and transported slowly with the tissue fluid flow and normal diffusion processes [29]. The API dissolution in the aqueous vehicle and tissue fluid is a major step in drug release from MCSs and depends on the API solubility, microcrystal size and shape and the fluid viscosity (**Equation 2a**). Thus, these parameters may be used to manipulate the drug release rate. Furthermore, API particle size and concentration influence rheology and viscosity of the formulation [33]. **Equation 2b** describes the dissolution rate of cubical particles with respect to particle size changes during the dissolution process. Accordingly, a relationship between the absorption profile of injected aqueous MCSs and the cube root law was found [34].

$$\text{a) } \quad dM/dt = S \cdot D \cdot (c_s - c_t)/h \qquad \text{b) } \quad \omega_0^{1/3} - \omega^{1/3} = k_2 \cdot t$$

Equation 2 Equations derived from the Noyes-Whitney equation based on Fick's law. **a)** Nernst-Brunner equation considering dM/dt = mass transported in the time interval dt , S = surface area of the drug particle, D = diffusion coefficient, c_s = drug solubility in the liquid unstirred boundary layer surrounding the drug particle, c_t = drug concentration in the well-stirred bulk fluid, h = thickness of the unstirred boundary layer [35]; **b)** Hixson – Crowell equation considering ω_0 = initial weight, ω = residual weight at time t , k_2 = constant, t = time [36].

In the next step, drug transfer through the tissue can influence the pharmacokinetics. *Kadir et al.* [31] compares the drug transport through the tissue with a reversed-phase chromatography, whereas the paracellular route resembles the mobile phase and the cells resemble the lipophilic stationary phase. Small, hydrophilic molecules should mainly be transferred by the paracellular route and passive diffusion and show therefore a faster drug absorption rate. Lipophilic APIs retard longer by partitioning over the transcellular route. Mathematical models of drug diffusion mechanisms in the tissue may be derived by the Fick's laws (**Equation 3**) and should follow first order kinetics. In general, there is a risk of incomplete drug release within the therapeutic relevant time for very lipophilic APIs suspended in aqueous vehicles, due to low drug solubility in the aqueous vehicle and tissue fluid as well as slow diffusion from the injection site [31].

$$F = -D \frac{\partial c}{\partial x}$$

Equation 3 Fick's first law of diffusion. F = rate of transfer per unit area of section (flux); c = concentration of the diffusing species, x = distance, D = diffusion coefficient (also called diffusivity) [37].

In vivo release and absorption oil-based solutions and MCSs

Oil-based vehicles stay longer at the injection site than aqueous media [38]. The disappearance rate of oils was investigated in different animal models [39-41]. In general, the results were highly variable and strongly depended on the animal model. It was assumed that the vehicle viscosity influenced the disappearance rate of oils; however, a clear correlation between vehicle viscosity and clearance rate was not found. Moreover, chemical hydrolysis of glyceride ester bonds should proceed very slowly at physiological pH [40]. Thus, solubilization or enzymatical degradation of oils which may be influenced by the oil composition seemed to mainly control the vehicle clearance rate [40] (**Fig. 3**). Furthermore, phagocytosis and uptake of small oil-droplets by the

lymphatic system was discussed to contribute on the vehicle disappearance [41]. For oil-based solutions, the overall drug absorption rate is described to follow first order kinetics [42]. The phase transfer of the API from the oil to the aqueous tissue fluid is assumed to play a major role in the release process [29] (**Fig. 3**).

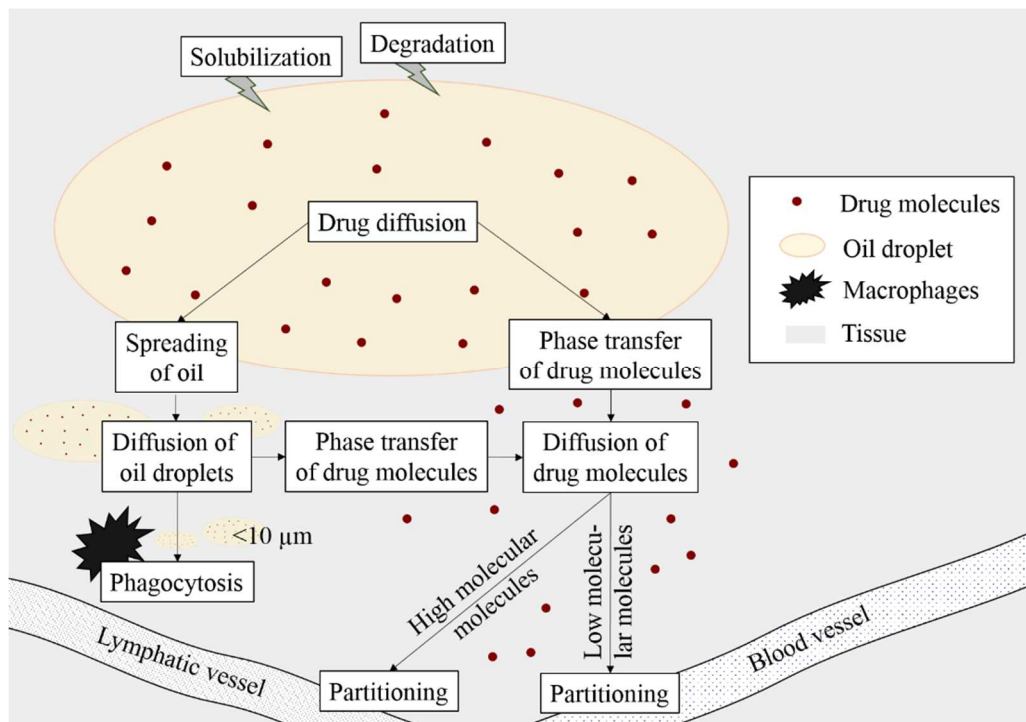


Fig. 3 Processes of drug delivery from oil-based solutions [29,38,40].

Thus, increased drug lipophilicity should not only sustain drug transport through the tissue, according to *Kadir et al.* [31], but also the vehicle to tissue fluid transfer. Indeed, prolonged drug absorption was shown by increasing the drug lipophilicity [43,44]. Moreover, the vehicle viscosity could theoretically influence the drug diffusion processes of dissolved drug molecules. However, the viscosity was found to be negligible for the drug absorption rate [42]. Prolonged drug absorption was shown with lower drug concentration in the vehicle (corresponding to a higher vehicle volume) in accordance to the Fick's law [45]. In addition, the shape of the oil-based depot, which is influenced by the interfacial tension, the physiology of the injection site, the injection volume and technique (e.g. speed), and body movement, impacts the drug diffusion processes [42,46,47]. Beside drug diffusion into the blood vessels, small drug-containing oil droplets are described to be cleared to lymphatic vessels available in the s.c. tissue [29,46,47]. Since the flow in the lymphatic system is slower than in the venous system, a second drug depot is built in the lymphatic system that release the API over a prolonged period of time to the system [47-49]. The drug uptake into the lymphatic system is nevertheless described to be less pronounced and occur mainly for very lipophilic and large molecules [29,48]. In general, the risk of residual lipophilic API that is not absorbed in the therapeutic time is lower for oil-based formulations than for aqueous MCSs [29]. The reason is that the API is kept dissolved in the oil which stays longer at the

injection site than water [29]. For extremely lipophilic APIs (e.g. perphenazine decanoate) with very high affinity to oils, the vehicle disappearance can be the release-controlling step [40]. In this case, degradation of the oil-based vehicle can influence the *in vivo* performance [47]. Compared with oil-based solutions, the drug release from oil-based MCSs is characterized by an additional step: the API dissolution (**Equation 2**). Drug release of oil-based MCSs is less often described in the literature, compared to aqueous MCSs and oil-based solutions. An oil-based MCSs might be an option when aqueous MCSs show an incomplete release within the therapeutic relevant time [29].

Application of injectable oil-based solutions and aqueous and oil-based MCSs

Examples of oil-based drug solutions are listed in **Tab. 2**. Whereas numerous i.m. and s.c. injectable aqueous MCSs are marketed, i.e. NPH insulin, vaccines (influenza virus antigen), or contraceptive steroids (**Tab. 4**), oil-based MCSs are rarely to find. Solganal® is a sesame oil MCS of aurothioglucose used in humans. Posilac® containing zinc bovine growth hormone dispersed in sesame oil is one of the most frequently sold veterinary product [38]. Furthermore, injectable oil-based MCSs are often used in earlier phases of drug development for first efficacy tests.

Tab. 2 I.m. and s.c. injectable oil-based drug solutions which are commercially available in Germany [13].

Products (German trade name)	API	Composition of oil-based vehicle	Dose interval in weeks
Androcur®-Depot	Cyproterone acetate*	Castor oil, benzyl benzoate	2
Faslodex®	Fulvestrant*	Castor oil, benzyl benzoate, ethanol, benzyl alcohol	4
Noristerat®	Norethisterone enanthate*	Castor oil, benzyl benzoate	8-12
Testoviron®-Depot	Testosterone enanthate*	Castor oil, benzyl benzoate	2-3
Nebido®	Testosterone undecanoate*	Castor oil, benzyl benzoate	2
Rheumon® i.m.	Etofenamate	Medium chain triglycerides	-
Flupentixol-neuraxpharm®	Flupentixol decanoate	Medium chain triglycerides	2-4
Ciatyl-Z® Depot	Zuclopenthixol decanoate	Medium chain triglycerides	2-4
Testosteron-Depot Jenapharm®	Testosterone enanthate*	Peanut oil	2-4
Lyogen® Depot	Fluphenazine decanoate	Sesame oil	2-4
Haldol®-Janssen Decanoat	Haloperidol decanoate	Sesame oil, benzyl alcohol	4

* API with a steroidal chemical structure

1.2.2 Organogels

General aspects and considerations for preparation

In principle, organogels can be considered as thickened formulation versions of oil-based MCSs or solutions (or, in a wider sense, of emulsions). Organogelators are added to oil-based MCSs or solutions mainly for two reasons: to reduce physical instabilities (sedimentation, aggregation) of

oil-based suspensions and to prolong the drug release of oil-based MCSs or solutions [50-52]. For the parenteral application, injectability and syringeability are crucial and must not be lost with increasing vehicle viscosity. Generally, most gels show a tremendous viscosity decrease under mechanical stress due to the breakdown of the organogelator network. This effect can be used advantageously to inject the formulations.

“...the colloid condition, the gel, is easier to recognize than to define”, is an often used cite of *D. Jordon Lloyd* [53] to describe the difficulty of defining a gel. Various gel definitions have followed and since today, they differ more or less from one literature source to the other. *Vintiloiu and Leroux* [54] describe gels as a semi-solid material containing low concentrations of gelator molecules that self-assemble in the presence of an appropriate fluid into an extensive mesh network. In the strict sense, organogels include self-assembled gelator molecules in a matrix of lipophilic vehicle. However, the term organogel is used broader in the literature. Some organogels also contain water beside gelator and lipophilic fluid [55,56]. These systems can be distinguished from hydrogels by the predominant lipophilic continuous phase [54]. The molecular structure of potential gelators and the preferentially gelled solvents is difficult to predict. Screening of molecules and solvents is necessary to find suitable gelling systems because many factors influence the organogelator aggregation [54]. The balance of the gelator's solubility and insolubility in the given fluid plays an important role in the fiber formation and prevents phase separation [54]. A good solvent is not gelled because the gelator-solvent interaction is too strong [57]. The solvent polarity and nature of the solvent molecules influence the shape of the gelator aggregates [58,59]. Vehicles for organogels are e.g. aliphatic and aromatic hydrocarbons, alcohols, silicone oil, dimethyl sulfoxide, and vegetable oils [57]. Sometimes additives i.e. co-surfactants are included, which can influence the gelation [60,61]. As abovementioned, anhydrous and water-containing organogels have been studied [54]. The absence of an aqueous phase is advantageously for APIs, which are unstable in water and reduce the risk of microbial contamination [57].

In contrast to hydrogels, organogels contain mostly low-molecular weight gelators [57] (**Fig. 4**). Whereas macromolecular organogelators interconnect via chemical, covalent or physical interactions, low-molecular weight organogelators are solely linked by physical attractions [54]. Attractive physical forces for gelation in non-aqueous vehicles are hydrogen bonding, van der Waals forces, π -stacking, electron transfer, solvophobic effects and metal coordination bonds [54,57,61]. Hydrophobic attractions, a major driving force for hydrogel formation, are either not operative or of minor importance in many organic liquids [61]. Organogelators self-assemble into various aggregates like rods, worm-like chains, tubules, ribbons, fan-like structures, fibres, and platelets [57]. Structural properties of the organogelator, i.e. functional groups, polarity, rigidity, and steric effects can influence the tendency of molecule aggregation and dictate the self-assembly and nature of gelator aggregates [54,57].

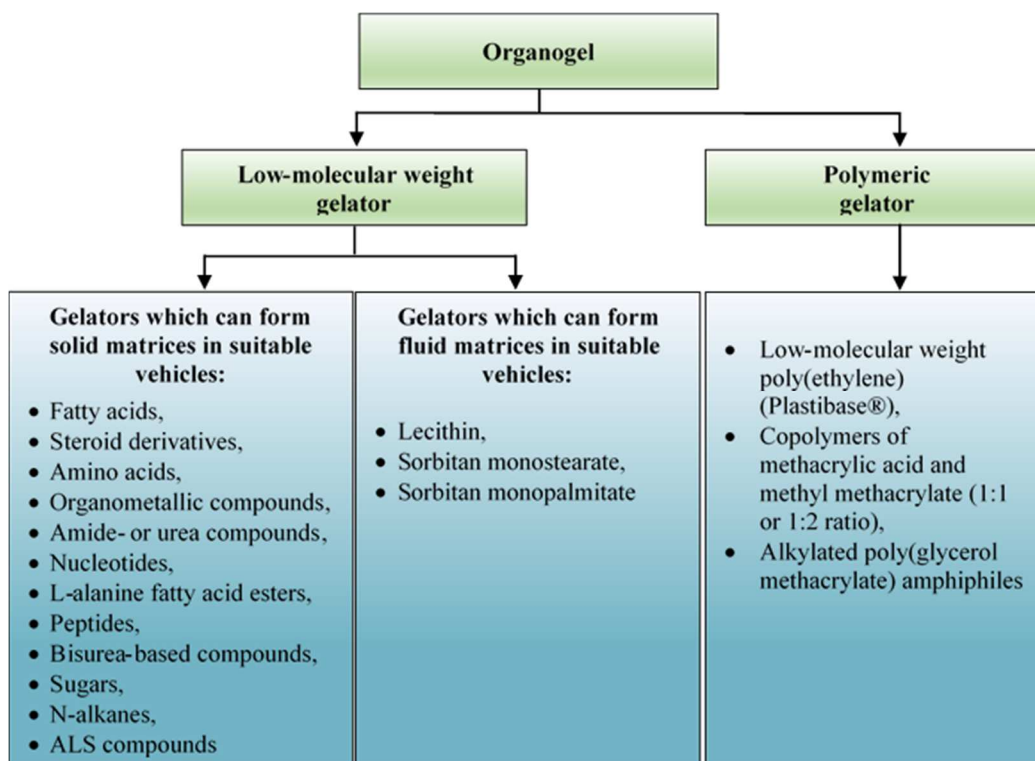


Fig. 4 Overview about organogelators [54,57,61].

Low organogelator concentrations of less than 15% are usually needed [54]. Very low gelator concentrations of 0.1% are necessary using sugar-derived supergelators [62]. The organogelator aggregates prevent the flow of organic solvent due to surface tension and, thus, lead to solvent gelation [54,57]. Low-molecular weight organogelators can be further divided into solid- and fluid-matrix gelators [61]. The resulting organogels of both types differ in their physical properties and kinetic behavior [54]. Solid-matrix organogels exhibit permanent solid-like networks in which the junction points are spatially extended (pseudo)crystalline microdomains [61]. They are obtained through a sharp sol-to-gel phase transition at a specific temperature [61]. The gels are usually prepared by dissolving the gelator in the hydrophobic vehicle at higher temperature. Thereafter, gelator-solvent affinity is decreased upon cooling, resulting in gelator self-assembling [54]. The gelator aggregates of solid matrices grow mostly uni-dimensional to fibers or rarely two-dimensional to microplatelet structures [61]. Furthermore, chirality of organogelators effects the growth and stability of fibrillar networks [63]. Fluid-matrix gels have transient networks in which junction points are most often simple chain entanglements or regionally limited organized microdomains [54,61]. Additional kinetic features such as chain breaking/recombination and dynamic exchange of gelator molecules with the bulk liquid may occur [54,61]. Fluid-matrix gels are prepared by suspending an amphiphilic molecules in mostly water, but rarely other solvent [63]. The surfactant molecules form reverse micelles aggregating into cylindrical structures that immobilize the solvent [54]. Organogelator chirality is described to be less important [54]. In contrast to solid-matrix gels, fluid-matrix organogels do not aggregate into higher order. The

formed organogels exhibit a “worm-like” or “polymer-like” network [54]. Thus, solid-matrix gels are described to be more robust than fluid-matrix gels [54,61].

The transition from a high viscous oil-based liquid to an organogel, is measurable by a simple visual test: When the reaction vessel is inverted and the sample does not flow, gelation is reached [57]. More objective measurement techniques include the falling drop and rheological methods [65]. When gelation is obtained by temperature changes, differential scanning measurement or hot-stage light microscopy for large organogelator aggregates can be used. Whereas the two latter methods analyze the point at which gelator aggregates are melted or no longer microscopically visible, the falling drop or rheological methods measure the flow of samples [61]. Thus, the sol-gel transition point can vary between the measurement methods. The rheological determination is described to be the best method to investigate the sol-gel transition: The system is gelled when the elastic modulus is higher than the viscous modulus [61,65] (**Fig. 5**). Furthermore, rheological measurements enable the characterization of the viscoelastic behavior of gels which may serve as an indicator for their physical stability [54,63].

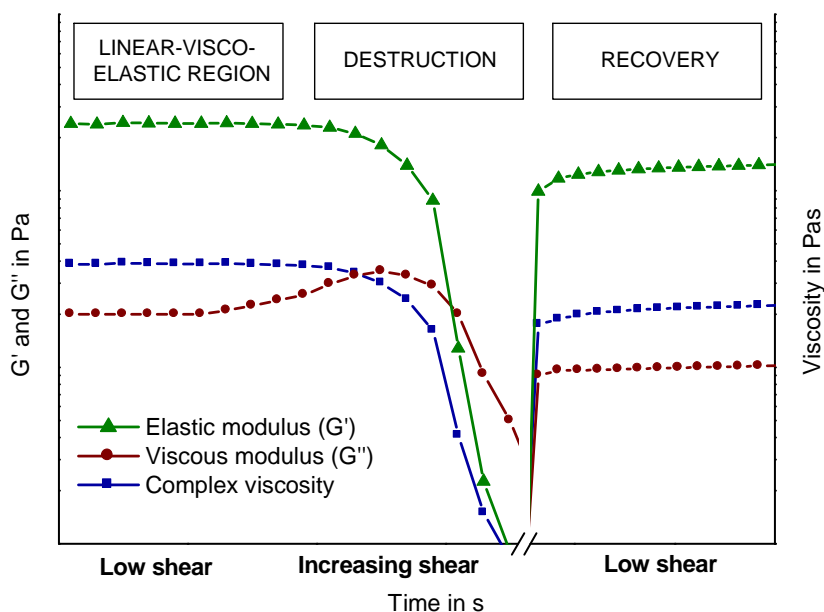


Fig. 5 Idealized rheological measurement profile of organogels at low/non-destructive shear stress, amplitude sweep, and low shear after destruction using an oscillatory test at constant frequency.

For the development of organogels as drug delivery systems, different organogel characteristics have to be considered. First, organogels are often prepared using elevated temperatures which can lead to degradation of thermolabile APIs [66]. Moreover, storage of organogels at high temperature could lead to gel network degradation due to the temperature-dependence of gel formation. Shrinkage of gel network during storage is a further typical unfavorable property of many gels that can lead to leakage of lipophilic fluid. Less literature is found about the drug-organogelator interaction [57]. The API can impede the interaction between organic solvent and organogelator,

which is essential for robust gel formation. Thus, possible interfering effects of the API on the gelator network have to be investigated.

***In vivo* release and pharmaceutical application**

So far, organogels are mainly studied and used in the chemical and technical industry, i.e. for enzyme immobilization for biocatalysis, temperature sensors, flatbed displays, and oil spill recovery [57,61]. Only a few organogels have been investigated as drug delivery systems, primarily in the field of dermal or transdermal drug delivery [54]. Rarely, oral or transmucosal (rectal, buccal, transnasal) organogels have been studied [64,67-69]. Furthermore, a few authors analyzed organogels as injectable drug delivery systems [50,51,60,70,71]. Because the research in organogels is not focused on drug development, many questions about organogels on the subject of pharmaceutical suitability are still unsolved [54]. One aspect is that the structural and physicochemical organogel properties are frequently well investigated, but the impact of drug incorporation on organogel characteristics is rarely described in the literature [57]. Moreover, less knowledge is found about the drug release mechanism and biocompatibility of organogels.

Basically, organogels form a depot at the injection site [57,60]. Enzymatical degradation by esterases and lipases should be one of the major factors that control the organogel disappearance from the injection site, comparable to oil-based vehicles without organogelators [71]. Furthermore, solubilization of the organogel matrix was found to cause the disappearance of organogels containing non-ionic surfactants [57,60]. Thus, organogels including surfactants were cleared fast (within days) due to penetration of interstitial fluid into the surfactant tubules that result in the emulsification and gel degradation [60,72]. Longer retention time of organogels was shown by *Gao et al.* [50]. The authors studied biodegradable organogels containing the contraceptive steroids levonorgestrel (LNG) and 17 α -ethinyl estradiol (EE) in a matrix of glyceryl fatty acid ester and derivatized vegetable oil. The respective organogels stayed relatively long at the s.c. injection site (5-6 weeks) and were able to prolong the drug efficacy compared to oil-based formulations without organogelators. The organogel degradation was assumed to control the efficacy duration. As long as the organogel matrix is persistent at the injection site, diffusional processes in the organogel matrix and phase transfer from the lipophilic vehicle to the interstitial fluid might influence the release of dissolved API from organogels. These processes are in accordance to the release mechanisms described for oil-based solutions (**section 1.2.1**). Since the viscosity is significantly higher in organogels, diffusional processes in the oil-based matrix should be decelerated, increasing their impact on drug release. For organogels containing suspended API, drug dissolution is necessary in the first step. If drug diffusion is the main rate-limiting step in drug release from organogels containing undissolved API, the mathematical models of release kinetics can be derived from **Equation 4**.

$$M_t = A \cdot \sqrt{D \cdot (2c_o - c_s) \cdot c_s \cdot t}$$

Equation 4 Higuchi equation, M_t = cumulative amount of released drug at time t , A = interfacial area of drug delivery system to the surrounding fluid, D = diffusion coefficient in the drug delivery system, c_s = API solubility in the drug delivery system, c_o = initial drug concentration, t = time [73,74].

However, for the correct use of Higuchi's equation and its derivations, several conditions must be fulfilled, i.e. constant shape of the semi-solid matrix and sink conditions [73,74]. It is often described in the literature that perfect sink conditions are not given in s.c. or i.m. tissue [75]. After drug release, drug transport through the tissue is assumed to be comparable with the mechanisms described for oil-based solutions and MCSs (**section 1.2.1**). Overall, there is a great potential for using organogels as controlled drug delivery systems, but more studies are needed specifically focusing on pharmaceutical aspects to give way to a broader pharmaceutical acceptability [50,54,57].

1.2.3 Biodegradable polymeric particulate systems – Poly(n-butyl-2-cyanoacrylate) (PBCA) and poly(D,L-lactid-co-glycolide) (PLGA) particles

General aspects and considerations for preparation

Micro- and nanoparticles are classified into capsules and spheres. Capsules consist of a polymer shell enclosing a core which is filled with i.e. gas or liquid. If the API is encapsulated in the core surrounded by a release rate-controlling, drug-free polymer shell, the capsules are called reservoir systems [74]. Reservoir systems enclose dissolved or dispersed API. Spheres consist of a polymer matrix. If they contain dissolved API (homogenously) distributed in the matrix, the spheres are called monolithic solution. When the API is dispersed in the matrix in concentrations that exceeds the drug solubility, the spheres are termed as monolithic dispersions [74]. In addition, the API can be adsorbed on the surface of spheres and capsules [76]. To find the optimal polymeric particulate system and preparation method, the following questions should be answered [17,23]:

- Which drug release rate meets the therapeutic drug concentration?
- What mass of polymer can be administered per unit?
- What are the API properties (pK_a , lipophilicity)?
- Are there drug-polymer interactions (drug-induced polymer degradation, e.g. drugs with amine groups in PLGA) or API instabilities (oxidation, humidity) expected?

The biggest advantage of using biodegradable polymers is their degradation during or shortly after the application that avoid surgical removal [77]. PBCA and PLGA are frequently used biocompatible and biodegradable polymers for particle preparation [23,78,79].

Various preparation methods are described for micro- and nanoparticles which can be divided into techniques using preformed polymer as starting material (examples are mentioned in **Tab. 3**) or techniques starting with a precursor/monomer (i.e. suspension, emulsion, interfacial

polymerization) [7,23]. The preparation of polymer particles can be challenging with regard to the following issues [7,17,23]:

- The use of organic solvents, which must be removed, is often essential. Costs and requirements of emission to environment must be considered. The toxicity of the solvent and the residual solvent concentration in the particles is important for operators and patients.
- Development of a robust and reproducible process which can be up-scaled is required, since a strong influence of process conditions on the final product is often observed.
- A negative impact of the manufacturing process on the API activity must be avoided (e.g. temperature, solvent, pressure).
- Lyophilization is frequently necessary to ensure storage stability.

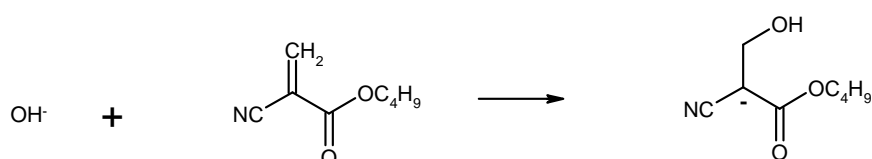
The preparation of PBCA and other poly(alkylcyanoacrylate) (PACA) particles have been intensively investigated and a large number of preparation methods are described [78,80-83]. One process to prepare PBCA nanospheres is **anionic emulsion polymerization**. For emulsion polymerization, the monomer solution is emulsified in the continuous phase, frequently water, in which the monomer is (scarcely) insoluble. Monomer droplets are formed in the continuous phase under agitation (i.e. stirring) [84]. If an emulsifier is added to the continuous medium in concentrations above the critical micelle concentration (CMC), the monomer can also be enclosed in these micelles [84]. The course of emulsion polymerization has been intensively discussed, mainly with regard to radicalic emulsion polymerization. The theories of *Smith, Ewart* and *Harkins* [85,86] describe the fundamentals of the process [84]. The authors postulated that the polymerization is primarily initiated in the monomer-swollen micelles which are present in a large number (micelle nucleation, interval I). The primary particles (nuclei) grow by monomer uptake from the continuous phase. The growing particle surface is stabilized by emulsifier leading to dissolution of emulsifier micelles. The nucleation phase is terminated when no more micelles are available (below CMC) [87]. Further monomer molecules diffuse from the monomer droplets to the growing particles. During this phase, the polymerization rate should be constant (interval II). Due to shrinking of monomer droplets, vacant emulsifier molecules diffuse to the growing polymer particles surface [87]. In the last phase (interval III), when all monomer droplets are disappeared, the monomer concentration in the reaction loci continuously decreases causing deceleration of the polymerization rate [87]. In contrast to the described processes of conventional emulsion polymerization, monomer droplets compete for initiators with emulsifier micelles in mini/microemulsion polymerization because small monomer droplets are available in a high number [88]. *Fitch, Hansen, Ugelstaad et al.* [89,90] assumed that the emulsion polymerization is initiated in the aqueous phase by reaction of dissolved monomer molecules with water-soluble initiator if the emulsifier concentration is below CMC. Over time, primary particles precipitate in the continuous phase (homogenous nucleation) [87].

The anionic polymerization of PBCA is shown in **Fig. 6**. The polymerization conditions influence the characteristics of resulting PBCA nanoparticles and were intensively investigated [78,83,91]. The pH adjustment of the aqueous phase was found to influence the particle size distribution (PSD) and molecular weight and is optimally set to pH 1-2.5 to obtain narrow distribution and small particle sizes [78,91]. Furthermore, the surfactant type and the surfactant:monomer ratio have a significant impact on the resulting PSD. Suitable surfactants are i.e. polysorbate, poloxamer, and octoxinol 9 [83,91]. The polymerization rate is additionally affected by the temperature [91].

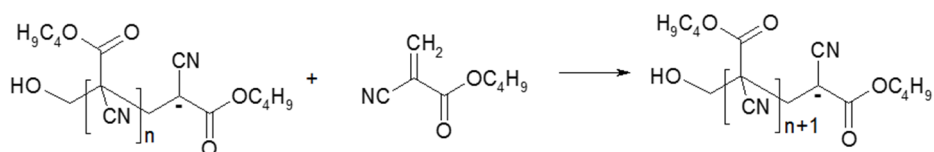
1. Autoprotolysis of water:



2. Initiation:



3. Propagation:



4. Termination:

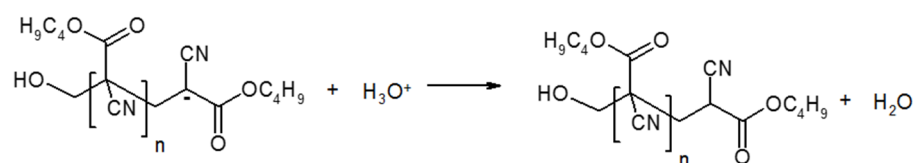


Fig. 6 Anionic polymerization of PBCA [83].

The API can be adsorbed on the surface of PACA nanoparticles, incorporated in the particle matrix, or encapsulated in the nanocapsules core. The drug adsorption could depend on the API characteristics (e.g. lipophilicity, charge), the drug concentration, the polymer material (e.g. hydrophobicity, charge), the surfactant (concentration), the electrolyte (concentration), pH, and the time point of drug addition [92-94]. Less often, direct drug incorporation into the polymer matrix of PACA nanospheres was shown [95]. Furthermore, the drug can be enclosed in the oil-based or aqueous filled core of PACA nanocapsules [96,97].

Beside PACA nanocapsules, PBCA microcapsules/ -bubbles are described in the literature [98,99]. They consist of a PBCA nanoparticle shell that surrounds an air- or partially liquid-filled core. *Schmidt et al.* [98] described the preparation of air-filled microcapsules from PBCA nanoparticles in dependence on various preparation parameters. In addition, various other materials have been investigated to prepare microbubbles [76]:

- Shell materials: lipids (e.g. phospholipids), proteins (e.g. albumin), sugars, polymers
- Core fillers: air, perfluorocarbons
- Liquids that partially fill the core: soybean oil, coconut oil

The API, which is adsorbed on or interact with the capsule surface, is incorporated into the capsule shell or included by dissolution in a liquid that partially fills the core [76].

Emulsion solvent evaporation/extraction preparation is one of the most often used methods to prepare polymer particles from pre-formed polymers and is frequently used to produce PLGA microspheres. First, a polymer solution is prepared in a suitable solvent (e.g. methylene chloride or ethyl acetate) and is emulsified into a continuous phase (frequently water) using impeller or static mixing, extrusion, membranes, sonication, electrostatic dripping, jet excitation, or other appropriate emulsification techniques [7]. The continuous phase contains low emulsion stabilizer concentrations (surface-active or viscosity-increasing agents) [7,100]. Poly(vinyl alcohol) (PVA) is mostly used as stabilizer due to the very good PVA/PLGA interaction [23]. After emulsification, the solvent is extracted from the dispersed phase by the continuous phase and then optionally evaporated using elevated temperature or reduced pressure. The polymer solvent must be slightly soluble in the continuous phase to enable solvent partitioning into the continuous phase and thus, polymer precipitation. The solvent extraction can be performed in one or two steps [100]. The combination of solvent extraction and evaporation is used to reduce the volume of continuous phase which is necessary for complete solvent dissolution and/or to accelerate the particle formation [100]. The resulting polymer particles are separated from the continuous phase by filtration or centrifugation followed by washing and drying under ambient conditions, reduced pressure, under heat or by lyophilization [100]. There are various methods to encapsulate lipophilic drugs during particle preparation by emulsion solvent evaporation/extraction (**Fig. 7**).

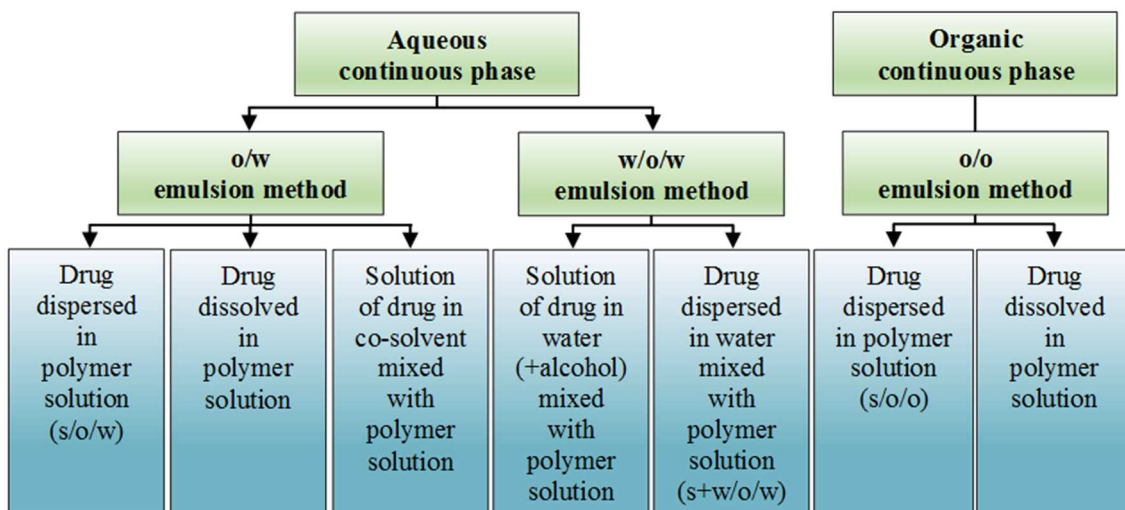


Fig. 7 Selected examples of emulsion solvent evaporation methods for lipophilic drugs [23,101].

Factors, which can influence the drug encapsulation efficiency, the particle morphology and size and, consequently, the drug release are summarized in **Fig. 8**. To ensure injectability, the prepared microparticles should have a particle size of less than 100-250 μm [1,23].

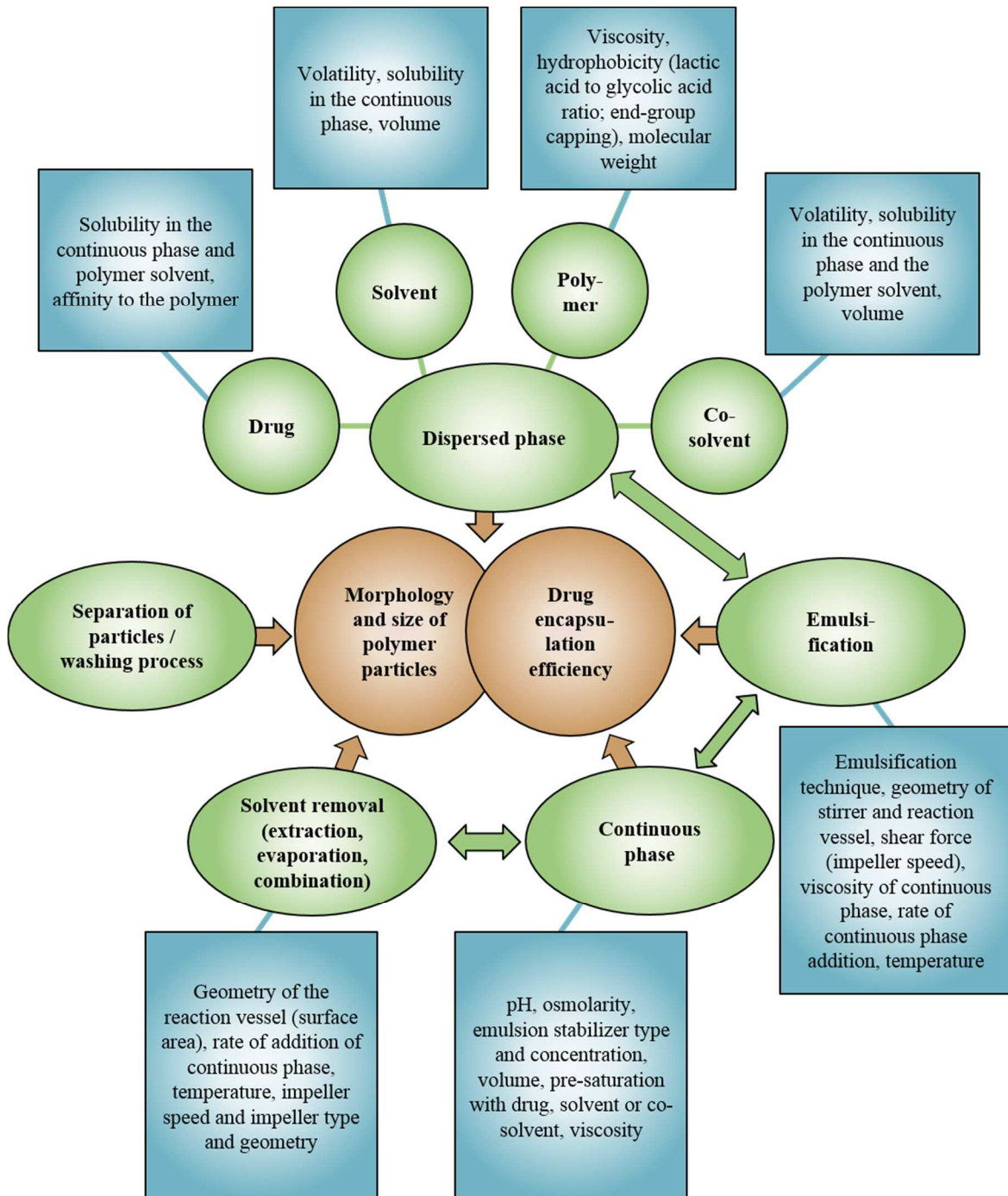


Fig. 8 Preparation parameters that can have an impact on the morphology and particle size of the resulting polymeric particles as well as on the drug encapsulation efficiency [23].

Stabilization of biodegradable drug delivery systems

Due to their susceptibility against hydrolytic degradation, biodegradable PBCA and PLGA drug delivery systems can be highly sensitive to humidity during storage. Although good long-term

stability was found for PBCA and other PACA particles in aqueous dispersion at low pH [102,103], drug diffusion from the particles into the aqueous dispersion media is possible during storage. In addition, water ingress into drug-loaded polymeric systems could initiate drug degradation, unwanted drug dissolution and precipitation as well as diffusion processes. Therefore, lyophilization or other techniques to dry the final product are often required to guarantee storage stability. The removal of water and other solvents by freeze-drying cause variety of stresses such as formation of dendritic ice crystals, increase of ionic strength, pH changes, or phase separation which may lead to the particle destruction [104]. Thus, stabilizers are often required to protect the polymeric particles during freezing (cryoprotection) and drying (lyoprotection) processes. Typical cryoprotectants are sugars/polyols, non-aqueous solvents, polymers, proteins, surfactants, and amino acids [104]. These cryoprotectants can also be applied as potential lyoprotectants except non-aqueous solvents [104]. Immediately before the application, the polymeric particles are re-constituted in the aqueous vehicle.

***In vivo* release**

Polymeric particles represent a possibility of real drug release control using suitable polymer materials and drug formulations, i.e. constant sustained or timed drug delivery may be achievable [6]. The drug release from polymeric drug delivery systems is a complex process that depends on the API and carrier characteristics as well as the environmental conditions (**Fig. 9**).

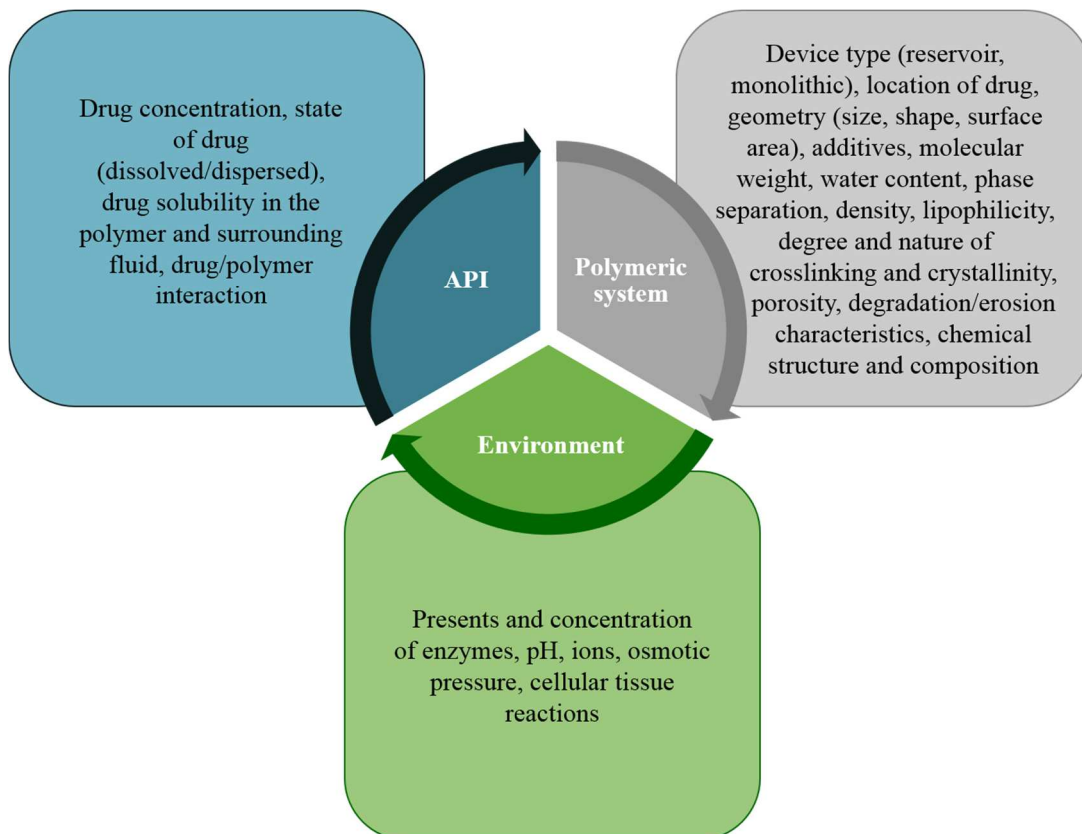


Fig. 9 Factors that influence the drug release from polymeric particulate drug delivery systems [23,74,105].

Upon contact with tissue fluid, various processes are initiated sequentially or in parallel that can influence the overall release pattern (**Fig. 10**). To understand and manipulate the drug release, it is important to know the rate-limiting step(s) in the process [74]. Biodegradation and bioerosion processes are involved in the biological elimination of polymeric systems from the injection site. Biodegradation is defined as polymer chain cleavage within a biological system. The polymer chain is split into oligomers or monomers [105]. The *in vivo* degradation is mainly caused by hydrolytic chain scission reaction or by active enzymatic reactions [77]. The rate of hydrolytic reaction depends on the polymer type (type of chemical bonds), co-polymer composition, the ability to take up water, and the environmental pH [77]. PBCA and PLGA carry chemical bonds that can be cleaved by hydrolysis [106]. On the other hand, bioerosion is referred to the loss of polymer bulk material within an organism including monomers, oligomers, parts of polymer scaffold and bulk [105]. If the polymer degrades slowly by random chain cleavage of ester bonds throughout the polymer, the erosion process is called homogeneous or bulk erosion [105]. If the polymer is carried off on the surface of system, the mechanism is termed as heterogeneous or surface erosion [105]. Two degradation pathways are described for PACA. Initial *in vitro* studies of PACA degradation indicated that formaldehyde and cyanoacetate ester are formed by disconnecting from the polymer chain under water addition based on inverse Knoevenagel reaction [107]. With regard to the toxicological potency of these products, the toxicity of PACA particles has been intensively discussed [108,109]. *Lenaerts et al.* [110] showed that poly(isobutylcyanoacrylate) particles mainly degraded by ester hydrolysis which is catalyzed by enzymes.

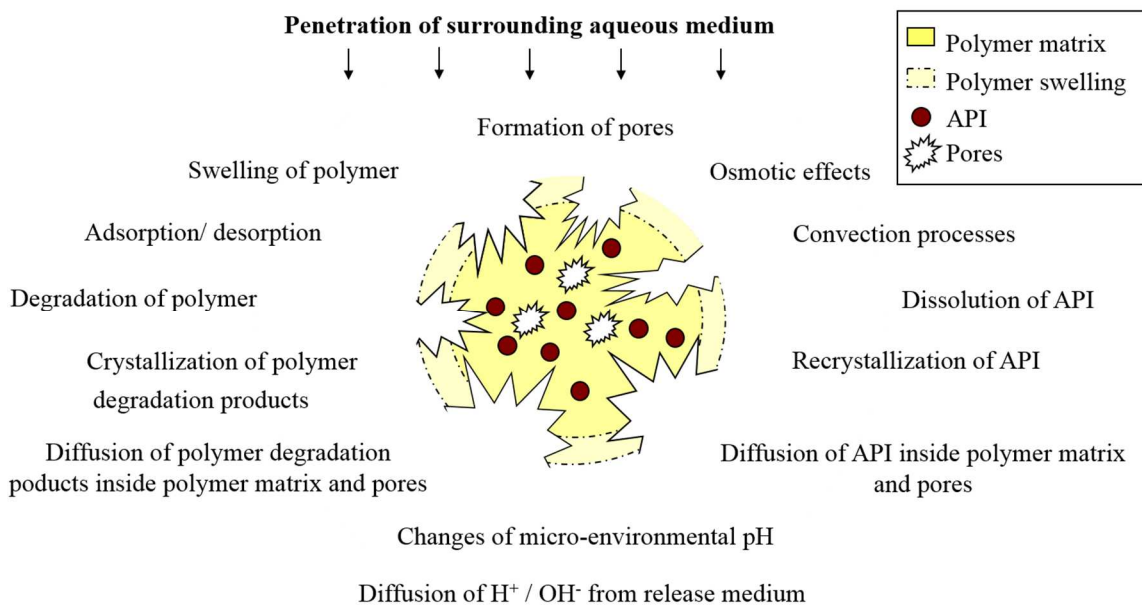


Fig. 10 Processes that can occur during drug release from polymeric drug delivery systems on the example of a monolithic device [74,105].

A strong influence of esterases on PBCA nanoparticle degradation, especially at pH 7 and 8, was also shown by *Scherer et al.* [111]. It is assumed that the ester side chains are hydrolyzed by esterases under formation of alcohol and water-soluble polycyanoacrylic acid derivatives [79]. These degradation products are less toxic. Furthermore, the toxic effect correlates with the polymer degradation rate: Slower degradation avoid high local concentration of degradation products and could therefore reduce adverse reactions at the injection site [112]. The degradation rate depends on the environmental conditions (e.g. pH, esterase concentration) and the alkyl side chain of the polymer [111,112]. *Kante et al.* [113] found that PACA nanoparticles induced cellular damage only at relatively high concentrations. A median lethal dose of 230 mg/kg was determined after i.v. injection of PBCA nanoparticles in mice [114]. Furthermore, neither necrosis nor irritation symptoms were observed 24 h after s.c. injection of PBCA nanoparticles at 10 mg/ml in mice [114]. Furthermore, the degradation of air-filled PBCA microcapsules was investigated previously [99]. Degradation of the PBCA nanoparticles wall leads to microparticles' burst. The degradation rate was found to depend on the particle wall thickness and the molecular weight of polymer. PLGA bears hydrolytically labile aliphatic ester linkages in their backbone and is cleaved into shorter chain alcohols and acids in contact with surrounding aqueous fluid [115]. The enzyme influence has been controversial discussed [113,116,117]. The degradation products lactic and glycolic acid are two naturally occurring substances in the human body. Thus, PLGA is intensively used for the preparation of biodegradable polymeric systems [106]. However, the acidic degradation products are known to autocatalyze further polymer degradation by decreasing the microclimate pH [115]. This phenomenon results into accelerated drug release [115]. Moreover, the acidic pH can cause degradation of acid-labile APIs [23]. Due to the relatively fast degradation, the bioerosion of nanosized PACA matrix systems is interpreted as surface erosion [118]. The bioerosion of microsized PLGA matrix systems is commonly interpreted as bulk erosion process, because water influx into the polymer systems is rapid compared to the subsequent polymer chain cleavage [119].

Mathematical modeling of drug release

Mathematical models including empirical and mechanistic realistic theories have been developed to interpret and understand drug release from polymeric systems [35]. Empirical models are only descriptive and do not characterize the exact physical processes. They are used as an approach for the evaluation of drug release results and to get a hint for the underlying release processes [105]. Empirical models include the Cooney and Hopfenberg model as well as the frequently applied Peppas equation [120-123]. In contrast, mechanistic models are based on the description of real effects involved in drug release such as dissolution, diffusion, or erosion [105]. Drug diffusion is often the most important or one of the major processes in drug delivery from polymeric systems. Derived from the Fick's laws (**Equation 3**) several mechanistic mathematical models were

established to describe diffusional processes in reservoir or matrix systems [74,124-126]. Other models consider drug diffusion in combination with polymer swelling [127]. Furthermore, the erosion/degradation of polymeric matrix alone or in combination with diffusional drug transport was investigated by several authors [128-130]. Finally, Monte Carlo simulation is applied to model the complex interplay of the various processes in drug release [131,132]. Using this approach, further processes such as the crystallization of polymer degradation products and microclimate pH effects can be considered. The drug release from PLGA microparticles with respect to drug diffusion, degradation, bulk erosion, porosity and the effect of accumulating acidic drug products was intensively analyzed using mathematical modeling [115,133,134].

Application

PLGA is approved by the US Food and Drug Administration agency (FDA) for the use in humans [23]. Thus, several PLGA particle products are commercially available on the market (**Tab. 3**).

Tab. 3 PLGA microparticles on the market [13,23,135-138].

Drug	Polymer	Trade name (Country)	Company	Dose interval / Injection	Encapsulation technique
Leuprolide acetate	PLGA (3:1)	Enantone® (DE)	Takeda	1 month, s.c.	w/o/w emulsion solvent evaporation
Octreotide acetate	PLGA (55:45)	Sandostatin® LAR® (DE)	Novartis	1 month, i.m.	Coacervation
Risperidone	PLGA (75:25)	Risperdal® Consta® (DE)	Janssen-Cilag	2 weeks, i.m.	o/w emulsion solvent extraction
Triptorelin acetate	PLGA (1:1)	Decapeptyl® (DE)	Ferring	1 month, s.c. or i.m.	Coacervation
Triptorelin pamoate	PLGA	Trelstar® (US)	Watson	1,3,6 months, i.m.	Hot extrusion cryogenic grinding
Buserelin acetate	PLGA (1:1)	Suprecur® MP (JP)	Mochida, Sanofi	1 month, s.c.	Spray drying
Lanreotide acetate	PLGA	Somatuline® LA (UK)	Ipsen-Beaufour	7-14 d, i.m.	Coacervation
Somatropin	PLGA	Nutropin® (US)	Genen Tech	2-4 weeks, s.c.	s/o cryogenic spray-congealing method
Naltrexone	PLGA (75:25)	Vivitrol® (US)	Alkermes	1 month, i.m.	o/w emulsion solvent extraction

PBCA and poly(isobutylcyanoacrylate) nanoparticles have been intensively studied as carrier systems for i.e. anticancer drugs, therapeutics for brain delivery, vaccines, peptides, gene therapeutics, antiretroviral agents, and ophthalmics [92-96,139-141]. Dermabond® is an FDA approved topical skin adhesive for surgeries containing 2-octyl cyanoacrylate [142]. In general, air-filled microcapsules prepared by various materials were developed as ultrasound contrast agents. Approved products are Albunex® and Optison™. More recently, gas- or liquid-filled microcapsules were investigated as drug or gene delivery systems i.e. in tumor, thrombosis, or inflammation therapy [76]. The API can be released after microcapsules' destruction i.e. using

ultrasound as trigger. So far, PBCA microcapsules have not been studied as drug delivery systems. The carrier systems offer a very interesting opportunity for timed or targeted drug release.

1.3 Combined drug delivery

Fixed-combination drug products are used to profit from the synergistic pharmacological effect of two or more APIs given together and improve the compliance by simplification of therapy regime [143]. Pharmacokinetic interaction of APIs should usually be avoided unless a synergistic effect is preferred [143]. Injectable contraceptives containing two steroids are typical examples for drug combinations. Both steroidal APIs are dissolved or dispersed in one vehicle. Combining APIs in one drug delivery system can be challenging if:

- Co-incorporation does not provide desired pharmacokinetics of each API (interaction).
- Co-incorporation of APIs with different physicochemical properties is not feasible.

Based on these considerations, multi-compartment or combinations of two or more drug delivery systems can be developed. An overview about currently investigated injectable multi-compartment or combined nano-, micro, and macrocarriers is given by *Zhang et al.* [144].

1.4 S.c. and i.m. injectable drug delivery systems for steroids

1.4.1 General aspects

Steroidal APIs are commonly lipophilic compounds interacting with intracellular steroid receptors. Steroidal APIs include mineralo-, glucocorticoids, sex hormone receptor agonists and antagonists and are used i.e. as antiinflammatory, antiallergic, analgesic, diuretic, anti-estrogenic/cytostatic drugs, for fertility control or hormone replacement therapy [13]. Their predominately insufficient water solubility has to be considered for drug manufacturing. Thus, injections of steroidal APIs are frequently manufactured as oil-based solutions or aqueous MCSs (**Tab. 2**, **Tab. 4**). One major group of steroidal i.m. and s.c. injections are contraceptive drugs.

1.4.2 Parenteral s.c. and i.m. injectable contraceptives

Several clinical studies have shown poor compliance with daily oral contraceptives which can lead to unintended pregnancy and irregular bleeding pattern [145]. For instance, it has been found that about 25% of users do not take their oral contraceptives within the recommended “window of hormonal safety” and approximately 30% of young users (18-30 years) miss one or more pills per month [145,146]. Parenteral long-acting contraceptives may not only overcome these compliance issues but may also avoid daily fluctuations of hormone plasma levels which are associated with oral contraceptives. Considering these aspects, there is a high medical need for the development of various prolonged-release parenteral drug delivery systems for contraception. Two commonly used approaches of long-acting drug delivery are i.m. or s.c. injectable formulations.

Tab. 4 Commercially available long-acting injectable contraceptives [147].

Trade name (Country)	Progestin/ Concentration	Estrogen/ Concentration	Formulation	Injection
<i>Progestin-only contraceptives</i>				
Depot Clinovir® (DE)	150 mg medroxy- progesterone acetate	-	Aqueous MCS	Every 3 months, i.m.
Noristerat® (DE)	200 mg norethisterone enanthate	-	Oil-based solution	Every 2-3 months, i.m.
Sayana® (DE)	104 mg medroxy- progesterone acetate	-	Aqueous MCS	Every 3 months, s.c.
<i>Combined contraceptives</i>				
Cyclofem® (MX)	25 mg medroxy- progesterone acetate	5 mg E2 cypionate	Aqueous MCS	Every 2 months, i.m.
Mesigyna® (MX)	50 mg norethisterone enanthate	5 mg E2 valerate	Oil-based solution	Every month, i.m.
Perlutan® (BR)	150 mg dihydroxypro- gesterone acetophenide	10 mg E2 enanthate	Oil-based solution	Every month, i.m.
Anafertin (MX)	75 mg dihydroxypro- gesterone acetophenide	5 mg E2 enanthate	Oil-based solution	Every month, i.m.

Injectable contraceptives for 1 month or longer are well established and effective contraceptives [147]. It is estimated that global use of injectable contraceptives will increase to almost 40 million users by 2015 [148]. Although less often used in Europe, these formulations represent the third most common method of reversible contraception worldwide, mostly used in low-income countries in Latin America and Asia [147,148]. Thus, expensive manufacturing costs should be avoided. Compared to oral contraceptives, benefits of injectable contraceptives include [148,149]:

- Less frequent dosing
- Circumvention of first-pass effect
- Discrete method
- Reduced risk of missing the administration (e.g. for travelers, shift workers)
- Administration by physician in an adequate dose interval possible for patients who are not able to intake oral contraceptives regularly
- Administration possible for users who have gastro-intestinal absorption problems

The first i.m. injectable contraceptive was the progestin-only Depot-Clinovir® (**Tab. 4**). Progestins are synthetic progesterone-like compounds. Sayana® is the first s.c. injectable contraceptive. The s.c. MCS is equally long effective but show a slightly lower maximum plasma concentration (C_{max}) and a lower overall dose of medroxyprogesterone acetate (MPA) than Depot-Clinovir® (**Tab. 5** and **Tab. 4**). Both products show comparable minimum plasma concentration (C_{min}) after 3 months and are re-injected after that time [147,150]. However, MPA can be found in the blood circulation for 6 months or longer which can cause a delay in return of fertility [147,151]. MPA-only contraceptives have a negative effect on the bone mineral density and should not be used for the

longer term (more than two years) [152,153]. There is no oral MPA formulation (in Germany and the United States) that is recommended for the use as contraceptive. For the progestin-only Noristerat® containing norethisterone enanthate (NET-EN), the serum concentration of the active metabolite norethisterone (NET) decreases in two phases: A fast first phase is followed by a second slower phase [14]. NET levels fall below the detectable limit within 46-110 d [147]. Combined oral contraceptives containing NET esters exhibit comparable NET C_{max} than Noristerat® (**Tab. 5**).

Tab. 5 Comparison of C_{max} values of injectable and oral medroxyprogesterone acetate (MPA), norethisterone (NET), and estradiol (E2) derivatives containing contraceptives [14,147,150,153-157]. For oral contraceptives, the C_{max} was measured in the steady state. E2 C_{max} of injectable contraceptives are conspicuous high compared to oral contraceptives and are highlighted in the table (n.c. = not considered, - = not included in the drug).

Drug Product	Progestin (active metabolite)	C_{max} progestin in ng/ml (min-max range) or \pm standard deviation	Estrogen (active metabolite)	C_{max} E2 in pg/ml (min-max range) or \pm standard deviation
Depot-Clinovir®	MPA	1-6	-	-
Sayana®	MPA	1.6 (0.5-3.1)	-	-
Cyclofem®	MPA	1.1 (0.9-1.4)	Estradiol	242 (191-308)
Noristerat® (1ml)	NET	12.2 \pm 2.7	-	-
Mesigyna®	NET	3.0 (1.9-4.7)	Estradiol	428 (237-768)
Estrostep® 21 (oral contraceptive)	NET	12.7 \pm 4.1	Ethinyl estradiol	n.c.
Qlaira® (oral contraceptive)	Dienogest	n.c.	Estradiol	70.5 \pm 25.9

However, the birth control effectiveness of Noristerat® (Pearl Index: 1.4 when injected every three months, 0.6 when injected every two months) is lower than that of the oral contraceptives and Depot-Clinovir® (Pearl Index: 0.3) due to the irregular decrease of NET plasma levels in the later phase [14,153,158]. Although NET-EN is metabolized to low EE amounts, it is assumed that Noristerat® may also reduce the bone mineral density. But up to now, there are no clinical studies [14,159]. In general, amenorrhea and other irregular bleeding patterns are associated with progestin-only injectable contraceptives which often lead to discontinuation of the contraceptive regimens [147]. Different approaches are and can be used to improve the efficacy, safety and compliance of injectable contraceptives:

Combination with estrogen derivatives

First injectable contraceptives combining estrogen and progestin were developed in the 1960s to improve bleeding patterns [147]. They must be injected more frequently than progestin-only contraceptives and contain estradiol (E2) esters which generate elevated estrogen plasma levels for 2-3 weeks (**Fig. 11**). Afterwards, a rapid decline of estrogen plasma levels causes an estrogen withdrawal bleeding [151]. Due to the combination with an estrogen derivative, the overall monthly progestin doses are lower than with progestin-only injectable contraceptives (**Tab. 4**). Furthermore, slightly lower C_{max} and similar C_{min} of MPA were observed with the combined drug Cyclofem® compared to progestin-only Depo-Clinovir® (**Tab. 4**). In accordance, NET C_{max} of the

combined drug Mesigyna® is lower than of the progestin-only Noristerat® and the combined oral contraceptive. Moreover, Cyclofem® and Mesigyna® provide lower overall monthly E2 ester doses than the combined oral drug Qlaira® due to the extensive first-pass metabolism. However, the initial exogenous E2 levels of both combined injectable contraceptives are considerably higher than that of Qlaira®. In addition to the improved bleeding patterns, the estrogen supplementation was found to have a protective effect against bone mineral density loss [160]. However, estrogens are associated with other adverse effects i.e. weight gain, edema, and increased blood pressure. This is due to the stimulation of angiotensinogen synthesis leading to sodium reabsorption and water retention [161]. Furthermore, the estrogen intake increases the risk of venous thromboembolism (VTE) [162].

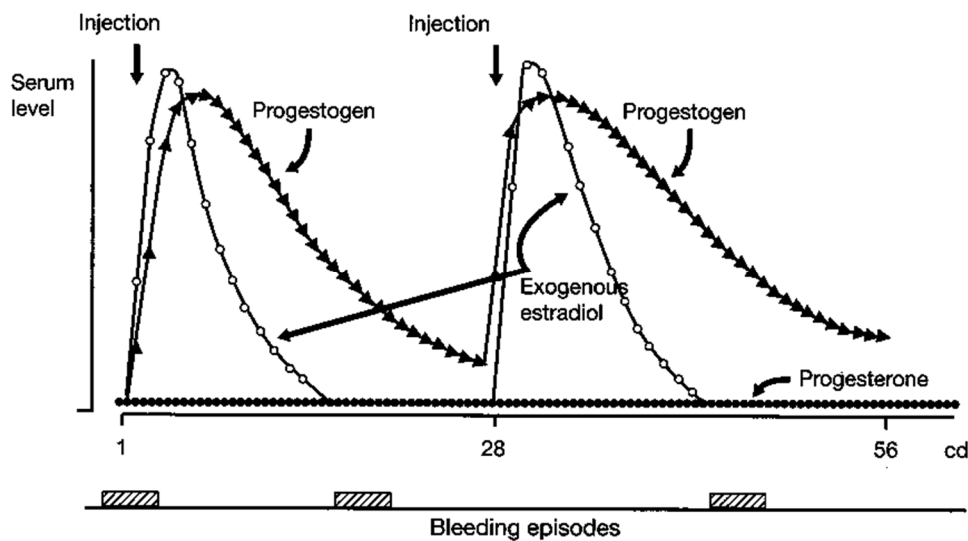


Fig. 11 Schematic pharmacokinetic and pharmacodynamic profile of combined estrogen progestin injectable contraceptives. A biphasic steroid profile is provided: The first "combined" phase is characterized by a progestin (progestogen) and estrogen increase and the second "progestin dominated" phase is shaped by decreasing estrogen levels after ca. 2 weeks (reprinted with permission from reference [147]).

Development of new steroids

The development of new progestins has been an ongoing goal to improve the compliance of steroidal contraceptives. NET-EN is a progestin of the first generation (**Tab. 4**). Structurally related to 19-nortestosterone, NET-EN bind to sex hormone-binding globulin (SHBG) leading to the competitive inhibition of testosterone and thus, increasing of free testosterone concentrations [163]. An androgenic activity of NET-EN is, however, only observed in higher and not in therapeutic dosages [14,161]. Some 17 α -hydroxyprogesterone derivatives or third generation progestins have antiandrogenic properties [161,164]. They inhibit androgen receptors, i.e. of the sebaceous glands and the hair follicles, and should therefore prevent acne and hirsutism [161].

According to naturally occurring progesterone, fourth generation progestins such as drospirenone (DRSP) provide antiandrogenic and additionally antimineralocorticoid activity. The antiandrogenic effect of DRSP is assumed to be caused by competitive binding to the androgen receptor, non-

binding to SHBG, the lack of counteracting estrogen-induced SHBG synthesis, and the suppression of androgen production [161]. Furthermore, DRSP and naturally occurring progesterone are aldosterone antagonists which increase the sodium/potassium ion and water excretion rate. Thus, they are assumed to counteract the aldosterone secretion stimulation which is caused by increased serum levels of natural estrogen during the menstrual cycle and by intake of combined contraceptives containing estrogen derivatives [161]. Unlike other progestins, progesterone and DRSP should therefore reduce symptoms which are associated with estrogen-induced water retention [161]. However, oral contraceptives containing DRSP and EE exhibited a significantly increased VTE risk [162]. The great majority of clinical studies showed a significantly higher VTE risk for the third and fourth generation combined oral contraceptives compared to the second generation (e.g. with LNG) [162]. It is controversially discussed if the VTE risk of fourth generation contraceptives is higher or the same compared to third generation contraceptives [162,165]. Furthermore, controversial results were found for the VTE risk of injectable contraceptives. Some studies suggest no increased risk, others revealed a significantly higher VTE risk compared to non-users [166-168]. The low incidence of VTE and the combination with other risk factors often impede precise risk estimates. Studies suggest that the VTE risk increases with higher overall estrogenicity of the contraceptive, but further research is needed [169].

Reduction of steroid dose

In order to optimize the safety-efficacy relationship, the World Health Organization reassessed combined injectable contraceptives and suggested a dose reduction in the 1970s [151]. Current dose optimized products are Mesigyna® and Cyclofem®. Furthermore, studies showed that products such as Anafertin® containing the half dose of estrogen and progestin are comparable effective with Perlutan® [147]. In the early 1980s, the EE dose in oral contraceptives was reduced from more than 50 µg to mainly 30 µg. Currently, contraceptives are available that contain a daily EE dose of 20 µg. The reason for this development is that estrogens were found to be associated with cardiovascular diseases, VTE, or nausea [162,170,171]. On the other hand, ultra-low dose contraceptives (equal or less than 20 µg of EE) were observed to may not sufficiently support bone formation in adolescents and may be related to irregular bleedings because the relative estrogen deficiency associated with contraceptives is not adequately compensated [172,173].

Optimized formulations

With respect to the safety-efficacy relationship, several injectable drug delivery systems have been developed that should obtain optimized control of drug release [6]. An option for the drug release improvement of injectable contraceptives is the encapsulation of contraceptive steroids into polymeric microparticles. The encapsulation of progestin and estrogen derivatives into various polymers i.e. PLGA has been studied by numerous groups [174-178]. Several authors conducted *in*

vivo studies that have shown prolonged drug release for polymeric microspheres containing steroidal drugs such as LNG, NET, EE, progesterone, and β -E2 over weeks to months [175,178-180]. Another possibility for drug release optimization is the inclusion of the contraceptive steroids into gel systems. *Gao et al.* developed organogels formulations which contain EE and LNG that show longer efficacy compared to conventional oil-based formulations [50,51] (**section 1.2.2**).

Modified schedule of administration

In the 1980s, multiphasic combined oral contraceptives were introduced with the aim to imitate the rising and falling of estrogen and progesterone during the normal menstrual cycle [181] (**Fig. 12**). This approach should result in a more physiologic course and studies indicate a better cycle control compared to monophasic combined oral contraceptives [181-183]. Furthermore, multiphasic oral contraceptives have been developed to decrease the total monthly steroid dose compared to monophasic products [181]. Combined injectable contraceptives provide biphasic steroid profiles (**Fig. 11**). However, there is a lack of more advanced multiphasic injectable contraceptive. As abovementioned, estrogen and progestin are combined in one matrix and, especially, the plasma level of the estrogen component is initially very high. Thus, there is a high need for the development of more advanced combined contraceptive. To obtain controlled drug delivery of both components, estrogen and progestin, multicompartiment or combined drug delivery systems are potential options.

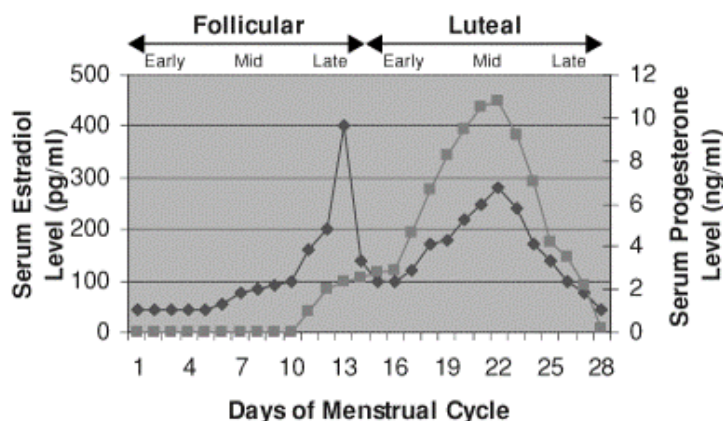


Fig. 12 17β -E2 and progesterone serum levels during a native menstrual cycle. Serum E2 concentrations are low during the first days (25- 50 pg/ml), and increases during the late follicular and early luteal phase (100-400 pg/ml), plateau during the mid-luteal phase (200-300 pg/ml), and decrease quickly to 25-50 pg/ml levels prior to menstruation. Serum progesterone levels are very low during the follicular phase (below 1 ng/ml), are highest during the mid-luteal phase (6-10 ng/ml), and then fall rapidly to levels below 2 ng/ml, prior to menstruation. The light grey line represents the E2 concentration, the dark grey line outlines the progesterone concentration (reprinted with permission from reference [184]).

1.4.3 The steroidal model APIs DRSP, EE, and ZK28

DRSP is used in contraceptives and for the treatment of diseases, disorders and symptoms associated with deficient endogenous estrogen levels in women [13,162]. The chemical structure is shown in **chapter 2**. DRSP is included in a dose of 3 mg in oral contraceptives in combination with

EE [13]. There is very little knowledge about parenteral DRSP formulations and no long-acting DRSP drug delivery system is available. EE is a semisynthetic and significantly more potent derivative of the naturally occurring steroid 17β E2 [185]. It is one of the most often used estrogens in contraceptive drugs and included in combined oral contraceptives as well as in transdermal and vaginal drug delivery systems [13]. EE exhibits a low oral bioavailability of only 45% [186]. Injectable EE drug delivery systems have been investigated but there are no marketed products available [176,180].

ZK28 is a 17β -hydroxysteroid dehydrogenase (17HSD) type 1 inhibitor. 17HSDs regulate the activity of sex hormones by redox reaction at position 17 of the steroid scaffold in many tissues [187,188]. 17HSDs catalyze the interconversions between highly active steroidal hormones, i.e. E2 and testosterone, and their corresponding less active steroidal hormones, i.e. estrone and androstenedione [187]. Recently, the research in the prognostic value of 17HSDs in breast and prostate cancer as well as endometriosis has been intensified [188]. Moreover, 17HSDs inhibitors are investigated as an approach against breast and prostate cancer [188]. In breast cancer, the reductive 17HSD type 1 activity dominates in malignant epithelial cells, while the oxidative 17HSD type 2 may be primarily present in non-malignant cells [187]. So far, suitable formulation approaches have not been investigated for 17HSD inhibitors. For first efficacy studies in the early stage of development, APIs are often included in aqueous or oil-based solutions or suspensions and injected i.m. or s.c.. The chosen dosage form can have a significant impact on the drug pharmacokinetics and may consequently influence the drug efficacy.

1.4.4 Summary

Steroids and, in particular, contraceptives are one of the most frequently used group of drugs worldwide. There is an ongoing need for the improvement of hormonal contraceptives. Since they are taken by (healthy) individuals over a very long period of time, the occurrence of undesired effects should be as low as possible. The contraceptive regimen, i.e. the progestin be used and whether a combination with an estrogen is favorable, depends on the individual medical history and requirements of the user. In general, further dose and compliance improvement of the current injectable steroidal formulations might be possible by using suitable drug delivery systems which should meet the following criteria:

- Prolonged and/or controlled drug release
- Optimal efficacy-dose relationship
- Improved side effect profile
- Self-administration

1.5 Objectives

The aim of this work was to investigate suitable i.m. and, in particular, s.c. injectable drug delivery systems for steroids. First, oil-based DRSP MCSs and DRSP organogels were characterized with regard to the physicochemical stability and the applicability. Furthermore, the pharmacokinetics of steroidal drug delivery systems have been analyzed, using the example of DRSP and ZK28. Finally, combination drug delivery systems of DRSP and EE were studied.

Oil based DRSP MCS

- Long-term chemical stability of DRSP MCSs with regard to DRSP epimerization
- Long-term physical stability of DRSP MCSs, which contain potential non-thickening stabilizing agents, in comparison to non-stabilized DRSP MCSs
- Syringeability / injectability via an autoinjector

DRSP organogels

- Rheological properties of DRSP organogels containing different organogelators
- Long-term physical stability of DRSP organogels in comparison to non-stabilized DRSP MCSs
- Syringeability / injectability via an autoinjector
- *In vitro* release of DRSP organogels in comparison to non-stabilized DRSP MCSs

Pharmacokinetics of injectable drug delivery systems for steroids

- *In vitro* release of DRSP formulations
- Pharmacokinetics of DRSP formulations
- Pharmacokinetics of ZK28 formulations
- Comparison of *in vitro* and *in vivo* results

Combined DRSP EE drug delivery systems

- Preparation and physicochemical characterization of EE PBCA and PLGA microparticles as well as DRSP PLGA microparticles
- Combinability of DRSP PLGA microparticles and EE PBCA or PLGA microparticles and investigation of the *in vitro* release
- Combinability of DRSP organogels and EE PBCA or PLGA microparticles and investigation of the *in vitro* release

References

- [1] J.C. Boylan and S.L. Nail, Parenteral Products, in: A.T. Florence and J. Siepmann (Eds.), *Modern Pharmaceutics Volume 1 Basic Principles and Systems*, Informa Healthcare, New York, 2009, pp. 565-610.
- [2] J.D. Ludwig, Parenteral dosage forms: Introduction and historical perspective, in: S. Nema and J.D. Ludwig (Eds.), *Pharmaceutical dosage forms: parenteral medications*, Informa Healthcare, London, 2010, pp. 1-6.
- [3] G.A. Brazeau, B. Cooper, K.A. Svetic, C.L. Smith, and P. Gupta, Current perspectives on pain upon injection of drugs, *J Pharm. Sci.*, 87 (1998) 667-677.
- [4] J.J. Cunningham, M.J. Kirchmeier, and S. Mittal, Formulation of depot delivery systems, in: S. Nema and J.D. Ludwig (Eds.), *Pharmaceutical Dosage Forms: Parenteral Medications, Formulation and Packaging*, Informa Healthcare, New York, 2010, pp. 158-193.
- [5] A.S. Hoffmann, The origins and evolution of "controlled" drug delivery systems, *J. Control. Release*, 132 (2008) 153-163.
- [6] J. Siepmann and F. Siepmann, Microparticles used as drug delivery systems, *Progr Colloid Polym Sci*, 133 (2006) 15-21.
- [7] N.K. Varde and D.W. Pack, Microspheres for controlled release drug delivery, *Expert. Opin. Biol. Ther.*, 4 (2004) 35-51.
- [8] M.A. Rodger and L. King, Drawing up and administering intramuscular injections: a review of the literature, *J. Adv. Nurs.*, 31 (2000) 574-582.
- [9] R.G. Strickley, Solubilizing Excipients in Oral and Injectable Formulations, *Pharm. Res.*, 21 (2004) 201-230.
- [10] B.S. Montgomery, J.P. Borwell, and D.M. Higgins, Does needle size matter? Patient experience of luteinising hormone-releasing hormone analogue injection., *Prostate Cancer Prostatic Dis.*, 8 (2005) 66-68.
- [11] S.C. Palmon, A.T. Lloyd, and Kirschm J.R., The effect of needle gauge and lidocaine pH on pain during intradermal injection, *Anesth. Analg.*, 86 (1998) 379-381.
- [12] MSD, Fachinformation Implanon® . <http://www.fachinfo.de> . 2008. Rote Liste Service GmbH. 19-8-2013.
- [13] Rote Liste. <https://www.rote-liste.de> . 2013. Rote Liste® Service GmbH. 8-2-2014.
- [14] Bayer, Fachinformation Noristerat® 200 mg Injektionslösung . <http://www.fachinfo.de> . 2013. Rote Liste Service GmbH. 23-12-2013.
- [15] Janssen-Cilag, Fachinformation Risperdal® Consta®. <http://www.fachinfo.de> . 2013. Rote Liste Service GmbH. 8-2-2014.
- [16] Takeda, Fachinformation Enantone® - Gyn Monats-Depot . <http://www.fachinfo.de> . 2012. Rote Liste Service GmbH. 7-9-2013.
- [17] Y. Shi and L.C. Li, Current advances in sustained-release systems for parenteral drug delivery, *Expert Opin. Drug Deliv.*, 2 (2005) 1039-1058.
- [18] G. Alexander, K. Greenway, A. Pollard, D. Pratt, and S. Stocks, Guidance on the administration to adults of oil-based depot and other long-acting intramuscular antipsychotic injections. Feetam, C. and White, J. www.hull.ac.uk/injectionguide. 2010. University of Hull. 31.03.2014.

- [19] Expert Committee Parenteral Products-Industrial, General Chapter <1> Injections. USP 36 - NF 31. <http://www.usp.org>. 2010. US Pharmacopeial Convention. 8-2-2014.
- [20] A.T. Florence, A short history of controlled drug release and an introduction, in: C.G. Wilson and P.J. Crowley (Eds.), *Controlled Release in Oral Drug Delivery*, Springer, New York, 2011, pp. 1-26.
- [21] X. Li, Design of controlled release drug delivery systems, in: X. Li and B.R. Jasti (Eds.), *Design of controlled release drug delivery systems*, McGraw-Hill, New York, 2013.
- [22] R.A. Siegel and M.J. Rathbone, Overview of Controlled Release Mechanisms, in: J. Siepmann, R.A. Siegel, and M.J. Rathbone (Eds.), *Fundamentals and Applications of Controlled Release Drug Delivery*, Springer, New York, 2012.
- [23] C. Wischke and S.P. Schwendemann, Principles of encapsulating hydrophobic drugs in PLA/PLGA microparticles, *Int. J. Pharm.*, 364 (2008) 298-327.
- [24] Handbook of Pharmaceutical Excipients. Rowe, R. C., Sheskey, P. J., Cook, W. G., and Fenton, M. E. [7]. 2013. www.medicinescomplete.com, Pharmaceutical Press. 13-9-2013.
- [25] W. Rungsevijitprapa, F. Siepmann, J. Siepmann, and O. Paeratakul, Disperse Systems, in: A.T. Florence and J. Siepmann (Eds.), *Modern Pharmaceutics Volume 1 Basic Principles and Systems*, Informa Healthcare, New York, 2009, pp. 357-421.
- [26] S. Nema, R.J. Waskuhn, and R.J. Brendel, Excipients and their use in injectable products, *PDA J. Pharm. Sci. Technol.*, 51 (1997) 166-171.
- [27] R.C. Moreton, Commonly used excipients in pharmaceutical suspensions, in: A.K. Kulshreshtha, N. Onkar, G. Singh, and M. Wall (Eds.), *Pharmaceutical suspensions: From formulation development to manufacturing*, Springer, New York, 2010, pp. 67-102.
- [28] J. Wong, A. Brugger, A. Khare, M. Chaubal, P. P.Papadopoulos, B. B.Rabinow, J. Kipp, and J. Ning, Suspensions for intravenous (IV) injection: A review of development, preclinical and clinical aspects, *Adv. Drug Deliv. Rev.*, 60 (2008) 938-954.
- [29] J. Zuidema, F. Kadir, H.A.C. Titulaer, and C. Oussoren, Release and absorption rates of intramuscularly and subcutaneously injected pharmaceuticals (II), *Int. J. Pharm.*, 105 (1994) 189-207.
- [30] N. Gulati and H. Gupta, Parenteral drug delivery: a review, *Recent Pat. Drug Deliv. Formul.*, 5 (2011) 133-145.
- [31] F. Kadir, J. Zuidema, Pijpers, A., A. Vulto, and J.H.M. Verheijden, Drug lipophilicity and release pattern of some beta-blocking agents after intra-adipose injection in pigs, *Int. J. Pharm.*, 64 (1990) 171-180.
- [32] J. Zuidema, F.A.J.M. Pieters, and G.S.M.J.E. Duchateau, Release and absorption rate aspects of intramuscular injected pharmaceuticals, *Int. J. Pharm.*, 47 (1988) 1-12.
- [33] S.S. Ober, H.C. Vincent, D.E. Simon, and K.J. Frederick, A rheological study of procaine penicillin G depot preparations, *J. Am. Pharm. Assoc.*, 47 (1958) 667-676.
- [34] K. Hirano and H. Yamada, Studies on the absorption of practically water-insoluble drugs following injection VIII: Comparison of the subcutaneous absorption rates from aqueous suspensions in the mouse, rat, and rabbit, *J. Pharm. Sci.*, 72 (1983) 608-612.
- [35] J. Siepmann, F. Siepmann, and A.T. Florence, Factors influencing oral drug absorption and drug availability, in: Alexander T.Florence and Juergen Siepmann (Eds.), *Modern Pharmaceutics: Basic Principles and Systems*, Vol. 1. Informa Healthcare, New York, 2009, pp. 117-154.

- [36] A. Dokoumetzidis and P. Macheras, A century of dissolution research: From Noyes and Whitney to the Biopharmaceutics Classification System, *Int. J. Pharm.*, 321 (2006) 1-11.
- [37] J. Siepmann and F. Siepmann, Modeling of diffusion controlled drug delivery. *J. Control. Release*, 161 (2011) 351-362.
- [38] N.J. Medlicott, N.A. Waldron, and T.P. Foster, Sustained release veterinary parenteral products, *Adv. Drug Deliv. Rev.*, 56 (2004) 1345-1365.
- [39] K. Hirano and H. Yamada, Studies on the absorption of practically water-insoluble drugs following injection VI: Subcutaneous absorption from aqueous suspensions in rats, *J. Pharm. Sci.*, 71 (1982) 500-505.
- [40] K. Schultz, B. Mollgaard, A.N. Fisher, L. Illum, and C. Larsen, Intramuscular rate of disappearance of oily vehicles in rabbits investigated by gamma-scintigraphy, *Int. J. Pharm.*, 169 (1998) 121-126.
- [41] O. Svendsen and T. Aaes-Jorgensen, Studies on the fate of vegetable oil after intramuscular injection into experimental animals, *Acta Pharmacol. Toxicol.*, 45 (1979) 352-378.
- [42] K. Hirano, T. Ichihashi, and H. Yamada, Studies on the absorption of practically water-insoluble drugs following Injection V: Subcutaneous absorption in rats from solutions in water immiscible oils, *J. Pharm. Sci.*, 71 (1982) 495-500.
- [43] P. Knudsen, L.B. Hansen, and N.E. Larsen, Pharmacokinetic implications of different oil vehicles used in depot neuroleptic treatment, *Acta Psychiatr. Scand. Suppl.*, 322 (1985) 10.
- [44] T. Aaes-Jorgensen, Pharmacokinetics of three different injectable zuclopenthixol preparations, *Prog. Neuro-Psychopharmacol. Biol. Psychiatry*, 13 (1989) 77-85.
- [45] H.W.L. Honrath, A. Wolff, and A. Meli, The influence of the amount of solvent (sesame oil) on the degree and duration of action of subcutaneously administered testosterone and its propionate, *Steroids*, 2 (1963) 425-428.
- [46] J.R. Howard and J. Hadgraft, The clearance of oily vehicles following intramuscular and subcutaneous injections, *Int. J. Pharm.*, 1 (1983) 31-39.
- [47] S.W. Larsen and C. Larsen, Critical Factors Influencing the *In Vivo* Performance of Long-acting Lipophilic Solutions - Impact on *In Vitro* Release Method Design, *AAPS J.*, 11 (2009) 762-770.
- [48] J.P. Luo, J.W. Hubbard, and K.K. Midha, The roles of depot injection sites and proximal lymph nodes in the presystemic absorption of fluphenazine decanoate and fluphenazine: Ex vivo experiments in rats, *Pharm. Res.*, 15 (1998) 1485-1489.
- [49] Y. Oh-E, H. Miyazaki, Y. Matsunaga, and M. Hashimoto, Pharmacokinetics of haloperidol decanoate in rats, *J. Pharmacobio-Dyn.*, 14 (1991) 615-622.
- [50] Z.-H. Gao, W.R. Crowley, A.J. Shukla, J.R. Johnson, and J.F. Reger, Controlled Release of Contraceptive Steroids from Biodegradable and Injectable Gel Formulations: *In vivo* Evaluation, *Pharm. Res.*, 12 (1995) 864-868.
- [51] Z.-H. Gao, A.J. Shukla, J.R. Johnson, and W.R. Crowley, Controlled Release of Contraceptive Steroids from Biodegradable and Injectable Gel Formulations: *In vitro* Evaluation, *Pharm. Res.*, 12 (1995) 857-863.
- [52] K. Klokke-Bethke, Suspensionen, in: F. von Bruchhausen (Ed.), *Hagers Handbuch der Pharmazeutischen Praxis*, Springer, Berlin, 1991, pp. 923-937.
- [53] D. Jordan Llyod, The problem of gel structure, in: J. Alexander (Ed.), *Colloid Chemistry*, The Chemical Catalog Co., New York, 1926, p. 767.

-
- [54] A. Vintiloiu and J.C. Leroux, Organogels and their use in drug delivery - A review, *J. Control. Release*, 125 (2008) 179-192.
- [55] P.L. Luisi, R. Scartazzini, G. Haering, and P. Schurtenberger, Organogels from water-in-oil microemulsions, *Colloid Polym. Sci.*, 268 (1990) 356-374.
- [56] Y.A. Shchipunov, Lecithin organogel. A micellar system with unique properties, *Coll. Surf. A. Phys. Eng. Asp.*, 183-185 (2001) 541-554.
- [57] S. Murdan, Organogels in drug delivery, *Expert Opin. Drug Deliv*, 2 (2005) 489-505.
- [58] P. Terech, Structure of non-ionic rod-like surfactant aggregates in apolar solvents : study of the influence of the nature of the solvent in steroid/hydrocarbon organogels, *J. Phys. France*, 50 (1989) 1967-1982.
- [59] S. Yamasaki and H. Tsutsumi, The dependence of the polarity of solvents on 1,3: 2,4-di-O-benzylidene-D-sorbitol gel, *Bull. Chem. Soc. Jpn.*, 68 (1995) 123-127.
- [60] S. Murdan and G. Gregoriadis, Sorbitan monostearate / polysorbate 20 organogels containing niosomes: a delivery vehicle for antigens, *Eur. J. Pharm. Sci.*, 8 (1999) 177-185.
- [61] P. Terech and R.G. Weiss, Low Molecular Mass Gelators of Organic Liquids and the Properties of Their Gels, *Chem. Rev.*, 97 (1997) 3133-3159.
- [62] O. Gronwald and S. Shinkai, Sugar-Integrated Gelators of Organic Solvents, *Chem. Eur. J.*, 7 (2001) 4328-4334.
- [63] A. Brizard, R. Oda, and I. Huc, Chirality effects in self-assembled fibrillar networks, *Top. Curr. Chem.*, 256 (2005) 167-218.
- [64] S. Murdan, T. Andrysek, and D. Son, Novel gels and their dispersions-oral drug delivery systems for ciclosporin, *Int. J. Pharm.*, 300 (2005) 113-124.
- [65] P. Terech, C. Rossat, and F. Volino, On the measurement of phase transition temperatures in physical molecular organogels, *J. Colloid Interface Sci.*, 227 (2000) 363-370.
- [66] A. Hafeti and B. Amsden, Biodegradable injectible in situ forming drug delivery systems, *J. Control. Release*, 80 (2002) 9-28.
- [67] S. Goto, M. Kawata, T. Suzuki, N.-S. Kim, and C. Ito, Preparation and evaluation of eudragit gels. I: Eudragit organogels containing drugs as rectal sustained-release preparations, *J Pharm. Sci.*, 80 (1991) 958-961.
- [68] Z. Cui and R.J. Mumper, Bilayer Films for Mucosal (Genetic) Immunization via the Buccal Route in Rabbits, *Pharm. Res.*, 19 (2002) 947-953.
- [69] S. Pisal, V. Shelke, K. Mahadik, and S. Kadam, Effect of organogel components on in vitro nasal delivery of propranolol hydrochloride, *AAPS PharmSciTech*, 13 (2004) 92-100.
- [70] A. Vintiloiu, M. Lafleur, G. Bastiat, and J.C. Leroux, In situ-forming oleogel implant for rivastigmine delivery, *Pharm. Res.*, 25 (2008) 845-852.
- [71] F. Plourde, A. Motulsky, A.C. Couffin-Hoarau, D. Hoarau, and J.C. Leroux, First report on the efficacy of l-alanine-based in situ-forming implants for the long-term parenteral delivery of drugs, *J. Control. Release*, 108 (2005) 433-441.
- [72] S. Murdan, G. Gregoriadis, and A.T. Florence, Interaction of a non-ionic surfactant-based organogel with aqueous media, *Int. J. Pharm.*, 180 (1999) 211-214.

- [73] T. Higuchi, Rate of release of medicaments from ointment bases containing drugs in suspension, *J. Pharm. Sci.*, 50 (1961) 874-875.
- [74] J. Siepmann and F. Siepmann, Modeling of diffusion controlled drug delivery, *J. Control. Release*, 161 (2012) 351-362.
- [75] U. Gietz, T. Arvinte, E. Mader, P. Oroszlan, and H.P. Merkle, Sustained release of injectable zinc-recombinant hirudin suspensions: development and validation of in vitro release model, *Eur. J. Pharm. Biopharm.*, 45 (1998) 259-264.
- [76] C.R. Mayer, N.A. Geis, H.A. Katus, and R. Bekeredjian, Ultrasound targeted microbubble destruction for drug and gene delivery, *Expert Opin. Drug Deliv.*, 5 (2008) 1121-1138.
- [77] A. Göpferich, Mechanisms of polymer degradation and erosion, *Biomaterials*, 17 (1996) 103-114.
- [78] S.J. Douglas, L. Illum, S.S. Davis, and J. Kreuter, Particle size and size distribution of poly(butyl-2-cyanoacrylate) nanoparticles - I. Influence of physicochemical factors, *J. Colloid Interface Sci.*, 101 (1984) 149-158.
- [79] P. Couvreur, L. Roblot-Treupel, M.F. Poupon, F. Brasseur, and F. Puisieux, Nanoparticles as microcarriers for anticancer drugs, *Adv. Drug Deliv. Rev.*, 5 (1990) 209-230.
- [80] N. Al Khouri Fallouh, L. Roblot-Treupel, H. Fessi, J.P. Devissaguet, and F. Puisieux, Development of a new process for the manufacture of polyisobutylcyanoacrylate nanocapsules, *Int. J. Pharm.*, 28 (1986) 125-132.
- [81] N. Behan and C. Birkinshaw, Preparation of Poly(butyl cyanoacrylate) Nanoparticles by Aqueous Dispersion Polymerisation in the Presence of Insulin, *Macromol. Rapid Commun.*, 22 (2001) 41-43.
- [82] P. Couvreur, B. Kante, M. Roland, P. Guiot, P. Bauduin, and P. Speiser, Polycyanoacrylate nanocapsules as potential lysosomotropic carriers: preparation, morphological and sorptive properties, *J. Pharm. Pharmacol.*, 31 (1979) 331-332.
- [83] C. Limouzin, A. Caviggia, F. Ganachaud, and P. Hémerly, Anionic Polymerization of *n*-Butyl Cyanoacrylate in Emulsion and Miniemulsion, *Macromolecules*, 36 (2003) 667-674.
- [84] A. van Herk and B. Gilbert, Emulsion Polymerisation, in: A.M. van Herk (Ed.), *Chemistry and technology of emulsion polymerisation*, Blackwell Publishing Ltd., Oxford, 2005, pp. 46-78.
- [85] W.D. Harkins, A general theory of the mechanism of emulsion polymerization, *J. Am. Chem. Soc.*, 69 (1947) 1428-1444.
- [86] W.V. Smith and R.H. Ewart, Kinetics of Emulsion Polymerization, *J. Chem. Phys.*, 16 (1948) 592-599.
- [87] C.S. Chern, Emulsion polymerization mechanisms and kinetics, *Prog. Polym. Sci.*, 31 (2006) 443-486.
- [88] F.J. Schork, Y. Luo, W. Smulders, J.P. Russum, A. Butte, and K. Fontenot, Miniemulsion polymerization, *Adv. Polym. Sci.*, 175 (2005) 129-255.
- [89] R.M. Fitch, The homogeneous nucleation of polymer colloids, *Br. Polym. J.*, 5 (1979) 467-483.
- [90] F.K. Hansen and J. Ugelstad, Particle nucleation in emulsion polymerization. I. A theory for homogeneous nucleation, *J. Polym. Sci. Polym. Chem.*, 16 (1978) 1953-1979.
- [91] U. Baudisch, Colloid-chemical investigations within the development of i. v. injectable polybutylcyanoacrylate nanoparticles: Synthesis, characterisation and stability. 2001. FU Berlin.

-
- [92] Z. Zhang, G. Liao, T. Nagai, and S. Hou, Mitoxantrone polybutyl cyanoacrylate nanoparticles anti-neoplastic targeting drug delivery system, *Int. J. Pharm.*, 139 (1996) 1-8.
- [93] T. Harmia, P. Speiser, and J. Kreuter, Optimization of pilocarpine loading onto nanoparticles by sorption procedures, *Int. J. Pharm.*, 33 (1986) 45-54.
- [94] J.L. Arias, V. Gallardo, M.A. Ruiz, and A.V. Delgado, Ftorafur loading and controlled release from poly(ethyl-2-cyanoacrylate) and poly(butylcyanoacrylate) nanospheres, *Int. J. Pharm.*, 337 (2007) 282-290.
- [95] M. Lianga, N.M. Davie, and I. Toth, Increasing entrapment of peptides within poly(alkyl cyanoacrylate) nanoparticles prepared from water-in-oil microemulsions by copolymerization, *Int. J. Pharm.*, 362 (2008) 141-146.
- [96] Lambert, Polyisobutylcyanoacrylate nanocapsules containing an aqueous core as a novel colloidal carrier for the delivery of oligonucleotides, *Pharm. Res.*, 17 (2000) 707-714.
- [97] M. Fresta, G. Cavallari, G. Giammonat, E. Wehrli, and G. Puglisi, Preparation and characterization of polyethyl-2-cyanoacrylate nanocapsules containing antiepileptic, *Biomaterials*, 17 (1996) 751-756.
- [98] W. Schmidt and G. Roessling, Novel manufacturing process of hollow polymer microspheres, *Chem. Eng. Sci.*, 61 (2006) 4973-4981.
- [99] C. Olbrich, P. Hauff, F. Scholle, W. Schmidt, U. Bakowsky, A. Briel, and M. Schirner, The in vitro stability of air-filled polybutylcyanoacrylate microparticles, *Biomaterials*, 27 (2006) 3549-3559.
- [100] S. Freitas, H.P. Merkle, and B. Gander, Microencapsulation by solvent extraction/evaporation: reviewing the state of the art of microsphere preparation process technology, *J. Control. Release*, 102 (2005) 313-332.
- [101] J. Herrmann and R. Bodmeier, Biodegradable, somatostatin acetate containing microspheres prepared by various aqueous and non-aqueous solvent evaporation methods, *Eur. J. Pharm. Biopharm.*, 45 (1998) 75-82.
- [102] P. Sommerfeld, U. Schroeder, and B.A. Sabel, Long-term stability of PBCA nanoparticle suspensions suggests clinical usefulness, *Int. J. Pharm.*, 155 (1997) 201-207.
- [103] M. Stein and E. Hamacher, Degradation of polybutyl 2-cyanoacrylate microparticles, *Int. J. Pharm.*, 80 (1992) R13.
- [104] W. Wang, Lyophilization and development of solid protein pharmaceuticals, *Int. J. Pharm.*, 203 (2000) 1-60.
- [105] J. Siepmann and A. Goepferich, Mathematical modeling of bioerodible, polymeric drug delivery systems, *Adv. Drug Deliv. Rev.*, 48 (2001) 229-247.
- [106] L.S. Nair and C.T. Laurencin, Biodegradable polymers as biomaterials, *Prog. Polym. Sci.*, 32 (2007) 762-798.
- [107] Leonard, Synthesis and degradation of poly(alkyl α -cyanoacrylates), *J. Appl. Poly. Sci.*, 10 (1966) 259-272.
- [108] R. Zange and T. Kissel, Comparative in vitro biocompatibility testing of polycyanoacrylates and poly(D,L-lactide-co-glycolide) using different mouse fibroblast (L929) biocompatibility test models, *Eur. J. Pharm. Biopharm.*, 44 (1997) 149-157.
- [109] G. Ciapetti, S. Stea, E. Cenni, A. Sudanese, D. Marraro, A. Toni, and A. Pizzoferrato, Cytotoxicity testing of cyanoacrylates using direct contact assay on cell cultures, *Biomaterials*, 15 (1994) 63-67.

- [110] V. Lenaerts, P. Couvreur, D. Christiaens-Leyh, E. Joiris, M. Roland, B. Rollman, and P. Speiser, Degradation of poly (isobutyl cyanoacrylate) nanoparticles, *Biomaterials*, 5 (1984) 65-68.
- [111] D. Scherer, J.R. Robinson, and J. Kreuter, Influence of enzymes on the stability of polybutylcyanoacrylate nanoparticles, *Int. J. Pharm.*, 101 (1993) 165-168.
- [112] C. Lherm, R.H. Müller, F. Puisieux, and P. Couvreur, Alkylcyanoacrylate drug carriers: II. Cytotoxicity of cyanoacrylate nanoparticles with different alkyl chain length, *Int. J. Pharm.*, 84 (1992) 13-22.
- [113] B. Kante, P. Couvreur, G. Dubois-Krack, C. de Meester, P. Guiot, M. Roland, M. Mercier, and P. Speiser, Toxicity of polyalkylcyanoacrylate nanoparticles I: Free nanoparticles, *J. Pharm. Sci.*, 71 (1982) 786-790.
- [114] P. Couvreur, L. Grislain, V. Lenaerts, F. Brasseur, P. Guiot, and A. Biernacki, Biodegradable polymeric nanoparticles as drug carrier for antitumor agents, in: P. Guiot and P. Couvreur (Eds.), *Polymeric Nanoparticles and Microspheres*, CRC Press, Boca Raton, 1986, pp. 27-93.
- [115] J. Siepmann, K. Elkharraz, F. Siepmann, and D. Klose, How autocatalysis accelerated drug release from PLGA-based microparticles: A quantitative treatment, *Biomacromolecules*, 6 (2005) 2312-2319.
- [116] D.H. Lewis, Controlled release of bioactive agents from lactide/glycolide polymers, in: M. Chasin and R. Langer (Eds.), *Biodegradable Polymers as Drug Delivery Systems*, Vol. 45. Marcel Dekker, New York, 1990, pp. 1-42.
- [117] J.M. Anderson and M.S. Shive, Biodegradation and biocompatibility of PLA and PLGA microspheres, *Adv. Drug Deliv. Rev.*, 2 (1997) 5-24.
- [118] R.H. Müller, C. Lherm, J. Herbort, T. Blunk, and P. Couvreur, Alkylcyanoacrylate drug carriers: I. Physicochemical characterization of nanoparticles with different alkyl chain length, *Int. J. Pharm.*, 84 (1992) 1-11.
- [119] F. Burkersroda, L. Schedl, and A. Göpferich, Why degradable polymers undergo surface erosion or bulk erosion, *Biomaterials*, 23 (2002) 4221-4231.
- [120] D.O. Cooney, Effect of geometry on the dissolution of pharmaceutical tablets and other solids: surface detachment kinetics controlling, *AIChE J.*, 18 (1972) 449.
- [121] H.B. Hopfenberg, Controlled release from erodible slabs, cylinders, and spheres, in: D.R. Paul and F.W. Harris (Eds.), *Controlled Release Polymeric Formulations*, ACS Symp. Ser. No. 33, American Chemical Society, Washington, 1976, pp. 26-32.
- [122] P.L. Ritger and N.A. Peppas, A simple equation for description of solute release. I. Fickian and non-Fickian release from non-swellable devices in the form of slabs, spheres, cylinders or discs, *J. Control. Release*, 5 (1987) 23-26.
- [123] P.L. Ritger and N.A. Peppas, A simple equation for description of solute release. II. Fickian and anomalous release from swellable devices., *J. Control. Release*, 5 (1987) 37-42.
- [124] R. Baker, *Controlled Release of Biologically Active Agents*, John Wiley & Sons, New York, 1987.
- [125] J. Crank, *The mathematics of diffusion*, Clarendon Press, Oxford, 1975.
- [126] T. Higuchi, Mechanisms of sustained action mediation. Theoretical analysis of rate of release of solid drugs dispersed in solid matrices. *J. Pharm. Sci.*, 52 (1963) 1145-1149.
- [127] R.W. Korsemeyer, S.R. Lustig, and N.A. Peppas, Solute and penetrant diffusion in swellable polymers. I. Mathematical modeling. *J. Polym. Sci. Polym. Phys.*, 24 (1986) 409-434.

- [128] J. Heller and R.W. Baker, Theory and practice of controlled drug delivery, in: R.W. Baker (Ed.), *Controlled release of bioactive materials*, Academic Press, New York, 1980, pp. 1-18.
- [129] P.I. Lee, Diffusional release of a solute from a polymeric matrix - approximate analytical solutions, *J. Membr. Sci.*, 7 (1980) 255-275.
- [130] A. Charlier, B. Leclerc, and G. Couarraze, Release of mifepristone from biodegradable matrices: experimental and theoretical evaluations, *Int. J. Pharm.*, 200 (2000) 115-120.
- [131] K. Zygorakis, Discrete simulations and bioerodible controlled release systems, *Polym. Prep. ACS*, 30 (1989) 456-457.
- [132] A. Göpferich and R. Langer, Modeling monomer release from bioerodible polymers, *J. Control. Release*, 33 (1995) 55-69.
- [133] N. Faisant, J. Siepmann, and J.P. Benoit, PLGA-based microparticles: elucidation of mechanisms and a new, simple mathematical model quantifying drug release, *Eur. J. Pharm. Sci.*, 15 (2002) 355-366.
- [134] D. Klose, F. Siepmann, K. Elkharraz, S. Krenzlin, and J. Siepmann, How porosity and size affect the drug release mechanisms from PLGA-based microparticles, *Int. J. Pharm.*, 314 (2006) 198-206.
- [135] Drugs@FDA. <http://www.accessdata.fda.gov/scripts/cder/drugsatfda/> . 2013. U.S. Food and Drug Administration, Silver Spring. 7-9-2013.
- [136] Fachinformation. <http://www.fachinfo.de> . 2014. Rote Liste® Service GmbH. 8-2-2014.
- [137] Mochida Pharmaceutical Co., SPC Suprecur® MP 1.8 for s.c. Inj. http://www.mochida.co.jp/dis/interview/scmp_n18.pdf . 2009. 7-9-2013.
- [138] Ipsen, SPC Somatuline® . <http://www.medicines.org.uk/emc/medicine/877/SPC> . 20-10-2010. Datapharm. 7-9-2013.
- [139] Y.C. Kuo, Loading efficiency of stavudine on polybutylcyanoacrylate and methylmethacrylate-sulfopropylmethacrylate copolymer nanoparticles, *Int. J. Pharm.*, 290 (2005) 161-172.
- [140] Y.C. Kuo and H.H. Chen, Effect of nanoparticulate polybutylcyanoacrylate and methylmethacrylate-sulfopropylmethacrylate on the permeability of zidovudine and lamivudine across the *in vitro* blood-brain barrier, *Int. J. Pharm.*, 327 (2006) 160-169.
- [141] D.T. O'Hagan, K.J. Palin, and S.S. Davis, Poly(butyl-2-cyanoacrylate) particles as adjuvants for oral immunization, *Vaccine*, 7 (1989) 213-216.
- [142] DermaBond™ - P960052. <http://www.accessdata.fda.gov/scripts/cdrh/cfdocs/cfTopic/pma/pma.cfm?num=p960052> . 2005. U.S. Food and Drug Administration, Silver Spring. 7-9-2013.
- [143] Draft Guideline on fixed combination medicinal products, European Medicines Agency, London, 2008.
- [144] H. Zhang, G. Wang, and H. Yang, Drug delivery systems for differential release in combination therapy, *Expert Opin. Drug Deliv.*, 8 (2011) 171-190.
- [145] M.J. Rosenberg, M.S. Burnhill, M.S. Waugh, D.A. Grimes, and P.J.A. Hillard, Compliance and oral contraceptives: A review, *Contraception*, 52 (1995) 141.
- [146] D. Oakley, S. Sereika, and E.L. Bogue, Oral contraceptive pill use after an initial visit to a family planning clinic, *Fam. Plann. Perspect.*, 23 (1991) 150-154.

- [147] C. d'Arcangues and Snow R.C., Injectable Contraceptives for women, in: T. Rabe and B. Runnebaum (Eds.), *Fertility Control Update and Trends*, Springer, Heidelberg, 1999, pp. 121-149.
- [148] B. Keith, Home-based administration of depot-subQ provera 104™ in the uniject™ injection system: A literature review, PATH, Seattle, 2011.
- [149] E.S. Linn, Progress in contraception: new technology, *Int. J. Fertil. Womens Med.*, 48 (2003) 182-191.
- [150] Pfizer, Clinical pharmacology and biopharmaceutics review(s) depo-subQ provera 104™. http://www.accessdata.fda.gov/drugsatfda_docs/nda/2005/021584s000_depo-subQ_biopharmr.pdf Application number 21-584. 2005. US Food and Drug Administration. 23-12-2013.
- [151] J. Garza-Flores, Pharmacokinetics of once-a-month injectable contraceptives, *Contraception*, 49 (1994) 347-359.
- [152] G. Hernandez, C. Lopez, F. Stanczyk, D. Taylor, and P. Segall-Gutierrez, Changes in bone mineral density among obese women on depot medroxyprogesterone acetate, *Contraception*, 78 (2008) 167-195.
- [153] Pfizer, Depot Clinovir® Fachinformation. <http://www.fachinfo.de> . 2011. Rote Liste Service GmbH. 1-10-2013.
- [154] A.R. Aedo, B.M. Langren, and E. Johannisson, Pharmacokinetic and pharmacodynamic investigations with monthly injectable contraceptive preparation, *Contraception*, 31 (1985) 453-469.
- [155] Bayer, Fachinformation Qlaira®. <http://www.fachinfo.de> . 2013. Rote Liste® Service GmbH. 23-12-2013.
- [156] Parke-Davis, Clinical pharmacology and biopharmaceutics review(s) Eurostep® . http://www.accessdata.fda.gov/drugsatfda_docs/nda/99/20130-s003_Eurostep.pdf Application number NDA 20130/S3. 1999. US Food and Drug Administration. 8-2-2014.
- [157] Pfizer, Fachinformation Sayana®. <http://www.fachinfo.de> . 2012. Rote Liste® Service GmbH. 23-12-2013.
- [158] H. Kuhl, Familienplanung, in: J.W. Dudenhausen, H.P.G. Schneider, and G. Bastert (Eds.), *Frauenheilkunde und Geburtshilfe*, De Gruyter, Berlin, 2003, pp. 59-89.
- [159] T. Rabe, M. Ludwig, E. Merkle, H.J. Ahrendt, K.J. Bühling, P. Hadji, A.O. Mueck, G. Merki, C. Egarter, K. König, and C. Albring, Depotgestagene zur Kontrazeption bei der Frau - Gemeinsame Stellungnahme der DGGEF e.V. und des BVF e. V., *J. Reproduktionsmed. Endokrinol.*, 10 (2013) 18-42.
- [160] B.A. Cromer, R. Lazebnik, E. Rome, M. Stager, A.Z.J. Bonny, and S.M. Debanne, Double-blinded randomized controlled trial of estrogen supplementation in adolescent girls who receive depot medroxyprogesterone acetate for contraception , *Am. J. Obstet. Gynecol.*, 192 (2005) 42-47.
- [161] R. Krattenmacher, Drospirenone: pharmacology and pharmacokinetics of a unique progestogen, *Contraception*, 62 (2000) 29-38.
- [162] O. Lidegaard, I. Milsom, R.T. Geirsson, and F.E. Skjeldestad, Hormonal contraception and venous thromboembolism , *Acta Obstet. Gynecol. Scand.*, 91 (2012) 769-778.
- [163] M. Ludwig, C. Grave, and U. Hugo, Orale Kontrazeptiva mit antiandrogen wirksamer gestagener Komponente Teil 1: Grundlagen, *Frauenarzt*, 47 (2006) 25-28.
- [164] A.M. Ochnik, N.L. Moore, T. Jankovic-Karasoulos, T. Bianco-Miotto, N.K. Ryan, M.R. Thomas, S.N. Birrell, L.M. Butler, W.D. Tilley, and T.E. Hickey, Antiandrogenic actions of

- medroxyprogesterone acetate on epithelial cells within normal human breast tissues cultured ex vivo, *Menopause*, 21 (2014) 79-88.
- [165] N. Gronich, I. Lavi, and G. Rennert, Higher risk of venous thrombosis associated with drospirenone-containing oral contraceptives: a population-based cohort study, *CMAJ*, 183 (2011) E1319-E1325.
- [166] Anonymous, Cardiovascular disease and use of oral and injectable progestogen-only contraceptives and combined injectable contraceptives. Results of an international, multicenter, case-control study. World Health Organization Collaborative Study of Cardiovascular Disease and Steroid Hormone Contraception, *Contraception*, 57 (1998) 315-324.
- [167] J. Goldstein, M. Cushman, G.J. Badger, and J.V. Johnson, Effect of depomedroxyprogesterone acetate on coagulation parameter: a pilot study, *Fertil. Steril.*, 87 (2007) 1267-1270.
- [168] A. van Hylckama Vlieg, F.M. Helmerhorst, and F.R. Rosendaal, The risk of deep venous thrombosis associated with injectable DMPA contraceptives or a Levonorgestrel intrauterine device, *Arterioscler. Thomb. Vasc. Biol.*, 30 (2010) 2297-2300.
- [169] M. Raps, F. Helmerhorst, K. Fleischer, S. Thomassen, F. Rosendaal, J. Rosing, B. Ballieux, and H. VAN Vliet, Sex hormone-binding globulin as a marker for the thrombotic risk of hormonal contraceptives, *J. Thromb. Haemost.*, 10 (2012) 992-997.
- [170] L. Chasan-Taber and M.J. Stampfer, Epidemiology of oral contraceptives and cardiovascular disease, *Annals of Int. Med.*, 128 (1998) 467-477.
- [171] M.J. Rosenberg, A. Meyers, and V. Roy, Efficacy, cycle control, and side effects of low- and lower-dose oral contraceptives: a randomized trial of 20 µg and 35 µg estrogen preparations, *Contraception*, 60 (1999) 321-329.
- [172] D. Scholes, L. Ichikawa, A.Z. LaCroix, L. Spangler, J.M. Beasley, S. Reed, and S.M. Ott, Oral contraceptive use and bone density in adolescent and young adult women, *Contraception*, 81 (2010) 35-40.
- [173] R.K. Zurawin and L. Ayensu-Coker, Innovations in contraception: a review, *Clin. Obstet. Gynecol.*, 50 (2007) 425-439.
- [174] D.T. Birnbaum, J.D. Kosmala, D.B. Henthorn, and L. Brannon-Peppas, Controlled release of beta-estradiol from PLGA microparticles: The effect of organic phase solvent on encapsulation and release, *J. Control. Release*, 65 (2000) 375-387.
- [175] B. Buntner, M. Nowak, J. Kasperczyk, M. Ryba, P. Grieb, M. Walski, P. Dobrzynski, and Bero, The application of microspheres from the copolymers of lactide and ε-caprolactone to the controlled release of steroids, *J. Control. Release*, 56 (1998) 159-167.
- [176] M.D. Dhanaraju, V. Kiran, R. Jayakumar, and C. Vamsadhara, Preparation and characterization of injectable microspheres of contraceptive hormones, *Int. J. Pharm.*, 268 (2003) 23-29.
- [177] S.R. Jameela, T.V. Kumary, A.V. Lal, and A. Jayakrishan, Progesterone-loaded chitosan microspheres: a long acting biodegradable controlled delivery system, *J. Control. Release*, 52 (1998) 17-24.
- [178] M.S. Latha, A.V. Lal, T.V. Kumary, R. Sreekumar, and A. Jayakrishan, Progesterone release from glutaraldehyde cross-linked casein microspheres: in vitro studies and in vivo response in rabbits, *Contraception*, 61 (2000) 329-334.
- [179] L.R. Beck, R.A. Ramos, C.E. Flowers, G.Z. Lopez, D.H. Lewis, and D.R. Cowsar, Clinical evaluation of injectable biodegradable contraceptive system, *Am. J. Obstet. Gynecol.*, 140 (1981) 799-806.

- [180] M.D. Dhanaraju, R. RajKannan, D. Selvaraj, R. Jayakumar, and C. Vamsadhara, Biodegradation and biocompatibility of contraceptive-steroid-loaded poly (dl-lactide-co-glycolide) injectable microspheres: in vitro and in vivo study, *Contraception*, 74 (2005) 148-156.
- [181] H. VAN Vliet, D.A. Grimes, L.M. Lopez, K.F. Schulz, and F.M. Helmerhorst, Triphasic versus monophasic oral contraceptives for contraception (review), *Cochrane Database Syst. Rev.*, 9 (2007).
- [182] J. Guillebaud, *Contraception: your questions answered*, Churchill Livingstone, Edinburgh, 1993.
- [183] R.W. Hale, Phasic approach to oral contraceptives, *Am. J. Obstet. Gynecol.*, 157 (1987) 1052-1058.
- [184] V.T. Martin and M. Behbehani, Ovarian hormones and migraine headache: understanding mechanisms and pathogenesis - Part 2, *Headache*, 46 (2006) 365-386.
- [185] R.B. Dickson and A.J. Eisenfeld, 17 Alpha-ethinyl estradiol is more potent than estradiol in receptor interactions with isolated hepatic parenchymal cells, *Endocrinology*, 108 (1981) 1511-1518.
- [186] Bayer, Fachinformation Yasminelle® . <http://www.fachinfo.de> . 2013. Rote Liste® Service GmbH. 14-12-2013.
- [187] P. Vihko, P. Härkönen, P. Soronen, S. Törn, A. Herrala, R. Kurkela, A. Pulkka, O. Oduwole, and V. Isomaa, 17-beta-hydroxysteroid dehydrogenases - their role in pathophysiology, *Mol. Cell. Endocrinol.*, 215 (2004) 83-88.
- [188] G. Moeller, D. Deluca, C. Gege, A. Rosinus, D. Kowalik, O. Peters, P. Droescher, W. Elger, J. Adamski, and A. Hillisch, Structure-based design, synthesis and in vitro characterization of potent 17 beta-hydroxysteroid dehydrogenase type 1 inhibitors based on 2-substitutions of estrone and D-homo-estrone, *Bioorg. Med. Chem. Lett.*, 19 (2009) 6740-6744.

CHAPTER 2

Parenteral oil-based drospirenone microcrystal suspensions - Evaluation of physicochemical stability and influence of stabilising agents

Published in International Journal of Pharmaceutics 416 (2011) 181– 188

<http://dx.doi.org/10.1016/j.ijpharm.2011.06.036>

Abstract

Drospirenone (DRSP) is a contraceptive drug substance with challenging physicochemical properties, due to insufficient solubility in aqueous and oil-based vehicles as well as low chemical stability in aqueous fluids. Although it is one of the most popular orally used progestins, no parenteral long-acting contraceptive containing the drug substance is marketed. An oil-based DRSP microcrystal suspension (MCS) might be an attractive formulation option. The main focus of this study was to investigate the physicochemical stability of such preparations. Moreover, syringeability and injectability via autoinjector were analysed using a materials testing machine. A high chemical stability of DRSP was found in oil-based vehicles. Span® 83, cholesteryl oleate, lecithin, methyl cholate, Aerosil® R972 and 200 Pharma were tested for increasing the physical stability of DRSP dispersions. Changes in viscosity, rheological properties, and solubility were analysed. The intention was to show a stabilising effect of the excipients without increasing viscosity and solubility. To evaluate the physical stability of DRSP MCS with and without addition of stabilising agents, sedimentation and particle growth after storage were examined. Especially, the silica derivatives Aerosil® 200 and R972 Pharma influenced the physical stability positively.

Konzeption:

Stefanie Nippe, Mitarbeit an Konzeption Sascha General

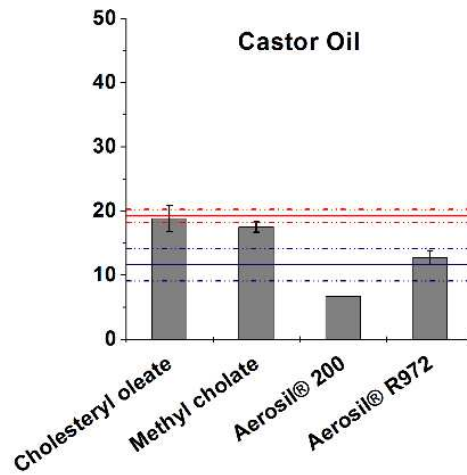
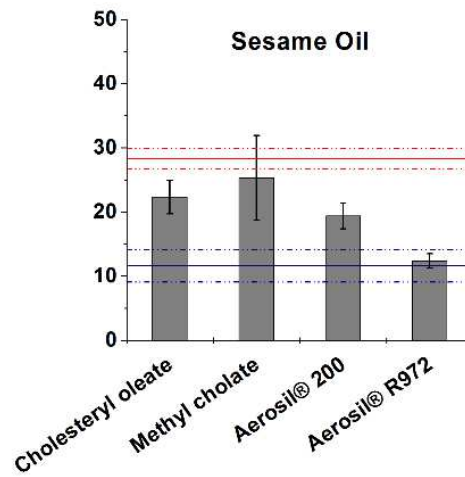
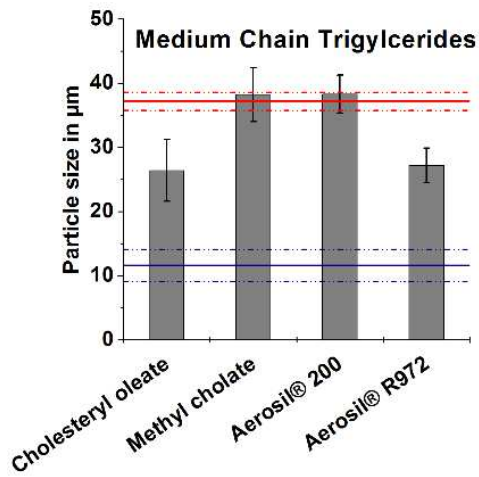
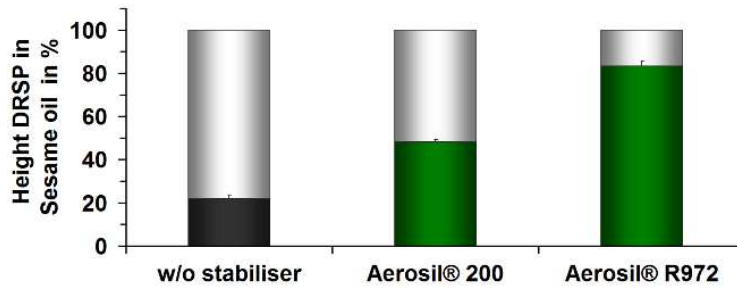
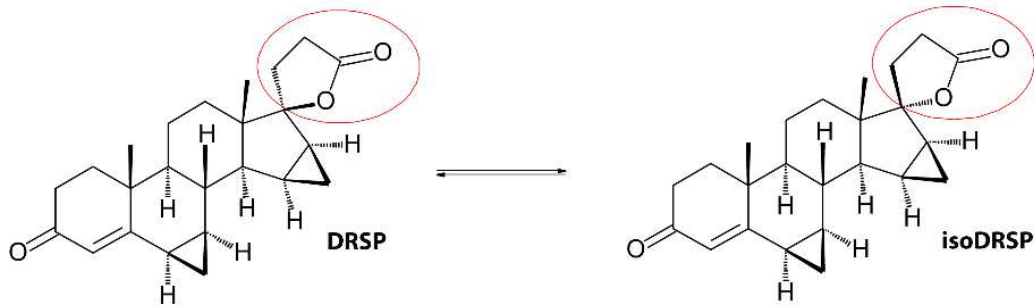
Durchführung:

Stefanie Nippe

Berichtsabfassung:

Stefanie Nippe

Graphical Abstract



1 Introduction

Parenteral injectable drug delivery systems allow a prolonged release of drug substance and avoid the first-pass effect [1,2]. Popular examples are long-acting parenteral contraceptives. They are effective, generally discreet, and reduce daily compliance challenges [3]. DRSP is a progestin which is known to be used in contraceptives and for treatment of diseases, disorders and symptoms associated with deficient endogenous levels of oestrogen in women. As analogue to spironolactone, this unique contraceptive exhibits both anti-mineralocorticoid and anti-androgenic activities [4,5]. Besides oral formulations, no parenteral formulation containing DRSP is on the market.

Long-acting parenteral contraceptives are mostly prepared as aqueous MCSs administered intramuscularly (i.m.) (Depot Provera®) or subcutaneously (s.c.) (Depot-subq Provera®). Or they are manufactured as oil-based i.m. solutions (Mesigyna®) [6,7]. Typical, parenteral applied oil-based vehicles are medium chain triglycerides (MCT) (e.g. in Ciatyl-Z® Depot), sesame oil (e.g. in Lyogen® Depot) or castor oil with addition of benzyl benzoate (e.g. in Noristerat®) [8]. Due to the challenging physicochemical properties of DRSP, an oil-based MCS might be a simple and reasonable formulation option for a once-a-month injection.

An ideal drug suspension for parenteral application should show no particle growth after storage, low sedimentation of suspended particles and easy application of homogeneous dosages [9,10]. Due to its physical instability, the preparation of suspensions is challenging [10,11]. Sedimentation could be an issue during manufacturing and filling processes and may lead to inhomogeneous content uniformity [12,13]. Furthermore, dispersed particles tend to crystal growth and aggregation during storage. However, the particle size of drug substance is an important factor influencing bioavailability, injectability and syringeability, product appearance as well as overall stability of i.m. or s.c. injectable suspensions [14]. For aqueous systems, numerous approaches are known to improve physical stability [12,15,16]. In contrast, oil-based systems have been less investigated. Not all techniques used to stabilise aqueous suspensions can be translated to oil-based formulations, due to differences in properties of vehicle and in drug-vehicle-interaction. Typically, surface-active additives were added decreasing the interfacial tension between drug substance and surrounding liquid phase [17]. Moreover, the addition of thickening agents should increase the viscosity of the external liquid phase, thus slowing down sedimentation and agglomeration of solid particles [18]. However, the rise in viscosity is possible up to the limit of injectability through a standard needle in a reasonable timeframe [2,19]. Furthermore, the solubility of drug substance in the oil-based vehicle was assumed to influence e.g. the release behaviour [20].

Considering these issues, six excipients are tested. In the following, they are referred to as stabilising agents. An increase in viscosity and solubility by addition of the excipients should be avoided. Lecithin is included in pharmaceutical products as dispersing, emulsifying, and stabilising

agent. It is contained in i.m. injections in a concentration of 0.3 – 2.3%. Sorbitan ester derivatives are used as wetting agent for insoluble drug substances in lipophilic bases in a concentration of 0.1 – 3% [21]. Further test substances are cholesteryl oleate, a cholesteryl fatty acid ester and methyl cholate, a cholic acid ester. Both have a sterol structure. The hydroxyl group at C-3 of cholesteryl ester derivative is associated with fatty acid. The carboxyl group of the cholic acid derivative is methylated. The excipients are assumed to interact with the suspended steroidal drug substance as well as with the external lipid phase. Colloidal silicon dioxide is added as suspending and thickening agent in a concentration of 2.0 – 10.0% and as emulsion stabiliser in a concentration of 1.0 – 5.0% (w/w) [21]. In high enough concentrations, e.g. methyl cholate, cholesteryl oleate, Aerosil® 200 Pharma, and Aerosil® R972 Pharma have a thickening effect on some lipophilic vehicle. Thus, they have to be used in low enough concentrations.

The aim was to evaluate the chemical and physical stability as well as the applicability as parenteral injection of oil-based DRSP MCS. Furthermore, a possible stabilising effect of the chosen excipients on oil-based DRSP MCS without increasing the viscosity or affecting the solubility of drug substance should be investigated.

2 Materials and methods

2.1 Materials

Drospirenone (micronised, Bayer Schering Pharma AG, Berlin, Germany), medium chain triglycerides (Myritol® 318 PH) (kindly provided by Cognis GmbH, Düsseldorf, Germany), castor oil (Riedel-de-Haen, Seelze, Germany), sesame oil (Fluka Chemie AG, Buchs, Switzerland), benzyl benzoate (Symrise GmbH & Co. KG, Holzminden, Germany), lecithin (L- α -Lecithin from soybean) (Calbiochem, Darmstadt, Germany), methyl cholate (Alfa Aesar, Karlsruhe, Germany), hydrophobic colloidal anhydrous silica (Aerosil® R972 Pharma), colloidal silicon dioxide (Aerosil® 200 Pharma) (both kindly provided by Degussa, Essen, Germany), cholesteryl oleate (Alfa Aesar, Karlsruhe, Germany), sorbitan sesquioleate (Span® 83, Sigma-Aldrich Chemie GmbH, Steinheim, Germany) were used.

2.2 Chemical stability of DRSP in oil and aqueous medium

70 mg/g of DRSP was added to MCT, sesame oil, or castor oil. The samples were mixed using a vortex mixer (Heidolph, REAK 2000, Heidolph Instruments GmbH, Schwabach, Germany). Thereafter, the suspensions were blended at 39 rpm for 24 h using a roller mixer (Britze, DA II). Afterwards, the samples were stored tightly closed in wide-neck brown glass flasks in an environmental chamber at 25°C and a relative humidity of 60%. After 1 year, the amount of DRSP as well as its degradation product isoDRSP was assayed as indicators for chemical stability. The suspensions were taken from storage and were blended using a roller mixer. Thereafter, 1 mL of

the samples was centrifuged twice at 7500 rpm for 10 min (Sigma Laborzentrifugen ZK15, Sigma Laborzentrifugen GmbH, Osterode, Germany). 0.5 mL of supernatant was pipetted into a volumetric flask and was mixed with 25 mL of acetonitrile. Then, the samples were analysed by high performance liquid chromatography with UV detection (HPLC/UV). Furthermore, 70 mg/g of DRSP was dispersed in USP phosphate buffer at pH 6.8 under stirring at room temperature using a magnetic stirrer (RT 15 power IKAMAG, Ika-Werke GmbH & Co. KG, Staufen, Germany). After 2 d, 14 d and 42 d, 2 mL of samples was filtered using syringe filter (Whatman® Spartan®, pore size 0.45 µm, Whatman GmbH, Dassel, Germany). The amounts of DRSP and isoDRSP were determined by using an Agilent 1100 series HPLC/UV system (Agilent Technologies Deutschland GmbH, Böblingen, Germany). 10 µL of samples was injected onto ODS Hypersil column (length 6 cm, inner diameter 4.6 mm, 3 µm; Agilent Technologies Deutschland GmbH, Böblingen, Germany) using as mobile phase a mixture of water and acetonitrile at a ratio of 60–40% (v/v) and a flow rate of 1 mL/min. The samples were detected at a wavelength of 270 nm. To calculate the amount of DRSP, a 6-point-calibration was performed using an external DRSP standard. The data were analysed by using the software Empower™ 2 (Waters GmbH, Eschborn, Germany). The relative ratio of isoDRSP and DRSP was determined by comparing the peak areas of both compounds. The retention times were known.

2.3 Solubility of DRSP with and without addition of stabilising agents

70 mg/g of DRSP was dispersed in sesame oil, castor oil or MCT with or without addition of a stabilising agent by sonication at 5 x 10% cycle, 100% power for 5 min using an ultrasound device (Bandelin Sonopuls HD2070, Bandelin electronic GmbH&Co.KG, Berlin, Germany). As stabilising agents, 0.2% (w/w) methyl cholate, Aerosil® 200 Pharma and R972 Pharma, as well as 2% (w/w) Span® 83, lecithin, and cholesteryl oleate were used. Thereafter, the samples were blended for 3 d using a roller mixer. Furthermore, 70 mg/g of DRSP was suspended in USP phosphate buffer pH 6.8. The amount of DRSP was analysed like described in **section 2.2** using HPLC with UV detection.

2.4 Determination of viscosity and rheological properties by a parallel plate rheometer

A rheological determination of viscosity was performed by a parallel plate system (Gemini II, Malvern Instruments GmbH, Herrenberg, Germany). Stabilising agents and preparation of samples was described in **sections 2.2 and 2.3**. Thereafter, suspensions were centrifuged at 2000 rpm for 30 min (Heraeus® Biofuge® Fresco, 4x15 mL, DJB Labcare Ltd., Buckinghamshire, UK) (castor oil suspensions were centrifuged twice). The clear supernatants were analysed using a plate with a diameter of 40 mm, at a gap width of 1 mm and 20°C. The samples were dropped on the tempered plate. After adjustment of the gap width and 15 min at rest without stressing, the measurements were started. Firstly, the viscosity of formulations was determined at low shear of 0.2 Pa and 1 Hz

every 10 s over 1 min simulating resting state. Furthermore, the instantaneous viscosity under shear stress was investigated. The shear rate was increased from 1 to 20 s⁻¹ and in the following decreased to 1 s⁻¹ over 2 x 180 s.

2.5 Evaluation of syringeability and injectability

The terms syringeability and injectability were defined in detail by *Boylan and Nail* [11] and *Crowder et al.* [22]. 1 mL of sesame oil or MCT was filled in glass syringes with 27 G ½ staked-on needles (n = 10). The cylindrical tube had an inner diameter of 6.35 mm. The syringes were clamped into a materials testing machine (Type Z010, Zwick Roell AG, Ulm, Germany). The liquid was expelled from syringes with a defined force. Time for depletion of formulation was determined. The syringes should be completely depleted within 10 s. Furthermore, 0.5 mL of MCT containing 70 mg DRSP was drawn into 1 mL plastic syringes (Tuberkulin 1x100 Soft-Ject, Henke Sass Wolf GmbH, Tuttlingen, Germany) (n = 5). The barrel had an inner diameter of 4.25 mm. Due to the smaller inner diameter, the force required to expel the suspensions from plastic syringe were assumed to be 2 – 2.5 times lower compared to glass syringes. The plastic syringes were applied with 23 G 25 mm or 27 G 13 mm needles. The prefilled syringes, inserted into the force tester, were emptied within 10 s. The force being necessary for complete depletion was recorded.

2.6 Particle size analysis of DRSP microcrystals by laser diffraction after storage

Changes in particle size during storage were determined exemplary on 1% (w/w) DRSP MCS. Prior to preparation, vehicles were saturated with DRSP to avoid any influence by drug solubility of vehicles and to achieve a constant amount of DRSP microcrystals in the suspensions. Thus, the vehicles were prepared by dispersing DRSP in castor oil, sesame oil, MCT, or water under stirring for 3 d using a roller mixer. Thereafter, the fluids were separated from undissolved drug substance by double suction filtration using filter papers (GF/B, Whatman®, Whatman GmbH, Dassel, Germany). For preparation of suspensions without stabilising agents, 200 mg of DRSP was added to 20 g of DRSP saturated vehicle. The mixtures were blended by magnetic stirrer and roller mixer. For preparation of suspensions with stabilising agents, the excipient was dispersed in 20 g of DRSP saturated vehicle by sonication at 5x10% cycle, 100% power until getting a clear solution. The tested stabilising agents and their used concentrations were described in **section 2.3**. After cooling, 200 mg of DRSP was added. All samples were stored tightly closed in wide-neck brown glass flasks in an environmental chamber at 25°C and a relative humidity of 60% for 1 year. The particle size of DRSP microcrystals was determined by laser diffraction (Sympatec GmbH System-Partikel-Technik, Clausthal-Zellerfeld, Germany) (sensor: Helos, dispersing unit: Cuvette; 50 mL, software: Windox 5). Before measurement, the samples were blended by a roller mixer for 12 h. A few drops of the suspensions were diluted in 50 mL of MCT saturated with DRSP under moderate stirring by a magnetic stirrer integrated in the measurement apparatus. All oil-based vehicles were soluble in

the fluid. The dilution medium was prepared by dispersing an excess of DRSP in MCT under stirring for 24 h and filtration of the undissolved drug substance by vacuum filtration (Nalgene sterile bottle filters, Nalgene® Labware, Fisher Scientific GmbH, Schwerte, Germany). The initial particle size distribution of DRSP microcrystals was determined by suspending the drug substance in the dilution medium. Aqueous DRSP suspension were diluted in 50 mL of water saturated with DRSP, prepared analogous to DRSP saturated MCT. Particle sizes between 0.5 and 175 μm were measured over 10 s. The optical particle concentration was allowed to range between 5 and 50%. For all samples, blank values of the dilution media were determined before measuring. Furthermore, blank tests of the vehicles with and without addition of stabilising agents were performed. The median particle sizes of volume-weighted particle size distribution were recorded.

2.7 Measurement of contact angle using static sessile drop method

Sessile drop method was an optical contact angle method for estimation of the wetting behaviour of liquids on a solid surface (**Fig. 1**). During static contact angle measurement, the size of the drop was not changed. The measurement was carried out on a DSA 10 calculating with software version 1.80 (Krüss GmbH, Hamburg, Germany). Prior to contact angle determination, pellets of DRSP were prepared using a materials testing machine. Therefore, about 100 mg drug substance was moulded by using pressing forces of 10 t for 30 min. The contact angles of sesame oil, castor oil and MCT were determined. For analysing the influence of stabilising agents on wetting behaviour, castor oil mixed with 0.2% (w/w) Aerosil® 200 or R972 Pharma, or 2% (w/w) cholesteryl oleate was used. To avoid dissolving of DRSP pellet during contact angle measurement, the liquids were saturated with DRSP. Preparation of samples was described in **sections 2.2 and 2.3**. Suspensions were centrifuged like described in **section 2.4**. The supernatants were dropped on the surface of the DRSP pellets. Therefore, the fluid was pumped through a capillary located above the solid and was dropped on the clean solid surface (**Fig. 1**). The angle between baseline of the drop and the tangent at the drop boundary was plotted over time ($n = 5$).

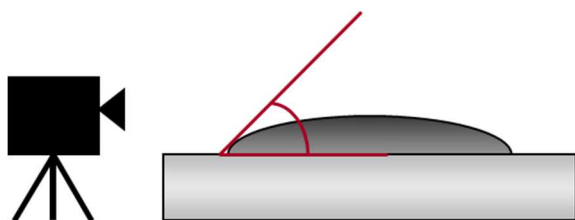


Fig. 1 Optical contact angle measurement by sessile drop method. Liquid was dropped on a solid surface. Thereafter, angles between baseline of the drop and tangent of the drop were determined.

2.8 Analysis of sedimentation using image analysis

Changes in particle size during storage were determined exemplarily on 1% (w/w) DRSP MCS. Preparation of samples with or without addition of stabilising agents was described in **section 2.6**. For analysing sedimentation, suspensions were photographed after 30 d. The level of sediment and

supernatant was measured. Therefore the software Axio Vision 4.5, Carl Zeiss Imaging Solutions (Carl Zeiss AG, Oberkochen, Germany) was used. The relative ratio between height of sediment and total height of sample was calculated. For evaluation of the results, the sedimentation volume F , the ratio between the volume of sediment and the total volume of the suspensions was calculated [12,23].

2.9 Statistics

The experiments were conducted in triplicate, where not otherwise stated. Arithmetic mean values as well as standard deviations were calculated. The 95% confidence interval was computed to compare two different sample groups.

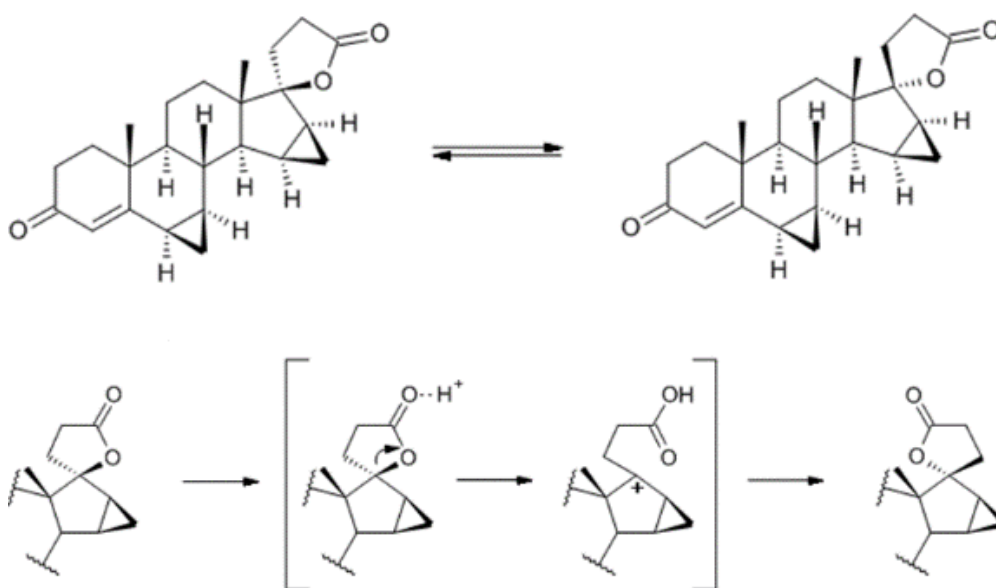


Fig. 2 DRSP and the epimer isoDRSP.

3 Results and discussion

3.1 Chemical stability of DRSP in aqueous and oil-based vehicles

With a solubility of $11.6 \pm 0.3 \mu\text{g/mL}$, DRSP was practically insoluble in USP phosphate buffer pH 6.8 and was furthermore chemically instable in aqueous medium, especially at acidic pH. During storage, the $15\beta,16\beta$ -methylene derivative of spironolactone isomerised due to a change in configuration at position 17 resulting in formation of the DRSP epimer isoDRSP (see **Fig. 2**). The extent of isomerisation in USP phosphate buffer pH 6.8 is presented in **Tab. 1**.

Tab. 1 Isomerisation of DRSP in USP phosphate buffer at pH 6.8 (n = 3).

Time of storage in d	Relative amount of isoDRSP in %
2	7.6 ± 0.7
14	10.9 ± 1.7
42	30.1 ± 5.2

After storage of 42 d, an obvious degradation of DRSP into isoDRSP was detected as measured by a relative ratio of 70% DRSP to 30% isoDRSP. On the other hand, no traces of isoDRSP were detected in MCT, sesame oil or castor oil after 1 year storage (see **Fig. 3**). Consequently, an oil-based solution or suspension would be an option for a chemically storage-stable formulation of DRSP.

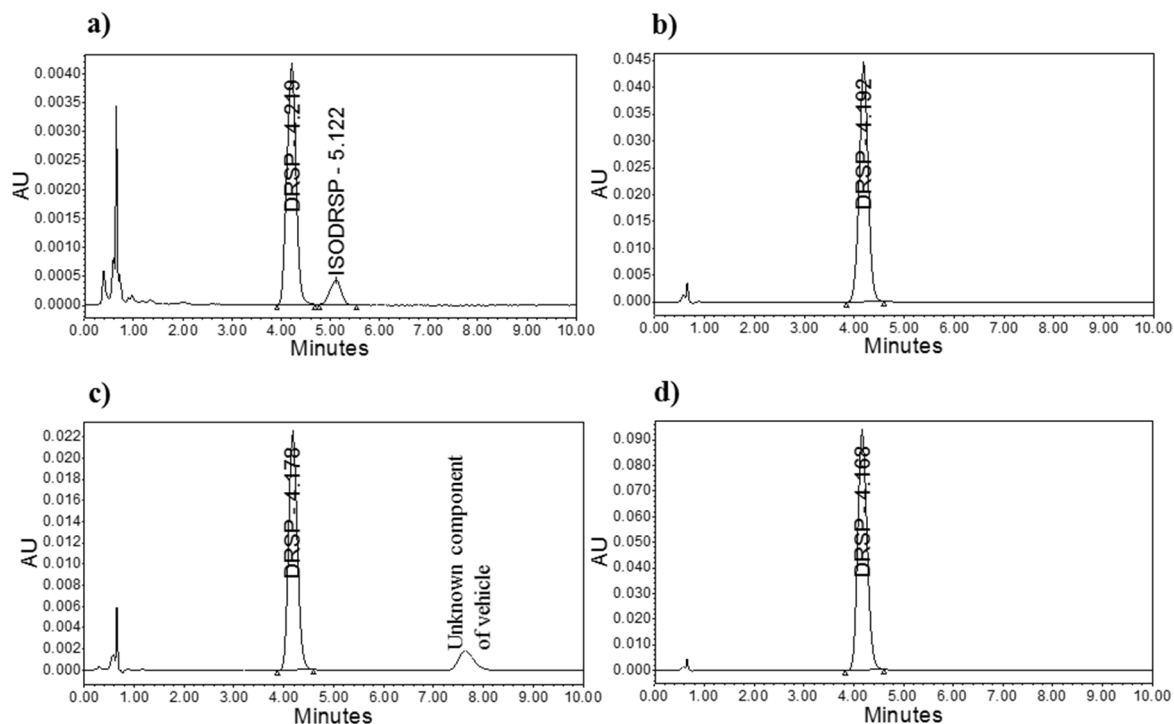


Fig. 3 HPLC chromatograms of DRSP suspended in **a)** USP phosphate buffer pH 6.8 after storage of 14 d at room temperature, **b)** MCT, **c)** sesame oil, and **d)** castor oil after storage of 1 year at 25°C (n = 3). IsoDRSP was only found in aqueous suspension.

3.2 Solubility of DRSP

First of all, an adequate DRSP dose for a once-a-month injection was calculated. Oral contraceptives contained 3 mg DRSP. 76% of the drug substance was bioavailable after oral administration [5]. A dose of at least 2 mg of DRSP per day was computed for i.m. or s.c. application, respectively. Therefore, at least 60 to 70 mg of DRSP should be necessary for a once-a-month injection. Depending on the injection site, the administered volume should be less than 5 mL for i.m. injection and less than 2 mL but optimally 0.5 mL for s.c. application [10,24]. With respect to the calculated dose, the solubility of DRSP in oil-based vehicles was tested (see **Tab. 2**). Less than 10 mg/mL DRS was soluble in MCT and sesame oil. Furthermore, about 12 mg/mL drug substance was dissolvable in castor oil.

Tab. 2 Viscosity and DRSP solubility of MCT, sesame oil, and castor oil without and with addition of stabilising agents. Viscosity was investigated at 0.2 Pa as well as at 20 s⁻¹ and 20°C using a rheometer (n = 3).

	Concentration in % (w/w)	Solubility of DRSP in mg/mL	Instantaneous viscosity at 0.2 Pa, 20°C in mPas	Instantaneous viscosity at 20 s ⁻¹ , 20°C in mPas
MCT + excipient				
-	-	6.9 ± 0.3	31.1 ± 1.1	30.2 ± 0.9
Lecithin	2	7.0 ± 0.1	-	-
Span® 83	2	6.7 ± 0.5	33.6 ± 0.0	32.2 ± 2.7
Cholesteryl oleate	2	6.5 ± 0.1	31.3 ± 0.9	30.3 ± 0.9
Methyl cholate	0.2	7.0 ± 0.5	31.9 ± 0.8	32.1 ± 1.5
Aerosil® 200 Pharma	0.2	7.0 ± 0.1	32.7 ± 1.9	27.6 ± 1.7
Aerosil® R972 Pharma	0.2	6.8 ± 0.1	31.3 ± 1.2	28.3 ± 3.6
Sesame oil + excipient				
-	-	3.9 ± 0.2	77.5 ± 0.3	79.6 ± 2.0
Lecithin	2	4.0 ± 0.4	-	-
Span® 83	2	3.9 ± 0.5	81.7 ± 1.1	79.5 ± 7.8
Cholesteryl oleate	2	3.7 ± 0.7	72.3 ± 1.2	73.3 ± 5.4
Methyl cholate	0.2	3.7 ± 0.4	75.1 ± 2.6	77.5 ± 2.7
Aerosil® 200 Pharma	0.2	3.8 ± 0.3	77.0 ± 0.8	76.1 ± 1.7
Aerosil® R972 Pharma	0.2	3.9 ± 0.7	79.5 ± 1.0	80.7 ± 5.9
Castor oil + excipient				
-	-	12.3 ± 0.4	1032.3 ± 34.1	942.2 ± 15.1
			1134.0 ± 54.4 ^a	1117.8 ± 29.3 ^a
Lecithin	2	12.4 ± 0.4	-	-
Span® 83	2	12.1 ± 0.4	1080.6 ± 14.3 ^a	1071.3 ± 25.1 ^a
Cholesteryl oleate	2	12.5 ± 0.2	1048.4 ± 12.5	1045.0 ± 23.3
Methyl cholate	0.2	12.1 ± 0.2	1137.4 ± 11.4 ^a	1126.8 ± 32.2 ^a
Aerosil® 200 Pharma	0.2	12.1 ± 0.7	1003.6 ± 10.6	978.8 ± 9.3
Aerosil® R972 Pharma	0.2	12.3 ± 0.8	1157.7 ± 16.8 ^a	1144.0 ± 32.5 ^a

^aBatch II of castor oil

3.3 Viscosity of oil-based vehicles

The viscosity of MCT, sesame oil and castor oil is shown in **Tab. 2**. With a dynamic viscosity of about 1000 mPas, castor oil was not suitable for parenteral administration. Nevertheless, the liquid was used as model vehicle for an oil-based DRSP suspension regarding storage stability in dependence on viscosity. MCT had the lowest viscosity.

3.4 Syringeability and injectability

Advantageously, using an autoinjector, the formulations could be injected s.c. by the patients themselves. It should be analysed if an injection of oil-based DRSP MCS via autoinjector was possible and which needle size should be used. Referring to *Rungseevijitprapa and Bodmeier* [25], formulations were easy to inject using injection forces of up to 50 N. Furthermore, injection forces over 100 N were evaluated to increase the risk of glass barrel burst during administration via autoinjector. However, over 100 N were necessary to inject 1 mL of sesame oil with 27 G syringes. Although, 1 mL of MCT passed through 27 G needles within 10 s using a force of 45 N, 1 mL of DRSP MCT suspensions could not be ejected applying a force below 100 N. Referring to the Hagen–Poiseuille equation (see **Equation 1**) different approaches might be possible to reduce the injection force.

$$\frac{dV}{dt} = \frac{\pi \cdot r^4}{8 \cdot \eta} \cdot \frac{\Delta p}{l}$$

Equation 1 where dV/dt = volumetric flow rate, r = internal radius of the tube, l = length of the tube, Δp = pressure drop and η = dynamic fluid viscosity. Hagen–Poiseuille law gave the voluminal laminar stationary flow of a uniform viscous fluid being incompressible, through a long cylindrical pipe with a constant circular cross-section [18].

One option was the prolongation of injection to 20 – 30 s. It was assumed that this would be less convenient for the patient's compliance and was therefore not followed up. Furthermore, the reduction of injection volume should decrease the injection force. However, about 30 N was still necessary to eject 0.5 mL of DRSP MCT dispersion from a plastic syringe through a 27 G needle. The force would be 2 – 2.5 times higher for injection with an autoinjector used with a glass barrel. Thus, this formulation might only be injected with difficulties. As needle size was shown to have no significant influence on injection pain, another possibilities was to use needles with larger inner diameter [26]. Most oil-based solutions and microparticulate formulations were administered with 19 – 25 G needles every 4 – 12 weeks [10]. For s.c. administration, 23 G or thinner needles were used [26,27]. An average force of only about 10 N was necessary to expel 0.5 mL of DRSP MCT suspension from plastic syringes with 23 G needles. Consequently, the formulation should be easy to inject via a conventional autoinjector used with 23 G needles. In general, DRSP sesame oil suspensions might not be s.c. applicable using an autoinjector with 23 G or smaller needles. Nevertheless, the formulations could be used for i.m. application.

3.5 Particle size analysis of DRSP MCS after storage

For micronised DRSP, an average median particle size of $11.6 \pm 2.5 \mu\text{m}$ was determined. In general, DRSP microcrystals had a median particle size of about $5 \mu\text{m}$ after micronisation measured by laser diffraction of dry powder samples (unpublished results). The discrepancy

between measurement results could be explained by particle growth during storage of DRSP powder or aggregation of microcrystals during sample preparation. Furthermore, particle size measurement could vary as a function of the type of instrument used for determination [13,20]. As expected, a relatively large median particle size was measured after storage of 1 year in aqueous suspension (see **Fig. 4**). DRSP was a relatively hydrophobic substance tending to agglomeration in aqueous fluids without stabilising agents. Furthermore, crystal growth could cause an increase of particle sizes. In general, median particle sizes were smaller in lipophilic vehicles than in aqueous medium. As higher the viscosity of oil-based vehicle was as smaller was the median particle size of DRSP microcrystals after storage. Like assumed, it seemed that a higher viscosity prevented growth of particles. Nevertheless, the median particle size of DRSP increased significantly in all tested fluids without addition of stabilising agents.

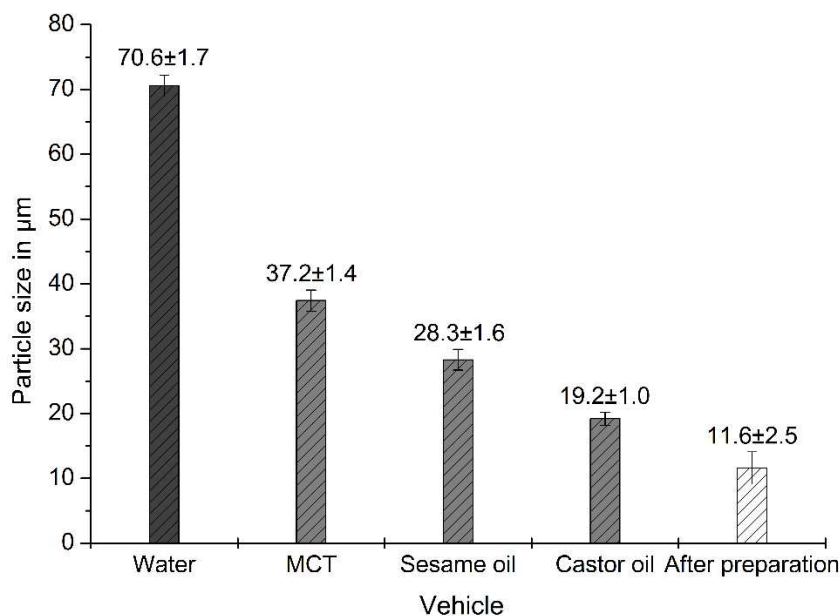


Fig. 4 Median particle sizes of DRSP suspended in water and different oils after storage of 1 year at 25°C and of the raw material suspended in dilution medium (n = 3).

The suspensions were also investigated by optical microscopy followed by determination via image analysis counting and sizing system [4]. No significant differences between number-weighted median particle sizes after storage of sesame oil, MCT, or castor oil suspensions were detected. For measurement, an object slide was pressed on the oil drop. Aggregated particles might be separated by the pressure indicating loose aggregation of particles.

3.6 Influence of stabilising agents on solubility of DRSP

The addition of stabilising agents could change the solubility due to solubilisation effects. No significant difference in solubility of DRSP with or without addition of stabilising agents is shown (**Tab. 2**).

3.7 Influence of stabilising agents on viscosity of vehicle

A possible thickening effect of stabilising agents was investigated (see **Tab. 2**). Even at a low shear, air bubbles were formed in samples containing lecithin (unpublished results). The rheometrical method did not seem to be suitable for this formulation. For MCT or sesame oil, the viscosity was slightly increased with addition of Span® 83. The excipient was a high viscous liquid being miscible with the vehicles. For MCT formulations including silica derivatives, viscosity at low shear was slightly higher compared to viscosity at high shear. Nevertheless, the differences were not significant. For preparation of castor oil DRSP suspensions, two different batches of the vegetable oil were used providing different viscosities. Stabilising agents caused no significant increase in viscosity.

3.8 Particle size analysis of DRSP MCS in addition of stabilising agents

The addition of the amphiphilic substances Span® 83 and lecithin did not affect the particle size of DRSP positively at storage, independently from the oil-based vehicle used (**Fig. 5**). In general, slight but no significant changes in median particle sizes could be observed for formulations containing methyl cholate. Interestingly, the addition of cholesteryl oleate to MCT and sesame oil suspensions led to median particle sizes being significantly smaller compared to non-stabilised suspensions indicating a stabilising effect. Due to just moderate particle growth in high viscous castor oil suspensions, only a slight influence on DRSP particle size was detected by addition of excipients.

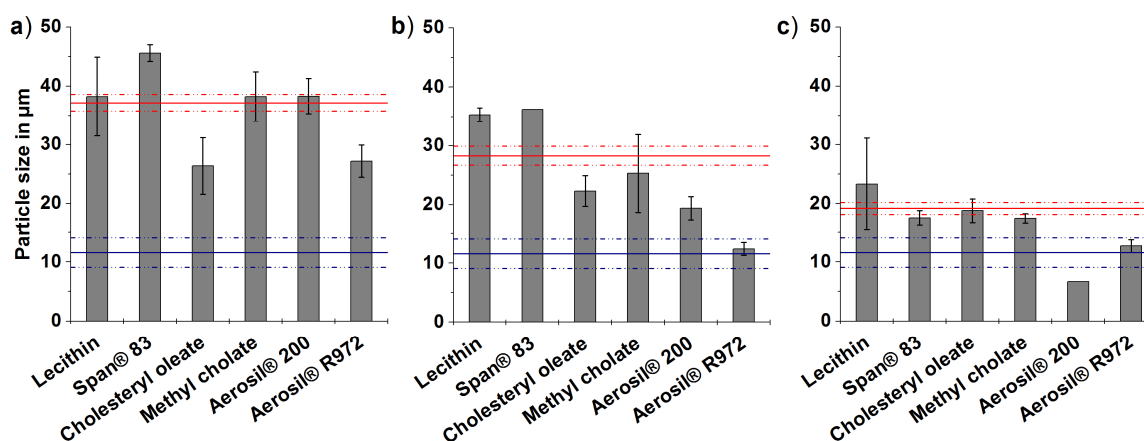


Fig. 5 Median particle size of DRSP microcrystals suspended in **a)** MCT, **b)** sesame oil, and **c)** castor oil with addition of stabilising agents after storage of 1 year at 25°C (n = 3). The median particle sizes of oil-based vehicles without addition of stabilising agents are shown as upper red line, the median particle size of DRSP in suspension before storage is shown as lower blue line (range of standard deviation in dotted lines).

Moreover, when Aerosil® 200 Pharma was added to sesame oil or castor oil suspensions, DRSP microcrystals had a significantly smaller median particle size after storage of 1 year in comparison to non-stabilised dispersions. The median particle size of DRSP in castor oil with addition of the

silica derivative was even smaller than median particle size determined after preparation of suspensions. They were comparable to particle sizes of DRSP powder analysed by laser diffraction of dry powder samples after micronisation. The results indicated that a slight aggregation of microcrystals might already take place during sample preparation before storage. No significant disparities were detected between particles suspended in MCT with or without Aerosil® 200 Pharma. The added amount of Aerosil® 200 Pharma might be too low to cause an effect.

A significantly positive effect of Aerosil® R972 Pharma on reduction of particle growth was observed for all test fluids. Stabilisation of suspensions by addition of small amounts of highly dispersed silicon dioxide in aqueous medium without increasing viscosity was described by *Turck and Schmelmer* [28]. Here, this effect could be shown for the tested oil-based systems with addition of hydrophobic colloidal anhydrous silica and without addition of any other stabilising agents. Silica derivatives possibly formed stabilising structures, before they gelled the vehicle. Furthermore, an interaction between DRSP molecules and silica molecule by van der Waals force could prevent aggregation.

3.9 Contact angle between DRSP and castor oil with addition of stabilising agent

The contact angle between DRSP and MCT or sesame oil without addition of stabilising agents were very small, due to relatively rapid spreading over time ($11.8 \pm 2.9^\circ$ for sesame oil, $2.1 \pm 2.2^\circ$ for MCT determined at 1 s). Furthermore, the uniform deposition of the oil droplet was challenging, resulting in a relatively high standard deviation. Hence, slight changes in contact angle by addition of stabilising agents were hard to detect. A contact angle of $42.1 \pm 5.5^\circ$ was determined between castor oil and DRSP, at 1 s. With addition of silica derivatives, influencing the particle sizes significantly, only slightly higher contact angles were determined (Aerosil® 200 Pharma $49.1 \pm 5.7^\circ$, Aerosil® R972 Pharma $49.9 \pm 5.6^\circ$). The difference was not significant. Cholesteryl oleate had an effect on DRSP particle sizes in sesame oil and MCT. The contact angles between castor oil with addition of cholesteryl oleate and DRSP were slightly lower in comparison to non-stabilised castor oil ($33.4 \pm 6.8^\circ$ at 1 s). Again, the disparity was not significant. Oil-based vehicles did not show the high surface tension of water. Thus, a stabilising effect of excipients decreasing the surface tension might be lower on oil-based vehicles.

3.10 Influence of stabilising agents on sedimentation of DRSP microcrystals

After 1 month of storage neither a marked sedimentation nor a clear supernatant occurred in castor oil suspensions with or without addition of any stabilising agent. Caking was no issue for all oil-based suspension with or without addition of stabilising agents. Even after storage of 1 year, all suspensions were easily redispersible. Span® 83, lecithin, cholesteryl oleate, and methyl cholate had no influence on sedimentation of microcrystals suspended in sesame oil or MCT (see **Fig. 6**).

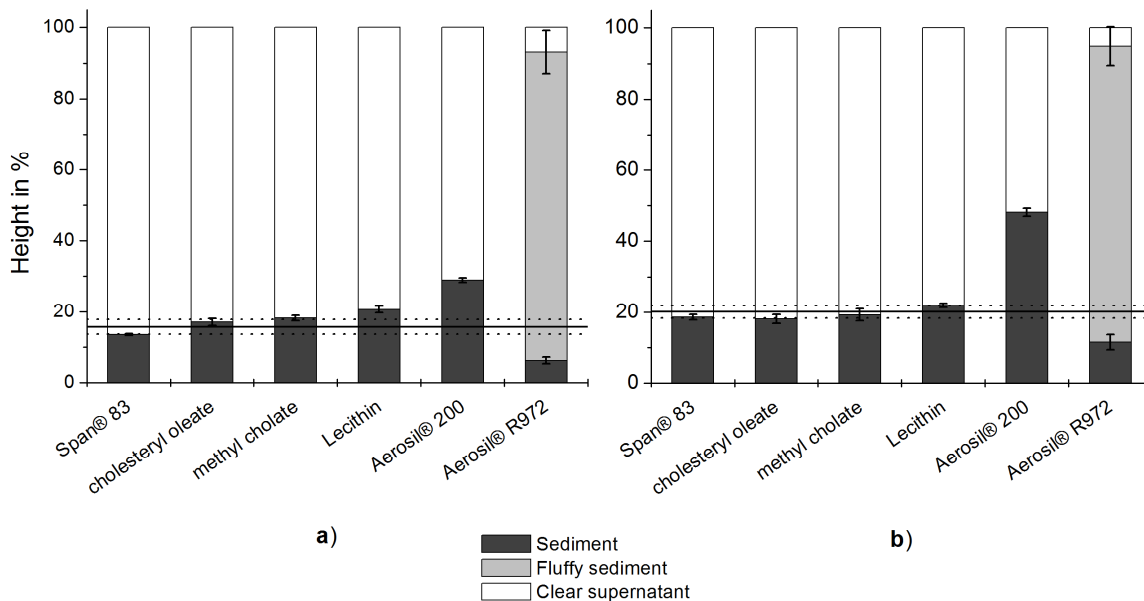


Fig. 6 Sedimentation of DRSP in **a)** MCT and **b)** sesame oil with or without addition of stabilising agents after storage of 1 month ($n = 3$). Sedimentation of MCT DRSP without addition of stabilising agents is shown as solid line (range of standard deviation in dotted lines).

Sediments of DRSP in MCT or sesame oil were fluffier by addition of Aerosil® 200 Pharma. Furthermore, the sedimentation was significantly slower compared to formulations without stabilising agent. The addition of 0.2% (w/w) Aerosil® R972 Pharma to MCT or sesame oil was found to have the highest impact on sedimentation; only low compact sediment was formed. The level of supernatant was relatively low ($F = 0.9$). As silica derivatives decreased sedimentation of DRSP microcrystals, this could result in decelerated particle growth and consequently in higher stability. Furthermore, sedimentation during manufacturing could be slowed down improving content uniformity. A possible explanation could be the formation of stabilising structures without significant increasing of vehicle viscosity. Interestingly, sedimentation was more reduced by addition of Aerosil® R972 Pharma, than by Aerosil® 200 Pharma although for complete immobilization of the liquid, higher amounts of hydrophobic colloidal anhydrous silica were necessary (12% (w/w) Aerosil® R972 Pharma, 3% (w/w) Aerosil® 200 Pharma in MCT; unpublished results). Less self-aggregation of Aerosil® R972 Pharma was caused by the lower amount of hydroxyl groups [29]. On the other hand, a stronger affinity between molecules of hydrophobic colloidal anhydrous silica and the steroidal drug substance via van der Waals bonds might be conceivable.

4 Conclusion

Oil-based DRSP suspensions showed a high chemical stability. Suspensions of the drug substance in MCT, sesame oil, and castor oil were investigated regarding their physical stability. High viscosity reduced sedimentation and particle growth. On the other hand, only low viscous MCT

was suitable for s.c. injection via an autoinjector. Sesame oil was i.m. injectable. Thus, it should be shown if the addition of excipients improved the physical stability of oil-based suspensions without increasing viscosity. All tested compounds did not influence the solubility of DRSP in the tested concentration. As desired, no thickening effect was observed with addition of any stabilising agent in the tested concentrations. The addition of Aerosil® 200 Pharma reduced particle growth of DRSP microcrystals in castor oil and sesame oil as well as sedimentation in all vehicles. Moreover, the addition of Aerosil® R972 Pharma even led to a decrease in particle growth and sedimentation in all tested DRSP formulations. It avoided an increase in median particle size completely in sesame oil and castor oil preparations in the tested timeframe. As a consequence, the physical stability of oil-based DRSP MCS during manufacturing and storage could be significantly increased by addition of silica derivatives. In contrast to crystalline silicone dioxide, sol-gel derived glasses containing silica did not induce significant toxicity, showed biocompatibility, and was excreted in soluble form through the kidneys. The degradation rate could be controlled by synthesis [30,31]. Therefore, a use in parenteral application might be possible.

References

- [1] B. Wang, T. Siahaan, and R. Soltero, *Drug delivery: principles and applications*, Wiley-Interscience, New Jersey, USA, 2005.
- [2] D.J. Burgess, D.J.A. Crommelin, A.S. Hussain, and Chen M.-L., *Assuring Quality and Performance of Sustained and Controlled Release Parenterals: Workshop Report*, *Eur. J. Pharm. Sci.*, 21 (2004) 679-690.
- [3] E.S. Linn, *Progress in contraception: new technology*, *Int. J. Fertil. Womens Med.*, 48 (2003) 182-191.
- [4] S. Nippe and S. General. 2010, *Formulation comprising drospirenone for subcutaneous or intramuscular administration*. [WO/2010/094623]. 12-2-2010.
- [5] Bayer, Fachinformation® Yasmin. <http://www.fachinfo.de>. 2010. Rote Liste® Service GmbH. 8-8-2010.
- [6] C. d'Arcangues and Snow R.C., *Injectable Contraceptives*, in: T. Rabe and B. Runnebaum (Eds.), *Fertility Control Update and Trends*, Springer-Verlag, Heidelberg, 1999, pp. 121-149.
- [7] S. Gupta, *Non-oral hormonal contraception*, *Curr. Obstet. Gynaecol.*, 16 (2006) 30-38.
- [8] Fachinformation. <http://www.fachinfo.de>. 2010. Rote Liste® Service GmbH. 8-8-2010.
- [9] M.J. Akers, A.L. Fites, and R.L. Robison, *Formulation design and development of parenteral suspensions*, *J. Parenter. Sci. Technol.*, 41 (1987) 88-96.
- [10] A. Rutz, *Ölige Suspensionen als parenterale Depotsysteme für rekombinante Proteine*. 2007. LMU München
- [11] J.C. Boylan and S.L. Nail, *Parenteral Products*, in: G.S. Banker and C.T. Rhodes (Eds.), *Modern Pharmaceutics*, Marcel Dekker, Inc., New York, 2002, pp. 576-625.
- [12] W. Rungseewijitprapa, F. Siepman, J. Siepman, and O. Paeratakul, *Disperse Systems*, in: A.T. Florence and J. Siepman (Eds.), *Modern Pharmaceutics Volume 1 Basic Principle and Systems*, Vol. 1. Informa Healthcare, New York, London, 2009, pp. 357-421.
- [13] J. Wong, A. Brugger, A. Khare, M. Chaubal, P. P.Papadopoulos, B. B.Rabinow, J. Kipp, and J. Ning, *Suspensions for intravenous (IV) injection: A review of development, preclinical and clinical aspects*, *Adv. Drug Deliv. Rev.*, 60 (2008) 938-954.
- [14] R. Nash, *Suspensions*, in: J. Swabrick (Ed.), *Encyclopedia of Pharmaceutical Technology*, Vol. 6. Informa Healthcare, New York, USA, 2006, pp. 3597-3610.
- [15] B.J. Bowman, C.M.I. Ofner, and H. Schott, *Colloidal Dispersions*, in: D.B. Troy and M.J. Hauber (Eds.), *Remington The Science and Practice of Pharmacy*, Lippincott Williams & Wilkins, Baltimore, 2005, pp. 293-318.
- [16] J. Swabrick, J.T. Rubino, and O.P. Rubino, *Coarse Dispersions*, in: D.B. Troy and M.J. Hauber (Eds.), *Remington The Science and Practice of Pharmacy*, Lippincott Williams & Wilkins, Baltimore, 2005, pp. 319-337.
- [17] T.F. Tadros, *Applied Surfactants: principles and applications*, Wiley-VCH Verlag GmbH & Co.KGaA, Weinheim, 2005.
- [18] Y. Ali, A. Kimura, M.J. Coffey, and P. Tyle, *Pharmaceutical Development of Suspension Dosage Form*, in: A.K. Kulshreshtha, O.N. Singh, and G.M. Wall (Eds.), *Pharmaceutical Suspensions: From Formulation Development to Manufacturing*, Springer, New York, 2010, pp. 103-126.

- [19] M.B. Dexter and M.J. Schott, The Evaluation of the Force to Expel Oily Injection Vehicles from Syringes, *J. Pharm. Pharmacol.*, 31 (1979) 497-500.
- [20] M. Martinez, M. Rathbone, D. Burgess, and M. Huynh, In vitro and in vivo considerations associated with parenteral sustained release products: A review based upon information presented and points expressed at the 2007 Controlled Release Society Annual Meeting, *J. Control. Release*, 129 (2008) 79-87.
- [21] R.C. Rowe, P.J. Sheskey, and P.J. Weller, *Handbook of Pharmaceutical Excipients*, Pharmaceutical Press, London, 2003.
- [22] T.M. Crowder, A.J. Hickey, M.D. Louey, and N. Orr, *A guide to pharmaceutical particulate science*, Interpharm/CRC, Boca Raton, London, New York, Washington D.C., 2003.
- [23] S. Kölling, *Die Stabilisierung öligiger Suspensionen*. 2007. Rheinischen Friedrich-Wilhelms-Universität Bonn.
- [24] R.G. Strickley, Solubilizing Excipients in Oral and Injectable Formulations, *Pharm. Res.*, 21 (2004) 201-230.
- [25] W. Rungseewijitprapa and R. Bodmeier, Injectability of biodegradable in situ forming microparticle systems (ISM), *Eur. J. Pharm. Sci.*, 36 (2009) 524-531.
- [26] B.S.I. Montgomery, J.P. Borwell, and Higgins D.M., Does needle size matter? Patient experience of luteinising hormone-releasing hormone analogue injection, *Prostate Cancer Prostatic Dis.*, 8 (2005) 66-68.
- [27] S.S. Ricci and T. Kyle, *Maternity and Pediatric Nursing*, Lippincott Williams & Wilkins, Philadelphia, 2009
- [28] D. Türck and Schmelmer V. 2001, Oral Suspension of pharmaceutical substances. [US 6184220]. 6-2-2001.
- [29] Evonik, Aerosil®, Product Information. 2010.
- [30] L. Hench and J. Wilson, Biocompatibility of silicates for medical use, in: M. O'Connor (Ed.), *Silicon Biochemistry*, Wiley, Chichester, 1986, pp. 231-246.
- [31] P. Korteso, Sol-gel derived silica gel monoliths and microparticles as carrier in controlled drug delivery in tissue administration. 2001. University of Helsinki.

CHAPTER 3

Investigation of injectable drospirenone organogels with regard to their rheology and comparison to non-stabilized oil-based drospirenone suspensions

Published in Drug Development and Industrial Pharmacy, 2014, Early Online: 1–11

<http://informahealthcare.com/doi/pdf/10.3109/03639045.2014.895375>

Abstract

The objective of this study was to evaluate organogels as potential injectable drug-delivery systems for drospirenone (DRSP). Recently, studies on organogel characterization with focus on the parenteral injection are rarely to find in the literature. DRSP organogels contained the drug suspended in medium-chain triglycerides and were stabilized by various organogelators. The DRSP organogels were assessed in comparison to non-stabilized DRSP microcrystal suspensions (MCSs). Furthermore, rheological properties of the organogels, in particular the elastic modulus (G'), the complex viscosity (η^*), and the elasticity, were evaluated with respect to the long-term stability, syringeability/injectability, and *in vitro* release. DRSP organogels showed significantly improved storage stability compared to non-stabilized MCSs with regard to sedimentation and particle growth. Furthermore, all of the DRSP organogels showed shear-thinning behavior. Thus, ejection from syringes was possible by an autoinjector using 23 G needles comparable to non-stabilized MCSs. Nevertheless, DRSP organogels exhibited significantly more sustained drug release than non-stabilized MCSs most likely caused by partial recovery of the organogelator structures at 37°C after destruction. Consequently, DRSP organogels were evaluated to be superior to conventional non-stabilized MCSs. Silica organogels which provided the highest elasticity, moderate G' and η^* , and avoided most efficiently particle growth are slightly more preferable compared to the other DRSP organogels.

Konzeption:

Stefanie Nippe, Mitarbeit an Konzeption Sascha General

Durchführung:

Stefanie Nippe

Berichtsabfassung:

Stefanie Nippe

1 Introduction

Gel formulations as injectable drug-delivery systems have been of growing interest in the past decades [1-3]. In contrast to microspheres, no toxic solvents are necessary for their preparation [4]. Gels are described as semi-solid materials containing low concentrations (< 15%) of gelator [3]. Compared with hydrogels, there is less knowledge about injectable gels formed in vegetable or semi-synthetic oils [1]. Gels of oils and organic solvents are mostly prepared by dissolving the gelator in the hydrophobic vehicle at a higher temperature. Thereafter, the gelator-solvent affinity is decreased upon cooling, resulting in the self-assembly of gelator molecules into a gel scaffold [5]. Gelator molecules cross-link to form various aggregates, such as rods, tubules, fibers, and platelets [1]. For the elementary assemblies of a gel network, the rod-like mode is the most efficient form [6]. Suspensions containing the drug dispersed in aqueous or oil-based gel matrices could have a higher stability than conventional suspensions. In general, suspensions could show physical instabilities, e.g. sedimentation, caking and particle growth [7,8]. These issues cause challenges during manufacturing, filling processes and injection as well as variation in bioavailability [9,10]. To overcome these issues, one possibility might be to increase the viscosity of the external phase by gelator addition. However, increased vehicle viscosity might affect the ability to inject the drug-delivery systems. With regard to these considerations, our aim was to investigate subcutaneous (s.c.) injectable gels containing the drug substance drospirenone (DRSP) suspended in the relatively low viscous oil medium-chain triglycerides (MCT). The progestin DRSP is typically used in oral contraceptives [11,12]. DRSP is insufficiently soluble in water and vegetable oils and is unstable in aqueous systems. Thus, an oil-based DRSP microcrystal suspension (MCS) might be a formulation option for the parenteral administration. The physicochemical stability and syringeability of DRSP MCT MCSs stabilized by the addition of non-thickening excipients was described previously [13]. Currently, we investigated DRSP MCSs stabilized by the addition of organogel-forming excipients in comparison to non-stabilized MCSs. Ideally, the organogels should provide increased storage-stability without losing syringeability/injectability. Furthermore, stabilizing organogelator structures should optimally partially recover after administration to influence the drug release positively. Moreover, the rheological properties of the DRSP organogels were investigated and compared with the results of stability, ejection force and drug release tests. Our intention was to identify viscoelastic properties which help to assess the suitability of the organogelators for preparing s.c. injectable DRSP organogels.

2 Material and methods

2.1 Materials

DRSP (Bayer HealthCare Pharmaceuticals, Berlin, Germany), MCT (Myritol®318 PH, Cognis, Düsseldorf, Germany), aluminum stearate (AS) (Fluka Chemie, Buchs, Switzerland), silica

(Aerosil®200 Pharma, Degussa, Essen, Germany), methyl cholate (MC), cholesteryl stearate (CS) (Alfa Aesar, Karlsruhe, Germany), dextrin palmitate derivatives Rheopearl®TL2 (RTL2), Rheopearl®KL2 (RKL2), dextrin palmitate / ethyl hexanoate Rheopearl®TT2 (RTT2) (S. Black, Moers, Germany), hydroxypropyl- β -cyclodextrin (Kleptose®HPB, Roquette, Lestrem, France), potassium dihydrogen phosphate and sodium azide (Merck, Darmstadt, Germany) were used.

2.2 Preparation of organogels without and with DRSP and non-stabilized MCSs

AS, silica, CS, MC and dextrin palmitate derivatives were used as organogelators. They were dispersed in MCT by sonication (Bandelin Sonopuls HD2070, Bandelin electronic, Berlin, Germany) at 5 x 10% cycle, 100% power for 3-5 min (depending on the vehicle volume) until a clear solution was obtained, which, after cooling, resulted in a gel. AS organogels were prepared by heating a mixture of organogelator and MCT to 200°C under magnetically stirring, followed by slow cooling to room temperature (RT). To prepare DRSP organogels, DRSP in a concentration of 70 mg/0.5 g (daily oral dose: 2 mg) and the organogelator were mixed before addition of MCT. AS organogels were cooled for 5 min before addition of DRSP and were then magnetically stirred until the mixture started to gel. For the preparation of non-stabilized MCSs, 70 mg/0.5 g of DRSP was added to MCT and was dispersed by sonication at 5 x 10% cycle, 100% power for 5 min. The sol-gel transition concentration was reached when moderate movement and tipping did not lead to the flow of formulations. The liquid phase should be completely immobilized after preparation. Visually, no sedimentation of the organogelator or DRSP, phase separation nor inhomogeneity should be observed. Furthermore, the organogel structure was analyzed using optical microscopy (Zeiss Axio Imager A1m, software: AxioVision Rel. 4.5, Carl Zeiss Imaging, Jena, Germany).

2.3 Rheological testing

Organogels containing 3.0% (w/w) silica or AS, 1.5% (w/w) MC, 5.0% (w/w) CS or dextrin palmitate derivatives were investigated by a parallel plate rheometer (CVOR 200, Malvern Instruments, Herrenberg, Germany) in an oscillatory mode using a plate diameter of 40 mm at a gap width of 2 mm and a constant frequency of 1 Hz. Complex viscosity (η^*), storage/elastic modulus (G') and $\tan \delta$ calculated by the quotient of G' and the loss/viscous modulus (G'') were analyzed. After preparation, the samples were stored for one week at RT to guarantee complete gel formation. Then, they were put on a tempered plate cautiously using a spatula. To allow the organogels to recover from the stress of sample preparation, all measurements were started 15 min after gap width adjustment. First, the viscoelastic behavior of organogels without and with DRSP was investigated using a constant, low shear stress (τ) of 0.2 Pa at 20°C. The optimal τ was previously identified using an amplitude sweep. Under the optimized non-destructive conditions, η^* , G' , and G'' were nearly constant, simulating the viscoelastic properties at rest. The parameters were plotted every 9 s over 15 min. The last five measuring points were used for the average

calculation. Second, the viscoelastic behavior of the DRSP organogels under increased τ was examined (amplitude sweep). τ was raised from 0.1 to 150 Pa over 2 min at 20°C. τ -values measured at the first time point when $G' < G''$ are termed destructive τ . The flow curves were fitted to rheological models described in the **Supplement**. The square of Pearson product-moment correlation coefficients (r^2) was calculated using Excel (Microsoft, Redmond, SEA). Finally, the recovery of the DRSP organogels after destruction was determined. Therefore, the viscoelastic properties were determined at 20°C and at 37°C after pre-shearing over 2 min. The plates were tempered before sample addition. The pre-shear stress (pre- τ) ranged from 25 to 100 Pa depending on the formulation. The optimal pre- τ for the tested formulations was determined before the respective experiment: τ had to be high enough to guarantee $G' < G''$, but movements that were too fast led to the ejection of the samples from the gap. After stopping pre- τ , η^* , G' and G'' were plotted against time at a low shear of 0.2 Pa. The viscoelastic properties of the DRSP organogels were compared 30 s after destructive pre- τ was stopped.

2.4 Stability testing

10 g of organogels without and with DRSP were stored in closed vials at RT over three months. Formulations containing 1.5%, 3.0% and 5.0% (w/w) of AS or silica; 0.75%, 1.5% and 3.0% (w/w) of MC; and 3.0%, 5.0% and 7.5% (w/w) of CS or dextrin palmitate derivatives were tested. As a reference, non-stabilized MCSs was used. For the stability evaluation, the flow behavior was tested as described in section **“Preparation of organogels without and with DRSP and non-stabilized MCSs”**. In addition, the stability was analyzed using multiple light scattering (Turbiscan, software: Turbisoft 1.13, Quantachrome, Odelzhausen, Germany). Because the Turbiscan vials were not siliconized, the formulations adhered to the wall (**Fig. 5 a**). This failure might not be important because only small amounts of the formulations were lost and the detection of sedimentation was not influenced. Transmission and backscattering spectrograms of the formulations were plotted over 50 mm (sample length ca. 25 mm) at 25°C after preparation and during storage. For organogels without DRSP, the formation of the organogel network was visible by the time-dependent decrease of transmission, which occurred constantly over the whole sample length. The organogel networks were considered stable if the difference in transmission was $< 5\%$ from one measuring point to the next. A difference between the bottom and the top backscattering of the sample indicates inhomogeneous distribution of organogelator and DRSP. Thus, organogels without and with DRSP were assessed as stable when the difference in backscattering between the bottom and the top was $< 5\%$ at all measuring points over 90 d of storage. Moreover, no increase in transmission, which indicates sedimentation, should occur at the top of the sample ($< 1\%$). The method was not suitable for transparent organogels. Furthermore, the organogels were photographed at all measuring points to evaluate the sedimentation visually. For DRSP formulations, the level of sediment was measured from the bottom to the boundary line of

supernatant using the microscopy software (Axio Vision Rel. 4.5, Carl Zeiss Imaging Solution, Jena, Germany). The height of the sediment was calculated as an average of the optically lowest and highest sediment levels. The sedimentation volume (F), the ratio between the volume of sediment and the total volume of the suspensions was calculated [14]. DRSP organogels were evaluated as stable when $F > 0.99$. In addition, 10 g of DRSP organogels containing the organogelators in concentrations, described in **section “Rheological testing”**, were destructed by shaking for 10 min using a laboratory shaker and afterwards by magnetically stirring for 15 min (at maximum stirring speed). Then, the samples were stored at 40°C over three months.

2.5 DRSP microcrystal size analysis

Changes in the particle size distribution (PSD) of the DRSP organogels were analyzed in comparison to non-stabilized MCSs. The organogelator concentrations used were described in **section “Rheological testing”**. The median of the volume-weighted PSD was determined using laser diffraction after three months of storage at RT (Sympatec System-Partikel-Technik, Clausthal-Zellerfeld, Germany; sensor: Helos, dispersing unit: Cuvette, software: Windox 5, Sympatec, Clausenthal-Zellerfeld, Germany). This method was previously described in detail [13]. Briefly, the initial PSD of non-stabilized MCSs was determined after preparation. Prior to measurement, preparations were blended for 3 min using a vortex mixer (Heidolph Instruments, Schwabach, Germany). For all samples, blank values of dilution medium were determined before measuring. Furthermore, blank tests of MCT were performed, and each organogel was also tested without DRSP addition.

2.6 Evaluation of the syringeability/injectability

The terms syringeability and injectability have been defined in detail [15,16]. The applicability of a conventional autoinjector for s.c. administration was evaluated. The autoinjector had a glass syringe with an inner diameter of 6.35 mm. The tested organogelator concentrations were described in **section “Rheological testing”**. To give samples time for complete consolidation, 1 ml plastic syringes (Tuberkulin 1 x 100 Soft-Ject, Henke-Sass Wolf, Tuttlingen, Germany) were pre-filled with 0.5 g of DRSP organogel 7 d before measurement. The plastic syringes with an inner barrel diameter of 4.25 mm were inserted into a materials testing machine (Type Z010, Zwick Roell, Ulm, Germany). The formulations were expelled in 10 s from syringes via 23 G, 25 mm or 27 G, 12 mm needles (B.Braun, Melsungen, Germany). The force necessary for complete depletion was determined ($n = 5$). Due to different tube diameters, the forces needed to expel the samples from the glass barrels were assumed to be 2 - 2.5 times higher than from the plastic syringes.

2.7 *In vitro* release test

DRSP organogels (0.5 g) or non-stabilized MCSs were injected into dialysis bags (MW cut off 12000 – 14000 Da, length 7 cm, flat width 1 cm, Spectra/Por, Spectrum laboratories, Rancho Dominguez, USA) using 1 ml syringes with 20 G needles to simulate administration stress. The DRSP organogels contained the organogelators in the concentrations described in section “**Rheological testing**” and were pre-filled into the syringe at least 24 h before the *in vitro* tests. The syringes were weighed before and after injection. The release test setup was described previously [17]. Briefly, the samples were placed in 50 ml of pre-heated USP phosphate buffer (pH 7.4) (containing 0.05% (w/w) sodium azide and 8% (w/w) hydroxypropyl- β -cyclodextrin) and were shaken at 100 rpm and 37°C. One milliliter samples were withdrawn and replaced with fresh medium. The release medium was withdrawn and replaced every 24 h to reduce the DRSP isomerization in the release medium. Finally, the possible residual drug amount in the dialysis bags was analyzed. The DRSP concentration was determined using HPLC/UV (Agilent 1100 series, Agilent Technologies, Böblingen, Germany) (injection volume: 10 μ L, linearity: 1.1 - 500 μ g/ml, LLOQ: 1.1 μ g/ml). The main reasons for the incomplete DRSP release were assumed to be isomerization, non-quantifiable drug concentrations at later sampling points, drug remaining in the dialysis bag and loss of drug during medium exchange. The drug release rates were calculated from the slopes of release profiles including all of the sampling points from 1 to 72 h.

2.8 Statistics

All experiments were conducted in triplicate where not otherwise stated. Arithmetic mean values and standard deviations were calculated. Because homoscedasticity and normal distribution were not tested, differences between two results were analyzed by a two-sample Welch *t*-test and a Mann-Whitney-*U* test ($\alpha = 0.05$). Differences between more than two groups were investigated using the Kruskal-Wallis test and the Welch’s ANOVA ($\alpha = 0.05$) (software: Excel, Microsoft, Redmond, SEA). When $p < 0.05$, the groups were evaluated as significant different. To evaluate the relationship between two groups, we used the Spearman correlation (software: SPSS Statistics, IBM, Armonk, NY). Because the calculated *p* value is inaccurate below 11 values, they were looked up in a table of critical values. Assuming normal distribution, r^2 was additionally calculated. Differences between drug release profiles were assessed by calculating the difference factor (f_1) and similarity factor (f_2). When $f_1 < 15$ and $f_2 > 50$, the profiles were evaluated as comparable [18,19]. All sampling points showing 10-85% drug release and one sampling point with drug release above 85% were considered.

3 Results and Discussion

3.1 Choice of the organogelator and determination of the sol-gel transition concentration

We screened numerous excipients for their suitability to form MCT organogels. The following excipients were found to gel MCT in our experiments and were tested as potential organogelators for DRSP MCSs. The low-molecular-weight gelators CS and MC formed intensively cloudy organogels. The steroidal skeleton induces growth of the gelator aggregates via van der Waals forces [3]. Furthermore, functional groups can interact by hydrogen bonding or/and π -interactions [3]. The hydroxyl group at the C3 position are assumed to play an important role for gelation [3,6]. CS organogels were stabilized by a plate-type network (**Fig. 1**).

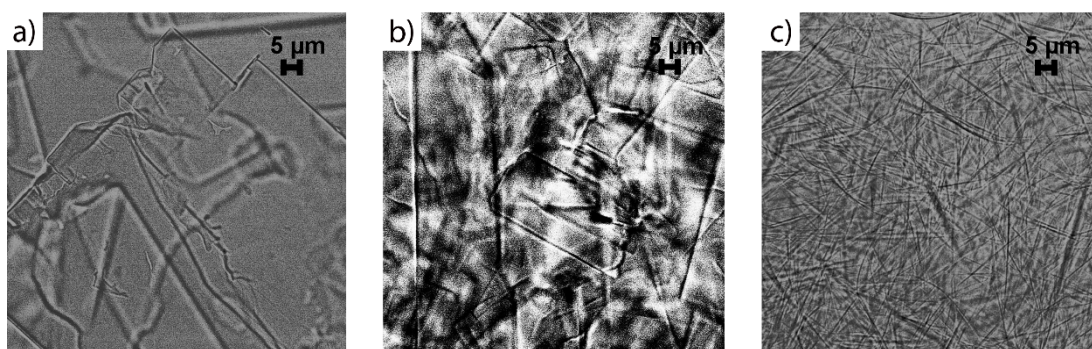


Fig. 1 Light microscopic images of organogel structures of **a)** and **b)** cholesteryl stearate and **c)** methyl cholate in MCT.

The MC organogel scaffold consisted of long rods. Rod-like structures were described to be highly efficient in self-assembling the organogel network [6]. Accordingly, only a low MC concentration was required to completely immobilize MCT (**Fig. 2 a**). AS and dextrin palmitate derivatives formed opaque MCT organogels. Gel networks were not detectable by optical microscopy. Generally, the low-molecular-weight gelator AS is an often used organogelator, which should aggregate via organometallic coordination bonding. Furthermore, the fatty acid chain influences the gelation process [6]. Dextrin palmitate derivatives are polymeric organogelators. The fiber network might be connected by polymer chain and physical interaction including hydrogen bonding between the hydroxyl groups of glucose units or van der Waals forces. Furthermore, silica is known to form gels in aqueous and oil-based systems [20]. Silica formed transparent MCT organogels. For gelation, heating was not necessary. With respect to the symmetric tetrahedral coordination of silica molecules, homogenous net-like gel scaffolds were formed [21]. The sol-gel transition concentrations of organogelators in MCT are shown in **Fig. 2 a**. The CS and MC formulations exhibited a sharp sol-gel transition, whereas silica formulations provided a smoother phase transition. For the conducted tests on physical stability, the lowest organogelator concentrations above the sol-gel transition were used to determine differences between the organogels, because their susceptibility to mechanical stresses might be high under these conditions.

3.2 Rheological behavior of DRSP organogels

The rheological properties of the organogels were investigated as an indicator for their physical stability during storage and application. First, we analyzed the viscoelastic parameters η^* , G' and $\tan(\delta)$ under low τ simulating rheological behavior at rest. In this linear viscoelastic region (LVR), η^* , G' and G'' showed a constant plateau on different levels [22]. Almost all of the organogels without and with DRSP showed $G' > G''$ at low τ . The result of $G' > G''$ indicated that the formulations acted more like viscoelastic solids than like viscoelastic fluids; they were gelled [22].

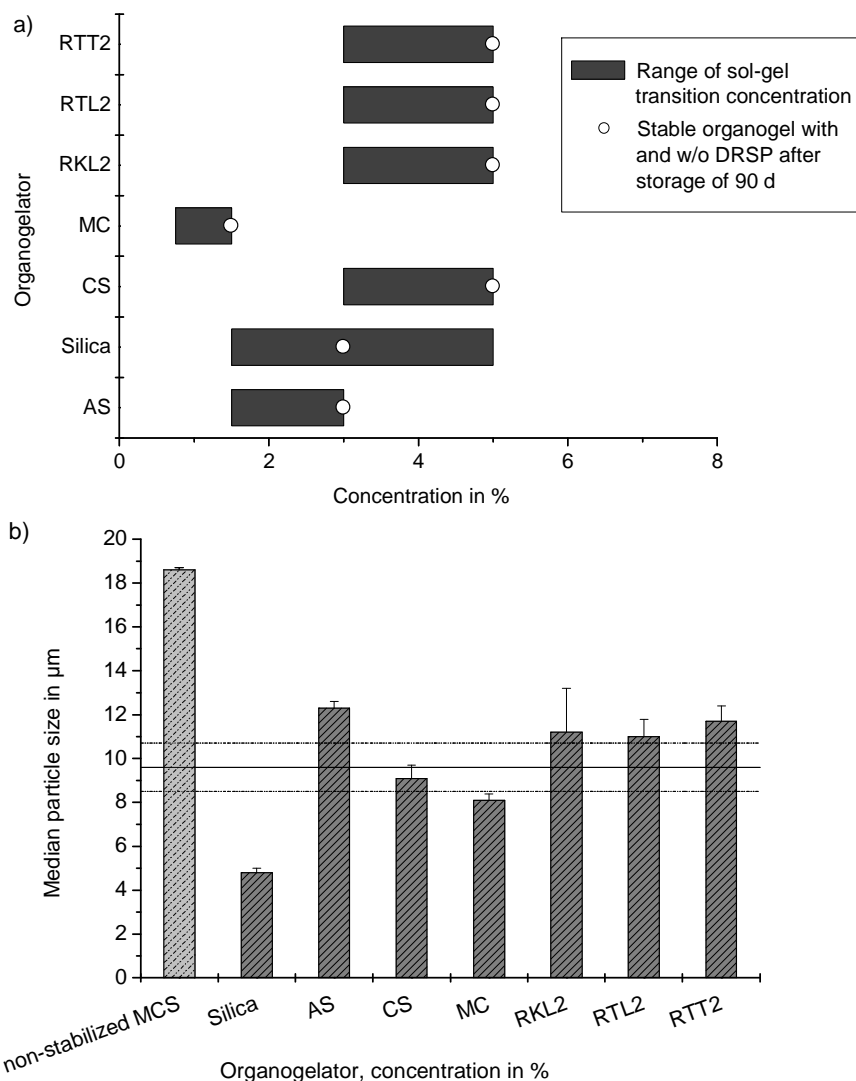


Fig. 2 a) Diagram of sol-gel transition concentration ranges and storage stability of organogels without and with DRSP ($n = 3$). The bars begin at the maximum non-gelling concentrations and end at the minimum gelling concentration. **b)** Average of median particle sizes of non-stabilized DRSP MCS and DRSP organogels after storage for three months at RT are presented in columns. The average of median particle size of non-stabilized MCS before storage is shown as a line (with the range of standard deviation in dotted lines) ($n = 3$).

The results are in agreement with the subjective determination of the sol-gel transition in **section “Choice of the organogelator and determination of the sol-gel transition concentration”**. Surprisingly, G' was relatively low for CS organogels and even lower than G'' for DRSP CS organogels although the formulations did not flow after preparation and showed no sedimentation

during storage (sections “Choice of the organogelator and determination of the sol-gel transition concentration” and “Storage stability of DRSP organogels”). It was assumed that the platelet structures of CS organogels were even destroyed at very low τ or during sample preparation for rheological tests. In general, the DRSP addition had a strong influence on the rheological properties of the organogels. η^* , G' but also $\tan(\delta)$ were primarily increased with DRSP addition (Fig. 3 a and b).

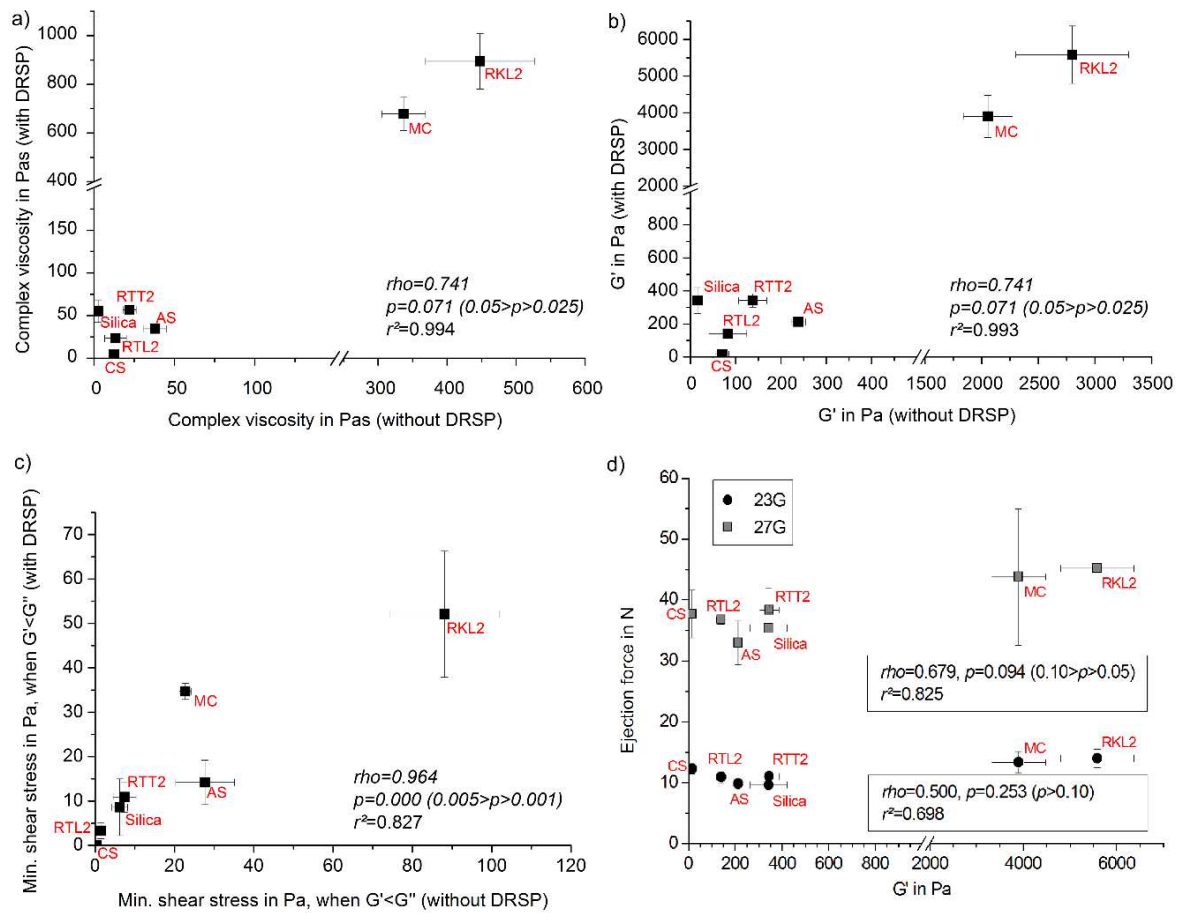


Fig. 3 Correlation between a) η^* , b) G' and c) destructive shear stress of organogels without and with the addition of DRSP ($n = 3$). d) Correlation between the ejection force required for expelling DRSP organogels from syringes via 23 G and 27 G needles ($n = 5$) and G' of DRSP organogels at rest ($n = 3$).

Relatively good correlation of G' and η^* was found between organogels without and with DRSP. However, a lower correlation was observed for $\tan(\delta)$ of organogels without and with DRSP ($\rho = 0.429$; $p > 0.1$; $r^2 = 0.259$). Due to the high impact of DRSP on the rheological behavior, the suitability of the different organogel formulation for the use as drug-delivery system should be evaluated with drug addition. All of the organogels showed shear-dependent behavior under the mechanical stress of an amplitude sweep (Fig. 4). With increasing τ , the end of LVR was reached by crossing the yield point. When $G' < G''$ (below the flow point), the formulations lost their gel character and showed more fluid-like properties [22]. Parenteral gel formulations are exposed to mechanical stress during transport, injection and in the human body after injection. The sensitivity

of organogels to mechanical stress is beneficial for the injectability /syringeability, but could be detrimental to the transport and storage stability. For a better characterization of the behavior under mechanical stress and the influence of DRSP on the gel network, we compared the experimentally measured flow curves with typical rheological models (**Tab. 1**).

Tab. 1 Correlation between experimental rheological profiles and theoretical rheological models. The square of Pearson product moment correlation coefficients is presented (r^2). The best correlation for each organogel is highlighted.

Formulation	r^2 (Herschel-Bulkley)	r^2 (Casson)	r^2 (Bingham)
	CS DRSP organogels: r^2 (Ostwald/deWaele)		CS DRSP organogels: r^2 (Newton)
<i>Without DRSP</i>			
A200	0.999	0.993	0.968
ALS	0.993	0.968	0.886
CS	0.997	0.979	0.946
MC	0.992	0.837	0.727
RKL2	0.941	0.730	0.543
RTL2	0.998	0.987	0.958
RTT2	0.998	0.965	0.921
<i>With DRSP</i>			
A200	0.993	0.956	0.904
ALS	0.998	0.968	0.901
CS	0.995	-	0.928
MC	0.992	0.843	0.683
RKL2	0.979	0.915	0.763
RTL2	0.909	0.407	0.390
RTT2	0.982	0.849	0.694

Because the organogels, except for DRSP CS formulations, showed a yield point/zone, the overall flow curves were fitted to typical non-linear plastic rheological models. Best correlation was found with the Herschel-Bulkley model using $n < 1$ (**Supplement**), indicating shear-thinning behavior. However, a closer look on the flow curves revealed that the shear-thinning behavior was not homogeneously over the whole range of τ (**Fig. 4 a-d**). The viscosity did not decrease constantly after crossing the yield point, but showed irregularities (shear-independent or even shear-thickening behavior) at certain intervals of τ (**Fig. 4 e and f**). This behavior was more pronounced for DRSP organogels showing consequently partially lower r^2 to the rheological models than drugless organogels. The reason might be that organogelator structures / DRSP particles or DRSP particles / DRSP particles entangle with increasing τ and therefore hinder the flow. The interaction between DRSP particles and gel structure could also be responsible for the partially lower destructive τ being necessary to reach $G' < G''$ (for AS, MC and RKL2) (**Fig. 3 c**).

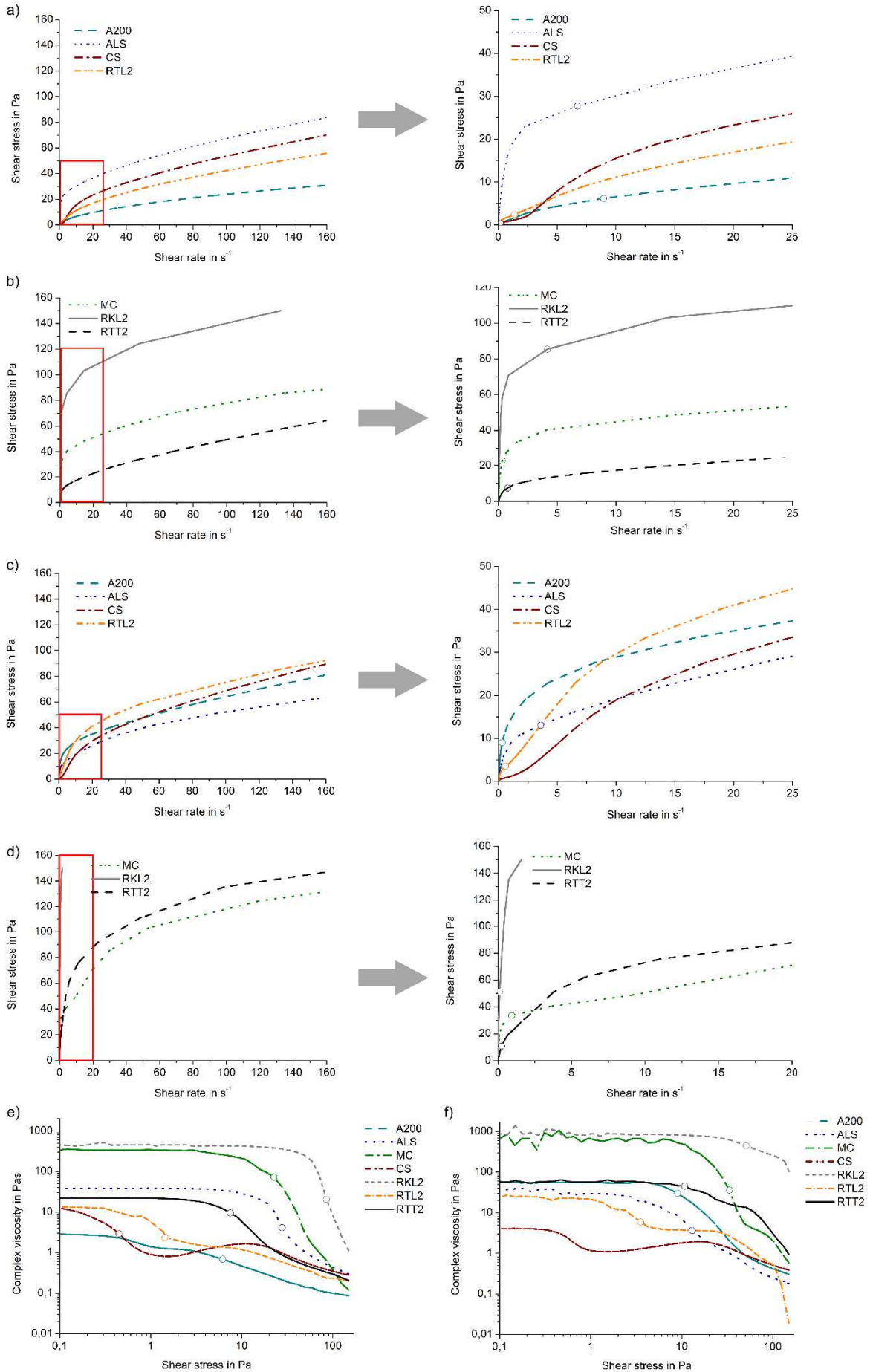


Fig. 4 a) and b) Flow curves of organogels without DRSP; **c) and d)** flow curves of DRSP organogels. Viscosity curve of organogels **e)** without DRSP and **f)** with DRSP versus shear stress (one example of each formulation). The dots mark the point where $G' < G''$.

Due to its high susceptibility to mechanical stress, the yield point was already reached for the (DRSP) CS organogel at the beginning of the amplitude sweep (or even at lower τ). The pronounced shear-thickening/-independent behavior of CS organogels was probably caused by the platelet organogelator structures, which require more volume during shear and interfere therefore with each other [23]. Furthermore, high variability of η^* was observed within the LVR especially for high viscous MC and RKL2 organogels, especially with the addition of DRSP. The variability might be caused by transient effects at low shear rates or, again, by interferences between organogelator and drug particles [22].

Next, we compared the destructive τ as an indicator for the robustness with the viscoelastic parameters measured at rest. The destructive τ correlated significantly with G' ($\rho = 0.893$; $p < 0.025$ and $r^2 = 0.950$) and η^* at rest ($\rho = 0.893$; $p < 0.025$ and $r^2 = 0.942$); the destructive τ increased with increasing G' and η^* at rest. No relationship was found between the destructive τ and $\tan(\delta)$ at rest ($\rho = -0.393$; $p > 0.10$ and $r^2 = 0.167$). Consequently, G' and η^* were used to evaluate the rigidity of DRSP organogels. G' and η^* of DRSP organogels at rest decreased in the following order (CS was excluded):

RKL2 > MC >> silica \approx RTT2 > AS > RTL2

Once destroyed, the viscoelastic properties of DRSP organogels were altered. The results determined at rest and at recovery were compared to investigate the elasticity. The elasticity of the organogelator network should be relevant for a consistent storage and transport stability. An organogel which is destructed during storage or transport, should ideally recover fast and should thereafter have a comparable rheological behavior to a non-destructed organogels to avoid sedimentation. In addition, a fast recovery of rigidity in the body after injection was assumed to have a positive effect on the drug release because organogelator structures might reduce spreading in the tissue and decelerate the drug diffusion [24-27]. Consequently, high G' and η^* of recovered organogels at 20°C and 37°C, being comparable with G' and η^* before destruction, should be advantageously for the stability and performance of the formulations. The relative ratios of the viscoelastic parameters determined before and after destruction decreased in the following order (CS was excluded):

G'

Silica (72%) > RTT2 (43%) > RTL2 (25%) > AS (12%) > MC (6%) > RKL2 (2%) at 20°C

Silica (50%) > RTT2 (36%) > RTL2 (30%) > AS (13%) > RKL2 (2%) > MC (0%) at 37°C

η^*

Silica (73%) > RTT2 (42%) > RTL2 (25%) > AS (12%) > MC (7%) > RKL2 (2%) at 20°C

Silica (51%) > RTT2 (37%) > RTL2 (31%) > AS (14%) > RKL2 (2%) > MC (0%) at 37°C

In general, softer organogels with lower G' and η^* at rest seemed to recover faster. The highest elasticity was shown in DRSP silica organogels. Silica organogels might regain their homogenous structure relatively quickly. It should be noted that $\tan(\delta)$ of silica organogels was primarily decreased especially at 37°C. $\tan(\delta)$ did not correlate with the destructive τ . However, the increased $\tan(\delta)$ indicated more pronounced viscous properties after destruction. DRSP CS organogels were only marginally influenced by pre- τ due to previous sample destruction. The lowest recovery of η^* and G' was observed for the stronger DRSP KL2 and MC organogels. The recovery was further decreased at elevated temperature. Nevertheless, the formulations showed differences in the time-dependent recovery. When the measuring time after destruction was prolonged from 30 s to 5 min at 37°C, a marked increase in η^* and G' was observed for DRSP RKL2 organogels ($G' = 87.4 \pm 5.1$ to 130.6 ± 10.0 Pa; $\eta^* = 14.6 \pm 2.1$ to 21.7 ± 1.0 Pas), whereas a slight increase in η^* and G' was examined for DRSP MC organogels ($G' = 1.7 \pm 1.3$ to 2.5 ± 1.4 Pa; $\eta^* = 0.3 \pm 0.2$ to 0.6 ± 0.1 Pas). A further decrease in η^* and G' over time was shown by DRSP CS organogels ($G' = 4.4 \pm 1.6$ to 3.1 ± 1.2 Pa; $\eta^* = 1.0 \pm 0.2$ to 0.7 ± 0.3 Pas). In short, high G' , η^* and elasticity might be important viscoelastic parameters to ensure robustness and consistent behavior of the organogels during transport, storage and after injection. In particular, the stronger organogels with high G' and η^* seemed to have a low elasticity; their rheological and consequently their physical properties were therefore markedly changed after destruction. Although the DRSP silica organogel provided a moderate G' at rest, it might have more preferable rheological properties with regard to elasticity.

3.3 Storage stability of DRSP organogels

First, homogeneity of organogels without DRSP was studied utilizing multiple light scattering. In general, organogels containing the minimum organogelator concentration necessary for gelation or higher were found to be stable in storage over three months (**Fig. 2 a**). Their respective organogelator networks were consolidated after 1 d, and thereafter, no major changes in transmission or backscattering were detected. Next, the stability of DRSP organogels was tested. Organogel scaffolds were sedimented together with DRSP microcrystals. Thus, sedimentation was visible by the formation of a clear supernatant. Non-stabilized MCSs had an F value of 0.58 ± 0.01 . DRSP formulations containing the organogelators in the minimum concentrations necessary for gelation, provided an $F > 0.99$. Local changes in DRSP particle concentrations were detected using multiple light scattering.

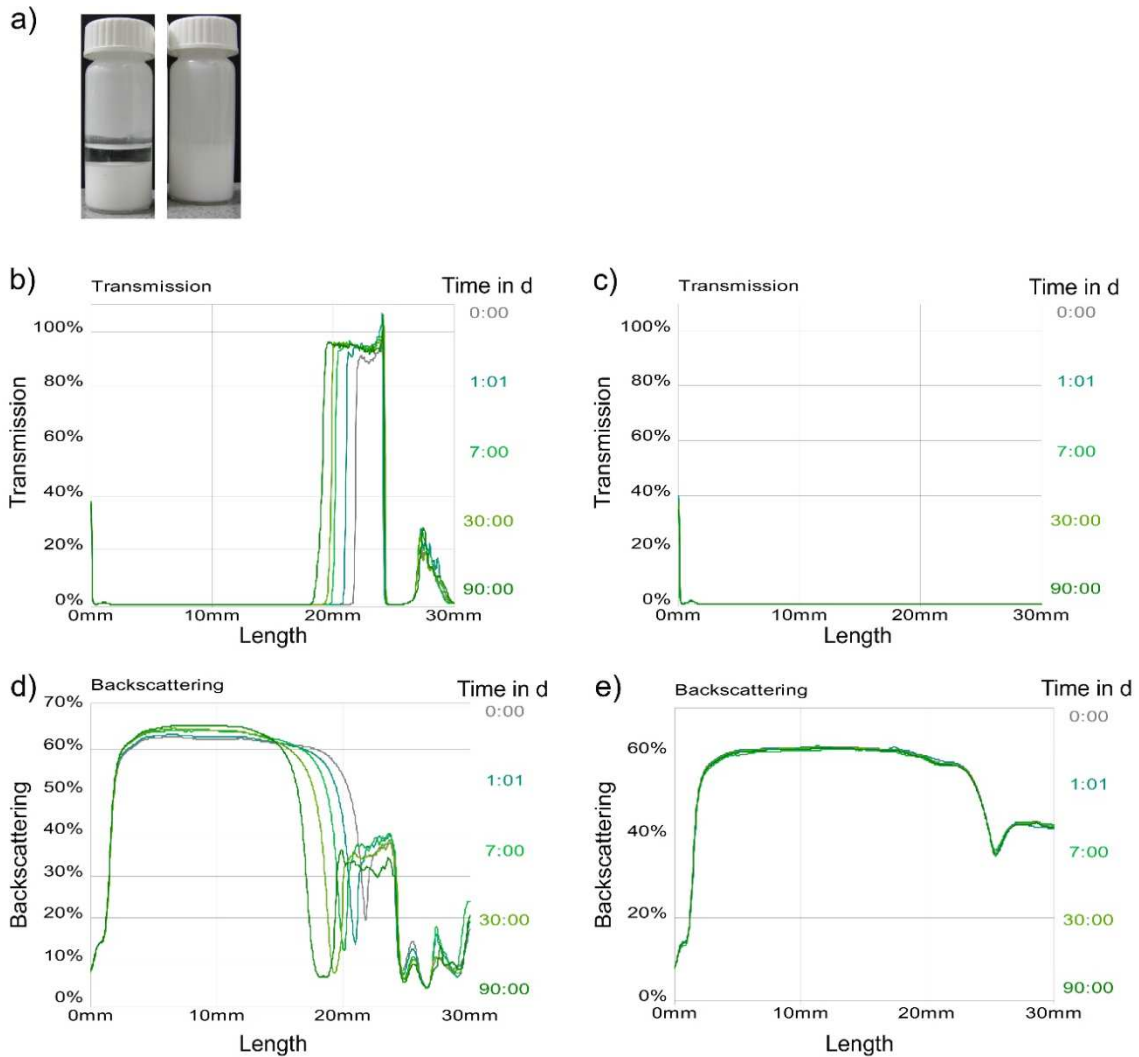


Fig. 5 a) Images of DRSP MCT formulations stabilized with 0.75% (w/w) and 1.5% (w/w) MC (from left to right) after storage for three months. Transmission spectra of DRSP MCS containing **b)** 0.75% (w/w) and **c)** 1.5% (w/w) MC, and backscattering spectra of DRSP MCT MCS containing **d)** 0.75% (w/w) and **e)** 1.5% (w/w) MC are shown (one example of each formulation).

The stability assessment of DRSP MC formulations is shown in **Fig. 5** as a representative example. The backscattering diagrams of organogels containing 1.5% MC showed a relatively constant plateau over the sample length (difference top and bottom backscattering: < 5%), indicating a homogenous drug distribution. Samples containing 0.75% MC showed a decrease of backscattering at the top and an increase of backscattering along the remaining sample length indicating sedimentation. Drug sedimentation could cause inhomogeneous filling processes during manufacturing, needle obstruction during injection or promote aggregation during storage; thus, it should be avoided [10,28]. Furthermore, the prevention of sedimentation could supersede agitation before administration. Thus, pre-filled in syringes, stable organogels would advantageously be ready-to-use. The minimum organogelator concentrations necessary to avoid DRSP sedimentation during storage were similar to the minimum concentrations necessary for gelation (**Fig. 2 a**). There was no tested organogelator that could not avoid sedimentation. Thus, DRSP organogels were

assumed to be generally markedly more physically stable than non-stabilized MCSs. The low recovery of DRSP CS organogels after mechanical stress (**section “Rheological behavior of DRSP organogels”**) was confirmed by a long-term storage experiment. The formulation did not regain their gel character after destruction during storage of 3 months at 37°C (moderate movement and tipping led to flow of the formulations) and showed clear phase separation. Furthermore, one of three DRSP MC organogels had not recover its gel character. DRSP RKL2 organogels and all of the other organogels regained their gel character after destruction during storage at 37°C (moderate movement and tipping led not to flow of the formulations).

Next, the PSD was investigated as an additional parameter for physical stability. The median particle size of non-stabilized MCSs was $9.6 \pm 1.1 \mu\text{m}$ after preparation (**Fig. 2 b**). A median DRSP particle size of approximately $5 \mu\text{m}$ was determined by laser diffraction of dry powder samples after micronization (unpublished results). The discrepancy between the measured results could be explained by particle growth during storage of the dry DRSP powder or by slight aggregation during sample preparation. Furthermore, the PSD could vary in dependence on the measuring instrument used [29]. Non-stabilized MCSs tended to particle growth. The median particle size increased significantly during storage (median particle sizes before and after storage: $p < 0.05$ for *U*- and *t*-test). However, crystal growth and aggregation could cause variation in bioavailability and increase the risk of needle obstruction during injection [30]. All of the tested organogelators were able to significantly decrease the DRSP particle growth. The increased viscosity and gel formation might have a high impact on the reduction of aggregation. Nevertheless, a significant correlation between G' or η^* and PSD was not found ($p > 0.1$; $\rho / r^2 < 0.1$). The results indicated that not only gel formation but also the interaction of organogelator and DRSP molecules might influence the particle growth. CS and MC were more capable to reduce particle growth than AS, RTL2 and RTT2 (*U*- and *t*-test: $p < 0.05$). CS and MC consisted of a steroidal structure that might interact with the steroidal DRSP more efficiently. Silica avoided particle growth most efficiently (*U*- and *t*-test: silica versus other: $p < 0.05$). Median particle sizes were comparable with those of DRSP powder measured after micronization, indicating that DRSP was aggregated in MCT even during preparation (non-stabilized MCSs after preparation versus silica organogel after storage: $p < 0.05$ for *U*- and *t*-test). The high benefit of the silica might be due to the inclusion of DRSP microcrystals in the homogenous, hydrophilic network of silica molecules. With regard to the particle growth, CS, MC and especially silica organogels should be preferred. In general, all of the DRSP organogels advantageously showed a significant better physical long-term stability with respect to sedimentation and particle growth compared with non-stabilized MCSs. DRSP CS formulations were determined to be most unfavorable with regard to the elasticity due to their irreversible loss of gel character after destruction.

3.4 Syringeability/injectability of DRSP organogels

For s.c. application, the injection needles should be ≥ 23 G and we consequently tested 23 G and 27 G needles [31,32]. Furthermore, we evaluated the applicability of an autoinjector. The device advantageously allows the drug administration by the patients themselves and that might increase the compliance. Ejection forces of > 100 N were considered to unacceptably increase the risk of bursting the glass barrel of the autoinjector. Moreover, *Rungseevijitprapa and Bodmeier* [33] recommended that formulations be evaluated as able to administer without difficulties using ejection forces < 50 N. The forces applied for passing DRSP organogels from the plastic syringes, used for syringeability testing, through the 27 G needles were > 30 N. Because the forces would be 2 - 2.5 times higher using the autoinjector with glass syringes, the administration of the organogels was evaluated as not possible or only possible with restrictions through 27 G needles. The ejection forces were markedly decreased using 23 G needles. Thus, the formulations should be syringeable without difficulties. The ejection forces differed slightly between the tested DRSP organogels (Kruskal-Wallis / ANOVA: 23 G: $p < 0.02$; 27 G: $p > 0.1$). As a slight enlargement of needle size was shown to cause no significant increase in pain during injection, 23 G needles are more preferable than 27 G needles [31]. Furthermore, we evaluated the relationship between the rheological properties and the ejection forces. No significant correlation was found between destructive τ and ejection stress ($p > 0.1$; 27 G: $\rho = 0.500$, $r^2 = 0.669$; 23 G: $\rho = 0.464$, $r^2 = 0.525$). The low correlation might be mainly caused by the entanglement of drug particles and/or gel structures leading to clogging of the passage from the syringe barrel to the needle (section “**Rheological behavior of DRSP organogels**”). Such an effect could not be simulated by τ . Moreover, no correlation was found between ejection forces and $\tan\delta$ (23G / 27G: $p > 0.1$; $\rho / r^2 < 0.1$). Nevertheless, in accordance to τ , ejection stress using 27 G needles showed better correlation tendency to G' (**Fig. 3 d**) and η^* (27 G: $0.1 > p > 0.05$; $\rho = 0.679$, $r^2 = 0.834$). With respect to the forces needed to eject the DRSP organogels using 23 G needles, an slight increase in G' and η^* by rising the organogelator concentration might be possible in order to improve the rigidity without losing syringeability.

3.5 *In vitro* drug release

The *in vitro* release was tested as an indicator for the stability of organogel networks after administration. With respect to the Fick's law, the *in vitro* release was assumed to depend on the drug diffusion being influenced by the vehicle viscosity. The DRSP solubility in the organogels, which can also influence the drug release, was comparable for all of the organogelators (data not shown). In fact, the drug release of DRSP organogels was significantly more sustained compared to non-stabilized MCSs ($f_2 < 50$ and $f_1 > 15$ for all of the organogels versus non-stabilized MCSs; comparison of drug release rates using Kruskal-Wallis / ANOVA: $p < 0.05$) (**Fig. 6 a and b**). With

respect to the results of rheological tests in section “**Rheological behavior of DRSP organogels**”, the organogel network recovered partially at 37°C after destruction. This restructuring seemed to cause deceleration of the *in vitro* drug release. Although the viscoelastic properties of the DRSP organogels were markedly different, the formulations did show no significantly or slightly different drug release ($f_2 > 50$ and $f_1 < 15$; comparison of drug release rates using Kruskal-Wallis: $p > 0.05$; however, ANOVA showed significant differences: $p < 0.05$). The comparison of drug release rates and viscoelastic properties indicated slightly decelerated drug diffusion with increasing η^* or G' (Fig. 6 c and d).

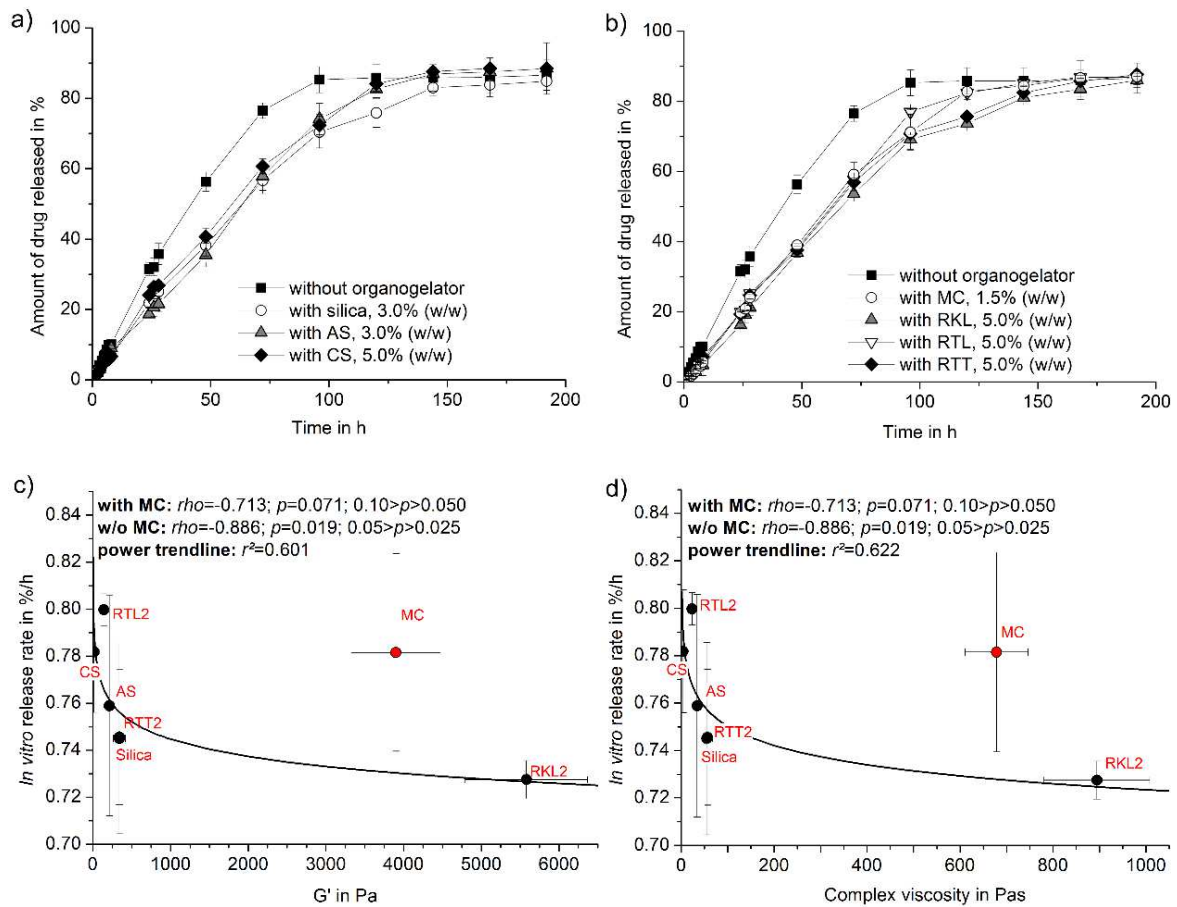


Fig. 6 Release profiles of non-stabilized DRSP MCS and of DRSP organogels containing **a)** AS, silica or CS and **b)** MC or dextrin palmitate derivatives ($n = 3$). **c)** Correlation between the *in vitro* drug release rate and G' of DRSP organogels at rest ($n = 3$); **d)** correlation between the *in vitro* drug release rate and η^* of DRSP organogels at rest ($n = 3$).

Accordingly, inverse proportionality between G' and drug diffusion from gel matrices was found previously [34]. However, the relationship between release rate and η^* or G' of MC organogels was low. Thus, corresponding to the results shown in sections “**Rheological behavior of DRSP organogels**” and “**Storage stability of DRSP organogels**”, very slow recovery of the MC organogel network after injection into the dialysis bag, might be the reason for the slightly accelerated drug release. RKL2 organogels recovered also slower than the other organogels but nevertheless faster than MC organogels at 37°C (sections “**Rheological behavior of DRSP**

organogels” and **“Storage stability of DRSP organogels”**). Consequently, the slower recovery rate of stronger organogels with higher η^* and G' could cause the non-linear correlation tendency between *in vitro* release and viscoelastic properties as well as the irregular behavior of MC organogels (**Fig. 6 c and d**). In accordance to our results, it was shown in a previous *in vivo* study that steroidal MC organogels showed a relatively high initial plasma level indicating a slow gel recovery after injection [17]. Thereafter, the *in vivo* plasma levels of the MC organogels declined slower than for the non-stabilized steroidal MCSs. This effect might be caused by a partial rebuilding of the MC structures in the body.

4 Conclusion

DRSP organogels were superior to non-stabilized MCSs with respect to the long-term storage and drug release. DRSP organogels showed improved storage-stability considering sedimentation and particle growth. The prevention of particle growth was assumed to be mainly caused by the molecular interaction of drug and gelator. All of the tested DRSP organogels showed shear-thinning behavior which is positive for injection. Thus, ejection from syringes was feasible with an autoinjector using 23G needles. The partially irregular rheological behavior (shear-thickening/-independent behavior) was possibly influenced by the entanglement of organogelator structures and drug particles. G' and η^* at rest were indicative for the behavior of organogels under mechanical stress (e.g. amplitude sweep, injection). All of the DRSP organogels show significantly more sustained drug release compared to non-stabilized MCSs which should be mainly caused by partial recovery of the organogelator structures found at 37°C after destruction. The organogels showed only slightly different DRSP release. Higher G' and η^* caused slightly more sustained drug release. Furthermore, softer organogels showed better elasticity which might be positive for the gel recovery after transport or injection stress. In summary, MCT organogels of DRSP could be a suitable formulation option for parenteral application. In general, a balance between rigidity and destructibility of organogels must be considered for an optimal formulation. Silica organogel might slightly more advantageously compared to the other organogels because it provided the highest elasticity, moderate G' and η^* and avoided most efficiently particle growth.

5 Supplement

5.1.1 Model functions for flow curves without a yield point

$$\tau = \eta \cdot \dot{\gamma}$$

Equation 1 Newton's law; τ = shear stress, η = viscosity $\dot{\gamma}$ = shear rate [22].

$$\tau = c \cdot \dot{\gamma}^n$$

Equation 2 Ostwald/de Waele (Power law); c = flow coefficient, n = power-law index, $n < 1$ shear thinning behavior, $n > 1$ shear-thickening behavior, $n = 1$ ideal-viscous flow behavior [22].

5.1.2 Model functions for flow curves including a yield point

$$\tau = \tau_B + \eta_B \cdot \dot{\gamma}$$

Equation 3 Bingham model equation; η_B = Bingham viscosity, τ_B = Bingham yield point [22].

$$\sqrt{\tau} = \sqrt{\tau_c} + \sqrt{\eta_C \cdot \dot{\gamma}}$$

Equation 4 Casson model equation; η_C = Casson viscosity, τ_c = Casson yield point [22]

$$\tau = \tau_{HB} + c \cdot \dot{\gamma}^n$$

Equation 5 Hershey/Bulkley model equation; τ_{HB} = yield point according to Herschel/Bulkley, c = flow coefficient (also called the Herschel/Bulkley viscosity), n = Herschel/Bulkley index, $n < 1$ shear thinning behavior, $n > 1$ shear-thickening behavior, $n = 1$ Bingham behavior [22].

References

- [1] S. Murdan, Organogels in drug delivery, *Expert Opin. Drug Deliv*, 2 (2005) 489-505.
- [2] C.B. Packhaeuser, J. Schnieders, C.G. Oster, and T. Kissel, In situ forming parenteral drug delivery systems: an overview, *Eur. J. Pharm. Biopharm.*, 58 (2004) 445-455.
- [3] A. Vintiloiu and J.C. Leroux, Organogels and their use in drug delivery - A review, *J. Control. Release*, 125 (2008) 179-192.
- [4] Z.-H. Gao, A.J. Shukla, J.R. Johnson, W.R. Crowley, and J.F. Reger, Controlled release of contraceptive steroids from biodegradable and injectable gel formulations: *In vivo* evaluation, *Pharm. Res.*, 12 (1995) 864-868.
- [5] A. Motulsky, M. Lafleur, A.C. Couffin-Hoarau, D. Hoarau, F. Boury, J.P. Benoit, and J.C. Leroux, Characterization and biocompatibility of organogels based on l-alanine for parenteral drug delivery implants, *Biomaterials*, 26 (2005) 6242-6253.
- [6] P. Terech and R.G. Weiss, Low molecular mass gelators of organic liquids and the properties of their gels, *Chem. Rev.*, 97 (1997) 3133-3159.
- [7] M.J. Akers, A.L. Fites, and R.L. Robison, Formulation design and development of parenteral suspensions, *J. Parenter. Sci. Technol.*, 41 (1987) 88-96.
- [8] T. Higuchi, Some physical chemical aspects of suspension formulation, *J. Am. Pharm. Assoc.*, 47 (1958) 657-660.
- [9] R. Nash, Suspensions, in: James Swabrick (Ed.), *Encyclopedia of pharmaceutical technology*, Informa Healthcare, New York, 2006, pp. 3597-3610.
- [10] J. Wong, A. Brugger, A. Khare, M. Chaubal, P. P.Papadopoulos, B. B.Rabinow, J. Kipp, and J. Ning, Suspensions for intravenous (IV) injection: A review of development, preclinical and clinical aspects, *Adv. Drug Deliv. Rev.*, 60 (2008) 938-954.
- [11] K.S. Hall and J. Trussell, Types of combined oral contraceptives used by US women, *Contraception*, 86 (2012) 659-665.
- [12] R. Krattenmacher, Drospirenone: pharmacology and pharmacokinetics of a unique progestogen, *Contraception*, 62 (2000) 29-38.
- [13] S. Nippe and S. General, Parenteral oil-based drospirenone microcrystal suspensions - Evaluation of physicochemical stability and influence of stabilising agents, *Int. J. Pharm.*, 416 (2011) 181-188.
- [14] J.E. Tingstad, Physical stability testing of pharmaceuticals, *J. Pharm. Sci.*, 53 (1964) 955-962.
- [15] T.M. Crowder, A.J. Hickey, M.D. Louey, and N. Orr, *A guide to pharmaceutical particulate science*, Interpharm/CRC, Boca Raton, London, New York, Washington D.C., 2003.
- [16] J.C. Boylan and S.L. Nail, Parenteral Products, in: G.S. Banker and C.T. Rhodes (Eds.), *Modern Pharmaceutics*, Marcel Dekker, Inc., New York, 2002, pp. 576-625.
- [17] S. Nippe, C. Preuße, and S. General, Evaluation of the in vitro release and pharmacokinetics of parenteral injectable formulations for steroids, *Eur. J. Pharm. Biopharm.*, 83 (2012) 253-265.
- [18] Guidance for industry dissolution testing of immediate release solid oral dosage forms. 1997. www.fda.gov, US Food and Drug Administration, Rockville. 21-10-2013.
- [19] J.W. Moore and H.H. Flanner, Mathematical comparison of curves with an emphasis on in vitro

dissolution profiles, Pharm. Technol., 20 (1996) 64-74.

- [20] R.C. Rowe, P.J. Sheskey, and P.J. Weller, Handbook of pharmaceutical excipients, Pharmaceutical Press, London, 2003.
- [21] R. Balasubramanian, A.A. Sughir, and G. Damodar, Oleogel: A promising base for transdermal formulations, Asian J. Pharm. Sci., 6 (2012) 1-9.
- [22] T.G. Mezger, The rheology handbook: for users of rotational and oscillatory rheometers, Vincentz Network GmbH&Co.KG, Hannover, 2006.
- [23] M.T.H. Nutan and I.K. Reddy, General principles of suspensions, in: A.K. Kulshreshtha, O.N. Singh, and G.M. Wall (Eds.), Pharmaceutical suspensions from formulation development to manufacturing, Springer, New York, Dordrecht, Heidelberg, London, 2010, pp. 39-66.
- [24] J. Zuidema, F. Kadir, H.A.C. Titulaer, and C. Oussoren, Release and absorption rates of intramuscularly and subcutaneously injected pharmaceuticals (II), Int. J. Pharm., 105 (1994) 189-207.
- [25] M. St'astný, D. Plocová, T. Etrych, M. Kovár, K. Ulbrich, and B. Ríhová, HEMA-hydrogels containing cytostatic drugs Kinetics of the drug release and *in vivo* efficacy, J. Control. Release, 81 (2002) 101-111.
- [26] S.W. Larsen and C. Larsen, Critical factors influencing the *in vivo* performance of long-acting lipophilic solutions - Impact on *in vitro* release method design, AAPS J., 11 (2009) 762-770.
- [27] Z.-H. Gao, A.J. Shukla, J.R. Johnson, and W.R. Crowley, Controlled release of contraceptive steroids from biodegradable and injectable gel formulations: *In vitro* evaluation, Pharm. Res., 12 (1995) 857-863.
- [28] W. Rungseevijitprapa, F. Siepmann, J. Siepmann, and O. Paeratakul, Disperse systems, in: Alexander T. Florence and Juergen Siepmann (Eds.), Modern pharmaceuticals: Basic principles and systems, Vol. 1. Informa Healthcare, New York, London, 2009, pp. 357-421.
- [29] M. Martinez, M. Rathbone, D. Burgess, and Mai Huynh, *In vitro* and *in vivo* considerations associated with parenteral sustained release products: A review based upon information presented and points expressed at the 2007 Controlled Release Society Annual Meeting, J. Control. Release, 129 (2008) 79-87.
- [30] E.J. Antal, C.F. Dick, C.E. Wright III, I.R. Welshman, and E.M. Block, Comparative bioavailability next term of two medroxyprogesterone acetate suspensions, Int. J. Pharm., 54 (1989) 33-39.
- [31] B.S.I. Montgomery, J.P. Borwell, and D.M. Higgins, Does needle size matter? Patient experience of luteinising hormone-releasing hormone analogue injection, Prostate Cancer Prostatic Dis., 8 (2005) 66-68.
- [32] S. Scott Ricci and T. Kyle, Maternity and pediatric nursing, Lippincott Williams & Wilkins, Philadelphia, 2009.
- [33] W. Rungseevijitprapa and R. Bodmeier, Injectability of biodegradable *in situ* forming microparticle systems (ISM), Eur. J. Pharm. Sci., 36 (2009) 524-531.
- [34] P.B. Pisal, S.S. Patil, and V.B. Pokharkar, Rheological investigation and its correlation with permeability coefficient of drug loaded carbopol gel: influence of absorption enhancers, Drug Dev. Ind. Pharm., 39 (2013) 593-599.

CHAPTER 4

Evaluation of the *in vitro* release and pharmacokinetics of parenteral injectable formulations for steroids

Published in European Journal of Pharmaceutics and Biopharmaceutics 83 (2013) 253–265
<http://dx.doi.org/10.1016/j.ejpb.2012.09.006>

Abstract

The aim of this study was to investigate the pharmacokinetics of injectable conventional dosage forms containing steroids. First, the *in vitro* release of drospirenone (DRSP) microcrystal suspensions (MCSs) was studied. Next, the pharmacokinetics of selected subcutaneously injected DRSP MCSs was analyzed in female Wistar rats and Cynomolgus monkeys. Furthermore, *in vivo* and *in vitro* results were fitted to mathematical models. Although the *in vitro-in vivo* correlation was partially good, the predictability of the *in vitro* test was assumed to be restricted. Nevertheless, mathematical calculations and *in vitro* results allow the interpretation of *in vivo* results and the identification of parameters influencing the drug release. DRSP microcrystal size had a marginal influence on the pharmacokinetics. The drug absorption was slower from aqueous MCSs than from peanut oil MCSs. Absorption profiles of aqueous DRSP MCSs correlated best with Hixson–Crowell model, whereas absorption profiles of oil-based DRSP MCSs showed a good fit to the Higuchi model. The established assumptions were used to interpret the pharmacokinetics of subcutaneously injected oil-based formulations of the steroid ZK28. In summary, low drug solubility in the vehicle and a high vehicle viscosity were assumed to result in slower and constant drug release.

Konzeption:

Stefanie Nippe, Mitarbeit an Konzeption Sascha General, Konzeption der Tierstudien Cornelia Preuße

Durchführung:

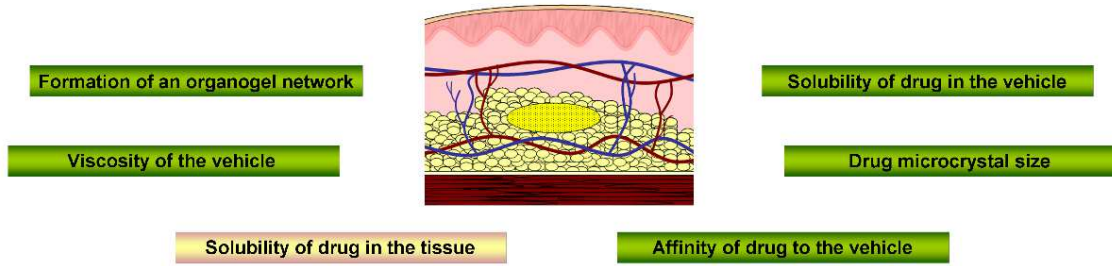
Stefanie Nippe, Durchführung der Tierstudien Cornelia Preuße

Berichtsabfassung:

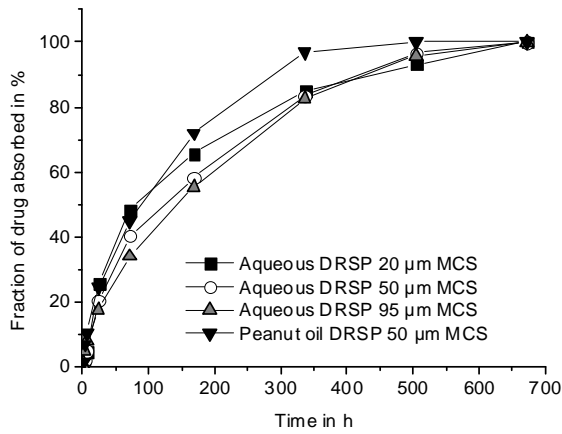
Stefanie Nippe

Graphical Abstract

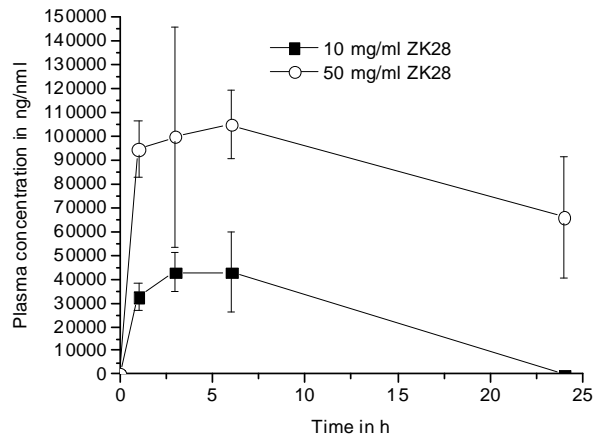
Parameters influencing the subcutaneous drug release



Absorption profiles of drospirenone microcrystal suspensions in Wistar rats



Pharmacokinetics of ZK28 medium chain triglycerides organogels in Wistar rats



1 Introduction

There is an ongoing need for developing steroidal formulations against hormone-dependent diseases or as contraceptives [1-4]. Long-acting steroidal drugs are commonly intramuscularly (i.m.) or subcutaneously (s.c.) injected conventional drug-delivery systems such as oil-based solutions or aqueous microcrystal suspensions (MCSs) [5-7]. The long-term use of daily administered oral drugs could reduce the patients' compliance and increase the risk of inconsistent drug intake [8,9]. To overcome these issues, parenteral injections are developed being administered advantageously less frequently. Conventional parenteral drug-delivery systems of steroids often seemed to provide typical pharmacokinetics. A peak serum level follows the injection exceeding largely the minimal effective dose. Thereafter, the plasma concentration decreases more or less rapidly over time [10,11]. The described plasma profiles were for example shown for oil-based testosterone undecanoate solutions used for the treatment of hypogonadism and for oil-based solutions or aqueous MCSs of contraceptive estradiol esters [10,12-14]. Despite the abovementioned advantage of long-acting injections, the acceptance of injectable contraceptives in middle Europe is low. The 3-months-syringe accounts for only 1% the contraceptive methods used [11]. One reason might be the pharmacokinetics of injectable contraceptives. A more constant release could allow for a lower dose with the same efficacy, while minimizing the side effects. In the following work, we investigated the pharmacokinetics of parenteral drug-delivery systems of two steroids drospirenone (DRSP) and ZK28. DRSP is a progestin used in contraceptives and for the treatment of diseases, disorders, and symptoms associated with deficient endogenous levels of estrogen in women [15]. DRSP is included in numerous oral contraceptives. However, the pharmacokinetics of injectable DRSP formulations has not been studied so far. The steroid has challenging physicochemical properties because it is insufficiently soluble in oils and practically insoluble and chemically unstable in water [16]. Thus, especially oil-based MCSs might be a formulation option. ZK28 is a 17β -hydroxysteroid dehydrogenase type 1 inhibitor, being responsible for the conversion of estrone to estradiol [3] (see **Fig. 1**). According to DRSP, it is insufficiently soluble in aqueous and oil-based vehicle. Formulations including this new drug compound have not been tested yet, and knowledge about its pharmacokinetics was low. First, we investigated the *in vitro* release of injectable steroidal formulations exemplary on DRSP-delivery systems. Our intention was to find formulation characteristics, influencing the drug release. For the initial assessment of injectable dosage forms, *in vitro* release testing is an important tool. Due to the absence of an official *in vitro* dissolution test for prolonged-release parenteral dosage forms, various methods were investigated in the past and are described in the literature. In general, membrane and non-membrane systems are used for *in vitro* release testing of parenteral drug-delivery systems [17-22]. The aim was to use an *in vitro* release test for the qualitative differentiation of formulations that is easy to perform on a large number of samples over a relative

long period of time. We employed a diffusion membrane system for the evaluation of DRSP MCSs. Diffusion membrane models were studied by numerous authors to analyze the drug release of parenteral particulate and lipid-based formulations [20,23-25]. We tested the influence of vehicles, drug microcrystal sizes, and organogelators on *in vitro* release of DRSP MCSs. To interpret the release behavior, theoretical release profiles calculated by mathematical models were fitted to the *in vitro* release profiles. Next, the pharmacokinetics of selected DRSP MCSs was investigated in female Wistar rats and in female Cynomolgus monkeys, considering the *in vitro* results. The plasma profiles were deconvoluted and compared with mathematical models of drug delivery. With respect to the *in vitro* characterization and correlation of DRSP absorption profiles to theoretical models, pharmacokinetic behavior of test formulations was evaluated. Our aim was to define factors affecting the pharmacokinetics of DRSP-delivery systems. To assess the *in vitro* release test, *in vitro* results were collated with the *in vivo* data. Furthermore, the pharmacokinetics in both animal models was compared with each other. During first efficacy studies, ZK28 formulations were injected into female Wistar rats. The pharmacokinetics of ZK28 included in high viscous oil and in an organogel of low viscous oil was compared with each other. Furthermore, different ZK28 doses were tested. The *in vivo* data were assessed based on the assumption established to interpret the pharmacokinetics of DRSP MCSs. In return, the *in vivo* results of ZK28 were used to draw conclusion for further investigations into DRSP MCSs in order to improve their pharmacokinetics.

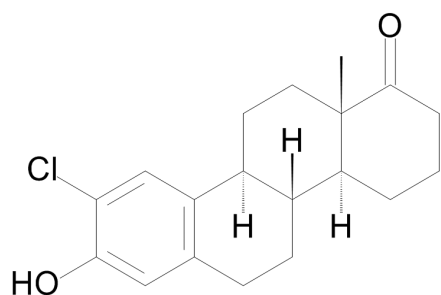


Fig. 1 Chemical structure of ZK28.

2 Materials and methods

2.1 Materials

DRSP micronized (median particle size below 5 μm), DRSP with median particle sizes of 20.82 μm , 48.34 μm , and 93.79 μm (see **Tab. 1**) specially prepared for the experiments, DRSP-d4, and ZK28 (Bayer HealthCare Pharmaceuticals, Berlin, Germany), medium chain triglycerides (MCT) (Myritol® 318 PH, Cognis, Düsseldorf, Germany), castor oil (co), buffer pH 7, and toluene (Riedel-de-Haen, Seelze, Germany), peanut oil (po) (Sigma–Aldrich Chemie, Steinheim, Germany), methyl cholate (Alfa Aesar, Karlsruhe, Germany), 2-hydroxypropyl- β -cyclodextrin (HP- β -CD) (Kleptose® HPBJ, Roquette, Lestrem, France), benzyl benzoate (bb), potassium

dihydrogen phosphate, ammonium acetate, 2-propanol, sodium azide, hydrochloric acid, sodium hydroxide, acetonitrile (ACN), methanol (MeOH), 1-chlorobutane (all from Merck, Darmstadt, Germany), Pefabloc buffer (Roche Diagnostics, Mannheim, Germany), physiological saline (Aguettant, Lyon, France), polysorbate 80 (Brenntag, Mühlheim, Germany), hydroxypropyl cellulose (Klucel® LF) (Hercules, Duesseldorf, Germany) were used.

Tab. 1 Particle size distribution of DRSP microcrystals (n = 3).

Raw material	d ₁₀ in µm	d ₅₀ in µm	d ₉₀ in µm
DRSP 20 µm	2.22 ± 0.19	20.82 ± 0.93	59.82 ± 0.74
DRSP 50 µm	5.49 ± 0.23	48.34 ± 0.50	145.96 ± 1.53
DRSP 95 µm	18.20 ± 0.82	93.79 ± 0.96	182.09 ± 6.29

2.2 Preparation of DRSP MCSs

Micronized DRSP (70 mg/0.5 ml) was dispersed in po, demineralized water, MCT, or a mixture of 60%:40% (w/w) co/bb by magnetically stirring (Ika-Werke, Staufen, Germany). DRSP and the oils were weighed. The density of the vehicles was determined prior to the *in vitro* tests by using a bending oscillator (DMA48, Anton Paar, Graz, Austria). Furthermore, 70mg/0.5 ml of DRSP 50 µm was blended in po, and 70 mg/0.5 ml of DRSP 20 µm were suspended in water by magnetically stirring. For the investigation into the *in vitro* release and its dependence on the presence of an organogelator, 70 mg/0.5 g micronized DRSP was dispersed in MCT with or without the addition of 1.5% (w/w) methyl cholate. The samples were mixed by sonication using an ultrasound device (Sonopuls HD2070, Bandelin electronic, Berlin, Germany) at 5 x 10% cycle with 100% power. They set into a gel after cooling. Shortly before solidification, 0.5 g of DRSP organogel was prefilled into a 1 ml syringe (Tuberkulin® 1 x 100 Soft-Ject, Henke Sass Wolf, Germany) at least 24 h before the *in vitro* tests started in order to give the organogelator network time to structure. For the *in vivo* testing of aqueous DRSP MCSs, 60 mg/0.5 ml of DRSP 20 µm, 50 µm, or 95 µm was dispersed in an aqueous solution, containing 0.25% (w/w) polysorbate 80, 1% (w/w) hydroxypropyl cellulose, and 98.75% (w/w) physiological saline by magnetically stirring at the earliest 1 d before injection. For the analysis of the *in vivo* testing of oil-based DRSP MCSs, 60 mg/0.5 ml of DRSP 50 µm was dispersed in po as described above.

2.3 Preparation of ZK28 formulations

15 and 50 mg/ml of pestled ZK28 were dispersed in 80%:20% (w/w) co/bb by magnetically stirring. Furthermore, 1.5% (w/w) methyl cholate was dispersed in a mixture of 75%:25% (w/w) MCT/bb using an ultrasound device at 5 x 10% cycle with 100% power until a clear solution, which set into a gel after cooling was obtained. Thereafter, 10 and 50 mg/ml of pestled ZK28 were

suspended in the organogel by sonication at 1 x 10% cycle with cooling. The samples were pre-filled in syringes to allow the organogel time to structure.

2.4 Determination of solubility and viscosity of oil-based vehicles

The determination of DRSP solubility in different vehicles was described previously ($n = 3$) [16]. The ZK28 solubility was tested analogously. Briefly, an excess of drug was dissolved in 60:40% (v/v) co/bb and 75:15% (v/v) MCT/bb ($n = 3$). The samples were stirred for 24 h and thereafter analyzed using the HPLC method described in **section 2.5**. The dynamic viscosity of MCT, po, and the mixture of 60%:40% (w/w) co/bb was determined by an automated microviscosimeter (AMVn, Anton Paar) ($n = 3$). Therefore, the samples were added to a capillary containing a ball of known size and density. The sphere descended through the liquids in the tube at an angle of 70°. The falling time was determined over a known distance at 20 °C. The viscosimeter was connected to the bending oscillator, because the determination of the density was necessary before measuring the viscosity.

2.5 *In vitro* release of DRSP

0.5 ml of DRSP MCSs was injected into a dialysis bag (Mw cut off 12,000–14,000 Da, length 7 cm, flat width 1 cm, Spectra/Por, Spectrum® laboratories, Rancho Dominguez, USA) using 1-ml syringes with 20 G needles (Sterican, B.Braun Melsungen, Melsungen, Germany) to simulate the mechanical stress of injection. The samples were weighed in the syringe before and after injection (drug amount of per g vehicle was known for the DRSP MCSs). No release medium was added into the tube. In the same way, 0.5 g of DRSP MCT MCSs and DRSP MCT organogels were injected into the bags. Afterward, the dialysis bags were placed in 100 ml Erlenmeyer flasks containing 50 ml USP phosphate buffer at pH 7.4 with addition of 0.05% (w/v) sodium azide and 8% (w/w) HP- β -CD preheated to 37 °C. The samples were put into a horizontal shaker (Innova 4230, New Brunswick Scientific, Edison, USA) at 100 rpm and 37 °C. At predetermined time intervals, 1 ml samples were withdrawn, assayed, and replaced with fresh medium. The complete release medium was changed every 24 h. Finally, the residual drug amount in the dialysis bags was determined. Therefore, the oil-based samples were diluted in ACN and then filtered (syringe filter, 0.45 μ m). The amount of DRSP and isoDRSP was analyzed by HPLC/UV (Agilent 1100 series, Agilent Technologies, Böblingen, Germany) as described previously (injection volume of 10 or 100 μ l) [16]. Before DRSP determination, a 6-point-calibration was performed. Therefore, the drug was accurately weighed into volumetric flasks and dissolved in ACN to prepare three stock solutions. Two standard solutions were prepared from each stock solution by diluting in ACN/phosphate buffer. Each standard solution was injected three times. Linearity was shown between 1.1 and 500 μ g/ml DRSP. The square of correlation coefficient (r^2) of regression line was above 0.999. The limit of quantitation (LOQ) was calculated from the 10-fold of signal/noise ratio in accordance to

[26]. The LOQ was 1.1 µg/ml. Values below the LOQ were not considered. The retention time was about 4.5 min for DRSP and about 5.3 min for isoDRSP. All of the *in vitro* release tests were performed in triplicate for each test formulation.

2.6 Animals

The female Wistar rats had an age of ca. 8 weeks and weighed about 200 g (supplier Charles River Laboratories, Berlin-Buch, Germany). The female Cynomolgus monkeys weighed about 2.7–5.4 kg and were 7–17 years old (supplier R.C. Hartelust BV, Tilburg, Netherlands). All animal studies were performed with the approval of the local authorities of Berlin (Landesamt für Gesundheit und Soziales, Germany) and in accordance with Recommendations from the Declaration of Helsinki and the German animal protection law.

2.7 Pharmacokinetics of DRSP MCSs

The pharmacokinetics of 60 mg/0.5 ml of DRSP 50 µm po MCSs and aqueous DRSP MCSs including 20 µm, 50 µm, or 95 µm DRSP was investigated in female Wistar rats after single s.c. administration. The formulations were not sterilized before injection. They were administered into the neck using a syringe for precision dosing (B.Braun Omnifix) and 20 G needles. The injection site was closed with Histoacryl to inhibit the loss of the administered formulations through the application site. The DRSP serum level was determined at 0.5, 1, 3, 6, 24, 72, 168, 336, 504, and 672 h, with n = 3 – 4 rats per sampling time. 1–2 blood samples were obtained from each rat. They were collected from the vena cava or by punctuation of the jugular vein at the final sampling time. The samples were diluted with 0.25 M aqueous Pefabloc phosphate buffer to inhibit esterase activity. Furthermore, 30 mg/0.25 ml of aqueous and po DRSP 50 µm MCSs were injected beneath the skin to female Cynomolgus monkeys using a syringe for precision dosing. The DRSP serum level was determined at abovementioned sampling times. Blood samples were collected from a punctured superficial limb vein. The samples collected from rats or monkeys were centrifuged to separate the blood cells and serum. They were stored at below -15 °C until required for later analysis. DRSP determination was conducted in monkey or rat serum with liquid–liquid extraction and separation by high-pressure liquid chromatography and tandem mass spectrometric detection (LC–MS/MS). For DRSP determination in rat serum, samples were mixed with an internal standard working solution containing DRSP-d4 or 80%:20% (v/v) water/MeOH for blank samples and with 1% hydrochloric acid in 50%:50% (v/v) water/ACN in extraction tubes. The samples were extracted with 1-chlorobutane for 2 min at 20 °C, centrifuged, and frozen in an acetone / dry ice bath. The organic layer was transferred to another extraction tube and was dried under nitrogen at 50 °C. The residue was redissolved in 80%:20% (v/v) water/MeOH. 75 µl samples were injected onto a HPLC column (Symmetry Shield C18, 2.1 x 100 mm, 3.5 µm, 40 °C, Waters, Milford, USA) at 200 µl/min. A gradient method was run from 50%:50% (v/v) water/MeOH to

15%:85% (v/v) water/MeOH for 7 min followed by an equilibration of the system using 50%:50% (v/v) water/MeOH for 2 min. The retention time was 6.2 min. Atmospheric pressure photo ionization was used. Toluene was the dopant. Multiple reaction monitoring (MRM) was performed in a positive mode. The m/z 367.3 to m/z 97.1 transition was monitored. For the DRSP determination in monkey serum, samples were mixed with internal standard working solution or buffer pH 7 for blank samples in extraction vials. They were extracted using a 98%:2% (v/v) toluene/2-propanol for 20 min at RT. After centrifugation and freeze out in an acetone/ dry ice bath, the organic phase was transferred to micro V-vials and dried under nitrogen at 50 °C. The residue was redispersed in 55%:45% (v/v) ACN/ammonium acetate buffer. 15 μ l samples were injected onto an HPLC column (comparable rat serum, RT). A gradient method was applied using eluent A, 55%:45% (v/v) water/ACN, and eluent B, 100% ACN, at 300 μ l/min. First, the solvent was set to 100% eluent A for 5 min. Then, a gradient was run from 100% eluent A to 100% eluent B for 2 min followed by an isocratic step applying 100% eluent B for 2 min. Then, the solvent was set to 100% eluent A within 0.2 min. The system was equilibrated using 100% eluent A for 1.4 min. The retention time of DRSP was about 4 min. A turbo ion spray ion source (TIS) was used. MRM was operated in a positive mode (collision energy 47 eV). The m/z 367.3 to m/z 97.1 transition is monitored. All of the *in vivo* studies were done in a GLP compliant facility, and the laboratory procedures were followed in accordance with the GLP guidelines. The method validation and the analysis of the study samples were performed in compliance with [27]. The results for the study samples were derived from sequences, which complied with the FDA acceptance criteria. The stock solutions of calibration standards and quality control (QC) samples were prepared from two separate weightings of the reference material. The calibration standards ranged from 0.2 to 200 ng/ml of DRSP in rat serum (1 sample per concentration). The lower LOQ (LLOQ) was 0.2 ng/ml, and the upper LOQ (ULOQ) was 200 ng/ml. QC samples were prepared from 0.6 to 160 ng/ml of DRSP in rat serum. The sample volume was 100 μ l. The regression type was linear and linearity ranged from 0.2 to 200 ng/ml. Calibration standards and QC samples ranged from 0.1 to 10 ng/ml of DRSP in monkey serum. The LLOQ was 0.1 ng/ml, and the ULOQ was 10 ng/ml. The linearity was shown from 0.1 to 10 ng/ml (2 sets of calibration standards) using a sample volume of 250 μ l. All of the rat and monkey serum samples were analyzed in analytical runs for which four out of six QC samples had a precision within 15% and accuracy within 85 - 115%. All samples were determined in analytical runs for which the blank and zero samples showed co-eluting peaks with responses of no more than 20.0% of the peak response at the LLOQ of DRSP and no more than 5.0% of the peak response of the internal standard. The assay methods showed no unacceptable carryover and no matrix effects. Concentration results of rat and monkey serum were transferred to Excel for further pharmacokinetic evaluation. The pharmacokinetic parameters were calculated from the individual serum concentrations by non-compartmental analysis using the Kincalc program (Version 2.50.02, Bayer, Berlin).

2.8 Pharmacokinetics of ZK28 formulations

ZK28 formulations were injected s.c. into the necks of female Wistar rats using a 1 ml syringe (Tuberkulin®) with a 20 G needle. The formulations were not sterilized before injection. Blood samples were drawn from the retrobulbar area of each animal twice after 1, 3, 6, and 24 h (2 – 3 rats per sampling point). Thereafter, the blood cells and plasma were separated by centrifugation. The samples were frozen until required for later analysis. The concentration of ZK28 in each plasma sample was determined by LC–MS/MS using TIS. 5 µl was injected onto a Thermo Quest Hypersil GOLD column (length 5 cm, inner diameter 2.1 mm, 1.9 µm, 25 °C) using ACN/water with addition of 0.1% methylmorpholine as mobile phase. A gradient was run from 25:75% (v/v) water/ACN to 5:95% (v/v) water/ACN at a flow rate of 300 µl/min over 4 min followed by a flow gradient at 5:95% (v/v) water/ACN from 300 µl/min to 600 µl/min for 1.35 min. Then, the solvent was set to 25:75% (v/v) water/ACN within 5 s. The system was equilibrated using 25:75% (v/v) water/ACN at 300 µl/min for 1.3 min. The retention time of ZK28 was 4.1 min. MRM was performed in a negative mode (collision energy -42 eV). The m/z 316.8 to m/z 280.9 transition is monitored. The method validation and the analysis of the study samples were performed in compliance with [27]. For the preparation of calibration standards and QC samples, rat plasma was spiked with ZK28. The calibration curve consisted of blank and zero samples and calibration standards containing 318.8 ng/ml – 1.59 mg/ml of ZK28. The LLOQ was 31.88 µg/ml, and the ULOQ was 1.59 mg/ml. Calculated from the QC samples, the precision was within ±15% and within 20% at LLOQ. The accuracy was within 85 – 115% and within 80 – 120% at LLOQ. Furthermore, calibration standards were prepared by dissolving ZK28 in concentrations from 318.8 ng/ml to 1.594 mg/ml in ACN/water. Calibration curves in buffer and serum were compared to exclude matrix effects. Pharmacokinetic parameters were calculated by Excel.

2.9 Calculation of theoretical drug release and comparison of *in vitro* drug release and *in vivo* drug absorption

Theoretical drug release profiles calculated by mathematical models were fitted to *in vitro* release and *in vivo* absorption profiles. Therefore, theoretical release profiles according to the Hixson–Crowell equation, the Higuchi equation, and the Nernst–Brunner equation were computed by Excel (see **section 6**). The release or absorption profiles were plotted against the theoretical release profile calculated by Higuchi or Nernst–Brunner. r^2 of linear regression was computed. The cube roots of total drug content minus cube roots of residual drug fractions were plotted versus time according to Hixson–Crowell and r^2 of linear regression line was computed. To compare the *in vitro* and *in vivo* results of DRSP, the drug serum concentrations were deconvoluted using the Wagner–Nelson method [28]. The fraction of drug absorbed divided by the volume versus time was calculated. The elimination rate constant was 0.107 h⁻¹ in Wistar rats and 0.062 h⁻¹ in Cynomolgus monkeys as determined previously [29]. The *in vitro* and *in vivo* results were

compared in a Levy plot. Therefore, absorption profiles and *in vitro* release profiles were normalized to 100%. The times being necessary to absorb/release drug fractions of 10 – 100% (5% steps) were interpolated and compared with each other. The calculations were performed using Excel.

2.10 Statistics

The arithmetic means and standard deviations were calculated for drug solubility, vehicle viscosity, and *in vitro* release profiles. Differences between two results were analyzed by a two-sample *t*-test ($\alpha = 0.05\%$). Differences between *in vitro* release and absorption profiles were evaluated by the difference factor (f_1) and similarity factor (f_2) as previously described [30]. The mean values of the cumulative release concentration at each time point of two formulations were compared. All sampling points with drug release between 10% and 85% were considered. Only one measuring point with drug release above 85% and below 10% was included in the calculation. The preparations were evaluated as not comparable when $f_1 > 15$ and $f_2 < 50$ [31]. To evaluate the pharmacokinetics of DRSP and ZK28, the geometric and arithmetic means and the related standard deviations were calculated from the individual concentration values and the derived individual pharmacokinetic parameters. The AUC and C_{\max} in female Cynomolgus monkeys were normalized for dose by dividing the serum concentration or the AUC by the individual dose (mg/kg body weight), resulting in the parameters C_{norm} and AUC_{norm} .

3 Results

3.1 *In vitro* release of long-acting parenteral DRSP formulations

Because DRSP is practically insoluble in aqueous medium, HP- β -CD was added to the release medium. 13.1 ± 0.2 mg/ml (at RT) of DRSP was soluble in the buffer containing HP- β -CD. Thus, sink conditions were given in the surrounding release medium. The buffer solution was changed every 24 h to reduce DRSP isomerization in the release medium. Below 1% of isoDRSP was found in the buffer at the last time point before medium exchange. Nevertheless, the drug isomerization might be one of the main reasons for the incomplete release beside non-quantifiable drug concentrations at later sampling points, drug remaining in the dialysis bag (residual drug concentrations in the dialysis bag below LOQ at the last sampling point), and loss of drug during medium exchange (see **Fig. 2**). Parameters influencing the drug release from parenteral steroidal formulations were studied on various DRSP MCSs. First, we tested aqueous and oil-based vehicles, being commonly used for injectable dosage forms (see **Fig. 2 a**). The vehicles differed in their viscosity and ability to dissolve DRSP.

The dynamic viscosity of the vehicles increased in the following order at 20 °C:

water < MCT (30.2 ± 0.7 mPas) < po (62.3 ± 0.3 mPas)
< 60%:40% (w/w) co/bb (98.8 ± 1.2 mPas)

The solubility of DRSP increased in the following order at RT:

water (15.4 ± 1.5 $\mu\text{g/ml}$) < po (2.3 ± 0.0 mg/ml) < MCT (5.9 ± 0.1 mg/ml)
< 60%:40% (w/w) co/bb (50.5 ± 0.6 mg/ml)

DRSP showed the fastest release from MCT. More than 80% of DRSP was released from MCT within 96 h. MCT was the lowest viscous lipophilic test vehicles and showed moderate DRSP solubility. DRSP was released markedly slower from co/bb ($f_2 = 53$, $f_1 = 17$). More than 80% of DRSP was released within 120 h. The addition of bb to co raised the DRSP solubility and decreased the vehicle viscosity dramatically. Thus, the vehicle showed the highest DRSP solubility. Nevertheless, co/bb provided the highest viscosity of all test vehicles. Po and aqueous DRSP MCSs exhibited the slowest drug release.

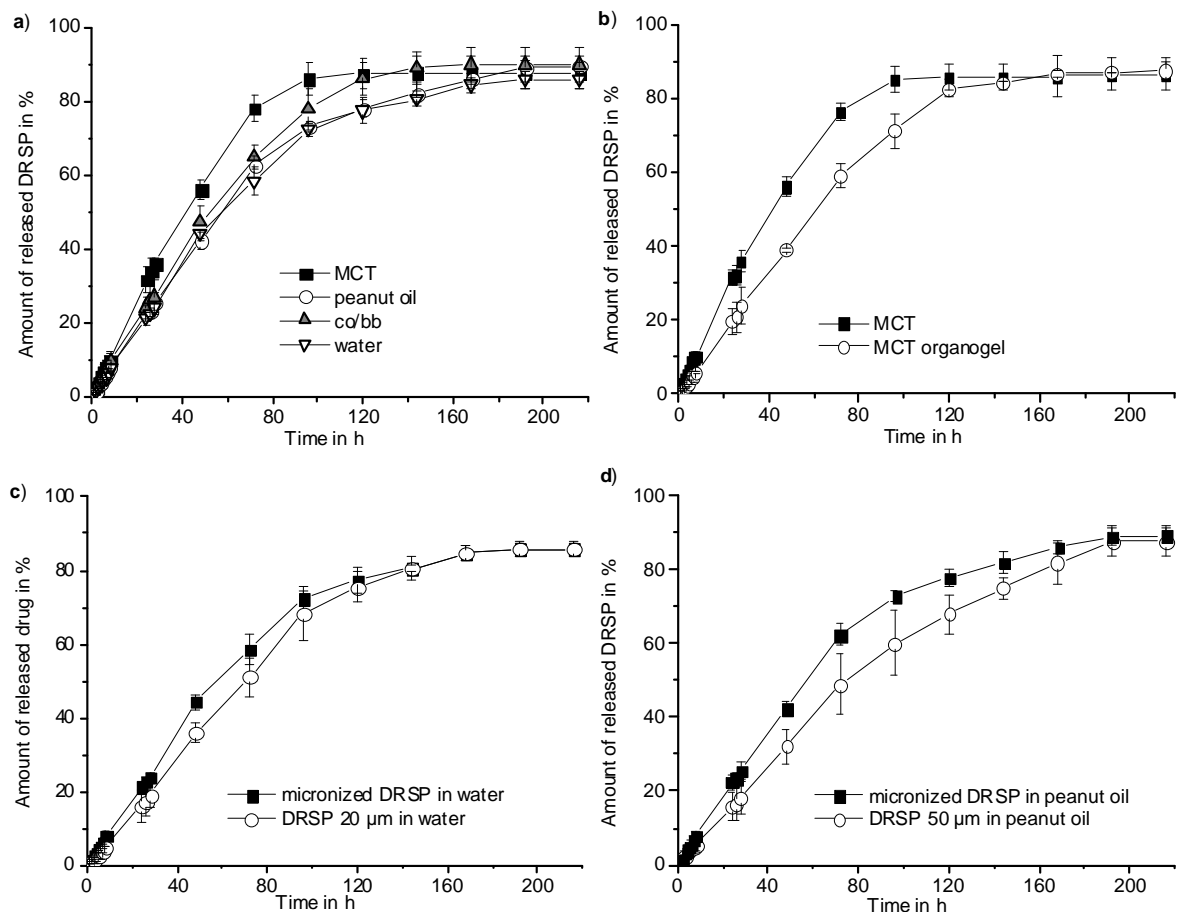


Fig. 2 *In vitro* release profiles of **a)** micronized DRSP suspended in po, water, co/bb and MCT in a concentration of 70 mg/0.5 ml, **b)** micronized DRSP dispersed in MCT and MCT organogel in a concentration of 70 mg/0.5 g, **c)** micronized DRSP and DRSP 20 μm suspended in water in concentration of 70 mg/0.5 ml, **d)** micronized DRSP and DRSP 50 μm suspended in po in concentration of 70 mg/0.5 ml (arithmetic means and standard deviations of $n = 3$).

They released the drug considerably slower than MCT DRSP MCSs (MCT versus po: $f_2 = 47$, $f_1 = 23$; MCT versus water: $f_2 = 45$, $f_1 = 24$) and slightly slower than co/bb DRSP MCSs (co/bb versus po: $f_2 = 68$, $f_1 = 9$; co/bb versus water: $f_2 = 65$, $f_1 = 10$). The drug release profiles of po and aqueous DRSP MCSs were rather comparable ($f_2 = 91$, $f_1 = 4$). Aqueous DRSP MCSs were only minimal slower. More than 80% of the drug from aqueous and po DRSP MCSs was released within 144 h. Both vehicles showed a low DRSP solubility. Po was the oil-based vehicle with the lowest DRSP solubility. However, the drug was almost 200 times less soluble in water. On the other hand, po had a relatively high viscosity, whereas water was the test vehicle with the lowest viscosity. In summary, high viscosity and low drug solubility seemed to decelerate the drug release. However, only MCT MCSs showed markedly different release profiles.

Tab. 2 Correlation between experimental absorption/release profiles and theoretical mathematical models. r^2 of linear regression line is calculated. For every test formulation, the highest r^2 is highlighted indicating the best fit to a mathematical model.

Formulation	r^2 (Nernst – Brunner ^a) (Zero-order release)	r^2 (Hixson-Crowell)	r^2 (Higuchi)
<i>In vitro</i>			
MCT DRSP MCS	0.876	0.925	0.965
Peanut oil DRSP MCS	0.975	0.980	0.984
Aqueous DRSP MCS	0.926	0.972	0.982
co/bb DRSP MCS	0.916	0.964	0.985
DRSP MCT organogel MCS	0.932	0.970	0.980
Aqueous DRSP 20 μm MCS	0.953	0.984	0.979
Peanut oil DRSP 50 μm MCS	0.930	0.999	0.985
<i>In vivo</i>			
Aqueous DRSP 20 μm MCS (rat)	0.833	0.971	0.968
Aqueous DRSP 50 μm MCS (rat)	0.882	0.992	0.986
Aqueous DRSP 95 μm MCS (rat)	0.905	0.992	0.990
Aqueous DRSP 50 μm MCS (monkey)	0.816	0.980	0.957
Peanut oil DRSP 50 μm MCS (rat)	0.965	0.971	0.981
Peanut oil DRSP 50 μm MCS (monkey)	0.906	0.980	0.988

^a Surface area, drug diffusivity and thickness of diffusion layer were assumed to be constant.

Next, the DRSP release from MCT organogels was analyzed. The addition of methyl cholate to the low viscous MCT immobilized the liquid phase completely and slowed down the sedimentation of drug microcrystal through the vehicle. The destruction of organogelator network by the mechanical stress enabled the injection by a syringe. The organogelator structure was partially recovered after

injection being visible by an increase in viscosity (see **Supplement**). Compared with DRSP MCT MCSs, the *in vitro* release was considerably decelerated ($f_2 = 44, f_1 = 27$) (see **Fig. 2 b**). The results confirm the assumption that the vehicle viscosity influences the drug release. Furthermore, DRSP MCT organogels showed a slightly slower drug release than co/bb DRSP MCSs and a slightly faster drug release than po and aqueous DRSP MCSs (co/bb: $f_2 = 63, f_1 = 11$; po: $f_2 = 77, f_1 = 5$; water: $f_2 = 75, f_1 = 5$). Finally, the influence of the DRSP particles size on the *in vitro* release was analyzed. MCSs containing DRSP with smaller microcrystals sizes and consequently with greater particle surfaces delivered the drug faster (see **Fig. 2 c and d**). However, a relative low impact of microcrystal size on drug release was found for the tested DRSP MCSs. The drug release from po MCSs including micronized DRSP was faster compared with po DRSP 50 μm MCSs ($f_2 = 52, f_1 = 19$). But aqueous MCSs containing micronized drug was only slightly faster compared with aqueous DRSP 20 μm MCSs although median drug particles were at least 4-fold smaller ($f_2 = 65, f_1 = 7$). The broad particle size distribution of the coarser drug microcrystals was assumed to cause relatively high standard deviations of the release profiles of DRSP 20 μm and DRSP 50 μm MCSs. Finally, mathematical models were fitted to the *in vitro* release profiles (see **Tab. 2** and **Fig. 3 a and g**). All mathematical models based on the Fick's law. The correlation between a theoretical zero-order profile calculated with Nernst–Brunner and the experimental release profiles was low. Nevertheless, the *in vitro* profiles correlated well to the model within the first hours. The Nernst–Brunner equation is true for particles with a constant surface. The Hixson–Crowell equation considers a decrease in the particle surface area during drug dissolution [32]. The correlation with this model was generally higher. Higuchi's equation described the release of suspended drug from an ointment matrix. Drug diffusion through the formulation matrix is the rate-limiting step in this process [33]. The best correlation was found using the Higuchi's equation with two exceptions. Po DRSP 50 μm MCSs and aqueous DRSP 20 μm MCSs showed a better fit to the Hixson–Crowell model. In general, the initial drug release was overestimated by the Higuchi model.

3.2 Pharmacokinetics of DRSP MCSs

The *in vivo* behavior was studied in two different animal models. First, the pharmacokinetics of DRSP MCSs was investigated in Wistar rats. In particular, the influence of the vehicle and of drug particles size on the pharmacokinetics was analyzed. The *in vitro* tests indicated that DRSP po MCSs and aqueous DRSP MCSs showed a slow drug release. Consequently, the pharmacokinetics of both formulations was analyzed. DRSP 50 μm was used, because the *in vitro* release was slightly decelerated with increased drug microcrystal size. Furthermore, the influence of microcrystal size was tested *in vivo* on aqueous DRSP MCSs containing the drug in three different particle sizes. For all aqueous formulations, the drug serum profiles were characterized by a fast increase of drug serum concentration within the first 24 h followed by a fast decrease of drug serum levels within the next 48 h resulting in a conspicuous initial plasma peak (see **Fig. 4 a**).

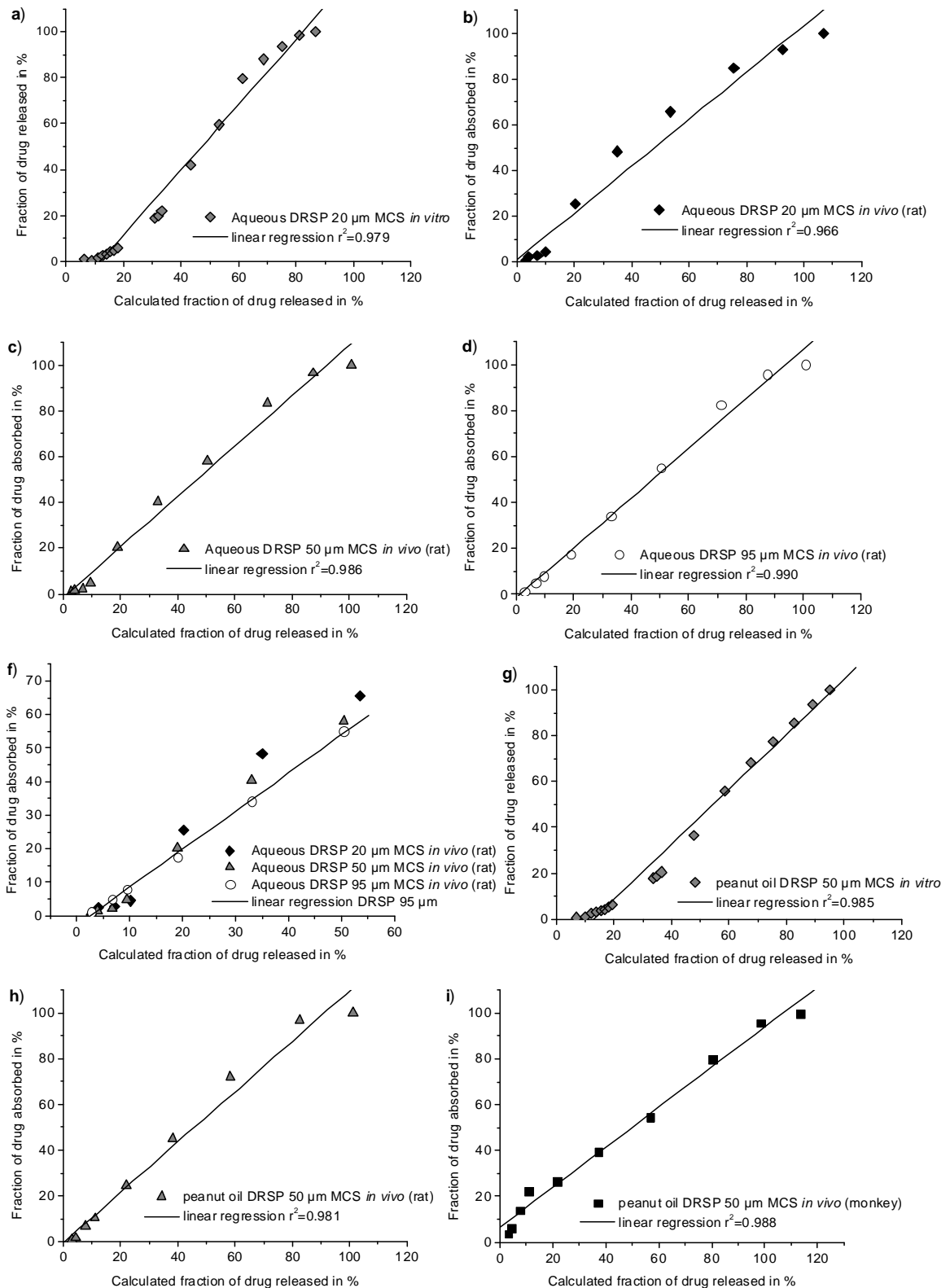


Fig. 3 *In vitro* release and *in vivo* absorption profiles correlated with the theoretical drug release profiles calculated by Higuchi's equation. **a)** *In vitro* release of aqueous DRSP 20 μm MCSs, **b)** *in vivo* absorption of aqueous DRSP 20 μm MCSs in Wistar rats, **c)** *in vivo* absorption of aqueous DRSP 50 μm MCSs in Wistar rats, **d)** *in vivo* absorption of aqueous DRSP 95 μm MCSs in Wistar rats, **e)** *in vivo* absorption of aqueous DRSP 50 μm MCSs in Cynomolgus monkeys, **f)** initial *in vivo* absorption of aqueous DRSP MCSs with different particle sizes in Wistar rats, **g)** *in vitro* release of po DRSP 50 μm MCSs, **h)** *in vivo* absorption of po DRSP 50 μm MCSs in Wistar rats, **i)** *in vivo* absorption of po DRSP 50 μm MCSs in Cynomolgus monkeys. r^2 of linear regression line is calculated.

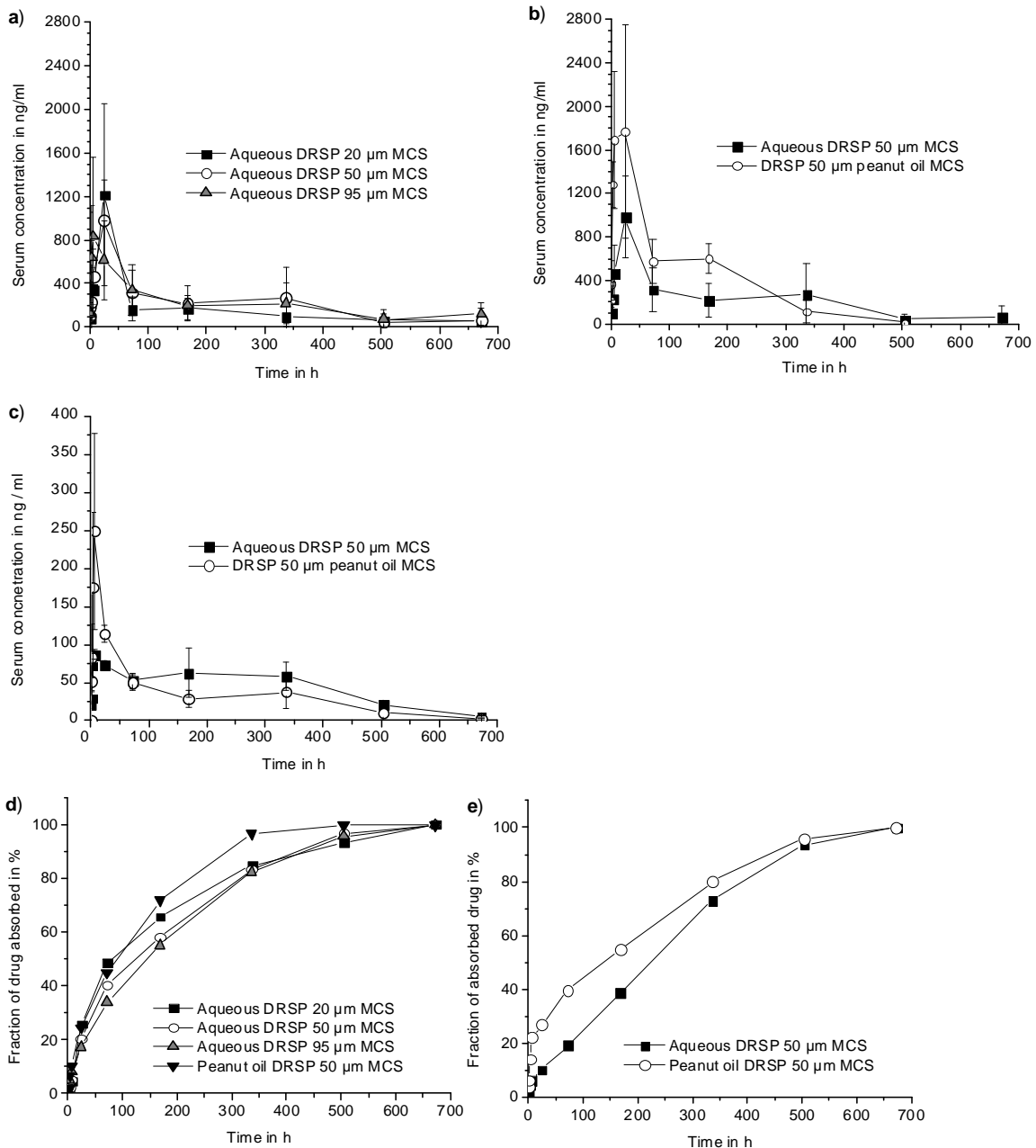


Fig. 4 Arithmetic mean of DRSP serum concentrations in female Wistar rats after single s.c. administration **a)** of aqueous DRSP MCSs in three different particle sizes and **b)** of po and aqueous DRSP 50 μm MCSs ($n = 3-4$). **c)** Arithmetic mean of DRSP serum concentrations in Cynomolgus monkeys after single s.c. administration of po and aqueous DRSP 50 μm MCSs ($n = 3$). **d)** Fractions of drug absorbed *in vivo* from aqueous and po DRSP MCSs in Wistar rats and **e)** Fractions of drug absorbed *in vivo* from aqueous and po DRSP MCSs in Wistar rats deconvoluted with the Wagner–Nelson method.

Thereafter, a more or less pronounced plateau drug serum level between day 3 and 14 was followed by a slow decline over time. As predicted *in vitro*, the influence of particle size was low on the drug release. The DRSP *in vivo* release was not prolonged using increased particle sizes because the lowest geometric mean of serum concentration (18.4 ± 5.7 ng/ml) was observed for aqueous DRSP 50 μm MCSs at the last sampling point. In addition, no correlation was found between particle size and AUC, t_{max} , or C_{max} (see **Tab. 3**).

Tab. 3 Pharmacokinetic parameters calculated from the individual DRSP serum profiles after single s.c. administration of DRSP MCSs to female Wistar rats (n=3-4).

Calculated parameter	Aqueous DRSP MCS (20 μm)	Aqueous DRSP MCS (50 μm)	Aqueous DRSP MCS (95 μm)	DRSP peanut oil MCS (50 μm)
AUC _(0-t_n) in (ng·h)/ml (arithmetic mean \pm arithmetic standard deviation)	98805 \pm 35519	128860 \pm 29370	152003 \pm 44331	229370 \pm 18597
AUC _(0-t_n) in (ng·h)/ml (geometric mean \pm geometric standard deviation)	94277.7 \pm 1.5 ^a	126425.8 \pm 1.3 ^a	148031.2 \pm 1.3 ^b	219590.1 \pm 1.0 ^b
C _{max} in ng/ml (arithmetic mean \pm arithmetic standard deviation)	1383 \pm 594	984 \pm 371	1142 \pm 607	2253 \pm 754
C _{max} in ng/ml (geometric mean \pm geometric standard deviation)	1300.5 \pm 1.5	927.0 \pm 1.6	1044.5 \pm 1.7	2160 \pm 1.4
t _{max} in h (arithmetic mean \pm arithmetic standard deviation)	17.0 \pm 12.1	24.0 \pm 0.0	5.0 \pm 1.7	11.0 \pm 9.6
t _{max} in h (geometric mean \pm geometric standard deviation)	12 \pm 3.3	24 \pm 1.0	4.8 \pm 1.5	7.6 \pm 2.4

^a t_n = 672 h, ^b t_n = 504 h

The absorption profiles were not markedly different, although DRSP 95 μm had an about 5-fold larger median particle size than DRSP 20 μm (20 μm versus 95 μm : $f_2 = 54$, $f_1 = 13$) (see **Fig. 4 d**). After an initial lag time, the absorption profiles of DRSP 20 μm and 50 μm MCSs increased significantly between 6 and 24 h (see **Fig. 3 f**). Compared with aqueous DRSP 50 μm MCSs, po DRSP 50 μm MCSs showed a conspicuously higher increase in serum concentrations within the first 24 h followed by a sharper decline within the next 48 h. (see **Fig. 4 b**). Thus, the initial serum peak was even more pronounced. However, C_{max} values did not differ significantly ($p = 0.10$). Then, a plateau phase was observed between day 3 and 7 followed by a decline in drug serum concentrations over time. Po and aqueous DRSP 50 μm MCSs showed considerably different absorption profiles ($f_2 = 52$, $f_1 = 17$) (see **Fig. 4 d**). Although the AUC of po MCSs was significantly higher ($p = 0.04$), the mean serum level was below LLOQ at day 28.

Tab. 4 Pharmacokinetic parameters calculated from the individual DRSP serum concentration after single s.c. administration of DRSP MCSs to female Cynomolgus monkeys (n = 3).

Calculated parameter	Aqueous DRSP MCS (50 μm)		DRSP peanut oil MCS (50 μm)	
	Geometric mean \pm geometric standard deviation	Arithmetic mean \pm arithmetic standard deviation	Geometric mean \pm geometric standard deviation	Arithmetic mean \pm arithmetic standard deviation
AUC _(0-t_n) in (ng·h)/ml	27707 \pm 1.3* ₁	28270 \pm 6949	20594 \pm 1.2* ₂	20829 \pm 3957
AUC _{(0-t_n)norm} in (kg·h)/l	3.2 \pm 1.2	3.2 \pm 0.5	2.3 \pm 1.7	2.5 \pm 1.5
C _{max} in ng/ml	92.8 \pm 1.1	92.9 \pm 5.2	229 \pm 1.8	253 \pm 124
C _{max, norm} in kg/l	0.010 \pm 1.080	0.011 \pm 0.001	0.025 \pm 1.284	0.026 \pm 0.007
t _{max} in h	14.5 \pm 8.6	59.0 \pm 94.4	9.5 \pm 2.2	12.0 \pm 10.4

^a t_n = 672 h, ^b t_n = 226-372 h

In the next step, po and aqueous DRSP 50 μm MCSs were injected into Cynomolgus monkeys (see **Tab. 4** and **Fig. 4 c**). Because the drug particle size was shown to have no effect in rats, only the influence of the different vehicles was tested in monkeys. Obviously, drug serum concentrations were considerably higher in rats mainly caused by the different dose and volume of distribution. Consequently, AUC and C_{max} were significantly lower. Nevertheless, the courses of DRSP serum profiles of po DRSP MCSs in rats and monkeys correlated well (see **Fig. 5 a**). For po DRSP MCSs, a sharp increase in drug serum concentrations was observed within the first 24 h resulting in high C_{max} . The serum peak was followed by a fast decrease of the serum level within the next 48 h. Subsequently, a plateau phase was reached proceeding in a phase of slow decline. For aqueous DRSP MCSs, the initial increase in drug serum levels was followed by a relatively slow decrease. Thus, the initial plasma peak was lower than for po MCSs and seemed to be less pronounced than shown in rats. Consequently, the C_{max} calculated by arithmetic mean values of drug serum concentrations was not reached within 24 h in contrast to all of the other formulations in rats and monkeys. The drug serum levels of aqueous and po DRSP MCSs were above LLOQ at day 28. $C_{\text{max, norm}}$ was significantly higher for po MCSs ($p = 0.02$), whereas AUC_{norm} were comparable with each other ($p = 0.5$). The absorption profiles of aqueous and po DRSP MCSs differed markedly ($f_2 = 44, f_1 = 27$) (see **Fig. 4 e**). Furthermore, the correlation between absorption profiles of aqueous DRSP MCSs in rats and monkeys was low (see **Fig. 5 b**).

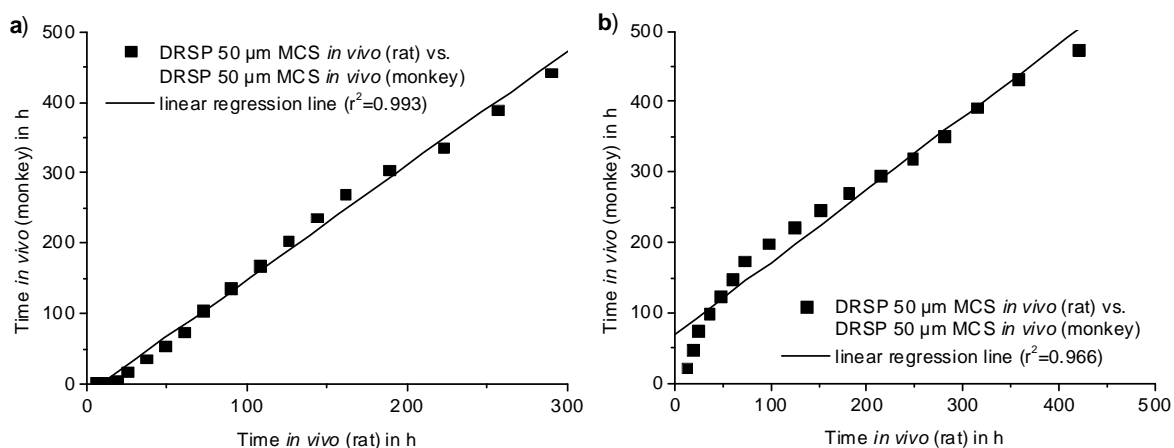


Fig. 5 Fraction absorbed *in vivo* from **a**) po DRSP 50 μm MCSs in Wistar rats versus fraction absorbed *in vivo* from po DRSP 50 μm MCSs in Cynomolgus monkeys, **b**) aqueous DRSP 50 μm MCS in Wistar rats versus fraction absorbed *in vivo* from aqueous DRSP 50 μm MCSs in Cynomolgus monkeys. r^2 of linear regression line is calculated.

The absorption rate of aqueous DRSP MCSs was considerably slower in monkeys within the first 72 h. Finally, the drug absorption profiles in rats and monkeys were compared with mathematical models (see **Tab. 3**, **Fig. 4**). The best correlation for aqueous DRSP MCSs was obtained with the Hixson–Crowell model. The best approximation to the absorption profiles of po DRSP MCSs was the Higuchi model.

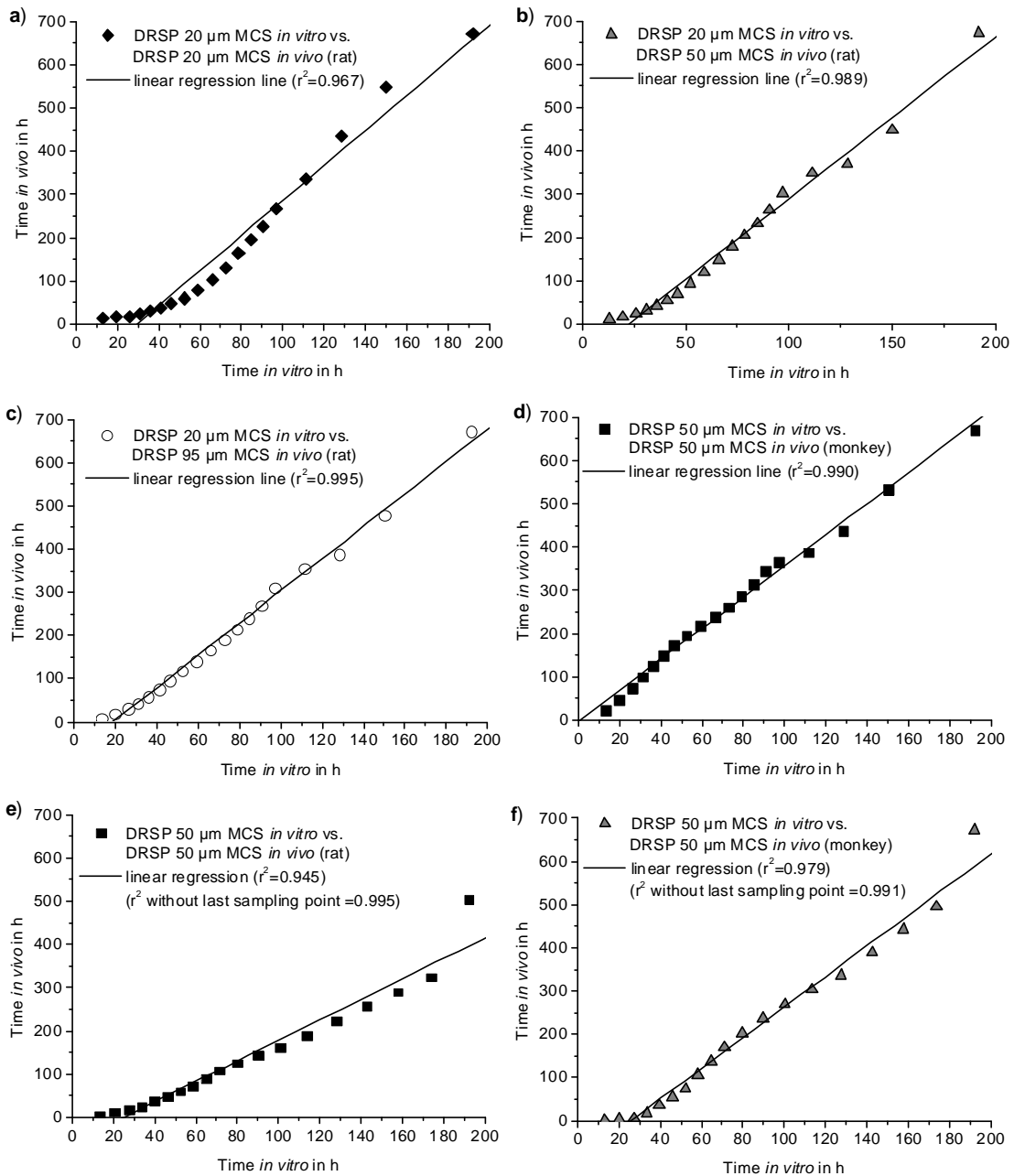


Fig. 6 Levy-plot of time necessary for DRSP *in vitro* release versus time necessary for DRSP *in vivo* absorption. *In vitro* release of aqueous DRSP 20 μm versus **a)** *in vivo* absorption of aqueous DRSP 20 μm MCSs in Wistar rats, **b)** *in vivo* absorption of aqueous DRSP 50 μm MCSs in Wistar rats, **c)** *in vivo* absorption of aqueous DRSP 95 μm MCSs in Wistar rats, **d)** *in vivo* absorption of aqueous DRSP 50 μm MCSs in Cynomolgus monkeys. *In vitro* release of po DRSP 50 μm MCSs versus **e)** *in vivo* absorption of po DRSP 50 μm MCSs in Wistar rats, **f)** *in vivo* absorption of po DRSP 50 μm MCSs in Cynomolgus monkeys. r^2 of linear regression line is calculated.

3.3 Comparison of *in vitro* and *in vivo* results

The best correlation was determined between *in vivo* and *in vitro* data of aqueous DRSP 95 μm MCSs and DRSP 50 μm MCSs (rat and monkey) (see **Fig. 6**). Interestingly, the correlation between *in vitro* profiles of aqueous DRSP 20 μm MCSs and absorption profiles of aqueous DRSP MCSs in rats was improved with increasing particle size of absorbed drug. Absorption profiles of

po DRSP 50 μm MCSs in rats and monkeys showed a lower overall fit to the *in vitro* profiles. Obviously, the time points of 100% absorption and 100% *in vitro* release did not match with each other. Nevertheless, with the exception of this point, the *in vitro-in vivo* correlation of po DRSP MCSs was rather well ($r^2 > 0.99$).

3.4 Pharmacokinetics of oil-based ZK28 formulations

With 38.3 ± 2.3 mg/ml, ZK28 was more soluble in co/bb than in MCT organogel (29.8 ± 3.0 mg/ml). The drug solubility was insufficient to dissolve higher ZK28 doses. In a first pharmacokinetic study, the *in vivo* behavior of ZK28 organogels and co/bb ZK28 formulations was examined in female Wistar rats (see Fig. 7). A fast increase in drug plasma concentrations of co/bb ZK28 formulations within 3 h was followed by a sharp decline within the next 3 h, resulting in a marked initial plasma peak in accordance to oil-based and aqueous DRSP MCSs. Thereafter, a plateau phase was observed for 50 mg co/bb ZK28 MCSs comparable to oil-based and aqueous DRSP MCSs. Similar behavior was shown for 15 mg co/bb ZK28 formulations. The plasma level was below the LLOQ after 6 h. ZK 28 MCT organogels showed a fast initial increase in drug plasma concentration within 1 h. In contrast to co/bb ZK28 formulations, the drug plasma concentrations decreased thereafter more constant. Plasma concentrations of 10 mg ZK28 organogels were below LLOQ within 24 h. 50 mg ZK28 organogels and 50 mg co/bb ZK28 MCSs exhibited comparable drug concentrations after 24 h. Calculated from the arithmetic mean, 50 mg co/bb ZK28 MCS had an $\text{AUC}_{(0-24\text{h})}$ of 1113 ± 570 $\mu\text{g/ml}$, whereas the MCT organogel, including 50 mg ZK28 provided an $\text{AUC}_{(0-24\text{h})}$ of 2091 ± 489 $\mu\text{g/ml}$. Due to the high standard deviation, the AUCs were not significantly different ($p = 0.086$). Furthermore, 15 mg co/bb ZK28 formulations had an $\text{AUC}_{(0-24\text{h})}$ of 96 ± 12.4 $\mu\text{g/ml}$, whereas the 10 mg ZK28 MCT organogels showed an $\text{AUC}_{(0-24\text{h})}$ of 839 ± 228 $\mu\text{g/ml}$. Consequently, the MCT organogel formulation showed a significantly higher AUC than the co/bb ZK28 formulation ($p = 0.005$).

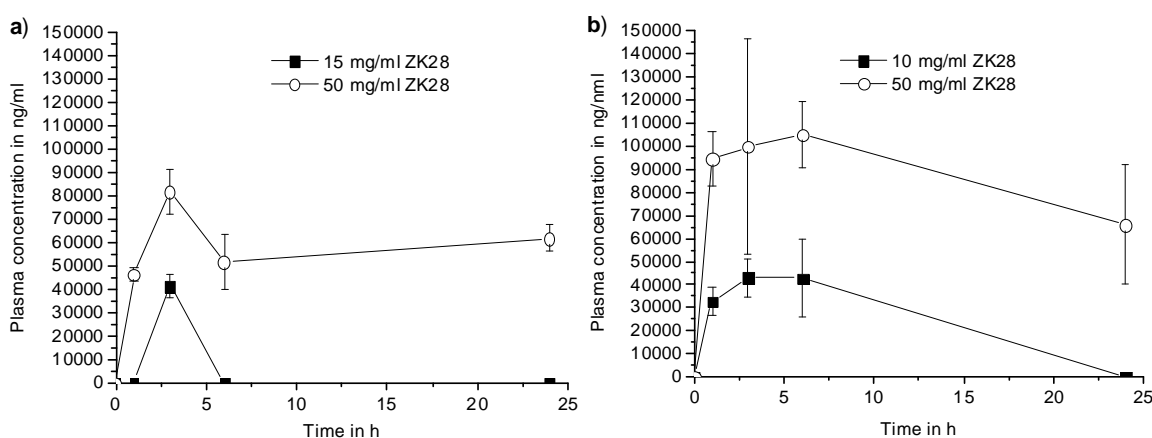


Fig. 7 Arithmetic mean plasma level of ZK28 in female Wistar rats after single s.c. administration of the drug substance dispersed in **a)** co/bb and **b)** MCT organogel ($n = 3$).

4 Discussion

The pharmacokinetics of the steroidal drugs ZK28 and DRSP was studied. Both drugs provide low water solubility as generally assumed for steroidal drugs and are insufficiently soluble in oil-based vehicles. We first investigated the *in vitro* release of DRSP MCSs and fitted mathematical models to the *in vitro* release profiles to understand influencing parameters on the *in vivo* behavior. All models require sink conditions, which were given in the release medium. Referring to Higuchi's equation, the surface area of drug formulation influences the release. A constant surface area of the DRSP formulation was ensured by inclusion in dialysis bags. The *in vitro* results indicated an impact of the physicochemical characteristics of the vehicle, in particular of the viscosity and drug solubility, on the drug release (see **Fig. 8 a**). The relationship between these parameters is expressed in Higuchi's equation. In accordance, the *in vitro* release profiles showed a relatively good correlation with the theoretical calculated release profiles (see **Tab. 2**). Over time, more and more DRSP was solvated in the aqueous vehicle and was transported to the release medium. The drug diffusion through the aqueous vehicle should be fast, due to the very low viscosity of the liquid. But, the aqueous DRSP MCSs showed, beside DRSP po MCSs, the most sustained release profiles. Thus, the low drug solubility in the aqueous vehicle should mainly cause the decelerated drug release compared with the other tested liquids. Po provided the lowest drug solubility of oil-based test vehicles. Nevertheless, drug solubility in po was significantly higher than in water. On the other hand, the drug diffusion through high viscous po should be significantly slower than in water. As a result, the drug release from po and aqueous DRSP MCSs was comparable. DRSP had the highest solubility in co/bb. This might explain the slightly accelerated drug release compared with po or water. However, the high drug solubility indicated that the relatively lipophilic DRSP had a higher affinity to the lipophilic vehicle than to the aqueous release medium. The attraction of the drug to the vehicle might cause a deceleration of the drug transfer to the release medium. In accordance, the influence of the drug distribution between the release medium and oil-based parenteral formulations on the drug release was previously described by several authors [34-38]. Another parameter which slows down the drug release from co/bb was its high viscosity. The viscosity of co alone was even too high for injection. Only with addition of bb, the vehicle became syringeable through 20 G needles used for the *in vitro* tests. Nevertheless, the mixture was the most viscous tested vehicle. The drug affinity to the vehicle and the high viscosity of co/bb were assumed to oppose the effect of high drug solubility on the release kinetics. As a result, a moderate drug release rate was observed for DRSP co/bb MCSs. Although the drug solubility was only slightly higher in MCT, the drug release was significantly accelerated compared with po. Thus, the significant lower viscosity of MCT compared with other oil-based vehicles could explain the faster drug release. In accordance, the drug release was significantly slowed down with addition of an organogelator. Apparently, the organogelator network decelerated the drug diffusion in the vehicle.

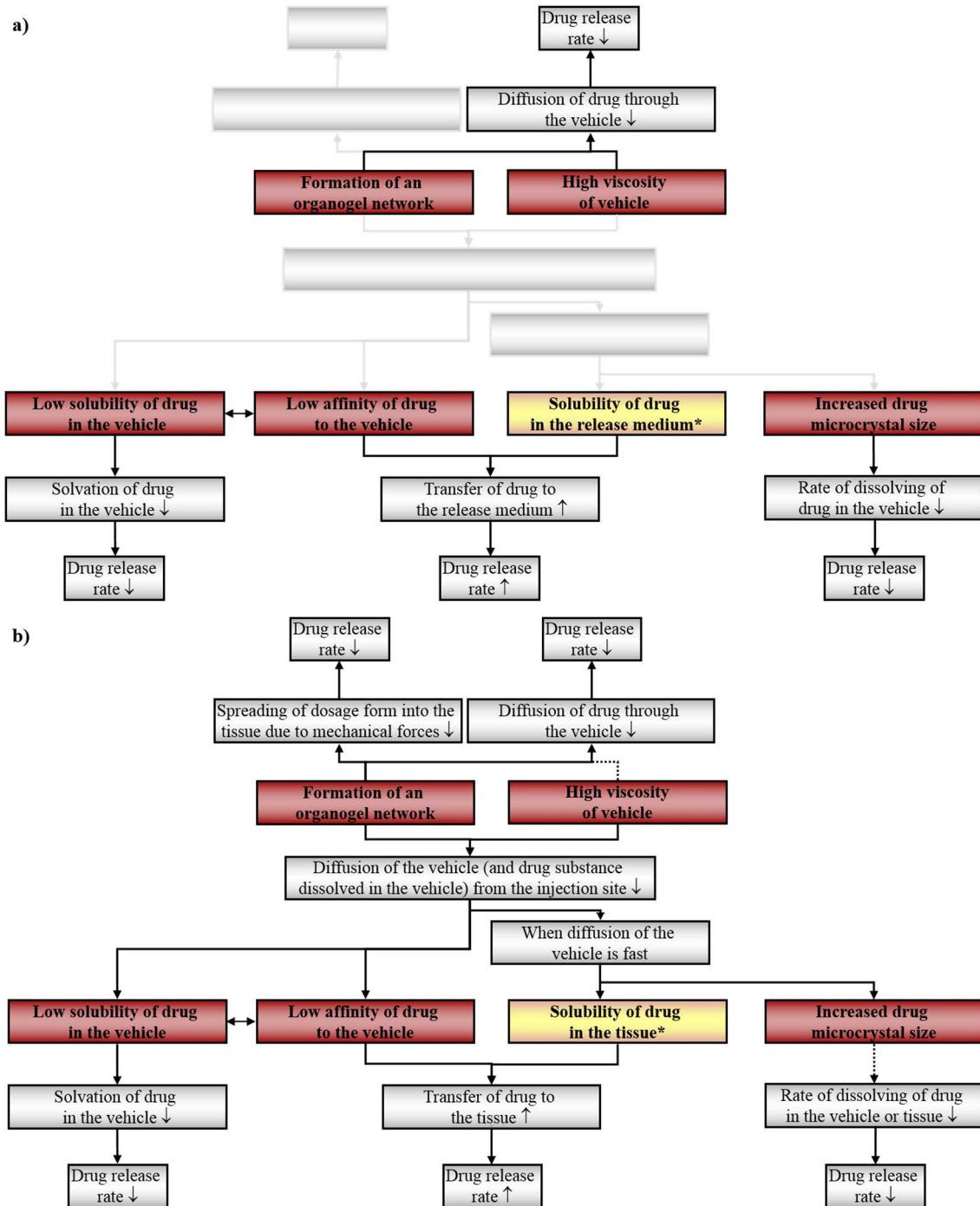


Fig. 8 Overview of parameters which were assumed to influence the drug release **a)** *in vitro* (light-gray-colored parameters were not simulated under *in vitro* conditions) and **b)** *in vivo* (dotted arrows symbolize that the parameter was assumed to have no significant influence the *in vivo* release; the clearance of vehicle was not considered); (*) parameter was constant and could not be influenced by the dosage form.

The addition of an organogelator enabled the increase of viscosity without losing syringeability. According to the Nernst–Brunner equation, the DRSP microcrystal size slowed down slightly the *in vitro* release. Interestingly, the release profiles of aqueous DRSP 20 μm MCSs and po DRSP 50 μm MCSs showed the best correlation with Hixson–Crowell’s model derived from Nernst–Brunner equation. The decelerated dissolution rate caused by large particle sizes might increase the

impact of drug dissolution on the drug release. In contrast, Higuchi's equation matches to systems in which dissolution is rapid, and diffusion is rate-controlling [39]. Furthermore, the length of diffusion pathway influenced the drug release in the Higuchi model. The larger particles might tend to sedimentation influencing the length of diffusion pathway. With respect to the Nernst–Brunner equation, the drug dissolution profile could be rather linear if the thickness of diffusion layer and the particle surface is constant and sink conditions in the release medium are given. Such a linear profile showed a good correlation with the experimental release profiles within the first hours. In the later course, the correlation became lower possibly by a decrease in drug particle size or in an increasing impact of diffusion. The decreasing particle size is considered by the Hixson–Crowell equation, which seemed to be most appropriate to explain the release behavior of MCSs including larger DRSP particles. The results indicated that only a marked increase in microcrystal size was able to prolong the drug release. In general, the theoretical profiles calculated by the Higuchi equation predicted a higher drug release rate within the first hours than observed experimentally (exemplary **Fig. 3 a** and **g**). According to the equation, the length of drug diffusion pathway increased over time. The drug release rate should consequently be high at the beginning and decelerate over time. On this consideration, the reduced initial drug release could be mainly caused by shaking of the *in vitro* systems. The movement of the *in vitro* system should avoid local saturation effects in the release medium and simulate mechanical *in vivo* stress. However, shaking influenced the drug distribution in the formulation which may reduce the time-dependent increase in the length of diffusion pathway. Moreover, the lag time could be caused by the surrounding drug-free dialysis membrane. *Higuchi* [33] described that drug release may be delayed until the first drug reaches the release medium. But, the lag time should be short because the dialysis membrane was much thinner than the matrix of MCSs, the membrane was freely permeable for DRSP, and drug dialysis rate was significant faster than the drug release rate (*in vitro* release rates were significantly slower than the dialysis rate (1.2 mg/h) of in release medium dispersed DRSP which was included in the dialysis membrane, data not shown). Furthermore, discrepancies between experimental and theoretical release profiles could be caused by the shape of drug formulations. Higuchi's equation describes the drug release from a thin layer. The dialysis bag had a cylindrical shape. Bottom and top of the cylinder are not available for diffusion as the dialysis tube is closed with clamps. The surface of the drug formulation was therefore calculated by computing the surface of the lateral area of the cylindrical tube. This approach did not give the precise mathematical model but an approximation. In summary, drug release was assumed to have a complex relationship between characteristics of the vehicle and of the steroidal drug (see **Fig. 8**). First, the suspended steroid is dissolved in the vehicle. This step might be decelerated by low drug solubility in the vehicle. Furthermore, a markedly larger drug particle size slows down the dissolution rate. Second, the dissolved drug is transported to the surface of the formulation. The drug diffusion to the phase boundary might be decelerated by high viscosity or by the addition of

an organogelator to the vehicle. Finally, the dissolved drug is distributed from the vehicle to the release medium. As the affinity of the drug substance for the vehicle increases, the transfer should be slower.

In the next step, the pharmacokinetics of steroidal injections was studied on DRSP and ZK28 formulations with respect to the *in vitro* results. In general, the *in vitro* DRSP release profiles were significantly faster than the DRSP absorption profiles. A possible reason might be that sink conditions exist *in vitro*. The drug must *in vivo* not only pass the vehicle, it has to diffuse through the s.c. tissue to reach the blood circulation where sink conditions exist. Although the slow drug release from po and aqueous vehicle was assumed to be caused by different effects, their *in vitro* release profiles were comparable. However, the pharmacokinetics of po and aqueous DRSP MCSs in rats differed significantly. It was shown that lipophilic drugs dispersed in aqueous vehicles tend to remain in the tissue over a long period of time increasing the risk of residual drug [38]. This phenomenon could explain the low AUC of aqueous DRSP MCS. Fitting mathematical models to the absorption profiles of aqueous and oil-based DRSP MCSs, the best correlation of aqueous DRSP MCSs was shown with the Hixson–Crowell model. It was described in the literature that an aqueous vehicle removed from the injection site within about 48 h [40,41]. An oil-based vehicle stayed longer at the injection site due to its higher viscosity. Whereas high viscous oil-based vehicles formed a sharply bounded depot, water spread wider into the surrounding tissue. Thus, undissolved particles remained widely distributed in the vicinity of the application site [40]. Referring to these processes described in the literature, it was assumed that the pharmacokinetics of aqueous DRSP MCSs was characterized by two phases of drug release.

At the beginning, DRSP is released by dissolution of drug in the vehicle, drug diffusion to the tissue and to the blood vessels in accordance to the mechanisms described by the Higuchi equation. Furthermore, depletion of aqueous vehicle containing dissolved drug could cause a faster drug absorption in this phase. In the second stage, remaining undissolved drug was slowly dissolved and diffused through the tissue to the blood vessels. The overall drug release process seemed to be mainly controlled by drug dissolution according to the Hixson–Crowell model in accordance to *in vitro* release profiles of DRSP 20 μm MCSs. Po was assumed to remain longer at the injection site. The dissolved drug was diffused through the vehicle and transferred to the tissue. The processes are mathematically expressed by the Higuchi equation, showing the best correlation to the absorption profile. With respect to the mathematical model, the shape of the drug-delivery system had a high influence on drug release. In contrast to the *in vitro* model, the shape was not controllable. This could explain the high *in vivo* variability. The absorption profile showed a decelerated drug release rate after 336 h, resulting in a slightly lower correlation between theoretical and experimental absorption profile of po DRSP MCSs (see **Fig. 6 e**). A possible explanation would be the complete depletion of the vehicle from injection site resulting in remaining undissolved DRSP thereafter.

Furthermore, the *in vitro* test indicated a slower drug release only with markedly larger drug microcrystal sizes. This effect was also shown *in vivo*. Interestingly, the fit of the theoretical release profiles to the absorption profiles increased with increasing drug microcrystal size. Within the first hours, aqueous DRSP 20 μm and 50 μm MCSs showed a delay in drug absorption (see **Fig. 3 f**). A distance between blood vessels and injection site could cause the initial lag time. Thereafter, DRSP 20 μm MCSs showed the highest serum concentrations. The increased concentration of drug released from DRSP 20 μm MCSs in this phase resulted in a lower correlation to the theoretical profile calculated with Higuchi or Hixson–Crowell and to the *in vitro* profile. The reason could be the depletion of the aqueous vehicle containing dissolved drug as abovementioned. The higher dissolution rate of DRSP with lower particles size might increase the deviation for DRSP 20 μm MCSs profiles. In accordance to the rat model, the drug absorption of po DRSP MCSs in monkeys was faster compared with aqueous DRSP MCSs. Higher drug solubility in oil and prolonged presence of the oil at the injection site might be the reason. Therefore, oil-based DRSP MCSs showed a better correlation with the Higuchi model in accordance to absorption in rats. Although the oil depot was previously shown to stay longer at the injection site, it was described that small oil droplets containing dissolved drug could be transported from the injection site to the lymphatic system [38]. This effect might cause the fast absorption rate of DRSP from oil-based MCSs within the first 24 h in monkeys (see **Fig. 4 e**). Aqueous DRSP MCSs correlated better to the Hixson–Crowell model because the drug dissolution might play the major role in drug absorption. In contrast to the absorption of aqueous DRSP 50 μm MCSs in rats, lower initial burst was observed in monkey within the first days. The influence of depletion of aqueous vehicle from injection site might be lower than in rats. In general, the pharmacokinetics of aqueous DRSP MCSs seemed to be more controlled by drug diffusion through tissue or other environmental influences in s.c. tissue of monkeys because the correlation to mathematical models is relatively low. With respect to the elimination rate constant in humans, the results of the animal models could be translated to humans. The blood of Wistar rats contained specific drug degrading esterases, which do not occur in humans. Thus, esterase inhibitors were added to the samples. The Cynomolgus monkey was used as animal model, because it was assumed to be closer to humans as previously shown [29]. Nevertheless, a good correlation of absorption profiles of po DRSP MCSs in rats and monkey was shown. In general, it was described that oil-based vehicles showed significant different behavior in various animal species after s.c. injection [42]. Thus, theoretical transfer of *in vivo* results from one species to another is restricted and has to be evaluated carefully. The *in vitro* model was useful to figure out characteristics of the drug formulation influencing the drug release (e.g., drug diffusion, dissolution, distribution). Although the *in vitro* profiles and absorption profiles correlated partially well, numerous factors which were identified to have an impact on *in vivo* results could not be simulated by the applied *in vitro* system (see **Fig. 8 a** and **b**). Consequently, the discriminatory power of the *in vitro* test was too low to differentiate between the po and aqueous DRSP MCSs

release profiles. Nevertheless, parameters influencing the drug delivery from DRSP MCSs were identified with respect to the *in vitro* and *in vivo* data. The results indicate that low drug solubility in the vehicle might be advantageously to reach slower drug release rate. Furthermore, a high vehicle viscosity might decelerate the drug diffusivity through the vehicle and reduce spreading in the tissue resulting in a smaller shape of s.c. depot. In addition, the data might be helpful to understand the *in vivo* behavior of comparable drug formulations such as ZK28 drug-delivery systems.

The *in vitro* release profiles of co/bb DRSP MCSs and of DRSP organogels fitted rather well to Higuchi's equation as shown for the release and absorption profiles of po DRSP MCSs. 50 mg ZK28 MCSs include the lipophilic steroid suspended in an oil-based vehicle in common with po DRSP MCSs. Referring to Higuchi's equation, the drug release rate of ZK28 MCSs should decrease potentially over time resulting in a fast initial drug release rate which is slowing down with time in dependence of vehicle viscosity and drug solubility. Co/bb is a relatively high viscous vehicle forming a depot at the injection site with unknown shape. Drug diffusivity through the vehicle should be relatively slow. The drug solubility is relatively high accelerating the drug release. The co/bb ZK28 formulations showed relatively high initial plasma concentrations followed by a fast decline of the plasma concentrations. The course of plasma profiles was comparable with the serum profiles of po DRSP MCSs showing sharp plasma peaks within the first 24 h. As the drug was already dissolved in co/bb 15 mg ZK28 formulations, drug release should be even faster than for 50mg ZK28 MCSs. Drug solubility of ZK28 in the MCT organogel was lower than in co/bb. However, the initial drug absorption from ZK28 organogels was higher. The reason might be the lower viscosity of the MCT organogel immediately after injection due to destruction of organogelator network. Due to partial recovery of the organogelator network the drug diffusivity should decrease according to the Higuchi model. This influence might explain the more constant decline of the plasma levels. Furthermore, formation of an organogelator network could decelerate the drug release by reducing spreading or depletion of the vehicle in the s.c. tissue. This effect would not be predicted with the *in vitro* test used for DRSP. ZK28 MCT organogels were the first ZK28 formulations suitable for efficacy studies in rats due to their higher and more constant plasma profiles. The transferability of ZK28 *in vivo* data on DRSP is restricted, because the *in vitro* tests indicates no significant differences between DRSP release from co/bb and MCT organogel. Furthermore, drug-specific characteristics such as drug diffusivity through tissue could influence the pharmacokinetics. Nevertheless, the results indicated that an *in vivo* investigation of DRSP MCT organogels could be promising to reach more constant plasma profiles.

5 Conclusion

Parenteral aqueous DRSP MCSs showed a slower absorption than po DRSP MCSs in rats and monkeys. The pharmacokinetics of aqueous and oil-based DRSP MCSs is characterized by an initial serum peak followed by a slower decline in serum levels. This behavior was also described in the literature for other conventional drug-delivery systems of steroids [10]. Although partially a good *in vitro-in vivo* correlation was found, the predictability of the *in vitro* test was assumed to be restricted. Nevertheless, *in vitro* characterization and the fitting of mathematical models to drug absorption profiles helped to interpret the pharmacokinetics of DRSP MCSs. With regard to the *in vivo* and *in vitro* data of DRSP MCSs, the *in vivo* data of ZK28 formulations were interpreted. The ZK28 MCT organogels showed a slightly more constant drug release possibly caused by slower drug diffusivity in the vehicle. Although further investigations are necessary to prove these results, an *in vivo* study of DRSP MCT organogels was evaluated to be promising to obtain slower or more constant drug delivery.

6 Supplement

$$dc/dt = S \cdot D \cdot (c_s - c_t) / V \cdot h$$

Equation 1 Nernst-Brunner equation considering the Noyes-Whitney equation based on Fick's law [43]. dc/dt = is the amount of drug dissolved in the time interval dt , S = surface area of the drug particle, D = the diffusion coefficient of the drug in the liquid unstirred boundary layer surrounding the drug particle, c_s = drug solubility in the liquid unstirred boundary layer surrounding the drug particle, c_t = drug concentration in release medium, V = volume of the bulk fluid, h = thickness of liquid surrounding the drug particle.

$$\omega_0^{1/3} - \omega^{1/3} = k_2 \cdot t$$

Equation 2 Hixson – Crowell equation [32]. ω_0 = initial weight, ω = residual weight at time t , k = constant, t = time.

$$M_t = A \cdot \sqrt{D \cdot (2c_o - c_s) \cdot c_s \cdot t}$$

Equation 3 Higuchi equation [39]. M_t = cumulative amount of drug release at time t , A = surface of drug delivery system, D = diffusion coefficient in the drug delivery system, c_s = drug solubility in the drug delivery system, c_o = initial drug concentration in the drug delivery system, t = time



Fig. 9 Picture of DRSP MCT organogel in aqueous buffer medium after depletion from a syringe.

References

- [1] J. Garza-Flores, P.E. Hall, and G. Perez-Palacios, Long-acting hormonal contraceptives for women, *J. Steroid. Biochem. Mol. Biol.*, 40 (1991) 697-704.
- [2] L. Harle, S. Basaria, and A.S. Dobs, Nebido: a long-acting injectable testosterone for the treatment of male hypogonadism, *Expert. Opin. Pharmacother.*, 6 (2005) 1751-1759.
- [3] G. Moeller, D. Deluca, C. Gege, A. Rosinus, D. Kowalik, O. Peters, P. Droescher, W. Elger, J. Adamski, and A. Hillisch, Structure-based design, synthesis and in vitro characterization of potent 17 beta-hydroxysteroid dehydrogenase type 1 inhibitors based on 2-substitutions of estrone and D-homoestrone, *Bioorg. Med. Chem. Lett.*, 19 (2009) 6740-6744.
- [4] K. Singh and S.S. Ratnam, New developments in contraceptive technology, *Adv. Contracept.*, 7 (1991) 137-157.
- [5] Nebido® 1000 mg Injektionslösung. 2011. www.rote-liste.de, Rote Liste Service GmbH, Frankfurt am Main. 20-11-2011.
- [6] C. d'Arcangues and Snow R.C., Injectable Contraceptives, in: T. Rabe and B. Runnebaum (Eds.), *Fertility Control Update and Trends*, Springer-Verlag, Heidelberg, 1999, pp. 121-149.
- [7] S. Gupta, Non-oral hormonal contraception, *Curr. Obstet. Gynaecol.*, 16 (2006) 30-38.
- [8] M.J. Rosenberg, M.S. Waugh, and S. Long, Unintended pregnancies and use, misuse, and discontinuation of oral contraceptives, *J. Reprod. Med.*, 40 (1995) 355-360.
- [9] M.J. Rosenberg, M.S. Waugh, and M.S. Burnhill, Compliance, counseling and satisfaction with oral contraceptives: a prospective evaluation, *Family Planning Perspectives*, 30 (1998) 89-92, 104.
- [10] J. Garza-Flores, Pharmacokinetics of once-a-month injectable contraceptives, *Contraception*, 49 (1994) 347-359.
- [11] H.P. Zahradnik, Depotgestagene, *Arch. Gynecol. Obstet.*, 257 (1995) 536-541.
- [12] M.A. Oriowo, B.M. Landgren, B. Stenström, and E. Diczfalusy, A comparison of the pharmacokinetic properties of three estradiol esters, *Contraception*, 21 (1980) 415-424.
- [13] G.Y. Zhang, Y.Q. Gu, X.H. Wang, Y.G. Cui, and W.J. Brenner, A pharmacokinetic study of injectable testosterone undecanoate in hypogonadal men, *J. Androl.*, 19 (1998) 761-768.
- [14] X.F. Zhou, Q.X. Shao, X.J. Han, L.J. Weng, and G.W. Sang, Pharmacokinetics of Medroxyprogesterone Acetate After Single and Multiple Injection of Cyclofem in Chinese Women, *Contraception*, 57 (1998) 405-411.
- [15] R. Krattenmacher, Drospirenone: pharmacology and pharmacokinetics of a unique progestogen, *Contraception*, 62 (2000) 29-38.
- [16] S. Nippe and S. General, Parenteral oil-based drospirenone microcrystal suspensions - Evaluation of physicochemical stability and influence of stabilising agents, *Int. J. Pharm.*, 416 (2011) 181-188.
- [17] Z.-H. Gao, W.R. Crowley, A.J. Shukla, J.R. Johnson, and J.F. Reger, Controlled Release of Contraceptive Steroids from Biodegradable and Injectable Gel Formulations: *In vivo* Evaluation, *Pharm. Res.*, 12 (1995) 864-868.
- [18] U. Gietz, T. Arvinte, E. Mader, P. Oroszlan, and H.P. Merkle, Sustained release of injectable zinc-recombinant hirudin suspensions: development and validation of in vitro release model, *Eur. J. Pharm. Biopharm.*, 45 (1998) 259-264.

- [19] V. Puri and A.K. Bansal, In Vitro - In Vivo Characterization of Release Modifying Agents for Parenteral Sustained-Release Ketorolac Formulation, *Drug Dev. Ind. Pharm.*, 30 (2004) 619-626.
- [20] K. Schultz, B. Mollgaard, S. Frokjaer, and C. Larsen, Rotating dialysis cell as in vitro release method for oily parenteral depot solutions, *Int. J. Pharm.*, 157 (1997) 163-169.
- [21] L. Söderberg, S. Björkman, H. Dyhre, and B. Roth, In-vitro release of bupivacaine from injectable lipid formulations investigated by a single drop technique - relation to duration of action in-vivo, *J. Control. Release*, 54 (2002) 747-755.
- [22] C. Gido, P. Langguth, J. Kreuter, G. Winter, H. Woog, and E. Mutschler, Conventional versus novel conditions for the in vitro dissolution testing of parenteral slow release formulations: Application to doxepin parenteral dosage forms, *Pharmazie*, 48 (1993) 764-769.
- [23] S.S. D'Souza and P.P. DeLuca, Methods to assess in vitro drug release from injectable polymeric particulate systems, *Pharm. Res.*, 23 (2006) 460-474.
- [24] D.B. Larsen, S. Joergensen, N.V. Olsen, S.H. Hansen, and C. Larsen, *In vivo* release of bupivacaine from subcutaneously administered oily solution. Comparison with *in vitro* release, *J. Control. Release*, 81 (2002) 145-154.
- [25] C. Nastruzzi, E. Esposito, R. Cortesi, R. Gambari, and E. Menegatti, Kinetics of bromocriptine release from microspheres: comparative analysis between different in vitro models, *J. Microencapsul.*, 11 (1994) 565-574.
- [26] ICH Topic Q 2 (R1) Validation of the Analytical Procedures: Text and Methodology. 1995. www.emea.europa.eu, European Medicines Agency, London. 8-5-2012.
- [27] Guidance for Industry - Bioanalytical Method Validation. 2001. www.fda.gov/cvm, US Food and Drug Administration, Rockville.
- [28] J.G. Wagner and E. Nelson, Kinetic analysis of blood levels and urinary excretion in the absorptive phase after single doses of drug, *J. Pharm. Sci.*, 53 (1964) 1392-1403.
- [29] Yasmin Pharmacology Review Part 1- Review and Evaluation of Pharmacology/Toxicology data. N21-098. 2000. www.fda.gov, US Food and Drug Administration, Rockville. 13-11-2011.
- [30] J.W. Moore and H.H. Flanner, Mathematical comparison of curves with an emphasis on in vitro dissolution profiles, *Pharm. Technol.*, 20 (1996) 64-74.
- [31] Guidance for Industry Dissolution Testing of Immediate Release Solid Oral Dosage Forms. 1997. www.fda.gov, US Food and Drug Administration, Rockville. 13-11-2011.
- [32] A. Dokoumetzidis and P. Macheras, A century of dissolution research: From Noyes and Whitney to the Biopharmaceutics Classification System, *Int J Pharm.*, 321 (2006) 1-11.
- [33] T. Higuchi, Rate of release of medicaments from ointment bases containing drugs in suspension, *J. Pharm. Sci.*, 50 (1961) 874-875.
- [34] K. Hirano, T. Ichihashi, and H. Yamada, Studies on the Absorption of Practically Water-Insoluble Drugs following Injection V: Subcutaneous Absorption in Rats from Solutions in Water Immiscible Oils, *J. Pharm. Sci.*, 71 (1982) 495-500.
- [35] D.H. Larsen, K. Fredholt, and C. Larsen, Assessment of rate of drug release from oil vehicle using a rotating dialysis cell, *Eur. J. Pharm. Sci.*, 11 (2000) 223-229.
- [36] S.W. Larsen and C. Larsen, Critical Factors Influencing the *In Vivo* Performance of Long-acting Lipophilic Solutions - Impact on *In Vitro* Release Method Design, *AAPS J.*, 11 (2009) 762-770.
- [37] T. Seki, J. Mochida, M. Okamoto, O. Hosoya, K. Juni, and K. Morimoto, Measurement of diffusion

coefficients of parabens and steroids in water and 1-octanol, *Chem. Pharm. Bull.*, 51 (2003) 734-736.

- [38] J. Zuidema, F. Kadir, H.A.C. Titulaer, and C. Oussoren, Release and absorption rates of intramuscularly and subcutaneously injected pharmaceuticals (II), *Int. J. Pharm.*, 105 (1994) 189-207.
- [39] J. Siepmann and F. Siepmann, Modeling of diffusion controlled drug delivery. *J.Control.Release*, 161 (2012) 351-362.
- [40] N.J. Medlicott, N.A. Waldron, and T.P. Foster, Sustained release veterinary parenteral products, *Adv. Drug Deliv. Rev.*, 56 (2004) 1345-1365.
- [41] A. Rutz, *Ölige Suspensionen als parenterale Depotsysteme für rekombinante Proteine*. 2007. Ludwig-Maximilians-Universität München.
- [42] S.W. Larsen, E. Rinvar, O. Svendsen, J. Lykkesfeldt, G.J. Friis, and C. Larsen, Determination of the disappearance rate of iodine-125 labelled oils from the injection site after intramuscular and subcutaneous administration to pigs, *Int. J. Pharm.*, 230 (2001) 67-75.
- [43] J. Siepmann, F. Siepmann, and A.T. Florence, Factors influencing oral drug absorption and drug availability, in: Alexander T.Florence and Juergen Siepmann (Eds.), *Modern Pharmaceutics: Basic Principles and Systems*, Vol. 1. Informa Healthcare, New York, London, 2009, pp. 117-154.

CHAPTER 5

Combination of injectable ethinyl estradiol and drospirenone drug-delivery systems and characterization of their *in vitro* release

Published in European Journal of Pharmaceutical Sciences 47 (2012) 790–800

<http://dx.doi.org/10.1016/j.ejps.2012.08.009>

Abstract

Our aim was to investigate the *in vitro* release and combination of ethinyl estradiol (EE) and drospirenone (DRSP) drug-delivery systems. DRSP poly(lactic-co-glycolic acid) (PLGA) microparticles and organogels containing DRSP microcrystals were prepared and characterized with regard to properties influencing drug release. The morphology and release kinetics of DRSP PLGA microparticles indicated that DRSP is dispersed in the polymer. The *in vitro* release profiles correlated well with *in vivo* data. Although DRSP degradation is known to be acid-catalyzed, DRSP was relatively stable in the PLGA matrix. Aqueous DRSP PLGA microparticle suspensions were combinable with EE PLGA microparticles and EE poly(butylcyanoacrylate) (PBCA) microcapsules without interacting. EE release from PLGA microparticles was faster than DRSP release; EE release is assumed to be primarily controlled by drug diffusion. Liquid-filled EE PBCA microcapsules were shown to be more robust than air-filled EE PBCA microcapsules; the bursting of microcapsules accelerating the drug delivery was therefore delayed. The drug release profile for DRSP organogels was fairly linear with the square root of time. The system was not combinable with EE PBCA microcapsules. In contrast, incorporation of EE PLGA microparticles in organogels resulted in prolonged EE release. The drug release of EE and DRSP was thus approximated.

Konzeption:

Stefanie Nippe, Mitarbeit an Konzeption Sascha General

Durchführung:

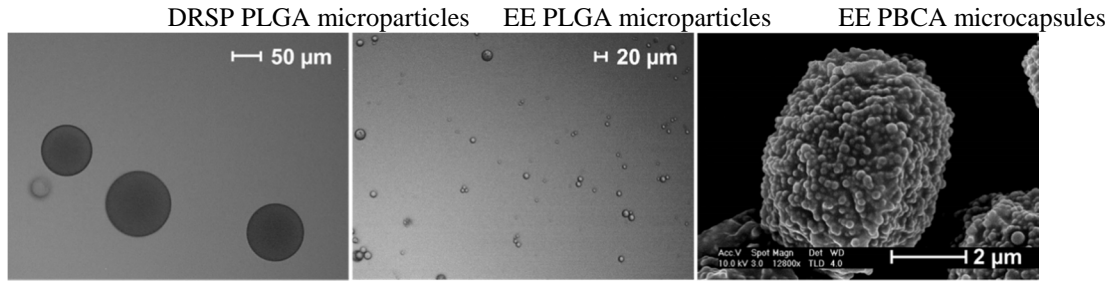
Stefanie Nippe

Berichtsabfassung:

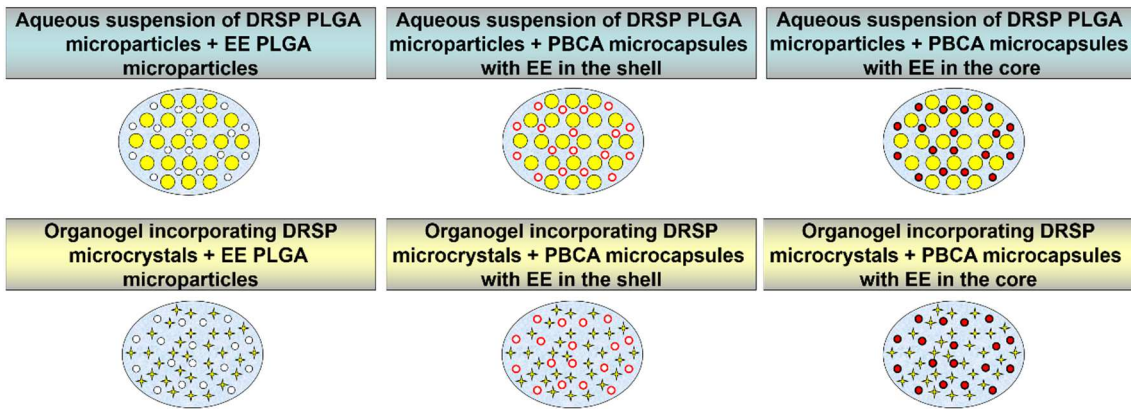
Stefanie Nippe

Graphical Abstract

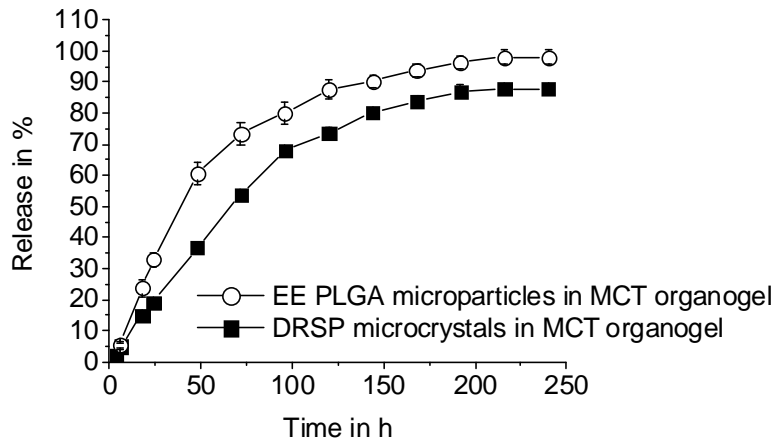
Preparation of EE and DRSP drug-delivery systems



Drug-delivery systems combining EE and DRSP



In vitro release



1 Introduction

In the last few decades, various parenteral drug-delivery systems (including polymeric particulate systems as well as gel formulations) have been developed to attain controlled and prolonged drug release after injection. For each drug, the optimal carrier system must be determined by considering the physicochemical characteristics of the drug substance and the targeted release profile. Patients are frequently treated with two or more drugs to increase efficacy or to antagonize an adverse reaction caused by one of the drugs [1]. Drugs may not only interact pharmacodynamically with each other, but they may also influence the pharmacokinetics of a co-administered drug formulation.

Based on these considerations, our intention at first was to study the *in vitro* release kinetics of chosen injectable drug-delivery systems for the lipophilic steroidal drugs ethinyl estradiol (EE) and drospirenone (DRSP). Stability, drug content, morphology, and particle size were investigated because these factors may influence drug release. Formulation development for long-acting injectable steroidal preparations has yielded conventional systems such as aqueous microcrystal suspensions and oil-based solutions [2]. These could cause an initial drug plasma peak that greatly exceeds the minimum effective dose [3,4]. Recently, controlled drug-delivery systems, including steroidal drugs, have been investigated and thoroughly described in the literature [5-7]. We prepared biodegradable DRSP poly(lactic-co-glycolic acid) (PLGA) microparticles and DRSP organogels to attain prolonged release of the progestin. PLGA microparticles are a well characterized drug-delivery system. Because DRSP is chemically unstable in aqueous fluids, especially under acidic conditions, we investigated the stability of DRSP during drug release from an acidic PLGA matrix. Furthermore, DRSP is poorly soluble in vegetable oils and aqueous systems, but it has been shown that DRSP displays high chemical stability in oil-based systems [8]. Thus, a DRSP organogel may be a suitable formulation. In contrast to hydrogels, semi-solid oil-based formulations are not as well studied [9]. Furthermore, we prepared polymer-based EE drug-delivery systems. To deliver EE over a prolonged period of time, the drug was encapsulated into PLGA microparticles. EE is a highly potent drug with a considerably lower dosage than DRSP and should therefore be encapsulated in significantly lower concentrations [10]. The difference between the *in vitro* release profiles of EE and DRSP PLGA microparticles should be analyzed. In addition, we studied the feasibility of preparing EE poly(butylcyanoacrylate) (PBCA) microcapsules. The microcapsules' shell consists of PBCA nanoparticles. The preparation of poly(alkylcyanoacrylate) nanoparticles has been investigated and reported by numerous authors [11-13]. Air-filled PBCA microcapsules have been analyzed for use as ultrasound contrast agents [14].

In the current study, we tested different techniques of encapsulating EE into PBCA microcapsules. PBCA microcapsules were assumed to release the drug in low amounts during the first few days. Biodegradation of the polymeric wall induces a natural bursting of PBCA microcapsules [15]. This phenomenon could be used for delayed release of higher EE doses. In the second part of our

investigation, our aim was to determine if the prepared DRSP and EE drug-delivery systems were able to combine with each other (see **Fig. 1**). The drug release profiles of the combined drug-delivery systems were analyzed for possible interactions. Combined drug-delivery systems may have a negative effect on each other, or a positive synergy could be achieved. Prolonged drug release from PDLLA microparticles incorporated into hydrogels and from PLGA microparticles enclosed in cubic phase-forming systems has been previously demonstrated [16,17]. The *in vitro* release of PLGA microparticles suspended in peanut oil has been investigated by *Kranz and Bodmeier* [18]. Based on their results, drug-loaded polymeric systems were included in the continuous outer phase of an organogel containing a second drug.

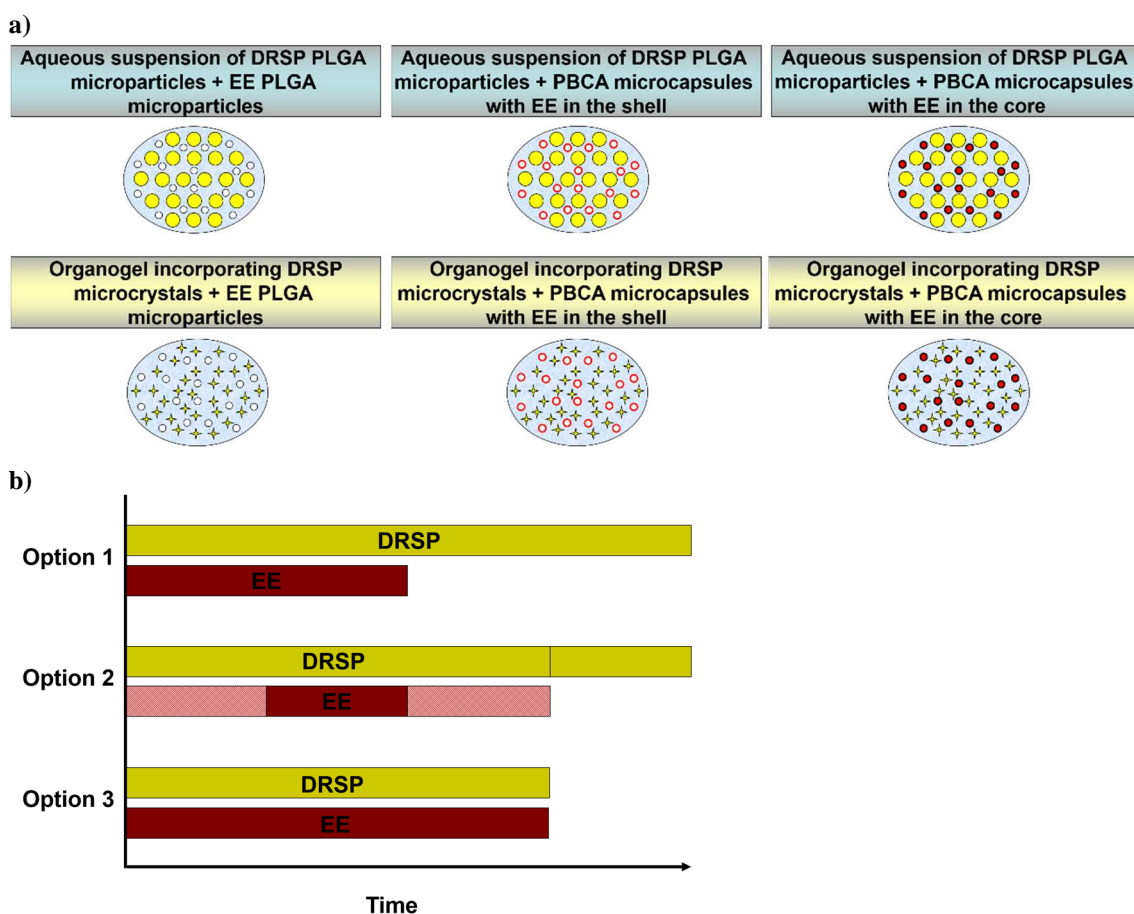


Fig. 1 Overview of **a)** the combined EE DRSP drug-delivery systems being investigated; **b)** the targeted EE and DRSP release profiles.

2 Materials and experimental methods

2.1 Materials

Micronized EE and DRSP (from Bayer HealthCare Pharmaceuticals, Berlin, Germany), PLGA (Resomer® RG 503 H, Boehringer Ingelheim, Ingelheim am Rhein, Germany), polyvinyl alcohol Mowiol 4-88 (MW 31.000) (PVA) (Sigma-Aldrich, Seelze, Germany), n-butyl cyanoacrylate (BCA) (Sicomet® 6000, Sichel-Werke, Hannover, Germany), medium-chain triglycerides (MCT)

(Myritol® 318 PH, Cognis, Düsseldorf, Germany), Polyvidone K15 < 18 (Kollidon® 17 PF, BASF, Ludwigshafen, Germany), dextrin palmitate (Rheopearl® KL2, S. Black, Moers, Germany), polysorbate 80 (Tween® 80), dichloromethane, Triton X-100, potassium dihydrogen phosphate, sodium azide (all from Merck, Darmstadt, Germany), and hydroxypropyl- β -cyclodextrin (HP- β -cyclodextrin) (Kleptose HPBJ, Roquette, Lestrem, France) were used.

2.2 Preparation of DRSP and EE PLGA microparticles

The general parameters for preparing drug-loaded PLGA microparticles described by *Luan and Bodmeier* [19] were used with some modifications to produce EE PLGA microparticles by a single oil-in-water solvent extraction / evaporation technique. 350 mg of PLGA and 39 mg of EE were dissolved in 3.0 g of dichloromethane. After injecting the mixture beneath the surface of 800 ml of 0.25% (w/w) aqueous PVA solution, the sample was emulsified using an Ultra-Turrax (T25 Basis Homogenizer, Ika-Werke, Staufen, Germany) at 13,000 rpm for 5 min. The solution was then magnetically stirred at 400 rpm and room temperature (RT) for 2 h. The samples were filtered (filter paper, 3 μ m) and washed with 1% (w/w) HP- β -cyclodextrin and water. The filter cake was re-suspended in water and then lyophilized without the addition of any lyoprotectant (ViTris AdVantage freeze dryer, SP Scientific, Stone Ridge, USA). The general parameters for preparing drug-loaded PLGA microparticles described by *Birnbaum et al.* [5] was used and modified to produce DRSP PLGA microparticles by a double emulsion solvent evaporation technique. 350 mg of PLGA and 150 mg of DRSP were dissolved in 5.0 g of dichloromethane. The solution was added to 60 ml of 0.5% (w/w) aqueous PVA solution. The mixture was emulsified under magnetic stirring at 500 rpm for 3 min. Then, it was added to 800 ml of water under stirring for 3 h. The samples were centrifuged (Heraeus Biofuge Fresco, DJB Labcare, Buckinghamshire, UK) at 2500 rpm for 30 min and was washed with 1% (w/w) HP- β -cyclodextrin and with water. The sediment was re-dispersed in water and then lyophilized without the addition of any lyoprotectant. The lyophilized samples were stored in closed glass vials at 2 – 8 °C. The particle size distribution (PSD) (see **section 2.7**) and the drug content of lyophilizates were analyzed after freeze-drying and after 3 months of storage. To determine the amount of drug encapsulated in PLGA microparticles, samples were weighed, dissolved in acetonitrile (ACN), and then filtered (syringe filter, 0.45 μ m). The drug concentration was quantified by HPLC/UV (Agilent 1100 series, Agilent Technologies, Böblingen, Germany). 10 μ l of samples was injected into an ODS Hypersil column (length 6 cm, inner diameter 4.6 mm, 3 μ m) using a 60/40% (v/v) water/ACN mixture as the mobile phase and a flow rate of 1 ml/min. Both drugs were detected at a wavelength of 270 nm. To calculate the drug amounts, 6-point calibrations were performed using external standards. Three standard stock solutions were prepared for each drug from different initial weights. The drug was accurately weighed into volumetric flasks and dissolved in ACN. Two standard solutions were then prepared from each stock solution by diluting with ACN. Each standard solution was injected three times. Linearity for DRSP was

observed from 1.1 to 500 $\mu\text{g/ml}$ and from 1.5 to 508 $\mu\text{g/ml}$ for EE. The squares of the correlation coefficients (r^2) of calibration curves were above 0.999. The lower limit of quantitation (LOQ) was calculated based on the tenfold of signal/noise ratio [20]. The LOQ for DRSP was 1.1 $\mu\text{g/ml}$ and 1.5 $\mu\text{g/ml}$ for EE. The data were examined using the software Empower™ 2 (Waters, Eschborn, Germany). Because an external standard of isoDRSP was not available, the relative isoDRSP / DRSP ratio was determined by comparing the peak areas of both compounds. Values below the tenfold of signal / noise ratio were not considered. EE had a retention time of about 3.5 min, DRSP of about 4.5 min and isoDRSP of about 5.3 min. The drug content was calculated from the drug amount found in the resulting PLGA microparticles divided by the overall weight of the resulting drug-loaded PLGA microparticles. The loading efficiency was the ratio between the drug amount found in the resulting PLGA microparticles and the total drug amount used for the preparation.

2.3 Preparation of air-filled PBCA microcapsules encapsulating EE in the core (PBCAEEC)

The PBCA nano- and microcapsules manufacturing process previously described by *Schmidt and Roessling* [14] was used with some modifications. Over a period of 60 min, a 5% (w/w) BCA solution was added dropwise to 2000 ml of 0.1% (w/w) Triton X-100 solution acidified with HCl to pH 2.2 at 4 – 7 °C using a syringe pump (Precidor, Infors, Basel, Switzerland). During the dropwise addition, the mixture was stirred at 300 rpm by a three-blade propeller stirrer (Eurostar®, Ika-Werke). After the addition of BCA, the Triton X-100 concentration of the mixture was increased to 1% (w/w) and the dispersion was stirred for a further 30 min in an ice bath. The samples were then removed from the ice bath and stirred until reaching RT; the polymer particle dispersion was separated from the coarser polymer material by filtration (filter paper, 12 – 25 μm). Air bubbles were then introduced into the PBCA nanoparticle dispersions with a sintered metal filter connected to a compressed air supply under moderate stirring using a three-blade propeller stirrer for 12 h. The PBCA microcapsule bulk dispersion was then purified by mixing with 0.1% (w/w) acidified Triton X-100 solution and separated using a separation funnel. Air-filled PBCA microcapsules were stored as a dispersion in 0.1% (w/w) acidified Triton X-100 solution in closed glass flasks at RT (5 mg/ml PBCA). PSD and PBCA amounts were determined after 0.5 and 1 years of storage.

For the encapsulation of EE in the core of unloaded air-filled PBCA microcapsules, 10 mg of EE was added to 7.5 ml of PBCA microcapsule suspension in a test tube. The suspension contained 5 mg/ml PBCA microcapsules suspended in a 1% or 0.1% (w/w) Triton X-100 solution. The solubility of EE in either water or a surfactant solution was determined by dispersing excess drug into the solutions under magnetic stirring for 4 – 7 h. The drug concentration in the supernatant was determined by HPLC after dilution (see **section 2.6**). The samples were then heated to the optimal loading temperature in a water bath under magnetic stirring. Prior to filling, the optimal loading temperature was determined. Due to a marked decrease in the PBCA microcapsule size, the

temperature range was determined by microscopy and spectroscopic measurement of PSD (see **section 2.7**). Exceedingly high temperatures led to the destruction of PBCA microcapsules. After 15 min at the loading temperature, the samples were cooled in an ice bath. The density of the samples was determined before and after filling using a bending oscillator (DMA 48, Anton Paar, Graz, Austria) at 20°C and by weighing predetermined volumes of the microcapsule dispersion. The PBCA microcapsules were washed with 1% (w/w) acidified Triton X-100 solution, rinsed with water, and then extracted using a separation funnel. To analyze drug and polymer amounts, PBCAEEC were re-dispersed in water and freeze-dried without the addition of any lyoprotectant to destroy the microcapsules. The samples were dissolved in ACN and were then filtered (syringe filter, 0.45 µm). The drug concentration was determined using HPLC/FD (Agilent 1100 series). Either 10 µl or 100 µl of sample was injected into an ODS Hypersil column (length 6 cm, inner diameter 4.6 mm, 3 µm) using an ACN/water mixture as the mobile phase and a flow rate of 1 ml/min. To separate the polymer, the following gradient was used: 25/75% (v/v) ACN/water to 45/55% (v/v) ACN/water over 10 min, followed by isocratic elution for 15 min. The solvent was then set to 70/30% (v/v) ACN/water for 12 min; afterwards, the column was equilibrated using 25/75% (v/v) ACN/water for 8 min. To calculate the amount of EE, 6-point calibrations were performed using an external standard. The standard solutions were prepared as described in **section 2.2**. The LOQ was calculated from the tenfold standard deviation of the y-intercept of the linear regression line divided by the slope of calibration curve [20]. Linearity was observed between 1.5 ng/ml and 4.2 µg/ml. The LOQ of EE was 24 ng/ml, and the retention time was approximately 7 min. The EE content was determined using an excitation wavelength of 210 nm and a detection wavelength of 315 nm. The drug content as calculated as described in **section 2.2**. The yield of PBCA microcapsules after filling was calculated by noting the difference between the weight of EE PBCA microcapsules and the amount of EE in the EE PBCA microcapsules. The theoretical maximum drug content was calculated using the **Equation 1**.

$$V_g = 4/3 \pi r^3$$

$$V_i = 4/3 \pi (r - d_{np})^3$$

$$V_{pw} = V_g - V_i$$

Equation 1 V_g = volume of EE PBCA microcapsules; r = radius of PBCA microcapsules after drug loading (vw-mp); V_i = volume of the core; d_{np} = diameter of PBCA nanoparticles (vw-mp); V_{pw} = volume of the polymer wall.

With respect to the density of PBCA (1.15 mg/ml), the weight of the polymer wall was calculated [14]. The drug amount in the microcapsule core was computed with regard to the drug solubility. Finally, the (theoretical) drug content was calculated as described in **section 2.2**. The PSD and *in vitro* release of purified PBCAEEC were determined immediately after preparation. 5 mg/ml PBCA microcapsule suspensions with and without encapsulated EE were freeze-dried with the addition of 10% (m/v) polyvidone. Lyophilizates were stored in closed glass vials at 2 – 8 °C for 3 months. After

re-dispersion, the PSD, the PBCA amount, and the drug content of washed microcapsules were analyzed.

2.4 Preparation of air-filled PBCA microcapsules encapsulating EE in the shell (PBCAEES)

EE PBCA nanoparticles were prepared by anionic emulsion polymerization. Prior to the preparation, EE was dissolved in BCA under magnetic stirring. Over a period of 5 or 18 min (depending on the monomer concentration), the solution was added dropwise to 100 ml of acidified Triton X-100 solution. The preparation conditions are described in **section 2.3**. The tested amounts of EE, surfactant, and BCA are listed in **Tab. 1**. To determine the drug content, the PSD, and the *in vitro* release of EE PBCA nanoparticles, 15 ml of the dispersions was centrifuged in 1.5 ml tubes at 10.000 rpm for 20 min (Sigma ZK15, Sigma Laborzentrifugen, Osterode, Germany). The sediments were washed with 1% (w/w) acidified Triton X-100 solution and with water. To prepare PBCAEES, air bubbles were introduced into the 1% (w/w) acidified surfactant solution containing EE PBCA nanoparticles over a period of 4 h. Immediately after preparation, the purified microcapsules were characterized with regard to the *in vitro* release, the PSD, the polymer and drug content as described in **section 2.3**. Furthermore, PBCAEES (1.4% BCA; 1% Triton X-100) were freeze-dried and analyzed after storage as described in **section 2.3**.

Tab. 1 Variation of synthesis parameters during preparation of EE PBCA nanoparticles.

Variation	Amount of EE in mg	Concentration of Triton X-100 in % (w/w)	Concentration of BCA in % (w/w)
1	180	0.1 ^a	5.0
2	180	1.0	5.0
3	50	1.0	1.4

^a increased to 1% after complete addition of BCA

2.5 Preparation of DRSP organogels

5% (w/w) dextrin palmitate and 70 mg/0.5 g DRSP microcrystals were dispersed in MCT by sonication at a 5 x 10% cycle and 100% power using an ultrasound device (Bandelin Sonopuls HD2070, Bandelin electronic, Berlin, Germany) for 3 min. The mixture set as a gel after cooling. 10 g of DRSP organogels were stored in closed glass vials at RT for 3 months. The PSD and DRSP / isoDRSP ratio were determined before and after storage. Sedimentation was determined by multiple light scattering (Turbiscan, Quantachrome, Odelzhausen, Germany) over a period of 1 month. Backscattering and transmission spectrograms were considered.

2.6 Preparation and *in vitro* release of combined EE and DRSP drug-delivery systems

To prepare aqueous suspensions containing DRSP PLGA microparticles and EE PBCA microcapsules, 150 mg of DRSP PLGA microparticles was dispersed in 2 ml of aqueous EE PBCA microcapsule suspension containing 5 mg/ml microcapsules and 0.1% (w/w) Triton X-100 using a vortex mixer for 2 min. To prepare aqueous DRSP EE PLGA microparticle suspensions, 3.5 mg of

EE PLGA microparticles and 150 mg of DRSP PLGA microparticles were dispersed in 1 g of 0.5% (w/w) aqueous polysorbate 80 solution using a vortex mixer for 2 min. To prepare DRSP organogels including EE PLGA microparticles, 3.5 mg of EE PLGA microparticles were added to 0.5 g of DRSP organogel. The suspension was then sonicated at a 1 x 10% cycle and 100% power under cooling for 1 min. All of the samples were prepared directly before the *in vitro* release test. The drug solubility in the release medium and dispersion media (surfactant solutions, MCT) was determined as described in **section 2.3**. For the investigation of the *in vitro* release, 2 ml of aqueous EE PBCA nanoparticles or microcapsules suspensions containing 0.1% (w/w) Triton X-100, 0.5 g of MCT organogel including 3.5 mg EE PLGA microparticles, or 0.5 g of 0.5% (w/w) aqueous polysorbate 80 solution containing 3.5 mg EE PLGA microparticles were injected into dialysis bags (length 7 cm, flat width 10 mm for 0.5–1 g, 25 mm for 2 ml, MWCO 12,000–14,000 Da, Spectra/Por, Spectrum® Laboratories, Rancho Dominguez, USA). The dialysis tubes were placed in a 100 ml Erlenmeyer flask containing 50 ml USP phosphate buffer at pH 7.4 with the addition of 8% (w/w) HP- β -cyclodextrin and 0.05% (w/w) sodium azide pre-heated to 37 °C. The samples were then put into a horizontal shaker (Innova 4230, New Brunswick Scientific, Edison, USA) at 100 rpm and 37°C. At predetermined time intervals, 1 ml samples were withdrawn, assayed and replaced with fresh medium. The *in vitro* release of 0.5 g of DRSP organogel containing EE PLGA microparticles, 1 g of aqueous EE DRSP PLGA microparticle suspension, and 2 ml of aqueous suspensions containing DRSP PLGA microparticles and EE PBCA microcapsules was analyzed as described above. All release medium was removed and replaced after the first 24 h and at each measuring point thereafter. To study the influence of the dialysis membrane, the dialysis rates of 70 mg/0.5 ml of DRSP or 1.5 mg/0.5 ml of EE dispersed in release medium were analyzed. EE was quantified by HPLC/FD, as described in **section 2.3**. DRSP was analyzed by HPLC/UV (see **section 2.2**). Two standard solutions were prepared from each stock solution by further diluting in 40/60% (v/v) ACN/phosphate buffer (LOQ for EE was 15 ng/ml and 1.1 μ g/ml for DRSP). The cumulative amount of drug released was calculated using Excel (Microsoft, Redmond, US) (see **Equation 2**).

$$M_t = 100 \cdot \frac{V_g \cdot C_t + \sum_{x=0}^{t-1} (C_x \cdot V_x)}{M_g}$$

Equation 2 M_t = Relative amount of drug released at time point t (in %); M_g = Overall mass of drug in the formulation; V_x = Sample volume at time point x ; V_g = Overall volume of release medium; C_t = drug concentration (w/v) in sample solution at time point t ; C_x = drug concentration (w/v) in sample solution at sampling point x before t ; $t-1$ = last sampling point before t .

Differences between release profiles were analyzed by calculating the difference factor (f_1) and the similarity factor (f_2) from mean values of cumulative release concentrations at each time t [21]. The preparations were evaluated as significantly different if f_1 was above 15 and f_2 was below 50. All sampling points showing 10 – 85% drug release and one sampling point with drug release above 85% were considered. The calculation included at least three sampling points [22]. The relative theoretical

drug release of a spherical monolithic solution (short- and long-term) was calculated using the equation described by [23] (see **section 5**). The relative theoretical drug release of a spherical monolithic dispersion was computed using the equation described by *Koizumi and Panomsuk* [24] (see **section 5**). The *in vitro* release profiles of DRSP PLGA microparticles were compared with *in vivo* results of DRSP PLGA microparticles described in the literature [25]. Briefly, 30 mg/0.5 ml aqueous DRSP PLGA microparticle suspensions containing 1% (w/w) sodium carboxymethyl cellulose were subcutaneously injected into female Wistar rats (age ca. 8 weeks, weight ca. 200 g, purchased from Charles River Laboratories, Berlin, Germany). The suspensions were administered into the neck (B.Braun Omnifix; 20 G needles). The DRSP serum level was determined over a period of 672 h (3–4 rats, 1–2 blood samples). Blood samples were collected from the vena cava or by punctation of the jugular vein at the final sampling time. The samples were diluted with a Pefabloc phosphate buffer to inhibit esterase activity and then centrifuged to separate the serum. They were stored at below -15 °C. DRSP was determined by LC-MS/MS (LOQ was 0.2 ng/ml; linearity was observed between 0.2 and 200 ng/ml). The animal study was performed with the approval of the local authorities of Berlin (Landesamt für Gesundheit und Soziales, Germany) and in accordance to the Recommendations from the Declaration of Helsinki and the German animal protection law. To compare *in vitro* and *in vivo* release, the drug serum concentrations were deconvoluted with the Wagner–Nelson method using Excel [26]. The amount of absorbed drug divided by the volume versus time was calculated. The elimination rate constant was 0.107 h^{-1} , as previously determined [27]. Due to the accelerated *in vitro* conditions, the measuring time points of *in vitro* release were multiplied by a factor that was calculated by dividing the last measuring point of *in vivo* release (672 h) by the measuring point of complete *in vitro* release (312 h) to compare the *in vivo* and *in vitro* data. The error in prediction caused by the incomplete *in vivo* release of DRSP PLGA microparticles after 672 h was acceptable and was expected to have little influence on data interpretation. To test the stability of EE PBCA microcapsules in MCT, PBCA microcapsules were dried on a glass plate and then dispersed in MCT.

2.7 Determination of morphology and particle sizes

The PSD of PBCA microcapsules diluted in 0.01% (w/w) Triton X-100 solution was measured by laser diffraction using an AccuSizer Model 770 (Particle Sizing Systems, Santa Barbara, USA). The apparatus utilizes a single particle optical sizing system. The PSD of PLGA microparticles dispersed in 0.001% (w/w) polysorbate 80 was determined using a Laser Diffraction Particle Size Analyzer series LS 13 320 (Module: ULM, Beckman Coulter, Brea, USA). The PSD of DRSP microcrystals dispersed in organogel was analyzed after dilution in MCT as previously described (laser diffraction, sensor Helos, Sympatec, Clausthal-Zellerfeld, Germany) [28]. All of the particle sizing systems employ comparable measurement principles. Although particle size measurements could deviate from each other when using different apparatuses, the results should be suitable for comparing the

drug-delivery systems with each other. PSD determinations of PBCA microcapsules using the different systems were comparable. Furthermore, the size and morphology of PLGA microparticles and PBCA microcapsules were characterized by optical microscopy (Zeiss Axio Imager A1m, software: Axio Vision Rel. 4.5, Carl Zeiss Imaging Solution, Jena, Germany). The PSD of PBCA nanoparticles diluted in 0.01% (w/w) Triton X-100 solution and Triton X-100 micelles in a 0.1% (w/w) surfactant solution were measured using photon correlation spectroscopy (PCS) (LB-550, Dynamic Light Scattering Nano-Analyzer, Horiba, Kyoto, Japan). To compare particle sizes of different formulations with each other, the median of volume-weighted PSD (vw-mp) was stated for all of the preparations. The difference between the median of number-weighted PSD (nw-mp) and vw-mp was used to evaluate the polydispersity of PBCA microcapsules [14]. The surface morphology of PBCA microcapsules was analyzed using a scanning electron microscope (SEM) (Philips FEI XL30 S-FEG, Oregon, USA). The samples were dried for 2 h on a glass plate and then coated with a thin coat of a gold/platinum mixture deposited on the surface of the sample by sputter coating (Cressington 208HR, Cressington Scientific Instruments, Watford, UK). Coating and imaging were performed under low vacuum.

2.8 Statistics

All of the experiments were conducted in triplicate unless otherwise stated. Arithmetic mean values and standard deviations were calculated. Two sample groups were assumed to be comparable if the 95% confidence intervals coincide.

3 Results and discussion

3.1 Characterization of EE drug-delivery systems

3.1.1 EE PLGA microparticles

The prepared EE PLGA microparticles had a mean drug content of $8.2 \pm 0.5\%$ and a vw-mp of $9.5 \pm 2.0 \mu\text{m}$ ($81.3 \pm 4.9\%$ loading efficiency). In accordance with *Birnbaum et al.* [5] and *Bodmeier and Paeratakul* [29], the state of encapsulated drug in the polymer matrix was optically evaluated with regard to the translucency of the particles. Microscopic pictures showed that EE PLGA microparticles were mainly transparent, indicating that the drug was molecularly dispersed (monolithic solution), at least at the microscopic level (see **Fig. 2 a**). Drug microcrystals, which could increase the initial drug release, were not observed as precipitates on the surface of EE PLGA microparticles using polarized-light microscopy. The drug content ($8.5 \pm 0.4\%$) and vw-mp ($11.3 \pm 4.9 \mu\text{m}$) were comparable after 3 months of storage.

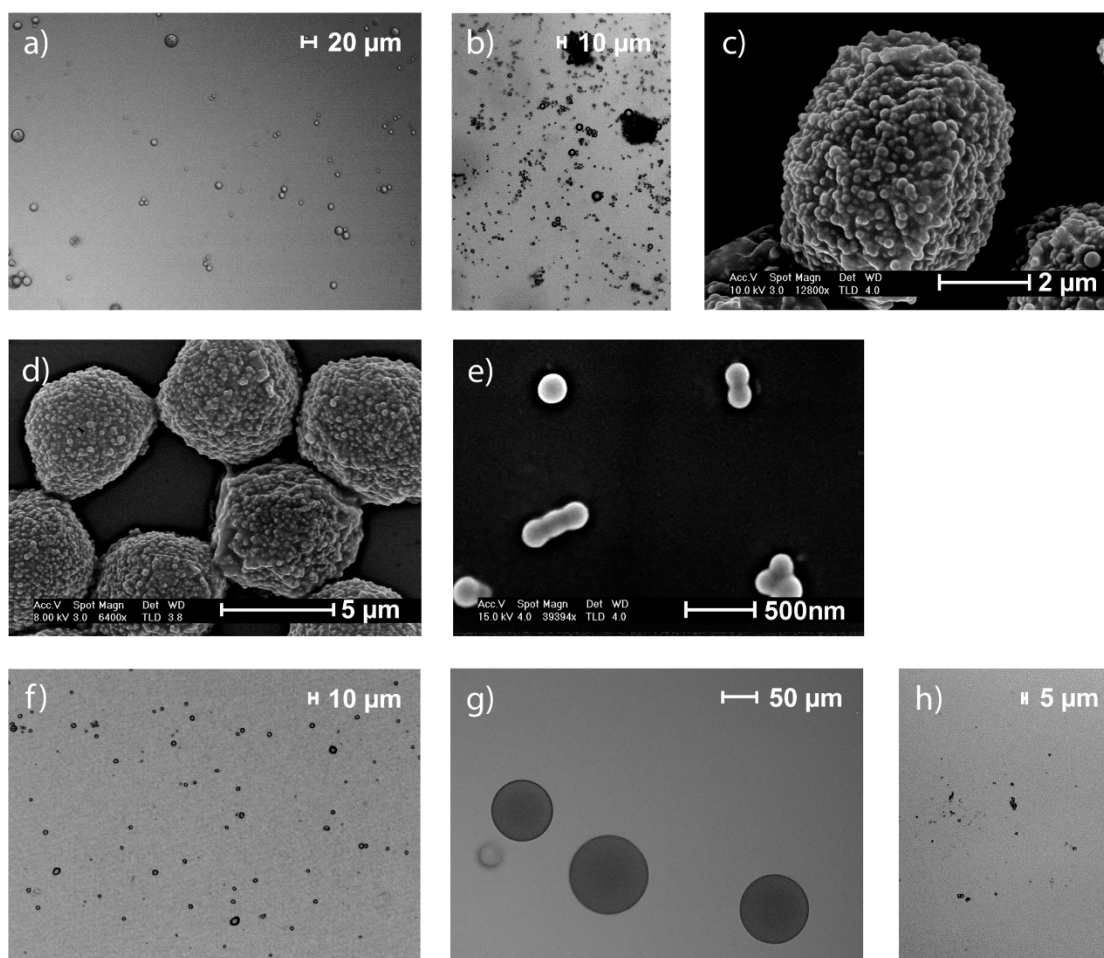


Fig. 2 Optical microscopic pictures of **a)** an aqueous suspension of EE PLGA microparticles; **b)** polymer aggregates after drug loading of PBCA microcapsules. SEM pictures of **c)** and **d)** PBCA microcapsules surrounded by a shell of PBCA nanoparticles and loaded with a solution of EE (PBCAEEC); **e)** small pieces of polymer wall consisting of PBCA nanoparticles after destruction of air-filled PBCA microcapsules during sample preparation under vacuum atmosphere. Optical microscopic pictures of **f)** PBCAEEC after lyophilization and re-dispersion in 0.01% (w/w) aqueous Triton X-100 solution; **g)** an aqueous suspension of DRSP PLGA microparticles; **h)** PBCAEEC at the last sampling point of *in vitro* release test.

3.1.2 PBCAEEC

PBCA nanoparticles were used as a starting material for PBCAEEC. The particle sizes of PBCA nano- and microcapsules without drug were controllable using the preparation parameters [14]. Relatively large PBCA nanoparticles (123 ± 49 nm) were prepared using a low surfactant/monomer ratio. The resulting air-filled PBCA microcapsules had relatively thick particle walls that should cause them to be more robust; this was assumed to be an advantage for targeted long-term use [15]. The mixing energy during preparation of PBCA microcapsules influenced the resulting microcapsule size. Utilizing a homogenizer, air-filled PBCA microcapsules with a size of 1 – 5 μm were previously prepared for intravenous administration to be used as an ultrasound contrast agent [14]. To prepare EE PBCA microcapsules administered intramuscularly or subcutaneously, the limits for particle sizes were broadened. For optimum drug loading, the microcapsules should have a capacious core. Under the given conditions, relatively large air-filled PBCA microcapsules (vw-mp 13.5 ± 4.3 μm / nw-mp 11.7 ± 0.6 μm) were prepared. For drug loading, air-filled PBCA microcapsules were heated to the

optimal loading temperature. Upon reaching the loading temperature, a marked decrease in the mean microcapsule size was observed, indicating the discharge of gas and the ingress of surrounding drug solution into the microcapsule core (vw-mp 7.3 ± 1.2 / nw-mp 5.8 ± 0.2 μm).

This process was also detectable by an increase in density. Before loading, the aqueous PBCA microcapsule dispersion had a density of 1.00 ± 0.00 mg/ml. After filling, the density increased to 1.03 ± 0.01 mg/ml. The vw-mp/nw-mp ratio was low before filling but increased during loading (35.9 ± 12.8 / 6.0 ± 1.3 μm) due to a few large polymer aggregates formed by the destruction of microcapsules (see **Fig. 2 b**). After purification, the vw-mp / nw-mp ratio decreased again (7.3 ± 1.2 / 5.8 ± 0.2 μm). Because the nw-mp stayed nearly constant, it was used to assess the rate of drug loading during filling. The yield of PBCA microcapsules was $86.6 \pm 15.3\%$ after filling / filtration. For the prepared air-filled PBCA microcapsules, the optimum loading temperature was between 54 and 58 °C with a narrow range of $\pm 1\%$ for each sample. Interestingly, drug-loaded PBCA microcapsules were not destroyed when exposed to low vacuum during SEM (see **Fig. 2 c** and **d**). The microcapsules were primarily round in shape and had intact nanoparticulate structures on their surface. In contrast, unloaded PBCA microcapsules disintegrated into smaller pieces when exposed to the same conditions, as described by *Olbrich et al.* [15] (see **Fig. 2 e**). The mean microcapsule and nanoparticle sizes measured by PCS and laser diffraction correlated well with the non-quantitative evaluation of particle sizes by SEM, although the hydrodynamic vw-mp detected by PCS should theoretically be higher than the diameter obtained from optical analysis. The ability to visualize PBCAEEC under these conditions without destroying them was another indicator that the drug solution had reached the core. It was assumed that liquid-filled microcapsules were more robust than air-filled microcapsules. PBCAEEC had a relatively low drug content of $0.27 \pm 0.02\%$; the main reason for the low drug content may be the low solubility of EE in an aqueous medium (14.5 ± 0.2 $\mu\text{g/ml}$). Furthermore, the microcapsules had residual gas content because flotation was possible. A maximum theoretical drug content of only 0.01% was calculated if only EE dissolved in water passed through the polymer, however, nearly 30 times higher drug content was observed. With the addition of surfactant, drug solubility in surrounding aqueous solutions significantly increased. A maximum theoretical drug content of 0.22% was calculated for EE solutions containing 0.1% (w/w) Triton X-100 (drug solubility of 0.28 ± 0.03 mg/ml) and a maximum theoretical drug content of 6.46% for EE solutions containing 1% (w/w) surfactant (drug solubility of 8.6 ± 0.4 mg/ml) when ingress of surfactant solution is assumed. However, the drug content did not increase with higher surfactant concentrations, indicating that EE encapsulated in surfactant micelles did not diffuse through the polymer wall. With a vw-mp of 6.5 ± 1.9 nm, Triton X-100 micelles might be too large to pass through the polymer wall. It is possible that single surfactant molecules could migrate through the wall; but it is more likely that the drug was not encapsulated in only the microcapsule core. No crystalline drug was visible on the surface of washed microcapsules in SEM

pictures (see **Fig. 2 c** and **d**), but the lipophilic EE had a certain affinity to the polymer (see **section 3.1.3**) and could therefore be enclosed in or absorbed onto the polymer wall. The location of EE influences its drug release kinetics. Furthermore, it was possible to lyophilize PBCA microcapsules with and without EE. Numerous lyoprotectants were tested in the past to stabilize air-filled PBCA microcapsules during lyophilization (unpublished results). Polyvidon K15 < 18 was determined to be a suitable lyoprotectant (see **Fig. 2 f**). Lyophilized microcapsules were easily re-dispersible in acidified 0.1% or 1% (w/w) Triton X-10 solution. The vw-mp/nw-mp of lyophilized microcapsules was not significantly different after 3 months storage (unloaded $10.9 \pm 3.1/10.5 \pm 1.0 \mu\text{m}$; loaded $8.0 \pm 1.3/5.9 \pm 0.6 \mu\text{m}$). Air-filled unloaded PBCA microcapsules suspended in acidic 0.1% (w/w) Triton X-100 solution were stable during 1 year of storage at RT ($5.1 \pm 0.3 \text{ mg/ml}$ PBCA). The results are in accordance with *Sommerfeld et al.* [30], showing high stability of PBCA at an acidic pH. It was observed that PBCAEEC released the drug through diffusion within days (see **section 3.3**). Thus, PBCAEEC were characterized immediately after preparation and lyophilized afterwards to avoid drug diffusion. The drug ($0.25 \pm 0.03\%$ after storage) and polymer content ($4.9 \pm 0.2 \text{ mg/ml}$ before storage, $4.8 \pm 0.1 \text{ mg/ml}$ after storage) of lyophilized microcapsules was comparable with those of unlyophilized PBCAEEC after preparation.

3.1.3 PBCAEEES

As described previously for unloaded PBCA nanoparticles by *Baudisch* [31] and *Schmidt and Roessling* [14], we found a linear correlation between the surfactant/monomer ratio and vw-mp for EE PBCA nanoparticles. However, the vw-mp was lower for drug-loaded nanoparticles, indicating that EE influenced nanoparticle formation (see particle sizes **Fig. 3** versus particle sizes in **section 3.1.2** and described by *Schmidt and Roessling* [14]).)

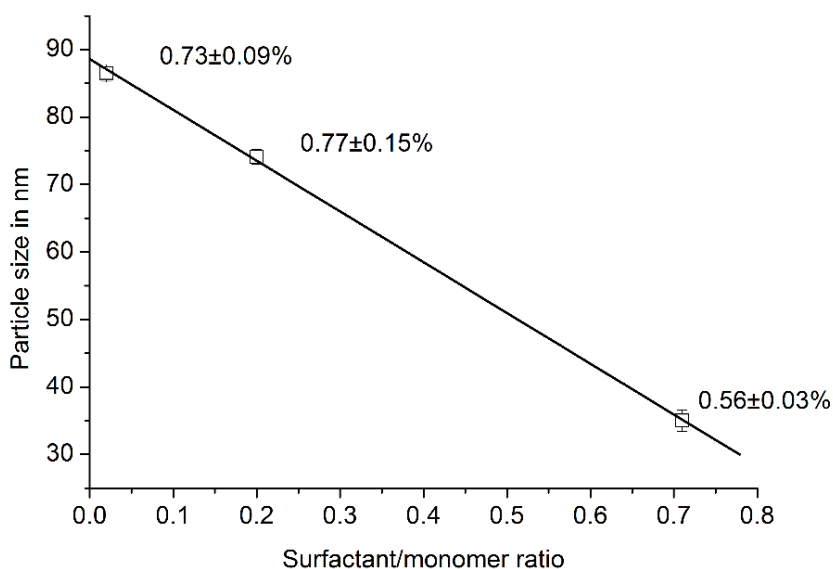


Fig. 3 Correlation between the surfactant/monomer ratios used for the synthesis of EE PBCA nanoparticles and the vw-mp of the resulting EE PBCA nanoparticles. The data labels contain the mean drug content of EE PBCA nanoparticles ($n = 3$).

With increasing nanoparticle size, more robust PBCAEES should be produced. Furthermore, the monomer amount had an impact on the drug content (see **Fig. 3**). This is understandable because an increased amount of the lipophilic BCA phase with a constant amount of the aqueous phase should lead to a higher drug content. However, the relationship between the surfactant concentration and the drug content is not completely understood. The surfactant molecules stabilized the growing nanoparticles during synthesis [32,33]. While a lower surfactant amount resulted in larger PBCA nanoparticles, a slight increase in drug content was obtained when using higher surfactant concentrations. It was assumed that EE was dissolved in surfactant micelles that participated in the formation of nanoparticles and that the surfactant amount could therefore influence the drug content of EE PBCA nanoparticles. PBCAEES did not have significantly different drug contents compared to EE PBCA nanoparticles used for their preparation (see **Tab. 2** versus **Fig. 3**); the loss of drug during preparation was low. The resulting PBCAEES had comparable vw-mp that was not dependent on the nanoparticles used for preparation.

Tab. 2 Drug content and mean particle sizes of PBCAEES. The synthesis parameter of shell-forming EE PBCA nanoparticles were varied (n = 3).

Parameters for EE PBCA nanoparticle synthesis	Surfactant/monomer Ratio	nw-mp (vw-mp) of EE PBCA microcapsules in μm	Drug content of EE PBCA microcapsules in %
5% BCA; 0.1% Triton X-100; 180 mg EE	0.02	11.8 \pm 2.7 (20.0 \pm 3.8)	0.69 \pm 0.27
5% BCA; 1% Triton X-100; 180 mg EE	0.20	12.9 \pm 5.1 (19.8 \pm 1.9)	1.09 \pm 0.20
1.4% BCA; 1% Triton X-100; 50 mg EE	0.71	10.8 \pm 3.6 (17.5 \pm 2.7)	0.55 \pm 0.17

PBCAEES released the drug by diffusion, as mentioned above, and should therefore be lyophilized. The vw/nw-mp, drug and polymer contents of lyophilized microcapsules were comparable to those of unlyophilized PBCAEES after preparation (vw/nw-mp of $19.3 \pm 2.0 / 10.9 \pm 1.2 \mu\text{m}$ and EE content of $0.53 \pm 0.05\%$ after storage; $4.9 \pm 0.2 \text{ mg/ml}$ PBCA before storage, $4.7 \pm 0.1 \text{ mg/ml}$ PBCA after storage).

3.2 Characterization of DRSP drug-delivery systems

Compared with EE, DRSP formulations had higher drug contents. DRSP PLGA microparticles were prepared as previously described for the *in vivo* tests used for comparison with the *in vitro* test results of the present study [25]. The prepared DRSP PLGA microparticles had a drug content of $39.6 \pm 1.1\%$ ($93.5 \pm 3.7\%$ loading efficiency). Furthermore, they provided a relatively large vw-mp ($55.2 \pm 18.5 \mu\text{m}$). In contrast to EE PLGA microparticles, DRSP PLGA microparticles were opaque, indicating that the drug was finely dispersed in the polymer and not completely dissolved (monolithic dispersion) (see **Fig. 2 g**). The dispersed or dissolved state of encapsulated drug in DRSP and EE

PLGA microparticles could have an impact on drug release. Furthermore, less than 0.1% of isoDRSP was found in DRSP PLGA microparticles. After 3 months of storage, the vw-mp, drug content, and the percentage of isoDRSP were comparable with freshly prepared microparticles. Oil-based dosage forms are advantageous for DRSP due to its instability in aqueous systems. Approximately 7 mg/ml of DRSP was soluble in MCT [8]. No change in drug solubility was observed with addition of dextrin palmitate. The organogelator immobilized the liquid phase completely, thus slowing down drug diffusion and sedimentation in the oil-based matrix. No sedimentation of DRSP microcrystals was observed after three months storage at RT. Furthermore, the vw-mp of DRSP microcrystals was not significantly different after 3 months storage ($9.6 \pm 1.1 \mu\text{m}$ before, $11.2 \pm 2.0 \mu\text{m}$ after storage). No isoDRSP was found before or after storage. The resulting organogels were opaque. The organogel network was not visible by optical microscopy.

3.3 Preparation and *in vitro* release of combined EE DRSP drug-delivery systems

The prepared EE and DRSP drug-delivery systems were able to be combined in various ways (see **Fig. 1 b**). The formulations were mixed with each other immediately before starting the *in vitro* release tests because the long-term stability was not tested. The particulate systems were prepared with the addition of low concentrations of surfactant to avoid aggregation. EE PLGA microparticles were stabilized with polysorbate 80 (a typical stabilizer for parenteral formulations), which was also used for the *in vivo* tests of EE PLGA microparticles described below. Triton X-100 was better able to stabilize PBCA microcapsules [31]. The surfactants could increase drug solubility in the dialysis bag, especially when micelles, which might not diffuse through the membrane, are formed. DRSP at a concentration of $0.45 \pm 0.10 \text{ mg/ml}$ was soluble in 0.1% (w/w) Triton X-100 solution, whereas $0.85 \pm 0.13 \text{ mg/ml}$ of EE and $0.98 \pm 0.16 \text{ mg/ml}$ of DRSP were dissolved in 0.5% (w/w) polysorbate 80 solution. With or without the addition of surfactant, sink conditions are provided for both drugs in the surrounding release medium due to the addition of HP- β -cyclodextrin. EE at a concentration of $7.5 \pm 0.3 \text{ mg/ml}$ and $13.1 \pm 0.2 \text{ mg/ml}$ of DRSP was dissolved in the buffer solution containing 8% (w/w) HP- β -cyclodextrin. In contrast to surfactants, HP- β -cyclodextrin did not interact with the oil-based formulations and was therefore used for all of the tested formulations. The dialysis bags were shaken to avoid local saturation effects. *In vivo*, the drug is released after dissolution and diffusion through the drug-delivery system; the drug must then diffuse through the tissue and reach the lymphatic or blood circulation [34]. *In vitro*, the drug is dissolved in the formulations matrix and must migrate through the drug-delivery system and then through the dialysis membrane into the release medium. The dialysis membrane avoided spreading of the oil-based formulations and therefore ensured a constant surface area. The membrane is freely permeable to both drugs because their molecular weight is much lower than the cutoff of the membrane. Less than 0.1% of EE or DRSP enclosed in the formulations remained in the dialysis bag at the endpoint of the release studies.

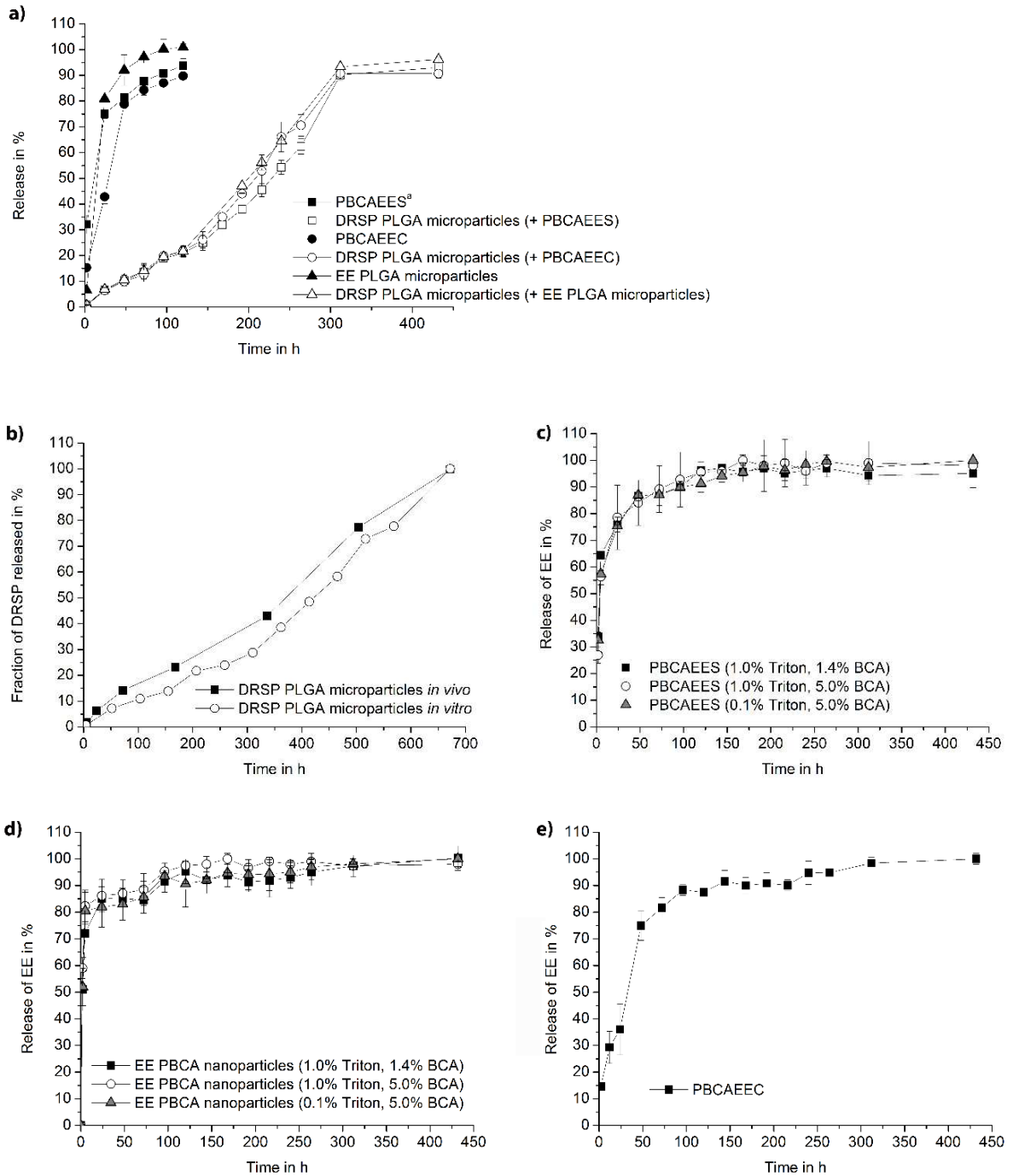


Fig. 4 *In vitro* release of aqueous dispersions containing **a)** DRSP PLGA microparticles and EE PBCA microcapsules or EE PLGA microparticles. **b)** Comparison between the relative amount of DRSP absorbed in Wistar rats and the relative amount of DRSP released *in vitro* from DRSP PLGA microparticles ($n = 3 - 4$; the measuring points of the *in vitro* release profile were multiplied by a factor of 2.15). *In vitro* release of aqueous dispersions containing **c)** PBCAEES; **d)** PBCA nanoparticles prepared under different conditions; **e)** PBCAEEC ($n = 3$). ^aPBCAEES prepared with 1.4% BCA and 1% surfactant.

To study the influence of the dialysis membrane, the dialysis rate of DRSP dispersed in release medium was determined. The suspension showed a mean dialysis rate of 1.2 ± 0.1 mg/h. For a dispersion containing 1.5 mg EE (EE drug-delivery systems contained lower drug amounts), a mean dialysis rate of 311 ± 29 μ g was found in the first hour. Because the release rates of the tested DRSP and EE formulations determined at each sampling point were significantly slower than the dialysis rate, one may conclude that the influence of drug diffusion through the membrane should be low. In an aqueous medium, DRSP isomerizes to isoDRSP. To reduce the degradation of DRSP after delivery into release medium, the buffer solution was replaced at specific time points. However, excessive medium exchange increased the risk of lowering drug concentrations below the LOQ at later sampling points. The degradation kinetics in phosphate buffer at pH 6.8 have previously been analyzed [8]. In the current study, less than 1% of isoDRSP was found in the release medium at pH 7.4 after 1 d. The proportion increased linearly over 24 h ($r^2 > 0.99$). The slope of the linear regression line was $0.025 \pm 0.000\%/h$ for the oil-based DRSP formulations. Because the isomerization is acid-catalyzed, the acidic PLGA matrix could accelerate the degradation [35,36]. However, the slope only slightly increased for DRSP PLGA microparticles ($0.026 \pm 0.002\%/h$). In summary, the main reasons for the incomplete release of DRSP were isomerization, non-quantifiable drug concentrations at later sampling points, drug remaining in the dialysis bag, and loss of drug during medium exchange (see Fig. 4 and Fig. 5). In contrast, aqueous EE and DRSP PLGA microparticle suspensions exhibited completely different release profiles. The drug release from polymer particles is mostly influenced by a complex interaction of different processes such as polymer degradation, erosion, drug dissolution, and diffusion [35,36].

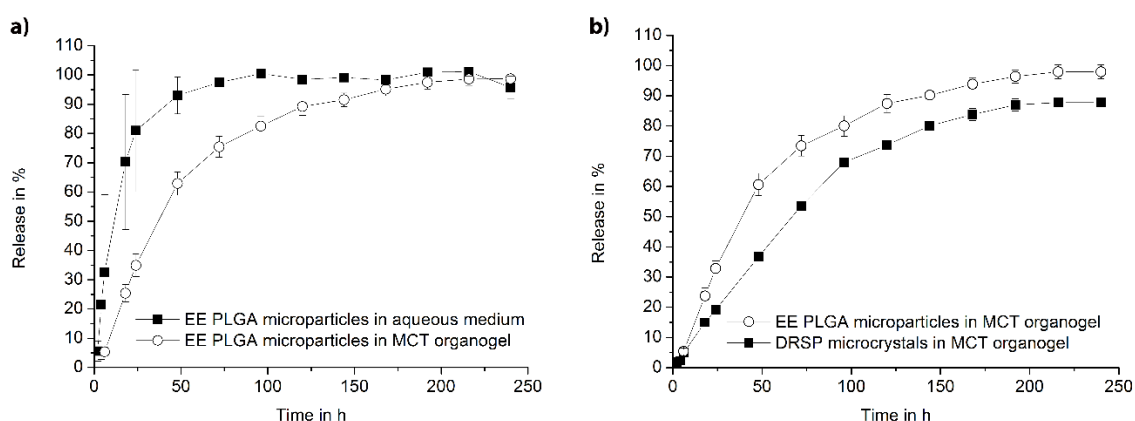


Fig. 5 *In vitro* release of **a)** EE PLGA microparticles dispersed in aqueous medium or MCT organogel without the addition of DRSP; **b)** MCT organogel containing DRSP microcrystals and EE PLGA microparticles ($n = 3$).

After reaching a maximum, the release rate of aqueous EE PLGA microparticle suspensions decreased gradually in the second stage (see Fig. 6 a). The continuous deceleration in the second stage indicated that constant diffusion of dissolved drug from the polymer matrix was the dominant process. The initial increase in release rate did not match the theoretical release profile; this may be

because the EE concentration was lower in the outer layers of microparticles, possibly caused by intensive washing or inhomogeneous distribution of drug during preparation. According to Fick's law, drug release from the bigger DRSP PLGA microparticles should be slower than from the smaller EE PLGA microparticles, but other mechanisms also appeared to influence drug release.

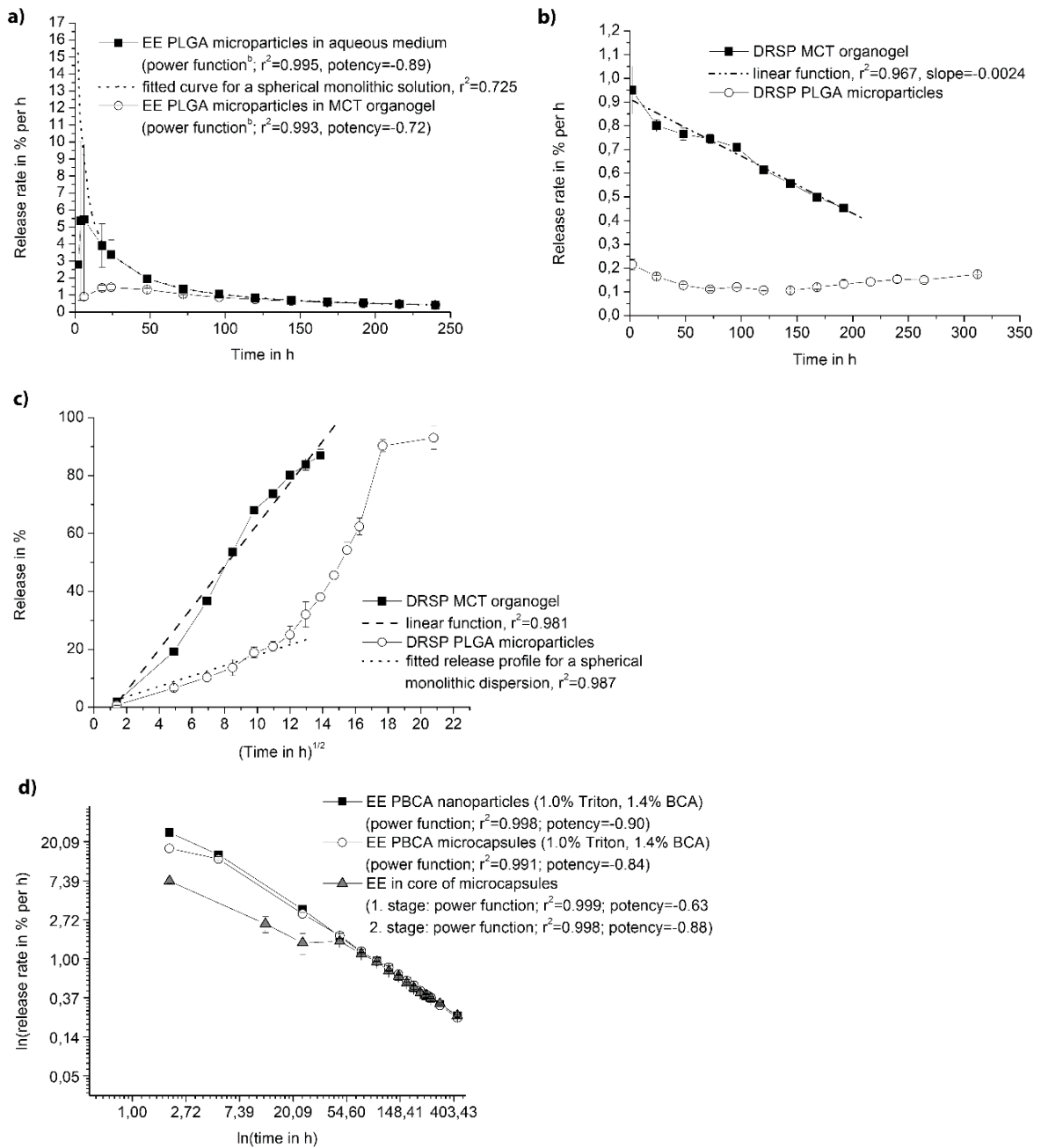


Fig. 6 *In vitro* drug release rates of **a)** EE PLGA microparticles dispersed in aqueous medium or MCT organogel and **b)** aqueous DRSP PLGA microparticle suspensions and DRSP MCT organogels. **c)** *In vitro* release of aqueous DRSP PLGA microparticle suspensions and DRSP MCT organogels over the square root of time. **d)** *In vitro* release rates of aqueous EE PBCA microcapsules and nanoparticle dispersions (logarithmic scales) ($n = 3$). ^bpower function includes all of the sampling points after reaching the maximum drug release rate.

During the first stage, the drug release profile of DRSP PLGA microparticles correlated relatively well with the theoretical drug release profile of a spherical monolithic dispersion [37] (see **Fig. 6 c**). According to the results in **section 3.2**, solid DRSP seemed to be dispersed in the polymer. The acceleration of drug release from PLGA microparticles during the later stage is well described in the literature [38,39] (see **Fig. 4 a** and **Fig. 6 b** and **c**). Acidic degradation product(s) of PLGA could decrease the micro-pH in the microparticles and therefore increase the autocatalysis of polymer degradation. Nevertheless, the percentage of isoDRSP in the release medium was still below 1% before daily medium exchange, indicating no significant increase in degradation. *In vitro*, DRSP was released at a constant rate from the polymer particles over 13 d. An *in vivo* study showed that subcutaneously injected DRSP PLGA microparticles provided constant drug release over more than 28 d, without a significant initial burst within the first 48 h [25]. The *in vitro* release rate was probably accelerated because of the employment of sink conditions *in vitro*, which may not exist *in vivo* [40]. Nevertheless, the *in vitro* and *in vivo* release profiles correlated well (see **Fig. 4 b**). Moreover, *in vivo* drug release from the prepared aqueous EE PLGA microparticle dispersions was faster compared to DRSP PLGA microparticles, in accordance with *in vitro* results (ca. 1 week until complete EE release in Wistar rats; unpublished results). As shown in the current *in vitro* experiments, a combination of EE and DRSP PLGA microparticles in an aqueous vehicle should be possible. DRSP PLGA microparticles were able to combine with EE PBCA microcapsules in an aqueous suspension. Both PBCAEES and PBCAEEC released the drug immediately after contact with the release medium. The greater surface area should cause a faster release from EE PBCA nanoparticles; in accordance, it was observed that the drug release rate from PBCAEES was initially slower (see **Fig. 4 c** and **d**). For both EE PBCA nanoparticles and microcapsules, the release rate followed a power function, indicating drug diffusion to be the main release process (see **Fig. 6 d**). The correlation coefficient was higher for EE PBCA nanoparticles. The release rate of EE PBCA microcapsules was comparable to the release rate of PBCA nanoparticles after 5 h. The reason for this could be the destruction of microcapsules. PBCA microcapsules are stable under acidic conditions (see **section 3.1.2**). In reference to [15], hydrolysis of the polymer is accelerated at pH 7.4 and starts within the first few hours. The bursting of microcapsules could be catalyzed by polymer degradation and could accelerate the drug release due to the greater surface area of microcapsule fragments. The destruction of microcapsules was observed during the release test by noting a decrease in the microcapsule concentration over time. Nevertheless, there were still isolated microcapsules and polymer fragments visible at the endpoint of drug release (see **Fig. 2 h**). Surprisingly, no influence of PBCA nanoparticle size on drug release was found. One reason for this may be inhomogeneous distribution of drug in the polymer matrix (e.g., higher drug concentrations near the surface of larger PBCA nanoparticles). Furthermore, the inhomogeneous drug distribution in the matrix, polymer degradation, or analytical variability could contribute to the irregular drug release profiles of PBCA nanoparticles and microcapsules at later stages (see **Fig. 4 c–e**). Compared with PBCAEES, the drug release from

PBCAEEC was initially significantly decreased (see **Fig. 4 e**). The *in vitro* tests were performed with unlyophilized liquid-filled PBCAEEC. The distribution of EE throughout the microcapsule could cause the slower initial release rate compared with PBCAEEES. Drug located mainly in the core should cause a spike in drug release after bursting. However, the release rate of PBCAEEC instead became closer to the drug release rate of EE PBCA nanoparticles in the later stage, indicating drug release from the polymer shell (see **Fig. 6 d**). PBCAEEC seemed to be more robust than PBCAEEES because the convergence phase started at a later time. Larger shell-forming nanoparticles did not significantly increase the robustness of PBCAEEES; the higher stability of PBCAEEC may primarily be due to the liquid filling. Finally, DRSP organogels were combined with EE drug-delivery systems. A combination of PBCA microcapsules and organogels was not producible; the PBCA microcapsules were destroyed within minutes of contact with MCT. On the other hand, the incorporation of EE PLGA microparticles in DRSP organogels was possible. The release of suspended DRSP from the organogel should mainly be controlled by the dissolution of drug microcrystals and the diffusion of dissolved drug to the release medium (see **Fig. 5**). Drug diffusion was decelerated by the organogel network [41]. In accordance with Higuchi's equation for the release of suspended drug from a semi-solid matrix, the drug release from DRSP organogel increased fairly linearly with the square root of time (see **Fig. 6 b**). Throughout the entire release test, the percentage of isoDRSP in the release medium was below 1% before daily exchange of medium. The organogels delivered DRSP faster than the PLGA microparticles; furthermore, embedding EE PLGA microparticles into the organogel influenced drug release. EE PLGA microparticles suspended in MCT organogel had significantly slower release compared with the aqueous suspensions although the solubility of EE in MCT (1.3 ± 0.1 mg/ml EE) was higher than in polysorbate 80 solution. The drug release rate of EE PLGA microparticles suspended in MCT organogel followed the same profile as the aqueous suspensions of EE PLGA microparticles; the main reason for the decelerated drug release may be lower diffusivity due to the higher viscosity of the surrounding organogel (see **Fig. 6 d**). EE release from PLGA microparticles was not influenced by the presence of DRSP microcrystals, and vice versa (EE PLGA microparticles in MCT organogel without and with DRSP: $f_2 = 82$, $f_1 = 3$; DRSP organogel without (data not shown) and with EE PLGA microparticles: $f_2 = 62$, $f_1 = 4$). In short, the incorporation of a particulate EE drug-delivery system into a surrounding continuous organogel phase caused a prolongation of EE release. The duration of DRSP and EE release was approximated.

4 Conclusion

Aqueous suspensions of EE PLGA microparticles released the drug relatively quickly; the release rate was mainly controlled by diffusion of dissolved drug. The drug release of PLGA microparticles including dispersed DRSP was significantly slower and was primarily influenced by drug dissolution and diffusion in the first stage. In the later stage, polymer degradation accelerated the release rate of DRSP. The *in vitro* release data correlated well with *in vivo* results. Although isomerization of DRSP

was accelerated under acidic conditions, only low concentrations of isoDRSP were found in PLGA microparticles after preparation, storage, and drug release. By varying the synthesis parameters of EE PBCA nanoparticles, the polymer wall thickness and drug content of the resulting PBCAEES were slightly changed. High doses of EE were delivered from PBCAEES and PBCAEEC within the first few days. Liquid-filled PBCA microcapsules were found to be more stable than air-filled PBCA microcapsules, thus the bursting of microcapsules, modifying the drug release in the later phase, was delayed. Polymer wall thickness did not significantly influence drug release in our experiments. EE drug-delivery systems were able to combine with aqueous DRSP microparticle suspension without influencing each other. In contrast, the combination of EE PBCA microcapsules with DRSP organogels was not possible due to immediate bursting of microcapsules. Both sedimentation and particle growth of DRSP microcrystals were decelerated in MCT organogels. DRSP organogels provided a nearly linear drug release with the square root of time; the drug release was mainly controlled by drug dissolution and diffusion. EE PLGA microparticles incorporated into DRSP MCT organogels released EE significantly slower than aqueous dispersions. The deceleration should mainly be caused by slowed drug diffusion. The drug release of EE and DRSP was thus approximated.

5 Supplement

$$\text{a)} \quad \frac{M_t}{M_\infty} = 6 \cdot \left(\frac{D \cdot t}{\pi \cdot R^2} \right)^{1/2} - \frac{3 \cdot D \cdot t}{R^2}$$

$$\text{b)} \quad \frac{M_t}{M_\infty} = 1 - \frac{6}{\pi^2} \exp\left(-\frac{\pi^2 \cdot D \cdot t}{R^2}\right)$$

Equation 3 Mathematical equation for quantifying the drug release from spherical monolithic solutions [23]; **a)** early time ($M_t/M_\infty \leq 0.6$), **b)** late time ($M_t/M_\infty \geq 0.4$). M_t = cumulative drug amounts released at time t ; M_∞ = cumulative drug amounts released at infinite time; D = diffusion coefficient in the drug delivery system; R = radius of sphere; t = time.

$$M_t = 4 \cdot \pi \cdot r^2 \cdot \left[\sqrt{2 \cdot (c_0 - c_s) \cdot c_s \cdot D \cdot t} + \frac{4 \cdot c_s \cdot D \cdot t}{9 \cdot r} \cdot \left(\frac{c_s}{2 \cdot c_0 - c_s} - 3 \right) \right]$$

Equation 4 Mathematical equation for quantifying the drug release from spherical monolithic dispersions [37]. M_t = cumulative amount of released drug at time t ; r^2 = radius of sphere; D = diffusion coefficient in the drug delivery system, c_s = API solubility in the drug delivery system, c_0 = initial drug concentration; t = time.

References

- [1] Draft Guideline on fixed combination medicinal products. www.ema.europa.eu. 2008. European Medicines Agency, London. 26.12.2011.
- [2] S. Gupta, Non-oral hormonal contraception, *Curr. Obstet. Gynaecol.*, 16 (2006) 30-38.
- [3] C. d'Arcangues and Snow R.C., Injectable Contraceptives, in: T. Rabe and B. Runnebaum (Eds.), *Fertility Control Update and Trends*, Springer-Verlag, Heidelberg, 1999, pp. 121-149.
- [4] H.P. Zahradnik, Depotgestagene, *Arch. Gynecol. Obstet.*, 257 (1995) 536-541.
- [5] D.T. Birnbaum, J.D. Kosmala, D.B. Henthorn, and L. Brannon-Peppas, Controlled release of beta-estradiol from PLGA microparticles: The effect of organic phase solvent on encapsulation and release, *J. Control. Release*, 65 (2000) 375-387.
- [6] M.D. Dhanaraju, K. Vema, R. Jayakumar, and C. Vamsadhara, Preparation and characterization of injectable microspheres of contraceptive hormones, *Int. J. Pharm.*, 268 (2003) 23-29.
- [7] Z.-H. Gao, W.R. Crowley, A.J. Shukla, J.R. Johnson, and J.F. Reger, Controlled Release of Contraceptive Steroids from Biodegradable and Injectable Gel Formulations: *In vivo* Evaluation, *Pharm. Res.*, 12 (1995) 864-868.
- [8] S. Nippe and S. General, Parenteral oil-based drospirenone microcrystal suspensions - Evaluation of physicochemical stability and influence of stabilising agents, *Int. J. Pharm.*, 416 (2011) 181-188.
- [9] S. Murdan, Organogels in drug delivery, *Expert Opin. Drug Deliv.*, 2 (2005) 489-505.
- [10] R.K. Zurawin and L. Ayensu-Coker, Innovations in contraception: a review, *Clin. Obstet. Gynecol.*, 50 (2007) 425-439.
- [11] N. Behan, C. Birkinshaw, and N. Clarke, Poly *n*-butyl cyanoacrylate nanoparticles: a mechanistic study of polymerisation and particle formation, *Biomaterials*, 22 (2001) 1335-1344.
- [12] S.J. Douglas, L. Illum, S.S. Davis, and J. Kreuter, Particle size and size distribution of poly(butyl-2-cyanoacrylate) nanoparticles - I. Influence of physicochemical factors, *J. Colloid Interface Sci.*, 101 (1984) 149-158.
- [13] D.C. Pepper, Anionic and zwitterionic polymerization of alpha-cyanoacrylates, *J. Polym. Sci. Pol. Sym.*, 62 (1978) 65-77.
- [14] W. Schmidt and G. Roessling, Novel manufacturing process of hollow polymer microspheres, *Chem. Eng. Sci.*, 61 (2006) 4973-4981.
- [15] C. Olbrich, P. Hauff, F. Scholle, W. Schmidt, U. Bakowsky, A. Briel, and M. Schirner, The *in vitro* stability of air-filled polybutylcyanoacrylate microparticles, *Biomaterials*, 27 (2006) 3549-3559.
- [16] A.R. Ahmed, A. Dashevsky, and R. Bodmeier, Reduction in burst release of PLGA term microparticles by incorporation into cubic phase-forming systems, *Eur. J. Pharm. Biopharm.*, 70 (2008) 765-769.
- [17] Q. Hou, D.Y. Chau, C. Pratoomsot, P.J. Tighe, H.S. Dua, K.M. Shakesheff, and F.R. Rose, *In situ* gelling hydrogels incorporating microparticles as drug delivery carriers for regenerative medicine, *J. Pharm. Sci.*, 97 (2008) 3972-3980.
- [18] H. Kranz and R. Bodmeier, A novel *in situ* forming drug delivery system for controlled parenteral drug delivery, *Int. J. Pharm.*, 332 (2007) 107-114.

-
- [19] X. Luan and R. Bodmeier, Influence of the poly(lactide-co-glycolide) type on the leuprolide release from in situ forming microparticle systems, *J. Control. Release*, 110 (2006) 266-272.
- [20] ICH Topic Q 2 (R1) Validation of the Analytical Procedures: Text and Methodology. 1995. www.emea.europa.eu, European Medicines Agency, London. 8-5-2012.
- [21] J.W. Moore and H.H. Flanner, Mathematical comparison of curves with an emphasis on in vitro dissolution profiles, *Pharm. Technol.*, 20 (1996) 64-74.
- [22] Guideline on the investigation of bioequivalence. 2010. www.emea.europa.eu, European Medicines Agency, London. 31-5-2012.
- [23] J. Siepmann and F. Siepmann, Modeling of diffusion controlled drug delivery, *J. Control. Release*, 161 (2012) 351-362.
- [24] T. Koizumi and S.P. Panomsuk, Release of medicaments from spherical matrices containing drug in suspension: theoretical aspects, *Int. J. Pharm.*, 116 (1995) 45-49.
- [25] S. General, 2010, Particles comprising drospirenone encapsulated in a polymer. [WO/2010/094624]. 12-2-2010.
- [26] J.G. Wagner and E. Nelson, Kinetic analysis of blood levels and urinary excretion in the absorptive phase after single doses of drug, *J. Pharm. Sci.*, 53 (1964) 1392-1403.
- [27] Yasmin Pharmacology Review Part 1- Review and Evaluation of Pharmacology/Toxicology data. N21-098. 2000. www.fda.gov, US Food and Drug Administration, Rockville. 13-11-2011.
- [28] S. Nippe and S. General. 2010. Formulation comprising drospirenone for subcutaneous or intramuscular administration. [WO/2010/094623]. 12-2-2010.
- [29] R. Bodmeier and O. Paeratakul, Evaluation of drug-containing films prepared from aqueous latexes, *Pharm. Res.*, 6 (1989) 725-730.
- [30] P. Sommerfeld, U. Schroeder, and B.A. Sabel, Long-term stability of PBCA nanoparticle suspensions suggests clinical usefulness, *Int. J. Pharm.*, 155 (1997) 201-207.
- [31] U. Baudisch, Colloid-chemical investigations within the development of i. v. injectable polybutylcyanoacrylate nanoparticles: Synthesis, characterisation and stability. 2001. FU Berlin. 6-1-2012.
- [32] R. Arshady, Suspension, emulsion, and dispersion polymerization: A methodological survey, *Colloid Polym. Sci.*, 270 (1992) 717-732.
- [33] A. van Herk and B. Gilbert, Emulsion Polymerisation, in: A. van Herk (Ed.), *Chemistry and technology of emulsion polymerisation*, Blackwell Publishing Ltd., Oxford, 2005.
- [34] J. Zuidema, F. Kadir, H.A.C. Titulaer, and C. Oussoren, Release and absorption rates of intramuscularly and subcutaneously injected pharmaceuticals (II), *Int. J. Pharm.*, 105 (1994) 189-207.
- [35] J. Siepmann and A. Goepferich, Mathematical modeling of bioerodible, polymeric drug delivery systems, *Adv. Drug Deliv. Rev.*, 48 (2001) 229-247.
- [36] J. Siepmann and F. Siepmann, Mathematical modeling of drug delivery, *Int. J. Pharm.*, 364 (2008) 328-343.
- [37] N. Faisant, J. Siepmann, and J.P. Benoit, PLGA-based microparticles: elucidation of mechanisms and a new, simple mathematical model quantifying drug release, *Eur. J. Pharm. Sci.*, 15 (2002) 355-366.

- [38] D. Klose, F. Siepman, K. Elkharraz, S. Krenzlin, and J. Siepman, How porosity and size affect the drug release mechanisms from PLGA-based microparticles, *Int. J. Pharm.*, 314 (2006) 198-206.
- [39] J. Siepman, K. Elkharraz, F. Siepman, and D. Klose, How autocatalysis accelerated drug release from PLGA-based microparticles: A quantitative treatment, *Biomacromolecules*, 6 (2005) 2312-2319.
- [40] S.S. D'Souza and P.P. DeLuca, Methods to assess in vitro drug release from injectable polymeric particulate systems, *Pharm. Res.*, 23 (2006) 460-474.
- [41] Z.-H. Gao, A.J.Shukla, J.R.Johnson, and W.R.Crowley, Controlled Release of Contraceptive Steroids from Biodegradable and Injectable Gel Formulations: *In vitro* Evaluation, *Pharm. Res.*, 12 (1995) 857-863.

CHAPTER 6

Summary - Zusammenfassung

1 Summary

The aim of this work was to investigate suitable i.m. and, in particular, s.c. injectable drug delivery systems for steroids. DRSP MCSs and DRSP organogels were studied as potential injectable formulations with focus on the physicochemical stability and applicability. The pharmacokinetics of steroids, in particular DRSP and ZK28, incorporated into injectable drug delivery systems, was analyzed. In addition, the ability to combine DRSP and EE drug delivery systems was studied.

DRSP MCSs

For once-a-month injections, an estimated dose of at least 60 - 70 mg of DRSP has to be included in 0.5 - 2.0 ml of vehicle for s.c. injection and in a maximum of 5 ml for i.m. injection. DRSP showed poor water solubility, a typical characteristic for steroids. Therefore, it would be predestined for the incorporation in aqueous MCSs. However, the chemical stability of aqueous DRSP MCSs was low due to isomerization to inactive isoDRSP (approx. 30% isoDRSP after 42 d). Advantageously, DRSP showed very high chemical stability in oils. After one year of storage, no traces of isoDRSP were determined in the tested oils sesame oil, co, or MCT. Because DRSP was insufficiently soluble in the tested oils as well, oil-based DRSP MCSs were analyzed as possible formulation options with regard to the physical stability, which is typically a critical issue for MCSs. High oil viscosity decelerated sedimentation and particle size growth. On the other hand, low viscous DRSP MCT MCSs were evaluated as suitable for s.c. injection with an autoinjector, which allows the drug application by the patients themselves.

The physical stability of oil-based DRSP MCSs was increased with the addition of suitable excipients. So far, the stabilization of oil-based MCSs is less investigated. The tested stabilizing agents were used in concentrations that affected neither the DRSP solubility nor the vehicle viscosity. Especially, silica derivatives influenced the physical stability positively. The addition of 0.2% (w/w) silica reduced DRSP sedimentation in all vehicles and particle size growth in co and sesame oil. The addition of 0.2% (w/w) hydrophobic silica even decelerated DRSP particle size growth and sedimentation in all tested oils and avoided increase of drug particle sizes in sesame oil and co completely over one year. The stabilizing effect was assumed to be caused by molecular interaction of API and stabilizer as well as the formation of sterically stabilizing structures by the excipient.

DRSP MCT organogels

Physical stability, applicability, and *in vitro* release of DRSP MCT organogels, containing different suitable organogelators, were assessed with respect to the rheological properties. In contrast to non-stabilized DRSP MCT MCSs and DRSP MCSs stabilized with non-thickening agents, DRSP organogels were completely stable against sedimentation. Thus, agitation of MCSs before injection would not be necessary. Pre-filled in syringes, stable organogels are ready-to-use. To

simulate transport and storage stress, DRSP organogels were mechanically destructed and stored at elevated temperature. All DRSP organogels restructured and showed no sedimentation except for CS and partially MC organogels. Furthermore, particle size growth was significantly reduced in all tested DRSP organogels during storage compared to non-stabilized DRSP MCT MCSs. The stabilizing excipient silica, which was used in increased concentrations for gelation, was even able to avoid particle size growth in MCT completely and was superior to the other organogelators. Advantageously, ejection of all DRSP organogels was still possible using an autoinjector, due to gel destruction during injection. Moreover, DRSP organogels exhibited significantly decelerated *in vitro* release compared to non-stabilized MCSs, most likely due to the recovery of the gel network after injection that was shown in the rheological tests. The *in vitro* release was slightly decelerated with increasing G' and η^* in dependence on the elasticity. The drug release profiles for DRSP organogels was fairly linear with the square root of time, according to Higuchi's equation. Overall, the rheological evaluation was useful to identify sol-gel transition, to differentiate between stronger and weaker gels and to assess the gel elasticity. A correlation between rheological properties and parameters of physical stability during storage and application was partially found.

Because DRSP silica organogels provided the highest elasticity, moderate G' and η^* , and avoided most efficiently particle size growth, they were evaluated as more preferable compared to the other DRSP organogels. In general, DRSP organogels were evaluated as superior to non-stabilized DRSP MCT MCSs with respect to storage stability and drug release.

Pharmacokinetics of steroids incorporated into injectable drug delivery systems

The aim was to identify parameters that influence the drug release and to obtain constant prolonged release kinetics. The *in vitro* release studies of DRSP MCSs showed an influence of the vehicle on drug release: Low API solubility in the vehicle and high vehicle viscosity decelerated the drug release. Po and aqueous DRSP MCSs showed the slowest *in vitro* release. With respect to the *in vitro* results, the pharmacokinetics of aqueous and po DRSP MCSs were studied after s.c. injection in female Wistar rats and Cynomolgus monkeys. Aqueous DRSP MCSs exhibited significantly slower absorption profiles compared to po DRSP MCSs. Conspicuously high initial serum peaks characterized the pharmacokinetics of aqueous and, in particular, po DRSP MCSs. Moreover, aqueous DRSP MCSs exhibited significant lower AUCs than po DRSP MCSs in rats. AUCs in monkeys were comparable. The high initial plasma peak of aqueous MCSs was probably caused by fast diffusion of the aqueous vehicle, which included dissolved DRSP, from the injection site. DRSP that remained at the injection site should slowly dissolve in the tissue fluid. In general, there is a risk that lipophilic APIs dissolve too slowly in the aqueous tissue fluid to reach therapeutic relevant concentrations. This effect might cause the low AUC of aqueous MCSs although the serum levels were already at very low levels at the end of measurement interval. Since oils stay longer at the injection site, the risk of residual API at the injection site after vehicle diffusion is

lower. Drug diffusion and partitioning to the aqueous tissue fluid should mainly influence the *in vivo* release of po MCSs. The dependence of both processes on the API concentration might explain the higher initial drug release.

With regard to the DRSP MCSs results, pharmacokinetics of non-stabilized ZK28 co/bb formulations and ZK28 MCT/bb organogels were evaluated in Wistar rats. In accordance to DRSP formulations, ZK28 co/bb preparations provided sharp initial plasma peaks. ZK28 organogels showed even higher initial absorption than ZK28 co/bb formulations which might be the result of gel destruction during injection and the low viscosity of MCT/bb compared to co/bb. Thereafter, ZK28 organogels advantageously exhibited more constant drug plasma levels and significant higher AUC compared to ZK28 co/bb formulations. The reason might be the partial restructure of gel network that was shown in rheological tests.

Overall, it is assumed that organogels could be also a suitable carrier system for other steroids, to obtain constant and prolonged drug release. The vehicle stays probably long enough at the injection site to dissolve the API completely. In the future organogels with faster gel recovery should be tested to avoid unfavorable high initial plasma peaks.

Combined DRSP and EE drug delivery systems

DRSP PLGA microparticles and organogels, EE PLGA and PBCA microparticles were successfully prepared. DRSP PLGA microspheres contained about 40% (w/w) DRSP dispersed in the polymer. EE PLGA microspheres included approx. 8% (w/w) EE dissolved in the polymer. DRSP and EE PLGA microspheres were prepared with high encapsulation efficiency (more than 80%). Shell thickness and EE content (optimum approx. 1% (w/w) of the high-potent API EE) of PBCAEES were adjustable by the synthesis parameters of the EE PBCA nanoparticles. PBCAEES were prepared by influx of aqueous EE solution into air-filled drugless PBCA microcapsules at the glass transition temperature. Due to the low EE water solubility, the drug content of PBCAEES was low (approx. 0.3% (w/w) EE) and was not increased by addition of solubilizing agents to the EE solution. So far, the preparation of drug-filled PBCA microcapsules was not described in the literature. The encapsulation efficiency of EE PBCA microcapsules was low but could be optimized in the future. EE PBCA microcapsules were lyophilizable with Polyvidon K15<18 addition without significant destruction.

Next, the ability to combine DRSP and EE drug delivery systems and their *in vitro* release was tested. A further target was to identify drug delivery systems, which release hormone doses that are as low as possible but efficient (i.e. by timed or sustained drug release). The EE PLGA and PBCA microparticles and DRSP PLGA microspheres were combinable in an aqueous vehicle without interfering each other. DRSP PLGA microparticles did not show significant initial burst effect and provided constant, significantly more sustained drug release than EE microparticles. The DRSP

release was assumed to be primarily influenced by drug dissolution and diffusion as well as polymer erosion in the later stage. The *in vitro* release correlated well with previous *in vivo* results. Although DRSP isomerization was accelerated under acidic conditions, low isoDRSP concentrations were found in PLGA microparticles after preparation, storage, and drug release. Overall, PLGA microparticles were evaluated as suitable sustained drug delivery systems for DRSP. Compared to EE PBCA nanoparticles, PBCAEES exhibited a lower unwanted initial burst effect, possibly due to the lower surface area of microcapsules. PBCAEEC showed significant decreased initial drug release, compared to PBCAEES, indicating drug release by diffusion from the core in the first phase. In the future, EE PBCA microcapsules could be further optimized to reach timed drug release, i.e. by increasing the stability of the polymer shell or by optimization of the core filling (e.g. by use of other EE vehicles). In contrast to DRSP PLGA microparticles, EE PLGA microparticles exhibited a fast *in vitro* release within 2 - 4 d, which was not influenced by polymer erosion.

Due to capsules' burst upon oil contact, EE PBCA microcapsules were not combinable with DRSP organogels. Incorporation of EE PLGA microparticles in DRSP organogels was possible. Compared to DRSP PLGA microparticles, the organogels provided a faster but more constant drug release rate. Advantageously, EE PLGA microparticles incorporated in organogel showed significantly prolonged and more constant EE release than aqueous EE PLGA microparticles dispersions. The system exhibited a nearly simultaneous drug release of EE and DRSP. Thus, EE PLGA microparticles incorporated into DRSP organogels were identified as excellent sustained drug delivery system for combined drug release.

2 Zusammenfassung

Ziel der vorliegenden Arbeit war es, potentielle intramuskulär und, insbesondere, subkutan injizierbare Freisetzungssysteme für steroidale APIs zu untersuchen. Zunächst wurden Drosiprenon (DRSP) Mikrokristallsuspensionen (MKS) sowie DRSP Oleogele, mit Fokus auf die physikochemische Stabilität und die Applizierbarkeit, analysiert. Darüber hinaus wurde die Pharmakokinetik verschiedener Steroidformulierungen, im Speziellen von DRSP und ZK28 Systemen, beleuchtet. Schließlich wurden zahlreiche Ethinylestradiol (EE) und DRSP Freisetzungssysteme miteinander kombiniert und deren *in vitro* Freisetzung untersucht.

DRSP MKS

Eine Dosis von mindestens 60 - 70 mg DRSP wurde für eine Ein-Monats-Applikation angenommen. Der Wirkstoff kann, für eine subkutane Injektion in 0,5 - 2,0 ml Vehikel bzw. für eine intramuskuläre Applikation in maximal 5 ml Trägerflüssigkeit dispergiert, verabreicht werden. DRSP zeigte eine schlechte Wasserlöslichkeit; eine charakteristische Eigenschaft für Steroide, die den Wirkstoff für eine wässrige MKS prädestiniert. Allerdings wies DRSP eine ungenügende chemische Stabilität in wässrigem Medium auf, da er sich in das inaktive Isomer isoDRSP umwandelte (ca. 30% isoDRSP nach 42 d). Sehr gute chemische Stabilität zeigte der Wirkstoff dagegen in öligen Grundlagen. Nach einem Jahr Lagerung, war kein isoDRSP in den getesteten Ölen Sesamöl, Rizinusöl bzw. mittelkettige Triglyceride (MKT) nachweisbar. Da DRSP eine ungenügende Löslichkeit in den Ölen aufwies, wurden ölige DRSP MKS als mögliche Formulierungsoption untersucht. Insbesondere wurde die physikalische Stabilität, als typischer kritischer Faktor einer Suspension, analysiert. Eine hohe Viskosität des Öls verlangsamte das Partikelwachstum und die Sedimentation. Andererseits wurde festgestellt, dass nur niedrigviskose DRSP MKS mit einem Autoinjektor subkutan applizierbar sind. Die Injektion mit dem Autoinjektor ermöglicht die Selbstapplikation durch den Patienten.

Mit dem Zusatz von geeigneten Hilfsstoffen, konnte die physikalische Stabilität von öligen DRSP MKS erhöht werden. Die Hilfsstoffe wurden in Konzentrationen eingesetzt, die weder die Viskosität noch die Wirkstofflöslichkeit im Öl signifikant änderten. Vor allem die Silicaderivate beeinflussten die physikalische Stabilität der öligen DRSP MKS positiv. Die Zugabe von 0,2% (m/m) Silica reduzierte die Wirkstoffsedimentation in allen Ölen und das Partikelgrößenwachstum in Rizinus- und Sesamöl signifikant. Die Zugabe von 0,2% (m/m) hydrophoben Silica konnte sogar das Partikelgrößenwachstum und die Sedimentation in allen Ölen deutlich reduzieren und verhinderte das Partikelgrößenwachstum in Rizinus- und Sesamöl vollständig über ein Jahr. Es wird vermutet, dass der stabilisierende Effekt durch molekulare Interaktion zwischen Hilfsstoff und DRSP sowie durch Ausbildung von sterisch stabilisierenden Strukturen erzielt wurde.

DRSP MKT Oleogele

Die physikalische Stabilität, die Applizierbarkeit sowie die *in vitro* Freisetzung von DRSP MKT Oleogelen, mit Zusatz von verschiedenen geeigneten Oleogelbildnern, wurden, im Hinblick auf ihre rheologischen Eigenschaften, evaluiert. Im Gegensatz zu DRSP MKT MKS, die nicht oder mit nicht viskositätserhöhenden Hilfsstoffen stabilisiert wurden, zeigten DRSP MKT Oleogele keine Wirkstoffsedimentation, wodurch eine Agitation der Suspensionen vor der Injektion unnötig ist. Abgefüllt in Fertigspritzen, könnte eine stabile DRSP Oleogelformulierung somit als „ready-to-use“ Anwendung genutzt werden. Darüber hinaus wurden Transport- und Lagerungsstress durch mechanische Zerstörung der DRSP Oleogele und anschließender Lagerung bei erhöhter Temperatur simuliert. Alle DRSP Oleogele restrukturierten sich, unter den gegebenen Bedingungen, und zeigten keine Sedimentation, mit Ausnahme von Cholesterylstearat- und, zum Teil, von Methylcholatoroleogelen. Im Vergleich zu nicht stabilisierten DRSP MKT MKS konnte das Partikelgrößenwachstum von DRSP während der Lagerung durch alle Gelbildner signifikant reduziert werden. In der verwendeten Konzentration konnte Silica nun auch das Partikelgrößenwachstum in MKT vollständig verhindern und war den anderen Gelbildnern überlegen. Durch die Zerstörung der Gelstruktur unter mechanischer Belastung, war der Ausstoß der DRSP Oleogele mit Autoinjektoren immer noch möglich. Darüber hinaus wiesen die DRSP Oleogele eine vorteilhaft langsamere Freisetzung im Vergleich zu nicht-stabilisierten DRSP MKT MKS auf. Die verzögerte Freisetzung wird vermutlich durch die partielle Gelrestruktuiierung nach Injektion, die auch bei den rheologischen Untersuchungen beobachtet wurde, verursacht. DRSP Oleogele mit höherem/r elastischen Modul und komplexer Viskosität zeigten in Abhängigkeit von der Elastizität eine leicht verzögerte *in vitro* Freisetzung. Die Freisetzungsprofile der DRSP Oleogele wiesen einen fast linearen Verlauf mit der Wurzel der Zeit auf, so dass sich das Freisetzungsverhalten durch die Higuchi-Gleichung beschreiben lässt.

Insgesamt zeigte sich, dass die rheologische Untersuchung der Oleogele sehr hilfreich für die Bestimmung des Sol-Gel-Übergangs, die Unterscheidung zwischen starken und schwachen Gelen sowie für die Beurteilung der Gelelastizität ist. Es wurde jedoch nicht immer eine eindeutige Korrelation zwischen rheologischen Eigenschaften und physikalischer Stabilität während Lagerung und Anwendung gefunden. Da DRSP Silica Oleogele die höchste Elastizität und ein moderate(s) elastisches Modul und komplexe Viskosität aufwiesen sowie das Partikelgrößenwachstums effizient verhinderten, wurden sie als vorteilhafter im Vergleich zu den anderen DRSP Oleogelen bewertet. Generell wurden DRSP Oleogele den nicht-stabilisierten DRSP MKT MKS als überlegen, in Bezug auf Lagerstabilität und Wirkstofffreisetzung, beurteilt.

Pharmakokinetik von Steroiden aus injizierbaren Freisetzungssystemen

Ziel war es, Parameter zu identifizieren, die die Wirkstofffreisetzung beeinflussen, sowie eine konstante Langzeitfreisetzung zu erzielen. *In vitro* Untersuchungen zeigten, dass das Vehikel die Wirkstofffreisetzung beeinflusste: Niedrige API Löslichkeit in der Grundlage und hohe Viskosität des Mediums verzögerten die *in vitro* Freisetzung. Die langsamste Freisetzung wiesen Erdnussöl- und wässrige DRSP MKS auf. Im Hinblick auf die *in vitro* Freisetzungsuntersuchungen, wurde die Pharmakokinetik von wässrigen und Erdnussöl-DRSP MKS nach subkutaner Injektion in weiblichen Wistar-Ratten und Cynomolgusaffen untersucht. Wässrige DRSP MKS wiesen eine deutlich langsamere *in vivo* Absorption als Erdnussöl-DRSP MKS auf. Die Serumspiegel der wässrigen und vor allem der Erdnussöl-DRSP MKS waren durch einen ungünstig hohen Anfangspeak gekennzeichnet. Wässrige DRSP MKS zeigten darüber hinaus in Ratten signifikant niedrigere AUCs als Erdnussöl-DRSP MKS. Die AUCs bei Affen waren vergleichbar. Der initiale Serumpeak der wässrigen MKS wird vermutlich durch das schnelle Wegdiffundieren des wässrigen Vehikels, das gelöstes DRSP enthält, verursacht. DRSP, das an der Injektionsstelle verbleibt, muss sich langsam in der Gewebsflüssigkeit lösen. Im Allgemeinen, besteht das Risiko, dass sich lipophile APIs, die an der Injektionsstelle verbleiben, zu langsam in der Gewebeflüssigkeit lösen, um wirksame Serumspiegel zu erzielen. Dieser Effekt könnte für die niedrigen AUCs der wässrigen DRSP MKS, trotz niedriger Plasmaspiegel zum Ende des Untersuchungsintervalls, verantwortlich sein. Da Öle länger an der Injektionsstelle verweilen, ist das Risiko, dass sich Wirkstoffe an der Injektionsstelle „einkapseln“, geringer. Wirkstoffdiffusion und Verteilung des APIs in die wässrige Gewebsflüssigkeit kontrollieren vermutlich hauptsächlich die *in vivo* Freisetzung aus öligen DRSP MKS. Beide Prozesse werden von der Wirkstoffkonzentration beeinflusst, was die höhere Initialfreisetzung des DRSP aus den öligen MKS erklären könnte.

Im Hinblick auf die Ergebnisse der DRSP MKS, wurde die Pharmakokinetik von nicht-stabilisierten ZK28 Rizinusöl/Benzylbenzoat Formulierungen und ZK28 MKT/Benzylbenzoat Oleogelen in Wistar-Ratten evaluiert. In Übereinstimmung mit den DRSP Formulierungen, war bei ZK28 Rizinusöl/Benzylbenzoat Formulierungen ein hoher initialer Plasmapeak zu beobachten. ZK28 MKT/Benzylbenzoat Oleogelee wiesen sogar eine höhere initiale Absorption als ZK28 Rizinusöl/Benzylbenzoat Formulierungen auf. Diese könnte durch die Zerstörung der Gelstruktur bei Injektion und die geringere Viskosität von MKT/Benzylbenzoat im Vergleich zu Rizinusöl/Benzylbenzoat verursacht werden. Im späteren Verlauf zeigten die Oleogelee jedoch konstantere Plasmaspiegel und signifikant höhere AUCs im Vergleich zu ZK28 Rizinusöl/Benzylbenzoat Formulierungen. Grund hierfür, könnte die partielle Restrukturierung des Gelgerüsts sein, die bei den rheologischen Untersuchungen gezeigt wurde.

Insgesamt, wurden Oleogelee als vielversprechende Trägersysteme für Steroide bewertet, mit denen eine konstante und verzögerte Wirkstofffreisetzung erzielt werden kann. Das Vehikel verweilt

vermutlich so lange an der Injektionsstelle bis der lipophile API vollständig gelöst ist. Oleogele, die eine schnellere Gelrestrukturierung nach mechanischer Belastung aufweisen, wären ein interessanter Ansatzpunkt, um hohe initiale Plasmapeaks zu vermeiden.

Kombinierte DRSP und EE Freisetzungssysteme

Zunächst wurden DRSP Poly(D,L-laktid-co-glykolid) (PLGA) Mikropartikel und Oleogele sowie EE PLGA und Poly(n-butyl-2-cyanoacrylat) (PBCA) Mikropartikel hergestellt. DRSP PLGA Mikrosphären enthielten ca. 40% (m/m) API, dispergiert in der Polymermatrix, während in den EE PLGA Mikrosphären ca. 8% (m/m) API gelöst vorlagen. Sowohl DRSP als auch EE PLGA Mikrosphären wurden mit einer hohen Verkapselungseffizienz hergestellt (größer 80%). PBCA Mikrokapseln, die EE in der Hülle enthalten (PBCAEES), werden von EE PBCA Nanopartikeln umhüllt, die in Abhängigkeit von den Syntheseparametern, in ihren Schichtdicken und ihrem EE-Gehalt (optimal ca. 1% (m/m) des hochpotenten API) variiert werden können. PBCA Mikrokapseln, die EE im Kern enthalten (PBCAEEC), wurden durch Einstrom einer wässrigen EE Lösung in luftgefüllte, wirkstofffreie PBCA Mikrokapseln hergestellt. Aufgrund der schlechten Wasserlöslichkeit von EE, war der Wirkstoffgehalt der PBCAEEC relativ gering (ca. 0,3% (m/m) EE) und konnte auch nicht durch Zusatz von Lösungsvermittlern erhöht werden. Bisher wurde die Herstellung von wirkstoffgefüllten PBCA Mikrokapseln noch nicht in der Literatur beschrieben. Die erstmals hergestellten EE PBCA Mikrokapseln wiesen eine niedrige Verkapselungseffizienz auf, die allerdings weiter optimiert werden kann. EE PBCA Mikrokapseln konnten unter Zusatz von Polyvidon K15<18 lyophilisiert werden.

Schließlich wurden die Kombinierbarkeit der EE und DRSP Freisetzungssysteme sowie deren Wirkstofffreisetzung geprüft. Ziel war es, Freisetzungssysteme zu identifizieren, die in der Zukunft eine möglichst geringe aber dennoch wirksame Hormondosis abgeben. EE PLGA bzw. PBCA Mikropartikel und DRSP PLGA Mikropartikel waren, ohne negative Wechselwirkungen, in wässrigem Medium kombinierbar. DRSP PLGA Mikrosphären zeigten eine signifikant langsamere *in vitro* Freisetzung als die EE Mikropartikel, ohne ausgeprägten initialen Bursteffekt. Die DRSP Freisetzung wurde vermutlich vor allem durch die Auflösung des Wirkstoffs sowie dessen Diffusion und, im späteren Verlauf, zusätzlich durch Polymererosion kontrolliert. Die Ergebnisse der durchgeführten *in vitro* Freisetzungstests an DRSP PLGA Mikropartikeln korrelierten gut mit früheren *in vivo* Daten. Obwohl die DRSP Isomerisierung in saurem Medium beschleunigt ist, wurden nur geringe isoDRSP Mengen nach Herstellung, Lagerung und Freisetzung in den Mikropartikeln gefunden. Insgesamt wurden PLGA Mikrosphären als sehr gut geeignete Langzeitfreisetzungssysteme für DRSP bewertet. Im Vergleich zu EE PBCA Nanopartikeln wiesen PBCAEES einen weniger ausgeprägten, unerwünschten initialen Bursteffekt auf, was vermutlich auf die geringere Oberfläche der Mikrokapseln zurückzuführen ist. Noch deutlich geringer war die initiale Freisetzung von PBCAEEC, was darauf hinweist, dass die Freisetzung in der ersten Phase

durch Wirkstoffdiffusion aus dem Kern gesteuert wurde. Zukünftig könnte eine gezieltere Wirkstofffreisetzung aus EE PBCA Mikrokapseln, zu einem bestimmten Zeitpunkt, durch Erhöhung der Polymerhüllenstabilität sowie durch verbesserte Kernbefüllung (z.B. Austausch des EE Trägerflüssigkeit) erreicht werden. Im Gegensatz zu DRSP PLGA Mikropartikeln, zeigten die EE PLGA Mikropartikel eine schnelle Freisetzung innerhalb von 2 - 4 d, die nicht durch Polymererosion beeinflusst wurde.

Da die EE PBCA Mikrokapseln nach Kontakt mit Öl sofort zerstört wurden, war eine Kombination mit DRSP Oleogelen nicht möglich. Allerdings konnten EE PLGA Mikrosphären in DRSP Oleogele inkorporiert werden. Im Vergleich zu DRSP PLGA Mikrosphären war die *in vitro* Freisetzungsrates aus den Oleogelen beschleunigt, aber auch konstanter. In Öl dispergiert, zeigten die EE PLGA Mikrosphären eine vorteilhafte, signifikant verlangsamte und konstantere Wirkstofffreisetzung als aus den wässrigen Suspensionen. Das Freisetzungssystem wies eine nahezu simultane Freisetzung von DRSP und EE auf und scheint hervorragend für eine synchrone und konstante Langzeitfreisetzung von EE und DRSP geeignet zu sein.

CHAPTER 7

Appendices

List of Publications

Original Research Articles

- 1) Nippe, S., General, S., Parenteral oil-based drospirenone microcrystal suspensions -Evaluation of physicochemical stability and influence of stabilising agents. *J. Int. Pharm* 416 (2011) 181–188
- 2) Nippe, S., General, S., Combination of injectable ethinyl estradiol and drospirenone drug-delivery systems and characterization of their in vitro release. *Eur. J. Pharm. Sci.* 47 (2012) 790–800
- 3) Nippe, S., Preuße, C., General, S., Evaluation of the in vitro release and pharmacokinetics of parenteral injectable formulations for steroids. *Eur. J. Pharm. Biopharm* 83 (2013) 253–265
- 4) Nippe, S., General, S., Investigation of injectable drospirenone organogels with regard to their rheology and comparison to non-stabilized oil-based drospirenone suspensions. *Drug Dev. Ind. Pharm.* Early Online: 1–11 (2014)

Patent Application

Formulation comprising drospirenone for subcutaneous or intramuscular administration, submitted on 12.02.2010

WO Patent Application No. WO2010094623A1

US Patent Application No. US20120064166A1

EU Patent Application No. EP2398461A1

CA Patent Application No CA2752805A1

Poster presentations

Nippe, S., General, S., Kleine, C.. Investigation of oil-based micro-crystal suspensions of Drospirenone regarding the release kinetics, the physical and chemical stability (Poster). Bayer Schering Pharma AG – Young Scientist Poster Session 2008, Berlin, Germany (10/29/2008).

Curriculum Vitae

Mein Lebenslauf wird aus Gründen des Datenschutzes in der elektronischen Fassung meiner Arbeit nicht veröffentlicht.